

University of Southampton Research Repository

Copyright © and Moral Rights for this thesis and, where applicable, any accompanying data are retained by the author and/or other copyright owners. A copy can be downloaded for personal non-commercial research or study, without prior permission or charge. This thesis and the accompanying data cannot be reproduced or quoted extensively from without first obtaining permission in writing from the copyright holder/s. The content of the thesis and accompanying research data (where applicable) must not be changed in any way or sold commercially in any format or medium without the formal permission of the copyright holder/s.

When referring to this thesis and any accompanying data, full bibliographic details must be given, e.g.

Thesis: Author (Year of Submission) "Full thesis title", University of Southampton, name of the University Faculty or School or Department, PhD Thesis, pagination.

Data: Author (Year) Title. URI [dataset]

University of Southampton

Faculty of Engineering and Physical Sciences

Chemistry

Prevention of silver corrosion issues in oil-filled power transformers

-

**Selective approaches for elemental sulfur quantification and its removal from
mineral insulating oil**

DOI [\[enter DOI\] hyperlink, optional](#)

by

Sérgio Barata Garcia

Thesis for the degree of Doctor of Philosophy

December 2021

University of Southampton

Abstract

Faculty of Engineering and Physical Sciences

Chemistry

Doctor of Philosophy

Prevention of silver corrosion issues in oil-filled power transformers - Selective approaches for elemental sulfur quantification and its removal from mineral insulating oil

by

Sérgio Barata Garcia

The electrical grid is one of the most complex and important systems of our era. The grid transmits and provides electricity to millions of homes, businesses, schools, hospitals, etc. in an impressive network that can reach extensions of thousands of miles. The power grid, in particular the power transformers, are constantly subjected to numerous stresses that degrade the mechanical and dielectric properties of the liquid insulating system (usually mineral oil), eventually compromising its function. The environmental and economic concerns regarding the disposal of used mineral insulating oil have driven to major efforts on extending the life time of the insulating system. A number of regeneration processes, usually referred to as reclamation processes, have been successful to reduce the level of contaminants and oil degradation products in the oil. Despite considerable effort, issues remain with the presence of elemental sulfur (S_8), typically found following some oil regeneration procedures, where procedures utilised to remove other corrosive sulfur compounds (e.g., dibenzyl disulfide) were proven ineffective for S_8 .

In recent decades, the occurrence of power transformer failures associated to the presence of corrosive sulfur in the insulating mineral oil has experienced a marked increase, and corrosion of silver-coated electrical contacts in switching compartments due to trace levels of elemental sulfur is a known contributor to this increase. It has been reported that S_8 levels, as low as 1 ppm, may be sufficient to induce silver corrosion within the power transformer. The standard corrosion test (DIN 51353) is time consuming, requires 18 h for completion, and is followed by a visual subjective rating process. Hence, the development of a rapid and reliable analytical method to monitor the presence of elemental sulfur is of critical importance. To improve this, two analytical techniques to detect trace levels of S_8 in insulating mineral oil have been developed, the analytical methods were optimised and laboratory results that demonstrate the potential of the approaches adopted are presented in this thesis. Both methods are based on the selective reaction of elemental sulfur with triphenylphosphine (TPP). The derivatisation of the elemental sulfur required minimal sample preparation and resulted in the formation of a single compound, namely triphenylphosphine sulfide (TPPS). The developed GC-MS method allowed S_8 concentrations to be monitored down to 0.5 ppm, while the UHPSFC-MS was able to quantify S_8 as low as 5 ppb. These methods can be used as a routine test or to confirm the presence of S_8 in samples where corrosion has occurred.

Herein is also presented an effective laboratory reclamation approach to selectively remove S_8 from insulating mineral oil using polymers loaded with trisubstituted phosphines. The general concept

of this method is based on the capability of the trisubstituted phosphine to react selectively with elemental sulfur present in the mineral oil. The reaction leads to the in-situ formation of the corresponding phosphine sulfide, converting the elemental sulfur in a suitable form to be removed. The use of the trisubstituted phosphine-loaded polymers enabled not only the selective and near-total removal of S₈ from mineral oil but also the possibility of the polymer to be regenerated and reused. The reliability and robustness of our method was demonstrated by evaluating the capability of four different polymers to selectively remove S₈ from a real transformer oil sample that was found to be corrosive towards silver. The results showed that the polymers were capable of efficiently removing ≥ 99.5% of the S₈ present in the oil sample, i.e., from *circa* 17 ppm to below 0.01 ppm. Which demonstrates the ability of our reclamation process to extend the life-time of oil insulated power transformers, by converting a corrosive sample into non-corrosive. Considering the operational conditions of our system, i.e., equipment, operational costs, time frame, efficiency, etc., a scale up to an industry level should be conceivable.

Table of Contents

Table of Contents	i
Table of Tables	vii
Table of Figures	xi
Table of equations.....	xix
Research Thesis: Declaration of Authorship.....	xxi
Acknowledgements	xxv
Definitions and Abbreviations	xxvii
TOPICS II Research Project Aims and Objectives	1
Chapter 1 Introduction	2
1.1 Electric grid system in the United Kingdom	2
1.2 Transformers.....	5
1.2.1 Insulating materials.....	6
1.3 Transformer failures linked to corrosive sulfur	9
1.3.1 Mitigation strategies	10
1.4 Desulfurisation of hydrocarbons.....	11
1.4.1 Critical evaluation	12
1.4.2 Removal of elemental sulfur from mineral oil.....	14
1.5 Detection of S ₈ in hydrocarbons	16
1.5.1 Introduction to chromatography	17
1.5.2 Mass spectrometry	22
1.5.3 Mass Analysers.....	25
1.5.4 Summary.....	26
1.6 Polymers	26
1.6.1 Free Radical Polymerisation (FRP) Technique	27
1.6.2 Nitroxide-Mediated Polymerisation (NMP).....	30
1.6.3 Polymer-supported reagents/scavengers	31
Chapter 2 Analytical experimental part	35
2.1 Chemicals.....	35

2.1.1	Transformer mineral oil samples.....	35
2.2	Analytical procedure	35
2.2.1	Stock solution and calibration	35
2.2.2	Sample preparation and derivatisation procedure.....	36
2.2.3	General procedure for the reclamation processes to selectively remove S ₈ from transformer mineral oil	36
2.3	Instrumentation	36
2.3.1	GC-MS	36
2.3.2	Non-polar column - Configuration	36
2.3.3	Polar column – Configuration.....	37
2.4	UHPSFC-MS.....	37
2.4.1	Ultra-Performance Convergence Chromatography system – Triple Quadrupole Detector (UPC ² – TQD)	37
2.5	Data processing.....	38
2.5.1	Xcalibur™	38
2.5.2	MassLynx™	39
Chapter 3 Determination and quantification of elemental sulfur in mineral transformer insulating oil using chromatography and mass spectrometry. 41		
3.1	Derivatisation method for elemental sulfur detection.....	41
3.1.1	Derivatisation efficiency.....	44
3.1.2	Optimisation of the derivatisation reaction	56
3.1.3	Summary	58
3.1.4	Derivatisation selectivity	58
3.1.5	Interference from the dilution solvent.....	60
3.1.6	Attempts to increase the rate of the derivatisation reaction: alternative P(III) compounds.	62
3.2	Development of the GC-MS method.....	64
3.2.1	Using a non-polar column	65
3.2.2	Using a polar column.....	66
3.2.3	Summary.....	67

3.3	Development of the UHPSFC-MS method.....	68
3.3.1	Sample Mixture Optimisation	68
3.3.2	Method validation.....	70
3.3.3	Is elemental sulfur present in the new mineral insulating oil A?.....	71
3.3.4	Analysis of ex-service mineral oil samples	72
3.3.5	Reproducibility of the UHPSFC-MS method when applied to ex-service mineral oil samples	74
3.3.6	Identification of elemental sulfur in mineral insulating oil - Standard corrosive test (DIN 51353) vs. Analytical approach	76
3.4	Summary of the chapter	81
Chapter 4 Reclamation process - Selective removal of elemental sulfur from mineral transformer insulating oil		83
4.1	Reclamation process using montmorillonite clay.....	83
4.1.1	Conclusion.....	85
4.2	Selection of trisubstituted-phosphine polymer scavengers used in the selective removal of S ₈ from mineral oil	85
4.3	Design and commission laboratory reclamation rig to be used on the selective removal of S ₈ from transformer mineral oil	92
4.3.1	Initial studies on the selective removal of S ₈ from transformer mineral oil ...	93
4.3.2	Design and optimisation of the reclamation rig	95
4.3.3	Optimised reclamation process to selectively remove S ₈ from transformer mineral oil	106
4.4	Summary of the chapter	121
4.5	Current and further work.....	122
Chapter 5 Conclusions		124
Chapter 6 Organic experimental part.....		127
6.1	Chemicals.....	127
6.2	Instrumentation	127
6.2.1	Nuclear Magnetic Resonance (NMR)	127
6.2.2	Fourier-transform - Infrared Spectroscopy (FT-IR)	127

6.2.3	Melting point.....	127
6.3	Preparation and characterisation of the compounds synthesised	128
6.3.1	Synthesis of triphenylphosphine sulphide.....	128
6.3.2	Synthesis of ethoxydiphenylphosphane.....	129
6.3.3	Synthesis of the poly(lauryl-methacrylate) resin-bound phosphine (B)	130
6.3.4	Synthesis of the polystyrene resin-bound phosphine (D).....	133
6.3.5	Attempt to the synthesis of the poly(lauryl-methacrylate) resin-bound phosphine (E) using a TEMPO based initiator.....	139
Appendix A		145
A.1	Copyright permissions to reuse - IEEE.....	145
Appendix B		147
B.1	Copyright permission for reuse – Analyst	147
List of References.....		149

Table of Tables

Table 1 - Summary of the key aims/objectives for WP 3 of the TOPICS II project.	1
Table 2 – Common types of insulating materials in transformers.	6
Table 3 – General specifications for transformer mineral oil. ¹³	8
Table 4 - Commonly used desulfurisation reagents and their reaction products. ⁴⁵	15
Table 5 - Physical properties of liquids, gases, and supercritical fluids. ⁷²	21
Table 6 - Inlet method for UHPUHPSFC.	38
Table 7 – Intraday and Interday reproducibility of the UHPSFC-MS method when analysing ex-service mineral oil samples.	76
Table 8 – Conditions tried for the synthesis of polymer B	88
Table 9 – Results of the preliminary reclamation experiment 1 to selectively remove S ₈ from mineral oil.	98
Table 10 – Results of the reclamation experiment 2 to selectively remove S ₈ from mineral oil.	99
Table 11 – Results of the preliminary reclamation experiment 3 to selectively remove S ₈ from mineral oil.	101
Table 12 – Results of the preliminary reclamation experiment 4 to selectively remove S ₈ from mineral oil.	101
Table 13 – Results of the preliminary reclamation experiment 5 to selectively remove S ₈ from mineral oil.	103
Table 14 – Summary of the obtained results of the preliminary reclamation experiments to selectively remove S ₈ from mineral oil.	103
Table 15 – Results of the reclamation of new transformer mineral oil sample spiked with S ₈ using polymer A to selectively remove S ₈	109
Table 16 – Results of the reclamation of ex-service oil sample B using polymer A to selectively remove S ₈	110

Table 17 – Results of the reclamation of ex-service oil sample B using polymer B to selectively remove S ₈	112
Table 18 – Results of the reclamation of ex-service oil sample B using polymer C to selectively remove S ₈	115
Table 19 – Results of the reclamation of ex-service oil sample B using polymer D to selectively remove S ₈	116
Table 20 - Results obtained from the reclamation processes experiments of the ex-service oil sample B.	117

Table of Figures

Figure 1 – Map of the electric transmission grid in the United Kingdom operated by National Grid UK. ³	2
Figure 2 – Graphical illustration of the electrical system network in the UK. ⁴	3
Figure 3 - Electricity transmission map for Great Britain and Ireland and respective electricity transmission operators. ⁶	4
Figure 4 – Electricity distribution map for Great Britain and Ireland and respective electricity transmission operators. ⁶	4
Figure 5 - Schematic of a single-phase transformer showing electro-magnetic induction – Faraday’s Law of Induction. ¹⁰	5
Figure 6 – Selected classes of sulfur compounds present in crude oil. ³⁶	12
Figure 7 - Chlorinolysis process.	13
Figure 8 – Derivatization reaction.....	16
Figure 9 - A standard GC configuration. ⁶⁷	18
Figure 10 – Scheme of a sulfur chemiluminescence detector (SCD) and conversion to sulfur chemiluminescent species. ⁷⁰ The sulfur containing compounds eluted from the column are injected into a burner, where they undergo oxidation/reduction reactions forming SO compounds. These are redirected to the reaction chamber where they react with ozone (O ₃), the change in states (i.e., excited to ground state) generates light that is detected by a photomultiplier.	19
Figure 11 – GC-SCD (top) and GC-MS (below) spectra obtained from the analysis of an in service mineral oil sample. ⁷¹	19
Figure 12 - Phase diagram of CO ₂ , showing the critical point, the triple point and the sublimation temperature. ⁷²	20
Figure 13 - Scheme of a supercritical fluid chromatography instrument. ⁷⁵ The sample is injected into the inlet and then swept onto a chromatographic column by the carrier gas (usually _{sc} CO ₂). The compounds are then separated and led to the ion source, where they are converted to ions. The ions of interest are then redirected to the	

detector. The detector sends the obtained data to a computer, where it can be	
visually displayed and stored.	21
Figure 14 - A schematic representation of an ESI interface. ⁸² Showing the main steps of ESI	
ionisation; from the sample introduction, to the ion formation and consequent	
transfer to the mass spectrometer.	23
Figure 15 - A schematic of an ion source. ⁸³ The compounds eluting from the column enter the ion	
source and are converted to ions, which are then transferred to the mass	
analyser.	24
Figure 16 - Process of ion formation in EI.	24
Figure 17 - Representation of a quadrupole (linear) analyser. ⁸⁶ When the ions enter the	
quadrupole the positively charged ions are separated and then transferred to	
the detector.....	25
Figure 18 – Common radical initiators and initiation steps: a) BPO b) AIBN c) Benzophenone	
(example of reaction with polylactic acid). ⁹⁷	28
Figure 19 – Different ways in which a mono substituted monomer can add to an active centre	
during the propagation step of the free radical polymerisation.....	29
Figure 20 – Termination of propagation by combination.	29
Figure 21 – Termination of propagation by disproportionation.	30
Figure 22 – Common types of NMP agents.....	30
Figure 23 – General mechanism for NMP, using TEMPO as NMP reagent, benzoyl peroxide as	
initiator and styrene as the monomer. ⁹⁹	31
Figure 24 – Illustration of the selective removal of impurities (acrolein) by a supported scavenger	
from API.....	32
Figure 25 - Sequence of analysis in UHPSFC-MS.	38
Figure 26 – GC-MS Total ion chromatogram (TIC) of 1 mg/mL of elemental sulfur in toluene. The	
large poorly resolved peak is due to elemental sulfur.....	42
Figure 27 –TIC GC-MS Chromatograms of new mineral insulating oil A and elemental sulfur,	
showing how the mineral oil peaks can obscure elemental sulfur.....	42

Figure 28 - Derivatisation reaction of elemental sulfur with TPP. ¹¹³	43
Figure 29 - GC-MS chromatogram of new mineral insulating oil A + 1.5 mg/mL of TPPS. The ion fragments correspond to $m/z = 183.19$ $[\text{C}_{12}\text{H}_8\text{P}]^{+\bullet}$, $m/z = 262.36$ $[(\text{C}_6\text{H}_5)_3\text{P}]^{+\bullet}$, and $m/z = 294.35$ $[(\text{C}_6\text{H}_5)_3\text{PS}]^{+\bullet}$. The peak with $t_R \sim 13.36$ min corresponds to 2,6-di-tert-butyl-p-cresol (BHT) and multitude of peaks with $t_R \sim 10 - 17$ min correspond to the hydrocarbon matrix (10 to 34 carbons).	43
Figure 30 – Proposed mechanism of the reaction of tertiary phosphines with elemental sulfur. ¹¹³	44
Figure 31 – Reciprocal of A vs. time of the derivatisation reaction and the associated residual plot.	47
Figure 32 - Calibration results obtained from the analysis of TPP standards (0.015, 0.023, 0.031, 0.038, 0.046 and 0.053 mmol) and a TPPS standard (0.027 mmol) using the ³¹ P NMR.	49
Figure 33 - ³¹ P NMR kinetic study of the derivatisation reaction at RT in 50% mineral oil and 50% toluene and the associated fractional conversion vs. time plot. (<i>Fractional conversion = (nTPP) reacted (nTPP) fed</i>).....	50
Figure 34 - ³¹ P NMR from kinetic study at RT in 50% mineral oil and 50% toluene after nine days.	50
Figure 35 - ³¹ P NMR kinetic study of the derivatisation reaction at RT in toluene and the associated fractional conversion vs. time plot. (<i>Fractional conversion = (nTPP) reacted (nTPP) fed</i>).....	52
Figure 36 - Reciprocal of PA vs. time of the derivatisation reaction.....	53
Figure 37 - ³¹ P NMR kinetic study of the derivatisation reaction between S_8 and TPP at RT in toluene with double the concentration of $[\text{S}_8]$ relative to TPP to study the order of the reaction and the associated fractional conversion vs. time plot. (<i>Fractional conversion = (nTPP) reacted (nTPP) fed</i>).....	54
Figure 38 - ³¹ P NMR kinetic study of the derivatisation reaction between S_8 and TPP at RT in toluene with double $[\text{TPP}]$ to study the order of the reaction and the associated fractional conversion vs. time plot. (<i>Fractional conversion = (nTPP) reacted (nTPP) fed</i>).....	55

Figure 39 – First derivatisation efficiency study using the optimised conditions.	56
Figure 40 – Derivatisation reaction (1 equiv. S_8 : 1.1 equiv. TPP) followed by ^{31}P NMR.	57
Figure 41 – GC-MS of the reaction of TPP with DBDS.	59
Figure 42 - GC-MS of the reaction of TPP with benzothiophene.	59
Figure 43 - GC-MS of the reaction of TPP with 4,6-Dimethyldibenzothiophene.	59
Figure 44 - TIC of DCM (#1,2) and toluene (#3,4) after reaction with TPP by UHPSFC-MS.	61
Figure 45 - SIR (m/z : 295) of DCM (#1,2) and toluene (#3,4) after reaction with TPP by UHPSFC-MS.	61
Figure 46 – Tertiary phosphines studied - trioctylphosphine (A), tri- <i>tert</i> -butylphosphine (B) and the ethyl diphenylphosphinite (C).	62
Figure 47 – ^{31}P NMR of the derivatisation reaction using the trioctylphosphine (A).	63
Figure 48 - ^{31}P NMR of the derivatisation reaction using tri- <i>tert</i> -butylphosphine (B).	64
Figure 49 - Standard concentrations of TPPS (20, 4 and 2 ppm) in new mineral insulating oil analysed by GC-MS with a non-polar column.	65
Figure 50 - SIR of the analysis of the mineral oil A using a non-polar column GC-MS.	66
Figure 51 - TICC and SIR analyses of a 20 ppm standard solution of TPPS in new mineral insulating oil using a polar-column GC-MS.	67
Figure 52 – ESI UHPSFC-MS SIM of TPPS at 1 ppm (S/N 161).	68
Figure 53 - UHPSFC-MS (SIR) of samples with 5 ppm of TPPS in different mixtures of mineral oil/toluene.	69
Figure 54 - Calibration curve obtained from TPPS standards (5 ppm, 2.5 ppm, 1 ppm, .0.5 ppm, 0.25 ppm, 0.1 ppm and 0.05 ppm) analysed using the UHPSFC-MS SIR method.	70
Figure 55 – ULOQ and LLOQ of the TPPS in mineral oil using the UHPSFC-MS SIR method.	71
Figure 56 – Integrated chromatograms for the TPPS found in new mineral insulating oil A by UHPSFC-MS using the SIR method.	72
Figure 57 – UHPSFC-MS SIR chromatogram from a real mineral oil sample doped with S_8	73

Figure 58 - UHPSFC-MS SIR chromatogram from the ex-service mineral oil sample B.....	73
Figure 59 - Corrosion test result of the ex-service mineral oil sample B subjected to the standard corrosion test (DIN 51353). The presence of the black colouration (silver sulfide) indicates that the oil is corrosive.....	74
Figure 60 – Reproducibility of analyses: Three different analyses of ex-service oil sample C showing similar TPPS peak areas ($t_R \sim 1.60$ min), indicating reproducibility of the method when applied to ex-service oil samples.	75
Figure 61 – Reproducibility of analyses: Three different analyses of ex-service oil sample D showing similar TPPS peak areas ($t_R \sim 1.60$ min), indicating reproducibility of the method when applied to ex-service oil samples.	75
Figure 62 – Silver strip (showing both sides) used as reference for the standard DIN 51353 corrosion tests.	77
Figure 63 - Corrosion test result of the oil sample spiked with 1 ppm of S_8 subjected to the standard corrosion test (DIN 51353). The silver strip (showing both sides) presents black colouration (silver sulfide), which indicates that the oil is corrosive.	77
Figure 64 - Corrosion test result of the oil sample spiked with 2 ppm of S_8 subjected to the standard corrosion test (DIN 51353). The silver strip (showing both sides) presents black colouration (silver sulfide), which indicates that the oil is corrosive.	78
Figure 65 - Corrosion test result of the oil sample spiked with 5 ppm of S_8 subjected to the standard corrosion test (DIN 51353). The silver strip (showing both sides) presents black colouration (silver sulfide), which indicates that the oil is corrosive.	78
Figure 66 - Corrosion test result of the oil sample spiked with 10 ppm of S_8 subjected to the standard corrosion test (DIN 51353). The silver strip (showing both sides) presents black colouration (silver sulfide), which indicates that the oil is corrosive.	78
Figure 67 - Compiled results from the oil samples spiked with 1, 2, 5 and 10 ppm of S_8 subjected to the standard corrosion test (DIN 51353).....	79
Figure 68 - Chromatogram of the oil sample spiked with 1 ppm of S_8	79

Figure 69 - Chromatogram of the oil sample spiked with 2 ppm of S ₈	79
Figure 70 - Chromatogram of the oil sample spiked with 5 ppm of S ₈	80
Figure 71 - Chromatogram of the oil sample spiked with 10 ppm of S ₈	80
Figure 72 – Representation of the molecular structure of montmorillonite clay. ¹²⁵ Reprinted from reference [125] with permission of Springer.	84
Figure 73 – GCs of a solution of DBDS and benzothiophene in <i>n</i> -hexadecane before filtration (left) and after filtration (right) using the montmorillonite clay.....	84
Figure 74 – Triphenylphosphine and benzyldiphenylphosphine polystyrene-bound (polymer A and C).	85
Figure 75 – Synthesis of polystyrene-bound 4-methylbenzyoxyphenyldiphenylphosphine (Polymer D).	86
Figure 76 – Synthesis of poly(lauryl methacrylate)-bound triphenylphosphine (polymer B).	87
Figure 77 –Literature, ¹³⁰ and our adapted approach to end-functionalised polymers.....	90
Figure 78 – Synthesis of the functionalised TEMPO initiator (NMP agent).	91
Figure 79 – Four different trisubstituted phosphine-loaded polymers used in the laboratory reclamation studies.	92
Figure 80 - Triphenylphosphine polymer-bound (100-200 mesh, extent of labelling: ~1.6 mmol/g loading, crosslinked with 2% Divinylbenzene (DVB), CAS N° 39319-11-4).	93
Figure 81 – Chemical transformation that occurs to the triphenylphosphine polymer-bound during the reclamation process.....	93
Figure 82 – GC-MS result for TPPS content of a reclamation process where the triphenylphosphine polymer-bound was added at two different stages.....	94
Figure 83 – Design of the lab scale reclamation rig.....	95
Figure 84 – How the reclamation rig can be adapted to the field.	95
Figure 85 – First working lab scale reclamation rig.....	96
Figure 86 - SFC-MS chromatogram showing the change in concentration of S ₈ in the second experiment.	100

Figure 87 - Column that was utilised in the optimised lab. reclamation rig.....	105
Figure 88 - Solvent effect on the swelling of the polystyrene-triphenylphosphine polymer....	105
Figure 89 - Optimised laboratory reclamation rig set-up used for the selective removal of elemental sulfur from mineral oil.....	106
Figure 90 – The different trisubstituted phosphine-loaded polymers that were studied in their ability to selectively remove S ₈ from mineral oil.....	107
Figure 91 - Strategy to study the effectiveness of our reclamation process in reducing silver corrosion.....	108
Figure 92 - Result of the silver corrosion test obtained from the oil sample B after being subjected to our reclamation process with polymer A. * Yellow colouration is due to the thermal stress.	111
Figure 93 – Results of the corrosion tests of the oil sample B after 32 and 44 h of reclamation with Polymer B.....	113
Figure 94 – Change in colour of the polymer B due to reclamation process of the oil sample B.....	114
Figure 95 - Result of the silver corrosion test obtained from the oil sample B after being subjected to our reclamation process with polymer C.	115
Figure 96 - Result of the silver corrosion test obtained from the oil sample B after being subjected to our reclamation process with polymer D.....	117
Figure 97 – ³¹ P NMR (Gel Phase) of the Polymer A after being used in all the reclamation experiments to remove S ₈ from mineral oil.	119
Figure 98 - ³¹ P NMR (Gel Phase) of the Polymer A after being chemically recycled.	120
Figure 99 - Synthesis of the phosphine-bound poly(lauryl-methacrylate) resin (B).	130
Figure 100 - Reduction of the of the poly(lauryl-methacrylate) resin-bound phosphine (B)....	132
Figure 101 - Synthesis of the phosphine-bound polystyrene resin (D).	133
Figure 102 - Synthesis of the poly(lauryl-methacrylate) resin-bound phosphine (E).....	139

Table of equations

Equation 1 – The Arrhenius equation.....	45
Equation 2 – Second-order rate equation.	46
Equation 3 - Integrated second-order rate equation.	46
Equation 4 – Second-order rate constant equation (UV-Vis).....	46
Equation 5 – Second-order rate constant (NMR).	52

Research Thesis: Declaration of Authorship

I, Sérgio Barata Garcia, declare that this thesis entitled “Prevention of silver corrosion issues in oil-filled power transformers - Selective approaches for elemental sulfur quantification and its removal from mineral insulating oil” and the work presented in it are my own and has been generated by me as the result of my own original research.

I confirm that:

1. This work was done wholly or mainly while in candidature for a research degree at this University;
2. Where any part of this thesis has previously been submitted for a degree or any other qualification at this University or any other institution, this has been clearly stated;
3. Where I have consulted the published work of others, this is always clearly attributed;
4. Where I have quoted from the work of others, the source is always given. With the exception of such quotations, this thesis is entirely my own work;
5. I have acknowledged all main sources of help;
6. Where the thesis is based on work done by myself jointly with others, I have made clear exactly what was done by others and what I have contributed myself;
7. Parts of this work have been published as peer reviewed journal papers (●), conference contributions (-) or conference presentations (*):

(●) S. B. Garcia, J. Herniman, P. Birkin, J. Pilgrim, P. Lewin, G. Wilson, G. J. Langley and R. C. D. Brown, “Quantitative UHPUHPSFC-MS analysis of elemental sulfur in mineral oil via derivatization with triphenylphosphine: Application to corrosive sulfur-related power transformer failure”, *Analyst*, 2020, **145**, 4782-4786, DOI:10.1039/D0AN00602E.

(●) S. B. Garcia, J. Herniman, P. Birkin, Neil J. Wells, J. Pilgrim, P. Lewin, G. Wilson, G. J. Langley and R. C. D. Brown, “Removal of elemental sulfur in mineral oil via a system based on trisubstituted phosphine-loaded polymers: Application to corrosive sulfur-related power transformer failure”, 2021, *In preparation*.

(●) M. S. A. Khiar, S. B. Garcia, P. Lewin, R. C. D. Brown, J. Pilgrim, G. J. Langley and G. Wilson, "On-Line Quantification of Corrosive Sulfur Content in Large Autotransformers," *IEEE Trans. Dielectr. Electric. Insul.*, **27**, 6, 1787-1794, 2020, DOI: 10.1109/TDEI.2020.008548.

(-*) S. B. Garcia, P. Birkin, J. Pilgrim, P. Lewin, G. Wilson, G. J. Langley and R. C. D. Brown, "Rapid analytical method for elemental sulfur detection in power transformer insulation," 2019 *IEEE*

Electrical Insulation Conference (EIC), Calgary, AB, Canada, 2019, 376-379, DOI: 10.1109/EIC43217.2019.9046559.

(-*) S. B. Garcia, P. Birkin, J. Pilgrim, P. Lewin, G. Wilson, G. J. Langley and R. C. D. Brown, "Identification of elemental sulfur in mineral insulating oil - Standard corrosive test (DIN 51353) vs. Analytical approach," *2020 IEEE International Conference on Dielectrics (ICD)*, Valencia, Spain, 2020. DOI: 10.1109/ICD46958.2020.9341889.

(*) S. B. Garcia, P. Birkin, J. Pilgrim, P. Lewin, G. Wilson, G. J. Langley and R. C. D. Brown, "Determination and quantification of elemental sulfur in insulating mineral oil used in power transformers" was presented at the *Euro TechCon 2018*, The Principal St David's Hotel, Cardiff, Wales, 4th – 6th of December 2018.

(*) S. B. Garcia, P. Birkin, J. Pilgrim, P. Lewin, G. Wilson, G. J. Langley and R. C. D. Brown, "TOPICS II - Removal of elemental sulfur and silver corrosion" was presented at the *UK CIGRE A2/D1 Liaison meeting*, Manchester, England, 9th December 2019.

Signature:Date:.....

Acknowledgements

First of all, I would like to express my sincere gratitude to National Grid plc for the financial support.

I would like to thank the whole team involved in this research project. Starting with my supervisor Professor Richard C. D. Brown, for his vital support and guidance throughout my studies. My co-supervisors, Prof G. John Langley and Dr Peter Birkin, for providing thoughtful comments and recommendations. To Dr Gordon Wilson for his invaluable insight and feedback. To the Tony Davies High Voltage Laboratory members, specially to Professor Paul L. Lewin and Dr James A. Pilgrim, for their availability and for introducing me to the engineering world.

I am really grateful to the Brown research group, past and present, whom have made my time in the laboratory so much more enjoyable, mainly in the less good times. With special thanks to Domenico Romano (for enduring with my poor Italian accent), Ana Folgueiras (for our good and deep conversations) and George Chambers (for bearing with me all these years... especially with my super clever questions about organic chemistry) with whom I have made lasting friendships with.

I would like to give a special thank you to my parents, Paulo Jorge Serrão Garcia and Gracinda Maria Carvalho Pereira Barata, to my brother Simão Barata Garcia and to Mafalda Incenso Pereira Catarro for their constant support, encouragement and understanding.

Definitions and Abbreviations

^1H NMR	Proton Nuclear Magnetic Resonance
$^{13}\text{C}\{^1\text{H}\}$ NMR	Carbon-13 Nuclear Magnetic Resonance
$^{31}\text{P}\{^1\text{H}\}$ NMR	Phosphorus-31 Nuclear Magnetic Resonance
A	Selectivity Factor
Ac	Acetate
APCI	Atmospheric Pressure Chemical Ionization
API	Atmospheric Pressure Ionization
BDS	Biodesulfurisation
CAD	Charged Aerosol Detection
CCC	Countercurrent Chromatography
CDCl_3	Deuterated chloroform
CI	Chemical Ionization
CLND	Chemiluminescence Nitrogen Detector
c_m	Molar Concentration in the Mobile Phase
cm	Centimetre(s)
cm^{-1}	Wavenumber(s)
C_s	Molar Concentration to the Analyte
DBDS	Dibenzyl disulfide
DBT	Dibenzothiophene
DCM	Dichloromethane
DESI	Desorption Electrospray Ionisation
DMF	Dimethyl Formamide

DMSO	Dimethyl Sulfoxide
DNOs	Distribution Network Operators
e⁻	Electron
EC-NCI	Electron Capture - Negative Chemical Ionisation
EDS	Energy-Dispersive X-ray Spectrometry
EI	Electron Ionisation
ELDS	Evaporative Light Scattering Detector
equiv.	Equivalent(s)
ESI	Electrospray Ionisation
ESI-MS	Electrospray Ionisation – Mass Spectrometry
Et	Ethyl
eV	Electron Volts
FAB	Fast Atom Bombardment
FCC	Fluid Catalytic Cracking
FID	Flame Ionisation Detector
FT-ICR	Fourier-transform - Ion Cyclotron Resonance
FT-IR	Fourier-transform - Infrared Spectrometry
g	Gram(s)
GC	Gas Chromatography
GC-MS	Gas Chromatography - Mass Spectrometry
h	Hour(s)
H	Height Equivalent to one Theoretical Plate
HDS	Hydrodesulfurisation
HPLC	High Performance Liquid Chromatography

HRMS	High Resolution Mass Spectrometry
HV	High Voltage
ICR	Ion-Cyclotron Resonance
ILs	Ionic Liquids
ISM	Isocratic Solvent Manager
K	Distribution Coefficient
K	Kelvin
K'	Capacity Factor
kV	Kilovolt(s)
LC	Liquid Chromatography
LC-MS	Liquid Chromatography - Mass Spectrometry
LLOQ	Lower Limit of Quantification
LOD	Limit of Detection
LRMS	Low Resolution Mass Spectrometry
M	Gas Phase
MALDI	Matrix-Assisted Laser Desorption/Ionization
Me	Methyl
MHz	Megahertz(s)
mol	Mole
Mo/ γ-Al₂O₃-H₂O₂	Molybdenum/Aluminium Oxide Mesoporous Catalyst
MP	Melting Point
mPa.s	Millipascal per second
MS	Mass Spectrometry
m/z	Mass/Charge ratio

N	Plate Number
NMP	<i>N</i> -methyl-2-pyrrolidone
NMR	Nuclear Magnetic Resonance
OATS	Olefinic Alkylation of Thiophenic Sulfur
ODS	Oxidative Desulfurisation
ppb	Parts per Billion
ppm	Parts per Million
QIT	Quadrupole Ion Trap
RF	Radio Frequency
RI	Refractive Index
Rs	Resolution
RT	Room Temperature
UHPSFC	Ultra-High Pressure Supercritical Fluid Chromatography
UHPSFC-MS	Ultra-High Pressure Supercritical Fluid Chromatography – Mass Spectrometry
SO_x	Sulfur Oxides
SIR	Selected Ion Recording
TBAS	Tetrabutylammonium sulphite
TCD	Thermal Conductivity Detector
TDHVL	Tony Davies High Voltage Laboratory
THF	Tetrahydrofuran
TIC	Total Ion Chromatogram
TLC	Thin Layer Chromatography
TPP	Triphenylphosphine
TPPS	Triphenylphosphine sulfide

TOF	Time of Flight
TOPICS	Transformer Oil Passivation and Impact of Corrosive Sulfur
ULOQ	Upper Limit of Quantification
UPC²-TQD	Ultra Performance Convergence Chromatography system – Triple Quadrupole Detector
UV	Ultra-Violet
V	Volt(s)
W_b	Peak Widths
W_{1/2}	Peak Widths at Half-Height
°C	Degree(s) Celsius

TOPICS II Research Project Aims and Objectives

In recent years, the University of Southampton and the National Grid plc (UK) have undertaken a programme of collaborative research called TOPICS (Transformer Oil Passivation and Impact of Corrosive Sulfur). TOPICS II was a three-year research project funded by National Grid plc (UK), that aimed to not only understand and identify the means by which silver corrosion occurs, but also to develop/improve the processes through which the existing oil within a transformer can be regenerated with respect to reducing silver corrosion. This was a multidisciplinary research project mainly based in the School of Chemistry and in the Tony Davies High Voltage Laboratory (TDHVL). The research team consisted of postgraduate researchers and research fellows, from Chemistry and from the TDHVL. The academic staff involved with the project are Prof R. C. D. Brown, Prof G. J. Langley, Dr P. R. Birkin, Prof P. L. Lewin, Dr J. Pilgrim and Dr G. Wilson from National Grid.

This research project is divided in four work packages (WP):

- WP 1 - Understanding ethylene production (Chemistry);
- WP 2 - Effect of the reclamation on the insulating paper (TDHVL);
- WP 3 - Removal of elemental sulfur and silver corrosion (Chemistry);
- WP 4 - Methods for corrosive sulfur detection (TDHVL).

The work presented in this thesis covers the WP 3, the key aims/objectives are shown below, in **Table 1**.

Table 1 - Summary of the key aims/objectives for WP 3 of the TOPICS II project.

Project aims and objectives
Understand the current knowledge of methods to remove sulfur from oils and fuels.
Report on novel methods for sulfur detection in transformer oil.
Design and commission laboratory reclamation rig for mineral oil.
Report covering effectiveness of laboratory reclamation strategies with respect to reducing silver corrosion.

The objective of this research project was to increase the understanding of power transformer failures related to the presence of elemental sulfur in the mineral insulating oil (i.e., silver corrosion) and develop methods to mitigate/prevent such failures. The intended approach consisted in the development of techniques that would allow the identification, quantification and selective removal of elemental sulfur from mineral insulating oil. The effectiveness of the developed methods was studied/demonstrated by the selective removal of elemental sulfur (using supported reagents) from new and ex-service mineral oil samples, the obtained results were verified using the in-house developed analytical methods and by the standard corrosive test (DIN 51353). The conducted experiments and respective findings are fully detailed, in this thesis.

Chapter 1 Introduction

1.1 Electric grid system in the United Kingdom

It was 1831 when Michael Faraday, the “Father of Electricity”, was able to induce the generation of an electric current.¹ These fundamental experiments lead not only to the development of Faraday’s law of induction, but also provided the stepping stones for the production of electrical power by mechanical means. Nowadays, electricity can be generated in numerous ways and from several sources, but, unlike other forms of energy, it cannot be stored. On the otherhand, electricity can be converted and stored in other forms of energy which can be later reconverted to electricity. This is valuable when there is a fluctuation in electricity supply, and there is more generation than demand. Electricity can be stored using a variety of technologies, which include mechanical storage (e.g., pumped hydro storage), electrochemical energy storage (e.g., batteries), chemical energy storage (e.g., hydrogen), high temperature energy storage (e.g., thermal energy) and electromagnetic storage (e.g, capacitors). Despite the sophistication of such technologies, some major disadvantages are still present; e.g., the scale of power/energy storage capacity available is still too low, unable to meet demand over prolonged periods, and are not yet cost efficient. Which means that electricity, nowadays, is still mainly generated as it is needed.² Since such generation is often carried far away from the place where is going to be used, an efficient and reliable distribution

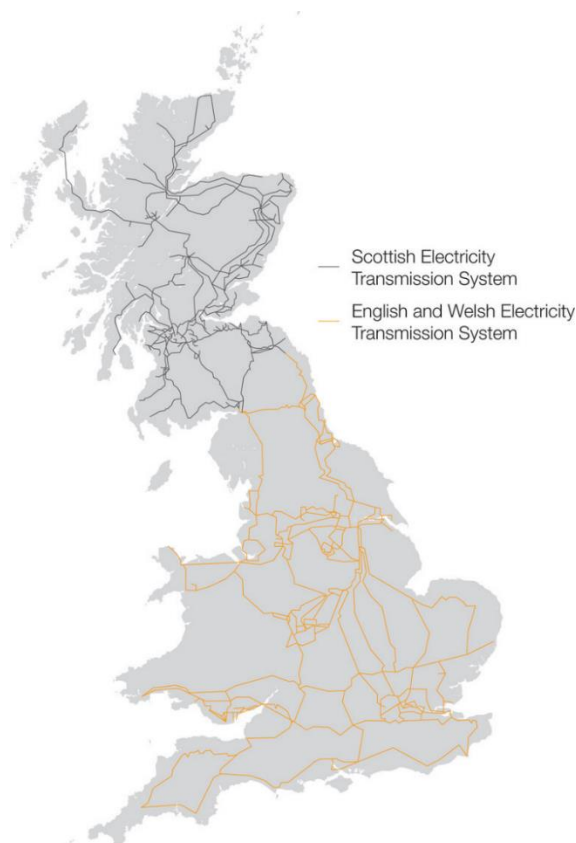


Figure 1 – Map of the electric transmission grid in the United Kingdom operated by National Grid UK.³

and transmission system of electricity had to be developed. The foundation of the electric grid system in Great Britain, generally referred to as “National Grid”, goes back to the 1930s - making it the first power grid system in the world. Today, the National Grid UK, takes care of 4474 miles of overhead line, 969 miles of underground cable, 326 substations at around 240 sites with a reliability of 99.99984% during 2017/2018.³ The location of their electricity transmission network can be seen above, in Fig. 1. Britain’s current electrical system can be divided in three main subsets: generation, transmission and distribution. The schematic representation of this infrastructure can be found in Fig. 2.

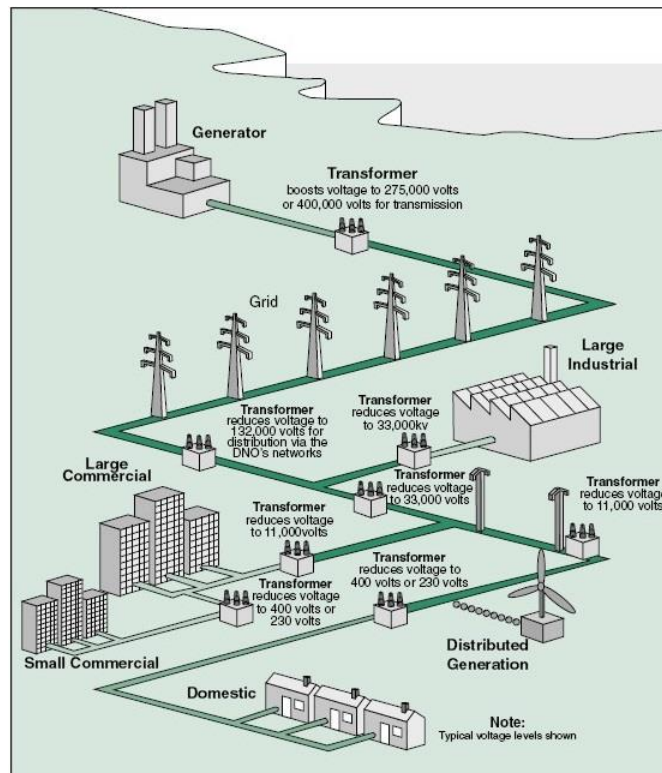


Figure 2 – Graphical illustration of the electrical system network in the UK.⁴

The electricity generation in the UK is based on many different sources, it goes from using the “old” fossil fuels to the use of the “new” renewable resources. Despite the fact that most of the electricity is still produced in thermal and nuclear power stations, a substantial increase in the use of renewable sources is expected in coming years.⁵ Once the electricity is generated in the power stations, its voltage is then increased by substation transformers, and then fed into the high voltage transmission network. Such a system allows the efficient transmission of the electricity over long distances. Currently, National Grid UK has the responsibility for controlling whole the transmission grid of the United Kingdom. When the electricity reaches the sources of demand, its voltage is reduced accordingly and distributed by the local electricity companies. At the moment, there are several licensed distribution network operators (DNOs), and each one is responsible for a different regional area. The up-to-date electricity transmission map and the electricity distribution map for Great Britain, are shown in Fig. 3 and Fig. 4, respectively.

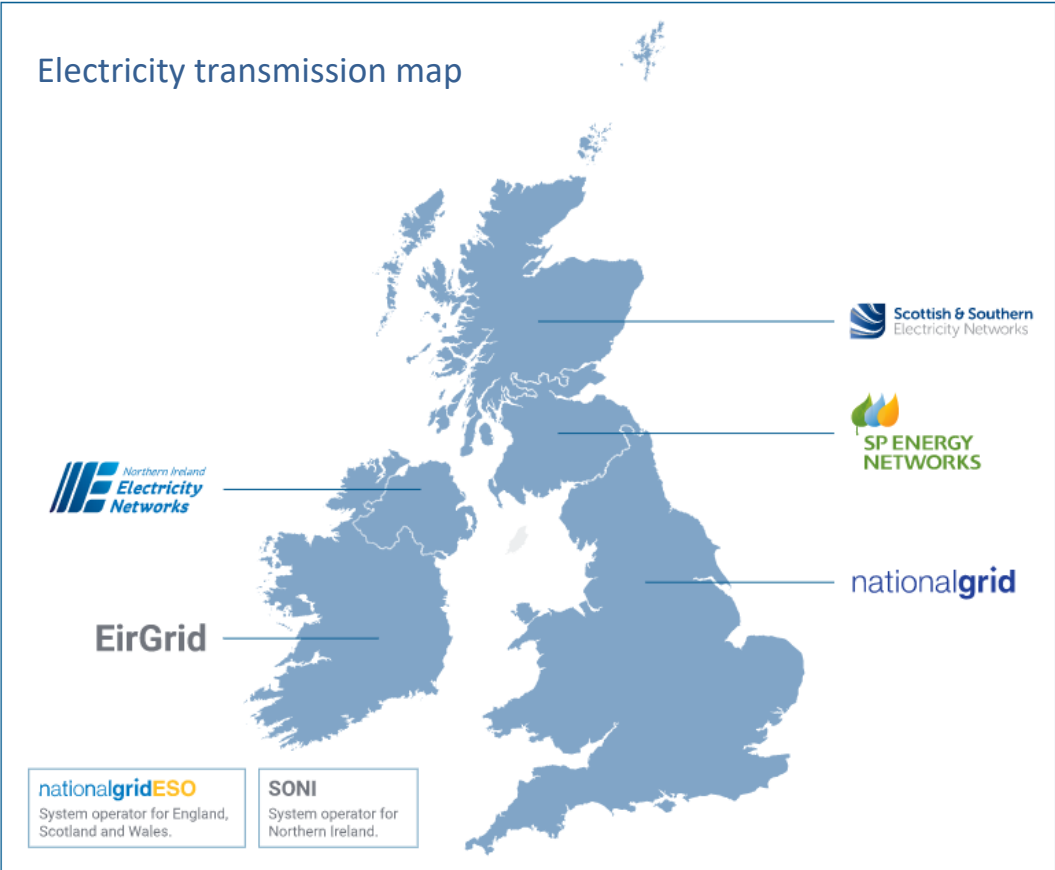


Figure 3 - Electricity transmission map for Great Britain and Ireland and respective electricity transmission operators.⁶

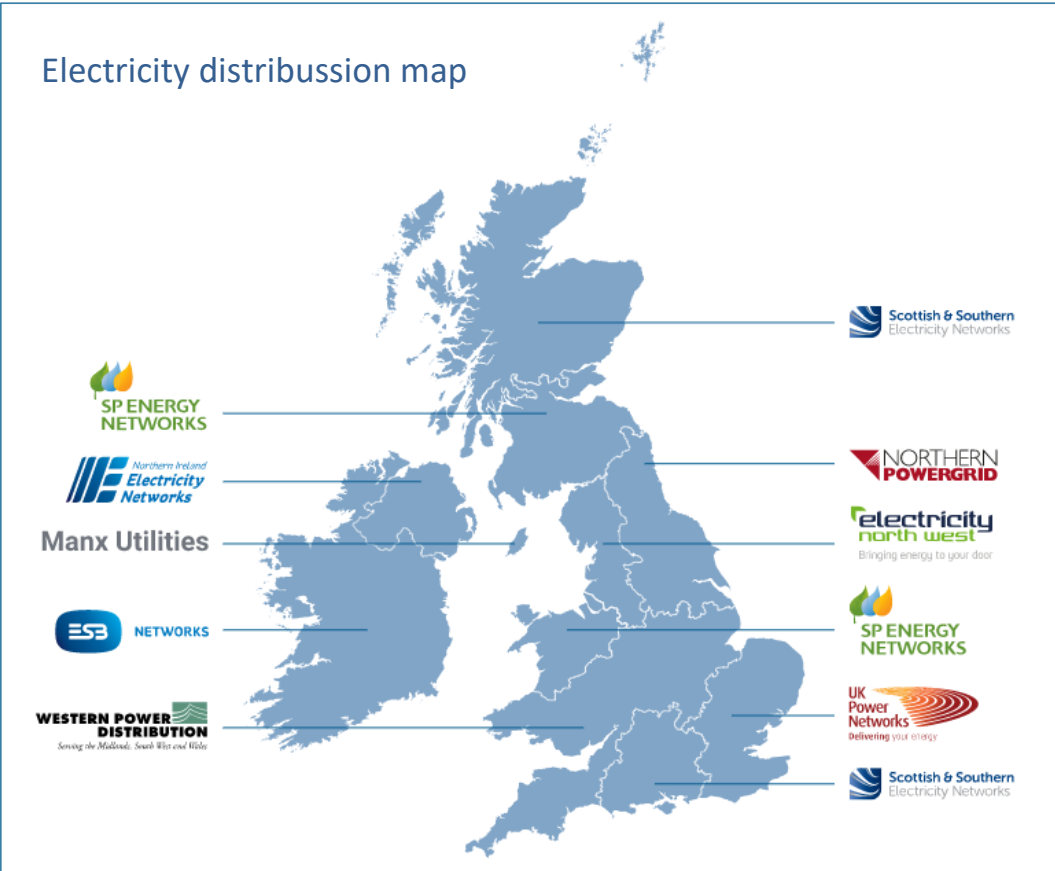


Figure 4 – Electricity distribution map for Great Britain and Ireland and respective electricity transmission operators.⁶

1.2 Transformers

An effective grid transmission is crucial when we think about the reliability, flexibility, and economic viability of the electrical system network.⁷ Maintaining an effective transmission is not an easy task, considering the countless complex interconnections present in the electricity grid. One of the key components which play a major role in the transmission effectiveness, is the power transformer (alternating current - AC), since its purpose is to modify the electrical current and voltage with minimal loss of energy during the electrical transmission.⁸ During the transmission several different voltages are used, to cope with this, many different transformers designs were developed and are nowadays available in the market. These “assets” are generally expensive, with High voltage (HV) super grid transformers costing millions of pounds. Therefore, the reliability and economic viability of power distribution are highly dependent on the availability, performance, and longevity of the power transformers.⁹

Having in mind the scope of the work described herein, and despite the clear engineering sophistication of the transformers, only a basic and brief description of how they work and how they are usually designed is presented. The power transformers are electrical devices that utilise Faraday’s Law of Induction to work. This means that they are able to convert electrical energy from one value to another, i.e., they are able to transfer electricity (by means of a magnetic field) from one electric circuit to another. During this energy transfer, change of voltage and current (AC) is possible but not the change in frequency nor the generation of electrical power. The basis for the energy transfer lies in the mutual induction (by a common magnetic flux) of the two electrical circuits, the schematic of a single-phase transformer is shown in Fig. 5.

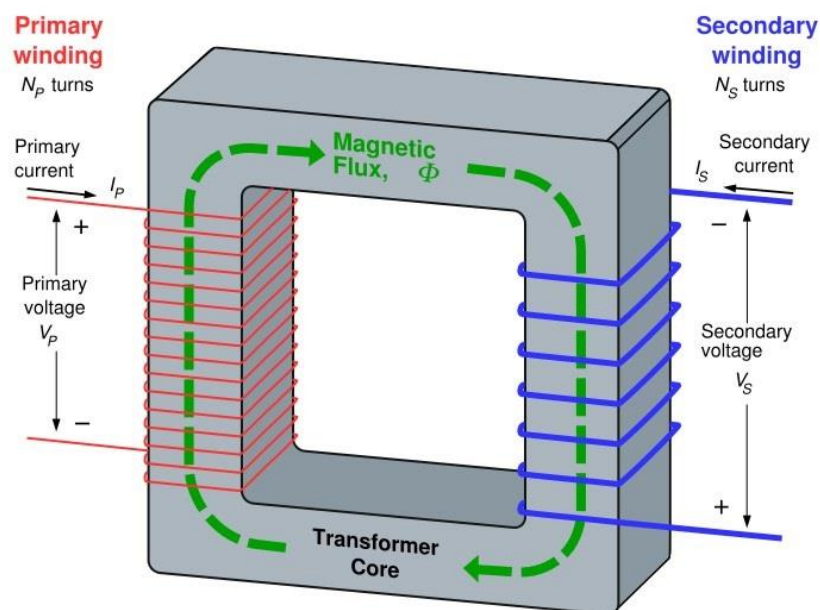


Figure 5 - Schematic of a single-phase transformer showing electro-magnetic induction – Faraday’s Law of Induction.¹⁰

As demonstrated in Fig. 5, a basic single-phase transformer is constituted by four primary parts: The input connections, the output connections, the windings (coils), and the transformer core. When an AC current (input voltage) is applied on the primary winding, and the current begins to flow a magnetic field is generated in the core. This magnetic flux induces the secondary winding, and AC voltage is produced in the secondary winding. The output voltage is directly proportional to the ratio of the number of turns between the two windings. This ratio will define the transformer as one of two different types:

- Step-up Transformer – The secondary winding has more turns of wire than the primary winding, which leads to the output voltage to be greater than the input voltage.
- Step-down Transformer – The primary winding has more turns of wire than the secondary winding, which leads to the input voltage being greater than the output voltage.

There are a number of other transformer types (e.g., Isolation, Instrument, Auto, etc.), that will possess a number of other components, characteristics, and configurations. As the focus of the project was to reduce the silver corrosion in power transformers, the main components of interest are the insulating materials, which will be discussed further below.

1.2.1 Insulating materials

To maintain efficient operation, transformers are equipped with an insulation system. This system, usually a combination of solid – fluid – gas components, provides the electrical insulation necessary to ensure an optimal working condition of the transformer. There are plenty of different insulating materials, the most common ones are summarised in Table 2.

Table 2 – Common types of insulating materials in transformers.

Types of Insulation	
Fluid/Liquid	Mineral oils (e.g., paraffinic, naphthenic, etc.) Synthetic oils (e.g., ester, polyglycols, etc.) Vegetable oils (e.g., soybean, etc.)
Gas	Hydrogen Air Fluorogases (e.g., SF ₆ , etc.)
Solid	Paper (e.g., Kraft, etc.)

In addition to providing insulation, they also provide structural support in the case of the solid materials and as a heat transfer agent in the case of the liquid materials. The use of an insulating liquid was first registered in 1892, when the company General Electric used a petroleum-based oil.¹¹

Since then, mineral insulating oil has been used world-wide, and up to the present day is still the most commonly used dielectric liquid by the industry. In recent years, mainly due to the environmental and safety risk associated with using mineral oil, several other types of liquid dielectrics have been tested. Silicon oils, owing to their superior thermal and chemical stability, have been found useful in situations where the risk of fire is of concern. Synthetic oils have been synthesised from vegetable oils, which provided good insulation properties with improved environmental credentials. Their higher cost of production, unfortunately, is still seen as a disadvantage. The transformer insulating samples provided by National Grid UK for this Project were mineral oil samples, so only the properties of this type of insulating oil will be further discussed here.

The transformer mineral oil is obtained from the distillation of crude petroleum. The chemical, electrical and physical properties of the oil obtained are not only associated with the boiling range of the collected fractions but are also unique and inherited from the crude oil.¹² Depending on the desired properties for the final product, the oil is then subjected to different refining processes. Usually, these processes are conducted in order to reduce the concentration of the contaminants (e.g., oxygen, nitrogen, sulfur, metals, etc.) and to tweak the ratio between the naphthenic and paraffinic components. To guarantee that the characteristics of the oil are suitable to be used as insulating oil in a power transformer, international standard specifications have been agreed upon. In this project, the mineral oil used complied with IEC 60296.¹³ The general specifications and relevant test methods of this standard are shown in Table 3. To meet specific requirements, additives such as oxidation inhibitors and pour point depressants are sometimes required. The oils are then classified accordingly, e.g., oils are referred to as inhibited when the addition of anti-oxidants was performed.^{13,14,15}

Several physical and molecular characteristics are important features when looking at insulating mineral oils. One of the main parameters is viscosity, which is one of the principal parameters relevant to heat transfer and the one that provides the ability to achieve an optimal working temperature for the transformer. Other important characteristics are flash point, pour point and high dielectric constant. Since they are outside the scope of this work they will be not discussed further.

The electrical grid, in particular the power transformers, are constantly subjected to numerous stresses that degrade the mechanical and dielectric properties of the insulating mineral oil, eventually compromising its function. This degradation will affect both the chemical and electrical properties of the oil. The chemical degradation mainly due to oxidation of the oil, will lead to an increase in its acidity and formation and precipitation of sludge.

Table 3 – General specifications for transformer mineral oil.¹³

Property	Test Method	Limits
Viscosity at 40°C	ISO 3104	Max. 12 mm ² /s
Viscosity at –30°C ^a	ISO 3104	Max. 1800 mm ² /s
Pour Point	ISO 3016	Max. –40 °C
Water content	IEC 60814	Max. 30 mg/kg ^b or 40 mg/kg ^c
Breakdown Voltage	IEC 60156	Min. 30 kV / 70 kV
Density at 20°C	ISO 3675 or ISO 12185	Max. 0.895 g/ml
DDF at 90°C	IEC 60247 or IEC 61620	Max. 0.005
Appearance	-----	Clear, free from sediment and suspended matter
Acidity	IEC 62021-1	Max. 0.01 mg KOH/g
Interfacial tension	ISO 6295	No general requirement
Total sulfur content	BS 2000 Part 373 or ISO 14596	No general requirement
Corrosive sulfur	DIN 51353	Not corrosive
Antioxidant additive	IEC 60666	(U) uninhibited oil: not detectable (T) trace inhibited oil: max. 0.08 % (I) inhibited oils: 0.08 – 0.40 %
2-Furfural content	IEC 61198	Max. 0.1 mg/kg
Oxidation stability ^d	IEC 61125 (method C)	-----
Total acidity	-----	Max. 1.2 mg KOH/g ^d
Sludge	-----	Max. 0.8 % ¹
Gassing	IEC 60628, A	No general requirement
Flash point	ISO 2719	Min. 135 °C
PCA content	BS 2000 Part 346	Max. 3 %
PCB content	IEC 61619	Not detectable

^a This is the standard LCSET for a transformer oil and can be modified depending on the climatic condition of each country. Pour point should be minimum 10 K below LCSET.; ^b For bulk supply.; ^c For delivery in drums and IBC.; ^d In some countries more stringent limits and/or additional requirements may be requested.

Usually, the degradation of the insulating oil is shown by the loss of dielectric resistance, a decrease of the breakdown voltage. The rate of oil degradation is also dependent on the initial properties of the oil. Since the condition of the oil is directly associated with the general condition of the transformer, regular monitoring of the oil quality and characteristics is of critical importance. Despite several different monitoring techniques being already available, major efforts have been taken to extend the lifetime of the insulating system. A number of regeneration processes/mitigation strategies, have been already applied with success to restore some of the properties of degraded/contaminated oil. Despite considerable effort, issues remain with the presence of S_8 , sometimes found following some oil regeneration procedures, where the same procedures utilised to remove other corrosive sulfur compounds (e.g., dibenzyl disulfide (DBDS)) were proven ineffective for elemental sulfur contamination.

1.3 Transformer failures linked to corrosive sulfur

The global problem of failures of transformers attributed to corrosive sulfur has been widely reported.¹⁴ The term corrosive sulfur is been used by the industry as a general denomination for all chemical sulfur species that are capable of corroding the metal parts of the transformer. The sulfur content of a transformer mineral oil can be from a number of different species with varying reactivities, such as thiophenes, polysulfides, mercaptans and S_8 among others. In the last decades, the risk of failure in electrical equipment owing to the presence of corrosive sulfur (usually associated with the presence of dibenzyl disulfide and/or S_8) in the mineral oil has increased. This risk has been understood for many decades but actual failures world-wide were very rare until around 2000. The International Council on Large Electric Systems (CIGRÉ) estimated the total number of failures due to corrosive sulfur to be in the region of 100 between 2000 and 2009.¹⁵ A number of these cases were associated with the presence of silver sulfide in silver-coated contacts, mainly in the tap-changers.¹⁶ Formation of surface metal sulfide will lead to overheating of the contacts followed by the detachment of conductive particles. These particles can cause breakdown and rated voltage stress.¹⁵ Transformer failures and/or repairs are expensive and should be avoided whenever possible. Outages, if not predicted in advance, can be expensive not only for generators, but also for networks. To avoid unexpected failures, diagnostic measures are necessary. Standard methods for corrosive sulfur detection in mineral oil have been published.^{13,17–20} These standards usually assess the corrosiveness of the oil towards a silver/copper strip, rather than performing chemical analysis. Since different corrosive sulfur compounds (e.g., DBDS) can be found in the mineral oil, it is important to highlight that these tests are not specific for S_8 . These tests are also time consuming and subjective due to a visual rating process. Hence, analytical methods that allow

rapid, reliable and reproducible quantification of S_8 in mineral transformer oil are needed. Techniques for the detection of S_8 in hydrocarbons are discussed below, see sub-chapter 1.5.

1.3.1 Mitigation strategies

The increase of power transformer failures related to corrosive sulfur in recent years led the industry to find different options to mitigate the risk. Many mitigation options were published in the literature,²¹⁻²⁷ which are mainly based on two different techniques, specifically, use of a metal passivator or the use of a process for regeneration of the oil. Although both techniques are employed to achieve the same end purpose, to make the oil suitable for use as insulating oil, they have distinct mitigation actions; therefore, each power transformer should be evaluated individually, so an appropriate strategy can be adopted/used.

The strategy for the first mitigation action, the use of a metal passivator, consists as the name suggests, in the addition of a metal passivator to the oil. These metal passivators are usually triazole derivatives added to the oil at a concentration of 100 mg/kg, meanwhile concentrations of less than 50 mg/kg are considered ineffective.²⁸ These compounds will adhere to bare copper surfaces, forming a coating layer that blocks/prevents the reactions of the copper with corrosive sulfur.²⁹ The second mitigation strategy, is based on chemical or physical (or both) treatment of the oil. The physical treatment, commonly denominated as oil reclamation/regeneration, usually uses an adsorption or extraction method (i.e., adsorbents or solvents) that will remove the corrosive sulfur compounds from the oil. On the other hand, chemical treatment, is typically employed in such a way that the reactive sulfur compounds are chemically converted into less reactive compounds or compounds that are more easily removed by the oil reclamation.^{30,31}

In the UK, the regeneration/reclamation process typically involves continuous filtration (using adsorption clays (e.g., Fuller's Earth, bauxite)) and consequent vacuum degassing of the mineral oil. These procedures are usually carried on-site in a so-called (mobile) reclamation rig, which not only provides the possibility to conduct such procedures in the field but also has significant economic advantage, since it is not necessary to turn off the transformer. The reclamation process is generally carried on a scale of thousands of litres of insulating mineral oil and the time frame is mainly linked to the initial condition of the oil, generally taking from a few days to a few weeks to be concluded.

Numerous examples are found in the literature where these different processes have been found successful in the removal of corrosive sulfur from oil. According to CIGRÉ, several of these examples were applied to on-site reclamation processes using reactivable clays. Even though the reclamation was effective in most of the cases, there were instance where the oil was found to be more corrosive after the reclamation.¹⁶ This corrosion was mainly towards silver, and silver corrosion is

mostly induced by the presence of S_8 in the oil. To tackle this issue the applicability of the metal passivator Irgamet® 39 to counteract silver corrosion was also tested. It was observed that Irgamet® 39 was not able to counteract corrosion in such oils in most of the cases, even when the passivator was added in high concentrations (up to 300 - 500 ppm).³² In order to improve understanding of this phenomenon, an extensive report by CIGRÉ was published in 2015.¹⁶ The report provided valuable contribution towards the understanding of how corrosive sulfur species present in mineral oil can lead to power transformer failures. These failures are mainly attributed to the formation of metallic sulfides (copper and silver) in the paper insulation and/or in active parts of the transformers. Progress in the comprehension of the mechanisms involved in the metallic sulfide formation on metal surfaces and paper was also described. The report also mentions important advances in the prevention/mitigation of such failures, which resulted in the establishment of several mitigation strategies and techniques. Despite the progress presented in the report, the ability to mitigate/remove the S_8 from mineral oil using existing reclamation set-ups remains limited.³³ Power transformer failures due to the presence of silver sulfide are usually linked to the presence of S_8 in the mineral oil, and low ppm concentrations of S_8 have been found to be corrosive towards silver.¹⁶ The silver sulfide is usually present in the on-load tap changer (OLTC), a key component that regulates the output voltage of a power transformer. The presence of silver sulfide can reduce the dielectric properties of the oil, which can enhance the possibility of local discharges and even breakdown of the oil.³⁴ In the next sub-chapter, a critical evaluation of desulfurisation methods to remove S_8 from mineral oil will be presented. In this thesis, the effectiveness of a laboratory reclamation strategy with respect to reducing silver corrosion will be also discussed.

1.4 Desulfurisation of hydrocarbons

Over recent years, environmental regulations have become increasingly rigorous with respect to the sulfur content of liquid oil fuels and the sulfur content became one of the most important parameters that reflect the quality of crude oil.³⁵ Consequently, the removal of sulfur from oil is one of the key processes in the oil refinery. There are many organic sulfur compounds present in crude oil, of which representative important classes are highlighted below in Figure 6, along with their relative reactivities.

The new requirements for low sulfur content demand effective approaches for desulfurisation, and challenges researchers to develop novel selective and cost-effective strategies. There are various reviews on desulfurisation, e.g., Javadli and Klerk;³⁶ Srivastava.³⁷ Most of the primary literature describing desulfurisation is focused on sulfur removal from light oils, such as gasoline, naphtha, diesel, etc. The following subchapter will provide a critical evaluation and highlight those methods that are feasible for desulfurisation of mineral oils.

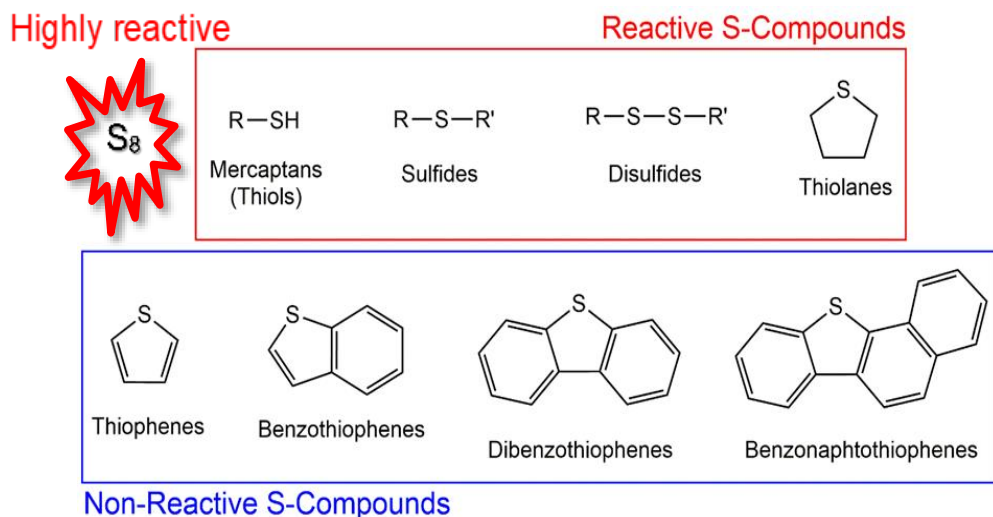


Figure 6 – Selected classes of sulfur compounds present in crude oil.³⁶

1.4.1 Critical evaluation

Most of the research in the field of desulfurisation is focused on oxidative desulfurisation (ODS), biodesulfurisation, and adsorption techniques. Despite this, the primary method for sulfur removal is still hydrodesulfurisation (HDS). In the context of the TOPICS II project, the different desulfurisation strategies reviewed are evaluated for applicability during the reclamation of mineral oil used in transformers.

Catalytic HDS of crude oil is carried out at high temperature ($> 300\text{ }^{\circ}\text{C}$) and pressure ($> 20\text{ atm}$), converting sulfur compounds to H_2S and hydrocarbons.^{38,39} HDS has been proven to be efficient for sulfur removal down to 500 ppm for gasoline and diesel, but it becomes inefficient for deep desulfurisation down to 10 ppm.⁴⁰ HDS can clearly be used to reduce the sulfur content of heavy oil by reduction of the more reactive sulfur-containing components. HDS either needs to be used together with other strategies if the less reactive sulfur species are to be removed, or different strategies need to be employed to achieve very low levels of sulfur. However, the more reactive sulfur compounds that are removed by HDS are also of the greatest concern in the context of corrosion of copper and silver surfaces. Furthermore, compounds resistant to HDS (e.g., benzothiophenes) may also serve protective functions (e.g., anti-oxidant properties) in mineral oil for application in transformers. When considering the appropriateness of HDS to be used during the reclamation of mineral oils in the field (e.g., mobile reclamation rig), it would clearly be challenging to implement the rather forcing conditions (i.e., high temperatures and pressure), and provide a cost-effective solution.

The use of desulfurisation methods based on adsorption has some advantages over the HDS process, i.e., the operation may be conducted at low temperature and does not require the use of H₂ gas or high pressure. There are two major challenges that the general adsorption approach faces when applied to desulfurisation of mineral oil. The first is to develop an easily recoverable adsorbent with a high adsorption capacity for sulfur compounds, as mineral oil loss and adsorbent recovery are important factors. The second challenge is to find adsorbents that selectively remove the corrosive sulfur compounds and discriminate from sulfur compounds that can have a protective function or other aromatic compounds that might be present. The adsorption capacity of many adsorbents has been low, and clay materials typically used in reclamation do not provide the selectivity desired for desulfurising mineral oil. Nonetheless, solid adsorbents such as bauxite are widely used in transformer reclamation.

The oxidative desulfurisation (ODS) process presents the same advantages as the adsorption methods over HDS, proceeding under conditions of low temperature and pressure.⁴¹ ODS involves two steps, and we must consider them separately. The oxidation step requires an oxidant that is totally consumed in the process and must confer selectively for the unwanted sulfur components. Some oxidants may cause undesirable side reactions that reduce the quantity and quality of the oil. The cost effectiveness of ODS is dependent on the cost and availability of the oxidant. However, for application during reclamation of mineral oil desulfurisation the mass of oxidant required should be relatively low and achievable on the required scale. The second step then requires the removal of the oxidised sulfur compounds using an adsorption technique, which is already in place in current reclamation processes.

The chlorinolysis-based strategies (Figure 7) have disadvantages such as the introduction of highly reactive species into the oil (e.g., Cl₂), or acidic by products produced in the chlorination (e.g., HCl). These species themselves are highly undesirable in insulating oil used in transformers. On the other hand, the alkylation of sulfur species leads to higher boiling and non-volatile components, which are separated by distillation of the oil. However, distillation is not practical as part of a typical transformer reclamation due to energy requirements and health and safety.

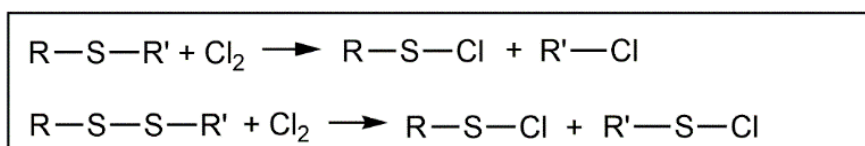


Figure 7 - Chlorinolysis process.

The biodesulfurisation (BDS) brings various potential benefits, but the application of this approach is really limited by the slow rate of the biodegradation process.⁴² The metabolism of sulfur

compounds is typically slow compared to the chemical reactions discussed. Despite considerable progress in BDS over the years, there are still some difficulties in the application of this method for desulfurisation of mineral oil. The biological systems must be kept alive to function under variable conditions in the transformer, and this is a problem since the rate of desulfurisation strongly depends on pH, temperature, and dissolved oxygen concentration. Separation of the cells from the oil can also be difficult, and immobilized cells have lower activity and limited lifetimes.

In conclusion, given all the pros and cons of the methods discussed in terms of their applicability for desulfurisation of mineral oil, adsorption methods and ODS have the greatest potential, as they only need an appropriate adsorbent/oxidant to be applied. Appropriate conditions in terms of optimum temperature, oxidants, solvent/oil ratio for extraction, and the impact of such solvents on the mineral oil quality will need a further assessment before the practical application is possible. Another approach, which may be readily integrated into the current reclamation process, is the introduction of a reactive absorbent capable of a selective chemical reaction with elemental sulfur.

1.4.2 Removal of elemental sulfur from mineral oil

During the process of oil refinement, the elemental sulfur present in the mineral oil is removed as hydrogen sulfide. The concentration of S_8 at the end of the process should be practically zero. Having this in mind, the reappearance of S_8 can happen during the usage of the oil. A number of different reasons have been proposed to explain such phenomena, most of them are linked to the improper storage/refining of the mineral oil, the most widely accepted are presented below:⁴³

- Overheating of oil during storage in buffer tanks;
- Catalytic cracking of oil entering hot columns;
- Incomplete combustion during reactivation of clay columns.

It is believed that elemental sulfur levels as low as 1 ppm may be sufficient to induce silver corrosion.⁴⁴ Elemental sulfur behaves as a chemical/molecular species, the dominant form of which at room temperature is an S_8 cycle, but under catalytic conditions or at elevated temperatures (as found in a standard Gas chromatography (GC) injector) an allotropic equilibrium (... $S_6 \leftrightarrow S_7 \leftrightarrow S_8$...) occurs.

Various reagents have been suggested for the removal of sulfur.⁴⁵ Some of the important reagents are listed in Table 4. Taking into consideration that most of the reagents are heavy metals, which are toxic, we decided to investigate the other ones. A desirable reagent needs to allow quantitative removal of elemental sulfur under mild conditions, and not participate in significant side reactions with common components of mineral oil. Therefore, we settled for triphenylphosphine (TPP). The

reaction of TPP with S₈ gives triphenylphosphine sulfide (TPPS), which is suitable for analysis by chromatographic techniques such as GC.

The use of TPP as a desulfurisation agent for mineral oil has great potential, as it is convenient to use (easy handling, rapid and selective reaction with S₈ and low cost). These properties offer the potential for application during the reclamation process used for transformer mineral oil. This potential will be demonstrated later on in the experimental chapter of this thesis.

Table 4 - Commonly used desulfurisation reagents and their reaction products.⁴⁵

Desulfurizing agent	Reaction product
Silver on silica gel (Ag/SiO ₂)	Ag ₂ S
Copper powder (Cu)	CuS
Mercury (Hg)	HgS
Copper amalgam (Cu/Hg)	CuS/HgS
Tetrabutylammonium sulphite (TBAS)	(TBA) ₂ S ₂ O ₃
Triphenylphosphine (TPP)	Ph ₃ P=S
Potassium hydroxide	S _x ²⁻
Superactive alumina (as column filling)	-----
Distilled water (ultrasonicating)	-----
Raney-nickel	NiS
Raney-copper	CuS
Silver nitrate on silica gel	Ag ₂ S

1.5 Detection of S₈ in hydrocarbons

Several analytical techniques have been applied to determine S₈ in hydrocarbons, but none specifically in mineral insulating oil. The use of gas chromatography (GC) and a number of variants (e.g., use of a selective detector for sulfur) can be found in the literature.^{46–50} Other methods include the use of polarography,^{51,52} liquid chromatography (LC),⁵³ and GC-Inductively Coupled Plasma-MS (GC-ICP-MS).^{54,55} One of the most common methods to detect sulfur in petroleum and in its derivatives, is the use of a sulfur chemiluminescence detector (SCD) coupled to a GC, a system. This commercially available instrumentation allows for specific detection and quantification of sulfur species at ppb levels, even in complex hydrocarbon matrixes.⁵⁶ Notable downsides are that it requires regular, costly, complex maintenance of the detector and the use of sulfur specific columns (e.g., Agilent J&W DB-Sulfur SCD GC column) and detector (SCD).⁵⁷ There are several other issues that can arise when applying these methods to quantify S₈ in transformer mineral oil. In mineral oil, at room temperature, elemental sulfur exists in an allotropic equilibrium (... S₆ ⇌ S₇ ⇌ S₈ ...) with S₈ being the predominant allotrope,⁵⁸ at elevated temperatures, as present in a standard GC injector, the equilibrium shifts to lower mass allotropes and this ensures that elemental sulfur does not elute from GC columns as a single and narrow chromatographic peak. Mineral oil also has miscibility issues with reversed phase HPLC solvents, while normal phase HPLC is more challenging to interface to MS. Even coupled with GC, ICP-MS systems would suffer from matrix interference due to the myriad hydrocarbons present in mineral oil.⁵⁹ UHPSFC can overcome the solubility issues related to the mineral oil, and when combined with a suitable derivatisation method and ESI-MS detection, may deliver simplified detection with minimal interference from the matrix. One derivatisation method, consists of a reaction of sulfur, independent of its allotropic composition, to give a single stable compound, namely triphenylphosphine sulfide (TPPS, Figure 8).⁶⁰

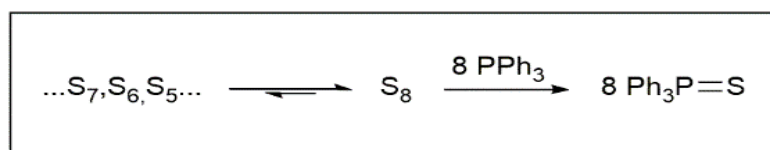


Figure 8 – Derivatization reaction.

The phosphine derivatisation method has been employed to determine elemental sulfur in different media.^{53,61,62} Another clear advantage of the derivatisation is an almost 9-fold increase in the mass concentration of the sulfur-containing species (1 µg mL⁻¹ of sulfur → 9.18 µg mL⁻¹ of TPPS).⁶⁰ In this thesis, two novel chromatographic-mass spectrometry methods *via* derivatisation with TPP that allow the detection of elemental sulfur in mineral oil down to ppb levels are described. The reported methods are capable of maintaining high sensitivity and accuracy when applied to

real mineral transformer samples. A brief introduction to chromatography, and to the different instruments/techniques employed during the project are discussed below.

1.5.1 Introduction to chromatography

The Russian-Italian botanist Twsett, often referred to as the father of chromatography, described the first chromatographic separation in 1906. This work reported the separation of plant pigments using column chromatography.⁶³ The term chromatography, nowadays is used to define several laboratory techniques that are used to separate mixtures. Separation is achieved through the use of two different phases: the stationary phase and the mobile phase.⁶⁴ Typically, the separation comprises the passage of a sample dissolved in a mobile phase through a stationary phase, which leads to resolution and isolation of the various components present in the sample. The separation of the analytes mostly depends on their relative affinity for each phase; affinity is related to the retention time of the components. The mobile phase (e.g., gas, liquid, or supercritical fluid), is defined as a phase that moves the materials over the stationary phase, separating compounds to different extents depending upon relative affinities for the phases. In some cases, modifiers and buffers are added to the mobile phase; this addition changes the chemical composition which can help (or hinder) in the separation of the analytes. On the other hand, stationary phases can be solid, gel, liquid, or solid support coated in liquid and are immobile.⁶⁴ They can vary in chemical composition and polarity, dictating the ability of the stationary phase to separate the analytes. Further developments in this field led into two different categories:⁶³

- Planar Chromatography: In this technique, the stationary phase is a flat surface, the analytes move across this support with the help of a liquid mobile phase. The different chemical compositions of each analyte will lead to different distances. Paper chromatography and thin-layer chromatography (TLC) belong to this category.

- Column chromatography: The main techniques in this category include GC, high-performance liquid chromatography (HPLC) and supercritical fluid chromatography (UHPSFC). They not only utilise different stationary and mobile phases, but also operate under different conditions (e.g. temperature and pressure).⁶⁴ This type of chromatography, as the name suggests, employs a column and two types of columns are typically used (packed or capillary). The capillary columns, present inside walls coated with the stationary phase. In contrast, in packed columns the stationary phase is bound to small particles (which can present different properties, i.e., sizes, origin, etc...). Nowadays, modern GC-MS systems usually are equipped with capillary columns, whilst UHPSFC and HPLC are routinely accomplished using packed columns. Depending on the stationary and mobile phase, these techniques are classified as “reversed phase” or “normal phase”. In the reversed phase

the stationary phase is of lower polarity compared to the mobile phase. In normal phase, the opposite occurs, with the stationary phase being more polar than the mobile phase. These techniques can produce different results depending on the parameters used for the separation, that is the stationary and mobile phase and the physical properties of the analyte. This means that a direct comparison of chromatographic separations using different techniques is not allowed; therefore, to make comparisons possible, separations are usually described by theoretical parameters. These theoretical parameters are often defined by mathematical equations, but, since this topic is out of the scope of the project they are not further discussed here.

1.5.1.1 Gas Chromatography

GC is a separation technique, that was first developed in the 1950s, in which the mobile phase (often described as the carrier gas) is a gas that is inert or unreactive (e.g., helium).⁶⁵ Modern GC provides good separation and narrow peaks due to the rapid diffusion of the molecules in the gas phase. However, is not suitable for the analysis of thermally labile and non-volatile compounds. This technique can be used quantitatively as well as qualitatively.⁶⁶ In GC samples are injected into the column, as either a vapour or a gas. The column is located in an oven, which can be programmed to be operated isothermally or with a temperature gradient (usually between 0 - 400 °C). In the column, the analytes interact with the stationary phase and are per consequence separated. This separation technique presents advantages such as high resolution, making it possible to be used quantitatively as well as qualitatively, reliability, relatively low cost, and requirement for small amounts of sample. Though, due to some limiting properties (e.g., volatility), not all the analytes can be separated using this technique (e.g., analytes with high boiling point). A standard GC configuration is shown in Figure 9.

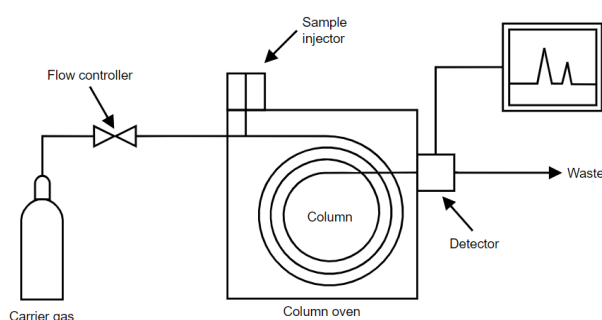


Figure 9 - A standard GC configuration.⁶⁷

Once the analytes elute from the column they are detected by a detector. Some common detectors include the flame ionisation detector (FID), mass spectrometer, electron capture detector (ECD) and a thermal conductivity detector (TCD).⁶⁸ The analysis of sulfur compounds is preferably conducted using a SCD detector. This detector has the capability not only of detecting and quantifying sulfur components but also to provide a linear and equimolar response to all sulfur

compounds, modest quenching effects of hydrocarbons, excellent sensitivity (low ppb levels) and good selectivity.⁶⁹ Since the SCD detector is only sensitive to sulfur compounds, it is able to detect trace amounts of sulfur containing species in complex matrixes such as hydrocarbons. In SCD, the detection is based on the generation of chemiluminescent species of sulfur. This generation is based in sequential reactions, the general process is presented below (Figure 10):

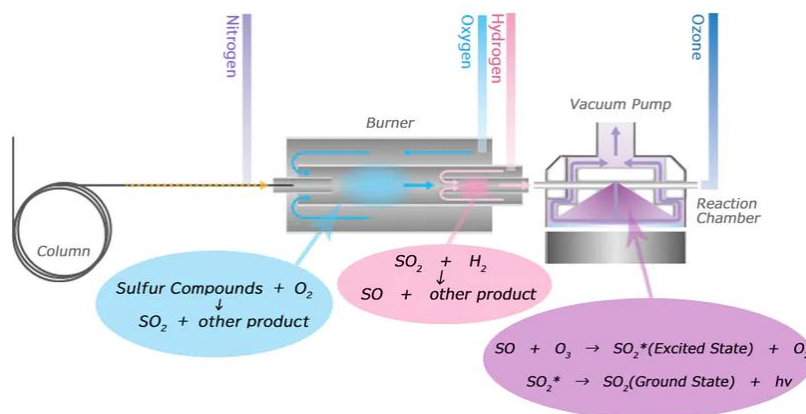


Figure 10 – Scheme of a sulfur chemiluminescence detector (SCD) and conversion to sulfur chemiluminescent species.⁷⁰ The sulfur containing compounds eluted from the column are injected into a burner, where they undergo oxidation/reduction reactions forming SO compounds. These are redirected to the reaction chamber where they react with ozone (O₃), the change in states (i.e., excited to ground state) generates light that is detected by a photomultiplier.

This generation of chemiluminescent species of sulfur process starts with oxidative combustion of the sulfur compounds which generate SO₂ species. Since, SO₂ does not (generate) chemiluminesce with ozone, a reduction reaction (with H₂) is required in order to produce the chemiluminescent species. These will then react with ozone to produce chemiluminescence.⁵⁷ An example of GC-SCD (and GC-MS) spectra is given below (Figure 11), which illustrates the utility of the SCD detector in the analysis of a transformer oil sample containing organosulfur compounds taken from an in service power transformer.⁷¹

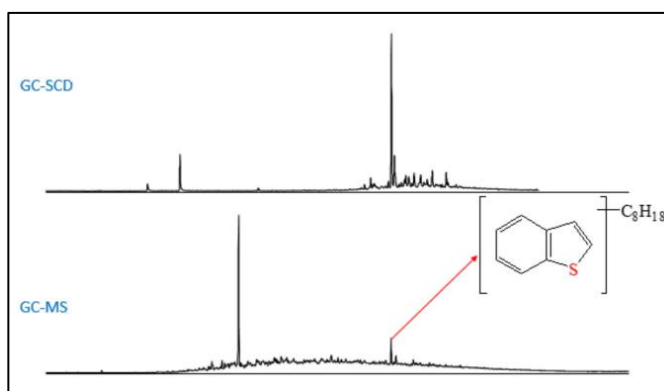


Figure 11 – GC-SCD (top) and GC-MS (below) spectra obtained from the analysis of an in service mineral oil sample.⁷¹

From Figure 11, when comparing the data obtained from the two analytical tools (GC-SCD and GC-MS), we can see that the use of GC-SCD provides increased sensitivity for sulfur compounds present in the oil sample than the GC-MS. As discussed above, a key attribute of the SCD detector is good selectivity and sensitivity for sulfur containing species even in complex mixtures such transformer oil.

1.5.1.2 Supercritical Fluid Chromatography

The properties of this technique are said to lie between gas and liquid chromatography, so UHPSFC is usually considered a hybrid of gas and liquid chromatography. This technique utilizes extreme conditions of temperature and pressure in such a way that the mobile phase remains as a supercritical fluid, which has properties intermediate between a liquid and a gas,⁷² giving supercritical fluids interesting and suitable properties to be used as mobile phases. The supercritical fluid state can be more easily understood with the help of a phase diagram, using carbon dioxide (CO₂) values as an example (Figure 12).

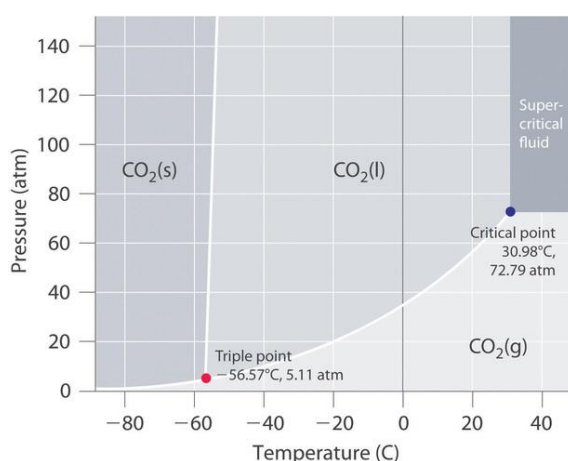


Figure 12 - Phase diagram of CO₂, showing the critical point, the triple point and the sublimation temperature.⁷²

Above certain temperatures, the substances can no longer exist as a liquid no matter how much pressure is applied, similarly, there is a pressure above which it can no longer exist as a gas no matter how high the temperature is.⁷³ These conditions are called the supercritical temperature and supercritical pressure, respectively. A substance is considered to be in a supercritical state when its temperature and pressure are higher than its critical temperature and pressure, respectively, where distinct liquid and gases do not exist, but below a pressure required to compress the substance into a solid. Supercritical fluids have good solvating properties and high diffusivity.⁷⁴ These properties can make UHPSFC up to ten times faster than HPLC, which is valuable where high throughput is desirable. The advantages come from the fact that the density, and diffusivity, of supercritical fluids are comparable to a liquid at the same time as viscosity is closely correlated to a gas (Table 5).

Table 5 - Physical properties of liquids, gases, and supercritical fluids.⁷²

Property	Liquid	Gas	Supercritical Fluid
Density (kg/m ³)	1000	1	200 - 800
Viscosity (mPa.s)	0.5 - 1.0	0.01	0.05 - 0.1
Diffusivity (cm ² /s)	10 ⁻⁵	0.1	10 ⁻⁴ – 10 ⁻³

In general, UHPSFC is considered a normal phase separation technique. Although several eluent systems have been used, the most successful and widely used is CO₂. Its use is usually owed to some of its properties; its low critical pressure (72.79 bar) and low critical temperature (30.98 °C) are major advantages, since they present values that are easily achieved and affordable with the current technology; CO₂ is non-flammable, non-explosive and usually its response in most detectors is negligible. Due to its non-polarity, addition of organic modifiers is often required (e.g., methanol, ethanol, acetonitrile, etc.) for improved analysis of polar compounds. This addition does not only increase the polarity of the mobile phase and but also changes the retention, efficiency, selectivity and its interactions with the stationary phase.

UHPSFC is generally more important in situations where neither GC nor HPLC can deliver the required analysis. One situation is in the analysis of petrochemical compounds; Mineral oil has miscibility issues with reversed phase HPLC solvents, while normal phase HPLC is more challenging to interface to MS. Even coupled with GC, ICP-MS systems would suffer from matrix interference due to the myriad hydrocarbons present in mineral oil.⁶⁰ UHPSFC can overcome the solubility issues

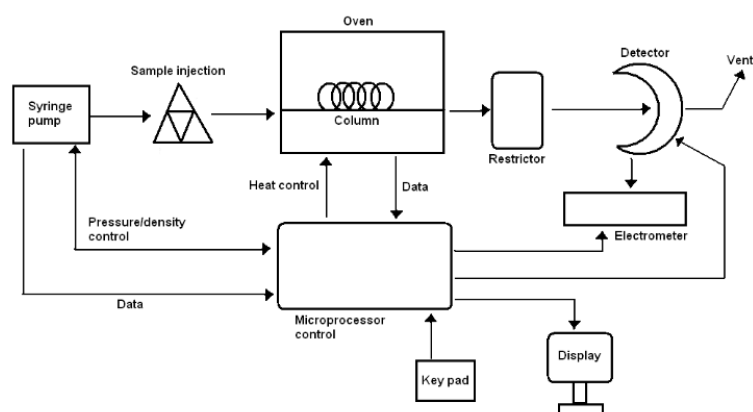


Figure 13 - Scheme of a supercritical fluid chromatography instrument.⁷⁵ The sample is injected into the inlet and then swept onto a chromatographic column by the carrier gas (usually _{sc}CO₂). The compounds are then separated and led to the ion source, where they are converted to ions. The ions of interest are then redirected to the detector. The detector sends the obtained data to a computer, where it can be visually displayed and stored.

related to the mineral oil, and when combined with a suitable derivatisation method and ESI-MS detection, may deliver simplified detection with minimal interference from the matrix. The main disadvantages of UHPSFC are the limited choice of mobile phases, limited analyte solubility in the mobile phase, unwanted reactions with the mobile phase (e.g., primary, and secondary amines can form carbamic acids in CO₂ under supercritical conditions) and repeatable and stable formation of a gradient which includes both supercritical CO₂ and a polar organic modifier.^{76,77} Figure 13 (above) presents a schematic representation of the main components of a UHPSFC instrument.

1.5.2 Mass spectrometry

Mass spectrometers are constituted of three main parts: the ion source, the mass analyser and the detector. As a quick summary of their standard operation, samples are firstly injected into the source where they are ionised. In the mass analyser, the ions (in the gas phase) are separated according to their mass/charge (m/z) ratio. The signals are then detected by an electron or photo-multiplier and the output is recorded by the data system (e.g., computer). Lastly, a mass spectrum is generated, which consists of a plot of relative ion abundance vs. m/z ratios. Many times, due to the complexity of the samples, prior separation is often required before sample injection and subsequent ion generation in the mass spectrometer. These separation methods include HPLC, GC, capillary electrophoresis, etc. Therefore, mass spectrometry can be used, and is usually used, in combination with prior separation techniques to attain high sensitivity and specificity for the analyses of an extensive diversity of complex samples.

1.5.2.1 MS ionisation sources

Currently, there are several types of ionisation methods available. The most common and widely used are the atmospheric pressure ionisation (API), which include techniques such as electrospray ionisation (ESI), atmospheric pressure chemical ionisation (APCI) and desorption electrospray ionisation (DESI). Other ionisation techniques include electron ionisation (EI), which is commonly employed in gas chromatography mass spectrometry (GC-MS), chemical ionisation (CI) and fast atom bombardment (FAB). The two different ionisation techniques utilised in this work are presented below.

1.5.2.1.1 Electrospray ionisation

ESI is a soft ionisation technique that transforms ions in solution into the gas phase. The basic concept of this technique was firstly described in the early 20th Century.⁷⁸ However, it was not until approximately 50 years later that John Fenn and colleagues,⁷⁹ demonstrated that ESI could be used as an ionisation technique for MS. In their work, they were able to ionise, and consequently analyse,

high molecular weight biological compounds. In recognition of this breakthrough, John Fenn was awarded a share of the 2002 Nobel Prize for Chemistry.⁸⁰ In ESI, the ionisation occurs at the same time as the solvent is nebulised, and subsequent evaporation leaves ionised particles in the gas phase. The nebulisation process occurs due to the presence of a high electrical field (2.5 - 6.0 kV) between the needle and the counter electrode. The resulting charged droplets shrink via evaporation, leaving small highly charged particles that are propelled towards the mass analyser.⁸¹ A schematic representation of the ESI interface is presented in Figure 14.

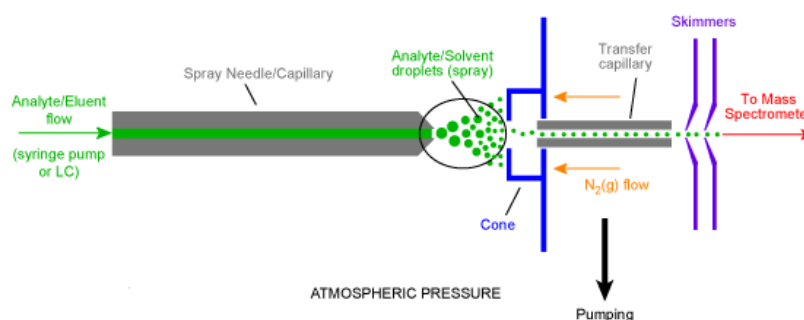


Figure 14 - A schematic representation of an ESI interface.⁸² Showing the main steps of ESI ionisation; from the sample introduction, to the ion formation and consequent transfer to the mass spectrometer.

ESI can be utilised to ionise a wide range of different compounds, but it is generally applied to the ionisation of involatile and thermally labile compounds. Electrospray Ionisation – Mass Spectrometry (ESI-MS) is now widely used, and it is in use in analytical laboratories all over the world. In this technique, the sample is typically dissolved in a solvent such as methanol, water, acetonitrile, or even a mixture of different solvents. The ionisation mode (i.e., negative or positive ionisation) is really dependent on the polarity and molecular weight of the analytes. As a general rule, ESI is most suited for the analysis of polar compounds. The main requirement for this type of analyses, is that the compounds of interest can be fully dissolved in a suitable solution.

1.5.2.1.2 Electron ionisation

In the electron ionisation method, molecules (M) are bombarded in the gas phase with high energy electrons (e^-), which results in the generation of radical cations $[M]^{+\bullet}$ and thermal energy free e^- . The graphic representation of an ion source is illustrated in Figure 15.

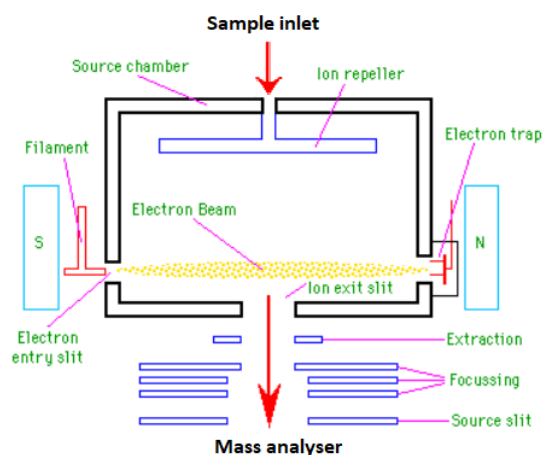


Figure 15 - A schematic of an ion source.⁸³ The compounds eluting from the column enter the ion source and are converted to ions, which are then transferred to the mass analyser.

Often the molecular ions formed are unstable and will undergo fragmentation to form a more stable ion (Figure 16).

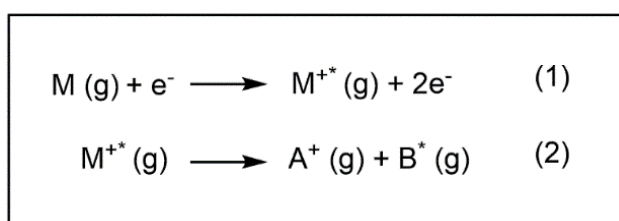


Figure 16 - Process of ion formation in EI.

Consequently, electron ionisation will result in high fragmentation of the analytes which can have both advantages and disadvantages for the analyses. This means that although the fragmentation can provide vital structural information, an extensive fragmentation can lead to a significant decrease of intensity of the ion observed in the spectrum or even to its complete disappearance, which can put at risk the determination of the molecular weight of the compound. A sample is suitable for this technique when it is volatile, so it can be converted to the gas phase and then undergo ionisation. In order to analyse some compounds that are poorly volatile, commonly the use of a gas chromatography system is connected to a mass spectrometer, giving rise to the GC-MS technique. Development and application of derivatisation agents to increase the volatility of poorly volatile compounds, or improve their chromatographic properties is a common approach in GC-MS. A common example is formation of methyl esters from carboxylic acids. A derivatisation method which allows the determination of trace levels of elemental sulfur is the basis of the research work described in this thesis, whereby the sulfur-containing sample is reacted with triphenylphosphine to form triphenylphosphine sulfide. The phosphine sulfide derivative exhibits improved chromatographic properties and can be readily detected with a flame ionisation detector (FID).

1.5.3 Mass Analysers

After the ions are produced, they need to be detected and this is accomplished by the use of a mass analyser. Once ionisation occurs, the sample (ions) are transferred from the ion source to the mass analyser. The choice of the analyser is much dependent on the requirements of the analysis and also reliant on the ionisation source. These instruments have the function to separate ions according to their m/z values, achieved using either a magnetic, or an electrical field or both. Most of the current mass analysers utilise electrical fields. Nevertheless, ion-cyclotron resonance (ICR) analysers, which utilise magnetic fields, are still used for the analysis of small molecules. The mass analysers include: quadrupole, quadrupole ion trap (QIT), time-of-flight (TOF) and Fourier transform ion cyclotron resonance (FT-ICR).⁸⁴ The type of mass analyser utilised in this thesis is discussed below.

1.5.3.1 Quadrupole

Quadrupole mass analysers are typically used in conjunction with HPLC, GC or UHPSFC but can also be used as stand-alone instruments using API techniques. The quadrupole ion trap, which is used as the base component in most of the current quadrupole analysers, was developed by Wolfgang Paul (awarded with the Noble prize in Physics for this invention) in 1989.⁸⁵ The quadrupole (linear) is made up of four parallel rods which have fixed direct current (DC) and alternating radio frequency (RF) potentials applied. The representation of the quadrupole analyser can be seen in Figure 17.

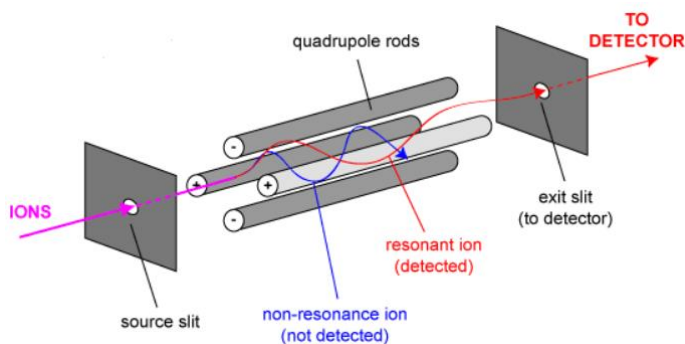


Figure 17 - Representation of a quadrupole (linear) analyser.⁸⁶ When the ions enter the quadrupole the positively charged ions are separated and then transferred to the detector.

In this type of analyser, the motion of the ions that travel along the quadrupole and will depend mainly on the electrical field applied at that particular time. This means that only ions with a specific m/z will be able to reach the detector when a particular field is applied. Those with unstable trajectories (i.e., different m/z ratios from the desired one) are deflected from the central axis and are not transmitted to the detector.

The different m/z ratios of interest are taken to the detector by varying the RF and DC, while keeping the ratio between them constant. The resolution of this analyser depends not only on the length and diameter of the quadrupole rods but also on the range of RF voltages that can be applied. However, MS/MS cannot be completed on single quadrupoles, resolution is on the nominal scale and the mass range is limited to 4000 m/z .⁸⁷

1.5.4 Summary

This sub-chapter provided not only a summary of the literature methods for S_8 detection in hydrocarbons, but also introduced the fundamental principles of chromatographic and mass spectrometry techniques used during the course of the project to detect and quantify S_8 and derivatives in mineral insulating oil. The use of the GC-MS and of the UHPSFC-MS equipment, coupled with the use of triphenylphosphine as the derivatisation reagent, allowed the detection and indirect quantification of S_8 with minimal sample preparation. The use of the UHPSFC combined with the ESI-MS, allowed for detection of TPPS with minimal interference from the matrix and consequently an accurate quantification of S_8 . The experimental methods and procedures for both of these techniques are described in detail in the next chapter.

1.6 Polymers

This sub-chapter starts with a brief introduction to the history of polymers, specifically describing the main advances in the synthesis of polymers and their impact/importance in our daily lives. This is followed, by a basic description of polymerisation techniques used in this work to synthesise two different polymer-supported reagents/scavengers for the selective removal of S_8 from mineral oil.

The use of naturally occurring polymers (e.g., rubber) can be dated back to ancient Mesoamerican civilizations. Historically, polymers have always been one of the bases of important goods. In the last couple of centuries, the necessity to replace and improve classical materials led to the discovery and production of synthetic polymers. Although, the definition of “polymer” experienced several modifications all over the years, the chemical term was introduced by Berzelius in the 1830s.⁸⁸ Despite significant advances in polymer synthesis in the 1800s, the concept of polymers and their molecular nature was only understood later on by H. Staudinger. For his discoveries in the field of macromolecular chemistry he received the Nobel prize in Chemistry in 1953.⁸⁹ During the next years, a significant period of innovation occurred. In 1963, K. Ziegler and G. Natta were awarded the Nobel Prize of Chemistry for their discoveries in the field of the chemistry and technology of high polymers.⁹⁰ Their innovations led to the development of a polymerisation process that enabled an inexpensive and versatile way to mass-produce polymers (mainly polyethylene (PE) and

polypropylene (PP)). Nowadays, polymers are extremely important industrial materials and many of them are easily found during our everyday lives. Their usage not only covers basic materials like plastics, coatings, fibres, etc. but also more complex engineered materials (e.g., with medical or/and electrical applications). It is also worthy of note that natural polymers are also the basis of life. Some examples of bio-polymers are polynucleotides (DNA and RNA) and polysaccharides (glycogen, cellulose, etc.).

One of the most important and versatile polymerisation methods is the free radical polymerisation (FRP). This process is utilised to produce almost half of all the polymers and synthetic rubbers in the world.⁹¹ In the last years, the growing demand for new materials with very specific applications, which are usually linked to complex structures and chemical properties, has demanded, and pushed for the development of new polymerisation techniques (e.g., “living” free-radical polymerisation techniques). These new methods allow controlling to great extent the average molar mass (the polydispersity (\bar{M}_w/\bar{M}_n)), the retention of the desired end chain, and in some cases the molecular architecture.⁹² Some of these “living” free-radical polymerisation techniques are: nitroxide-mediated polymerisation (NMP),⁹³ atom-transfer radical polymerisation (ATRP)⁹⁴ and the reversible addition-fragmentation chain-transfer (RAFT) polymerisation.⁹⁵ Polymers synthesised for the work reported in this thesis used the FRP and NMP techniques, which are summarised below.

1.6.1 Free Radical Polymerisation (FRP) Technique

This type of polymerisation consists of three general steps: The first, the initiation, where the radical/active centre is created. This step is followed by the propagation stage, where the polymer chain grows, due to the sequential and rapid addition of the monomer to the active centre. The third and last step, the termination stage, where the radical active centre becomes “inactive” and prevents any further propagation.

1) Initiation

The polymerisation reaction begins with the formation of the radical species. These radicals are usually obtained by the use of molecules denominated “initiators”. Under certain conditions, initiator compounds decompose and generate the radical species. There are several ways of inducing the generation of said species, the most common ones being thermal and photochemical decomposition. Some common initiators are peroxides (e.g., benzoyl peroxide (BPO)) and azo compounds (e.g., 2,2'-azobis(2-methylpropionitrile) (AIBN)) which are thermally decomposed. Other common initiators are photoinitiators (e.g., benzophenone, 2,2-dimethoxy-2-phenylacetophenone) which are ultraviolet (UV) triggered. The general radical initiation mechanism of some of these examples can be found below (Figure 18). In the case of BPO (a), the

production of carbon dioxide (CO₂) (i.e. formation of the phenyl radical), is usually linked to the reactivity of the substrate (e.g., monomer), the type of reaction (i.e., thermal or photochemical) and to the solvent used.⁹⁶ An example of the mechanism of the photosensitizer benzophenone (c), not shown in full in Figure 18, starts with the adsorption of UV light (wavelength: 200-400 nm). Benzophenone is excited to a singlet state, which reverts to a reactive triplet state (through intersystem crossing) that leads to H-abstraction from a polymer substrate and formation of a radical.⁹⁷

Once the radical is formed, the “second step” of the initiation occurs, comprising the reaction of the radical with a monomer (e.g., vinyl monomer) yielding the formation of a new radical species. It is important to notice that some of the radicals/initiators produced may suffer decompositions, or even recombine, thus forming inactive products, meaning that only a portion of the initiator molecules will take part in the polymerisation. Nowadays, mathematical equations to calculate the efficiency and even the rate of initiation can be found in the literature.⁹⁸ Since, it is out of the scope of the project, mathematical treatments will be not further discussed.

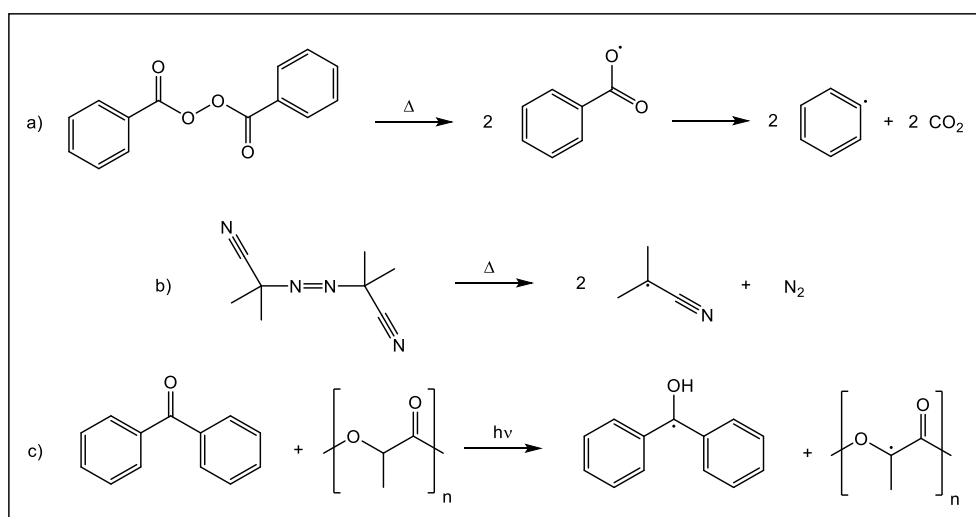


Figure 18 – Common radical initiators and initiation steps: a) BPO b) AIBN c) Benzophenone (example of reaction with polylactic acid).⁹⁷

2) Propagation

During the propagation step, the polymer chain grows by the sequential addition of monomers. The increase of the chain length occurs at a constant rate, due to the general assumption that all the propagation steps have the same rate constant. During the propagation each alkene monomer has the possibility to be added to the radical molecule in different ways to give regioisomers (and stereoisomers). An example of the different configurations in which the alkene can add to the active centre is shown below in Figure 19. It is frequently the case that one of the configurations will be more prevalent, mainly owing to steric and radical stabilisation properties.

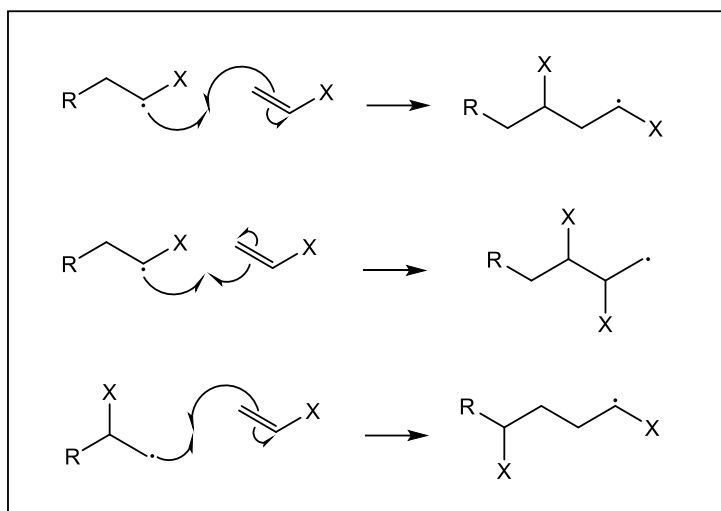


Figure 19 – Different ways in which a mono substituted monomer can add to an active centre during the propagation step of the free radical polymerisation.

(R = Radical Initiator, X = Any substituent that is not Hydrogen)

3) Termination

Although in theory, the propagation should only stop once all the monomers are consumed, in reality, this does not happen. It stops once the concentration of radical molecules is depleted; this usually occurs via two main ways:

- Termination by combination – In this case, two different radicals react with each other forming a single non-radical polymer chain (Figure 20).

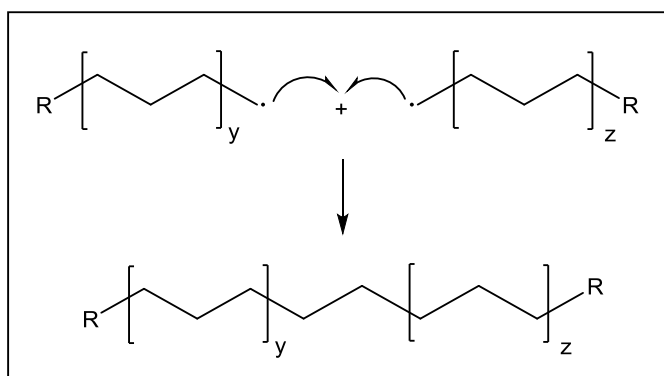


Figure 20 – Termination of propagation by combination.

- Termination by disproportionation – In this termination, a hydrogen (H) atom is abstracted by one radical from another giving two nonreactive polymers, one saturated and the other unsaturated (Figure 21).

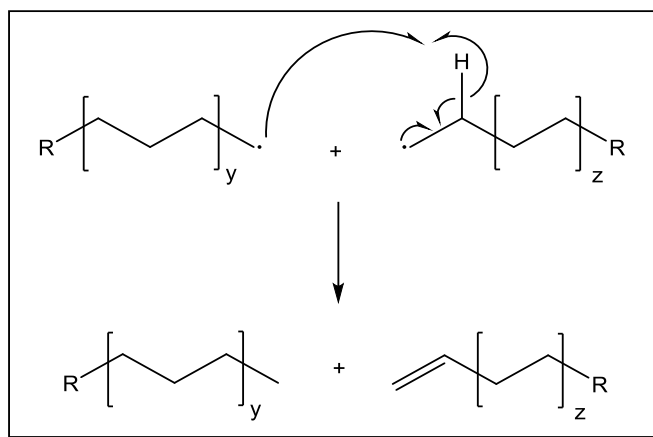


Figure 21 – Termination of propagation by disproportionation.

1.6.2 Nitroxide-Mediated Polymerisation (NMP)

The technique of Nitroxide-Mediated Polymerisation (NMP) was first introduced by D. Solomon and his colleagues in 1986.⁹⁸ NMP is usually performed under the same conditions as the FRP, and only requires the addition of an NMP agent. The NMP agent is a sterically hindered alkoxyamine that possesses a thermally labile C-ON bond, which enables the control of the propagation rate of the polymer. Some common NMP agents are shown in Figure 22 ((a) 2,2,6,6-tetramethyl-1-piperidinyloxy (TEMPO); b) 2,2,5-trimethyl-4-phenyl-3-azahexane-3-nitroxide (TIPNO); c) 2,2,5-trimethyl-4-(isopropyl)-3-azahexane-3-nitroxide (BIPNO)). Several different types of polymers have been successfully synthesised using this technique, these polymers include polystyrenes, polyacrylates, polymethacrylates among others.⁹⁹

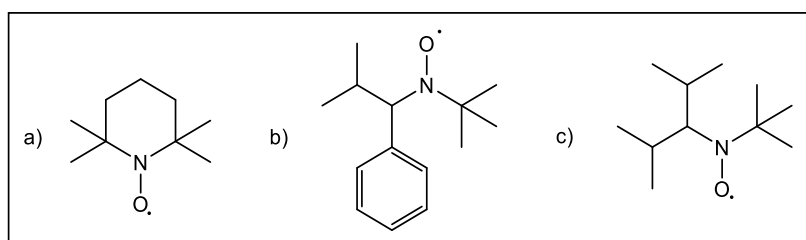


Figure 22 – Common types of NMP agents.

Although, NMP still suffers from slow polymerization rates which require high temperatures and long polymerization it provides an “easy” way to synthesise polymers that were once believed to be difficult or not worth the effort to synthesise.¹⁰⁰ Its wide utilisation comes mainly from some key advantages, such as the possibility to predict and prepare polymers with narrow molecular weight distribution, define the end groups and different types of polymer architecture (e.g., star, comb, gradient). These benefits were demonstrated by C. Hawker in 1994,¹⁰¹ using TEMPO to trap a styrenyl radical initiated by benzoyl peroxide. For a better understanding, the overall mechanism of the reaction is shown below in Figure 23.

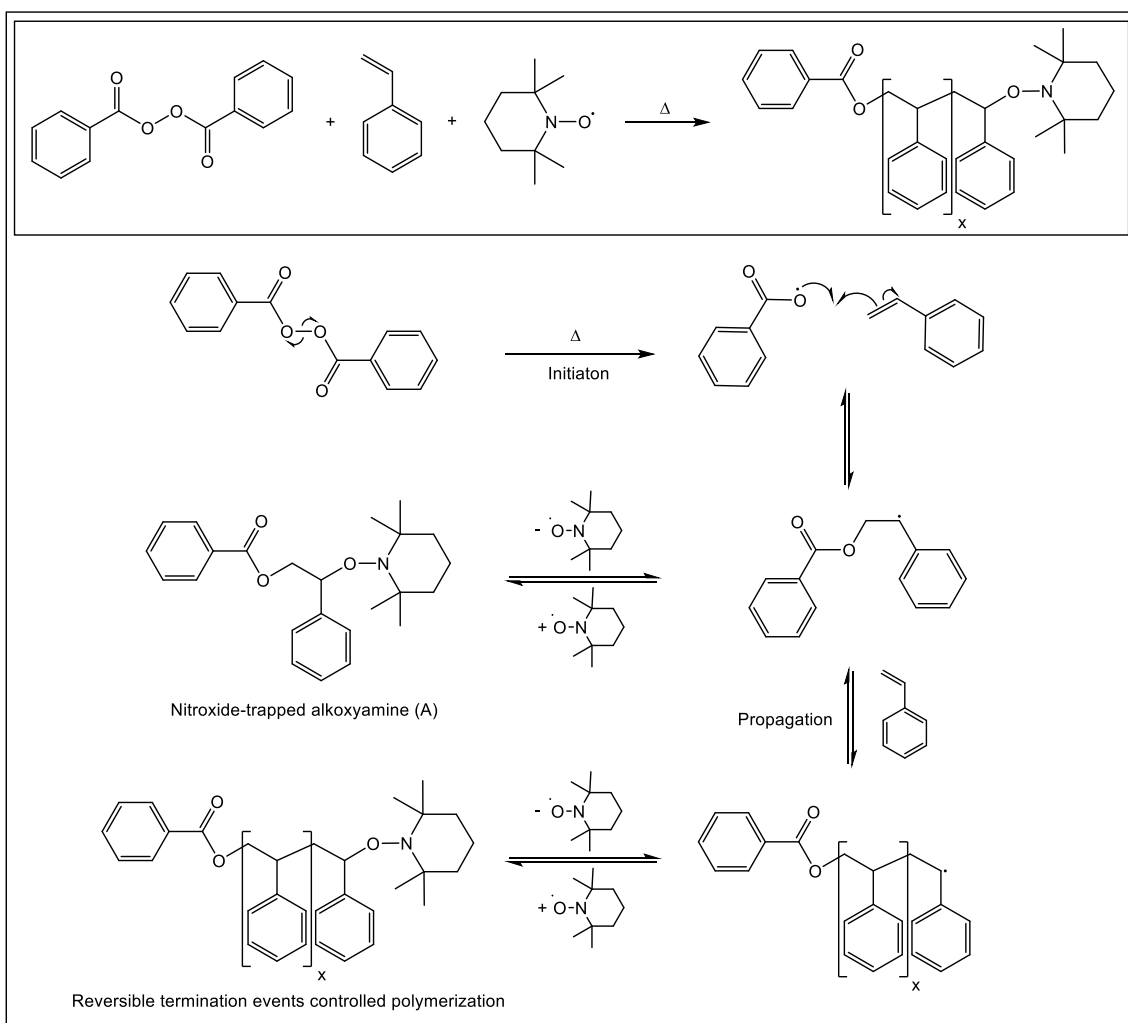


Figure 23 – General mechanism for NMP, using TEMPO as NMP reagent, benzoyl peroxide as initiator and styrene as the monomer.⁹⁹

Due to the reversible termination that the nitroxide-trapped alkoxyamine (A) provides, a high degree of polymerisation (DP) and low dispersity (\mathcal{D}) can be achieved. Usually, it is accomplished by ensuring that the rate of the reversible termination is much higher than the rate of the propagation step, which leads to low concentrations of active polymer chains, lowering the probability of irreversible termination reactions occurring.¹⁰²

1.6.3 Polymer-supported reagents/scavengers

Nowadays, the utilisation of supported materials as reagents, scavengers or even catalysts is something common;¹⁰³ In the figure 24, an example of application of scavengers is demonstrated, showing a supported scavenger that selectively removes acrolein from an active pharmaceutical ingredient (API) named iodixanol.¹⁰⁴

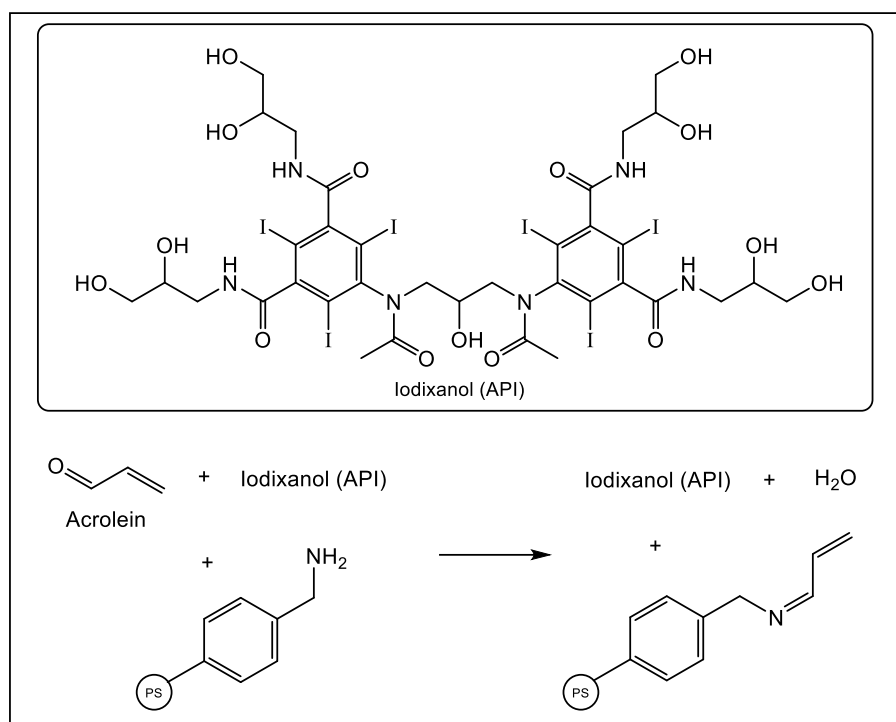


Figure 24 – Illustration of the selective removal of impurities (acrolein) by a supported scavenger from API.

- Supported reagents is usually the designation given to a support material that transform a substrate(s) into new chemical product(s), with the advantage that the excess or used reagent, which remains on the polymer, can be easily removed by filtration.
- Supported catalysts are supported materials that can be used in sub-stoichiometric amounts that are able increase the rate of transformation of a substrate(s) to the desired product(s). The principle advantage is the ease with which supported catalysts can be removed by filtration, so that they can be recycled and reused.
- Supported scavengers are compounds that can selectively remove/quench/sequester by-product(s) of a reaction or remove excess/unreacted starting material(s). They usually present the same advantages as the other supported materials.

The use of supported reagents, catalysts and scavengers can facilitate clean, practical, and effective preparation of complex compounds. One of the pioneers in the development of new methodologies for chemical synthesis on a solid support was R. Merrifield.¹⁰⁵ His work, showed it is possible to conduct organic synthesis using a substrate supported into a polymeric resin. This technique became the general process for solid-phase organic synthesis, and since then new modifications and techniques have been introduced.¹⁰⁵⁻¹⁰⁸ Despite wide acceptance and employment of solid-supported synthesis, there are some limitations associated with this approach. The reaction time can be extended relative to their solution phase counterparts, i.e., the reactivity of the free substrate is usually higher than when linked to the solid support. Another important notable

disadvantage is in relation to the techniques that are used to monitor the reaction progress (e.g., FTIR, gel phase and MAS NMR, etc.), which are usually more complicated to implement and present inferior quality analysis when compared to the more conventional techniques that are employed in solution-phase techniques (e.g., GC-MS, NMR, etc.). In the work described within this thesis, scavenger type polymers are used, which were obtained from commercial suppliers or synthesised by the procedures described. The rationale for selecting the polymer-supported scavengers and the methods for their synthesis is described in detail in Chapter 4. The full synthetic procedures can be found in Chapter 5. The different polymers will be used to selectively remove S_8 from the mineral oil samples; the solid support is insoluble in the media so it can be removed by filtration.

Chapter 2 Analytical experimental part

2.1 Chemicals

All solvents and chemicals were used as supplied and without any further purification, drying or treatment. Methanol (Liquid Chromatography – Mass Spectrometry (LC-MS) grade), *n*-hexadecane (> 95%) and dichloromethane (DCM) (HPLC grade) were purchased from ThermoFisher Scientific (Loughborough, UK). Food grade carbon dioxide was purchased from BOC Special Gases. Thianaphene (benzothiophene) (98%), 4,6-dimethyldibenzothiophene (95%) were purchased from Fluorochem Ltd (Glossop, UK) and formic acid was purchased from Riedel-de Haën (Seelze, Germany). All the other chemicals were purchased from Sigma–Aldrich (Gillingham, U.K.). National Grid plc (London, UK) kindly supplied representative mineral oil samples.

2.1.1 Transformer mineral oil samples

National Grid plc provided mineral oil samples for analysis, some of which are believed to possess corrosive properties and all with varying compositions and chemistries. The samples were collected from a diverse range of transformers, presenting different working conditions and ages.

2.2 Analytical procedure

2.2.1 Stock solution and calibration

The autosampler vials were prepared at a concentration of 10% of the sample and 90% of toluene for GC-MS and at a concentration of 50% of the sample and 50% of toluene for the Supercritical Fluid Chromatography – Mass Spectrometry (UHPSFC-MS) (solvent mixture optimum). A working stock solution of TPPS was made in 50:50 mineral oil/toluene (v/v) at a concentration of 100 µg/mL (ppm). Dilutions of the working solution with 50:50 mineral oil/toluene (v/v) were used to prepare calibration standards. The calibration standards were prepared by dilution with 50:50 mineral oil/toluene (v/v) to give concentrations of 0, 0.05, 0.10, 0.25, 0.50, 1.0, 2.5 and 5.0 µg/mL of TPPS. These provide concentrations at the lower limit of the quantification (LLOQ) and upper limit of quantification (ULOQ) for TPPS.

2.2.2 Sample preparation and derivatisation procedure

Mineral oil samples were stirred at room temperature, and then 5.0 mL of each sample was transferred to a round bottom flask to which 5.0 mL of toluene was added. For derivatisation, 20 mg of TPP was added to each round bottom flask and the mixture was stirred at 60 °C. Sufficient TPP is available for oil samples with a concentration of elemental sulfur up to 490 µg/mL. In this work, the samples were allowed to react for 3 h before being diluted (in an appropriate ratio) with 50:50 new mineral oil/toluene(v/v) and loaded into autosampler vials. All samples were analysed by UHPSFC-MS immediately after preparation.

2.2.3 General procedure for the reclamation processes to selectively remove S₈ from transformer mineral oil

The general procedure for removal of S₈ from mineral oil samples involved loading of the polymer-bound triphenylphosphine (2-7 g) to an empty column (glass column without frit – Figure 85 or Biotage® Sfär - empty 10 g column with frits - Figure 87). The stirring sample of mineral oil (50-250 mL) in a RBF was warmed using a aluminium heat transfer block placed on a heating plate (60 °C). The warm oil was continuously pumped through the column containing the polymer. Analyses for S₈ content was performed at intervals of 6-8 hours. The oil samples were analysed using the TPP derivatisation method (described in Chapter 3), and SFC-MS SIR (see below for detailed method – 2.4). The experiment was terminated once the concentration of S₈ present in the oil sample reached ≤ 100 ppb. The pump used was a Masterflex L/S digital miniflex pump (item number: WZ-07525-40) and the tubing was Masterflex L/S® precision pump tubing (part number: 06424-16). The general reclamation process set-up used in our experiments can be found in Figure 89.

2.3 Instrumentation

2.3.1 GC-MS

2.3.2 Non-polar column - Configuration

Samples were analysed using a Thermo (Hemel Hempstead, UK) Trace GC-MS single quadrupole mass spectrometer. Gas chromatography was performed using a Phenomenex ZB5-MS 30 m x 0.25 mm 0.25 µm thickness non-polar column using helium as a carrier gas at 1.2 mL/ min. The injector temperature was set at 220 °C and 1 µL of sample was injected in splitless mode. The temperature program used was 60 °C for 3 min which then increased at 10 °C/min to 320 °C and then held for 10 min. A positive EI mass spectrometry with a Selected Ion recording (SIR) method was also

created for the ions of interest m/z 183, 262 and 294 which correspond to TPPS. Low resolution positive ion electron ionisation mass spectra were recorded over a mass range of m/z 40-500 at 70 eV. The ion source temperature was 200 °C and the detector voltage of 350 V.

2.3.3 Polar column – Configuration

All the samples were analysed using a Thermo (Hemel Hempstead, UK) Trace GC-MS single quadrupole mass spectrometer. Gas chromatography was performed using a J & W Innowax 60 m x 0.25 mm 0.5 μ m thickness polar column using helium as a carrier gas at 1.0 mL/min. The injector temperature was set at 220 °C and 1 μ L of sample was injected in splitless mode. The temperature program used was 40 °C for 10 min which then increased at 10 °C/min to 240 °C and then held for 20 min. Low resolution positive ion electron ionisation mass spectra were recorded over a mass range of m/z 20-500 using at 70 eV. The ion source temperature was 200 °C and the detector voltage of 350 V.

2.4 UHPSFC-MS

2.4.1 Ultra-Performance Convergence Chromatography system – Triple Quadrupole Detector (UPC² – TQD)

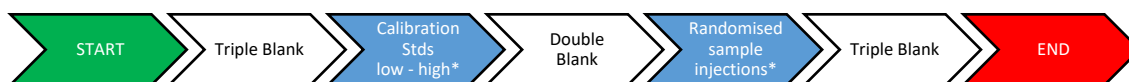
2.4.1.1 UHPSFC Method

An Acquity UPC2 system (Waters Corp., Milford, MA, USA) was employed for all analyses. This system is equipped with a binary solvent manager, a heated column manager and an internal autosampler with a cooled sample tray. A HSS C18 SB column (1.8 μ m, 3.0 x 100 mm) was used. The column was held at 40 °C in a column oven and 2.0 μ L of each sample solution was injected. A mobile phase modifier, methanol (25 mM ammonium acetate) was used. The supercritical (sc) CO₂ back pressure of the system was set to 150 bar. A 3 min gradient elution was performed using the method described in Table 6 and a 1 min pre-run was used for column equilibration.

Before the analyses, three blank injections of methanol were performed to ensure system stability and cleanliness. Analyses commenced with triplicate injections of the calibration curve solutions (low concentration to high); each standard solution was followed by two blank injections. Study samples (triplicate measurements) were then analysed in a randomised order to minimise bias due to batch effects. The sequence of analysis is shown in Figure 25.

Table 6 - Inlet method for UHPUHPSFC.

Time (min)	Solvent A (CO ₂) %	Solvent B (methanol + 25 mM ammonium acetate) %
0.00	98	2
2.00	60	40
2.30	60	40
3.00	98	2



* A blank was conducted in between samples.

Figure 25 - Sequence of analysis in UHPSFC-MS.

2.4.1.2 ESI-MS Method

A Waters TQD (Waters Corp., Milford, MA, USA) triple quadrupole mass spectrometer was used. An Internal Solvent Manager (ISM) was used to introduce make up solvent, methanol + 1% formic acid, after chromatographic separation at a flow rate of 0.5 mL/min to enhance ionisation and ensure a stable spray. The operating conditions for the positive ion ESI were as follows: capillary voltage 3.5 kV, cone voltage 20 V, source temperature 150 °C, desolvation temperature 500 °C. Nitrogen was used as the desolvation gas at a flow of 300 L/h. Full scan data over the m/z range of 100 – 800 were acquired for each injection. A positive ion ESI mass spectrometry single ion recording (SIR) method was created for the ion of interest m/z 295, which corresponds to protonated TPPS [TPPS + H]⁺.

2.5 Data processing

2.5.1 Xcalibur™

Xcalibur™ software (version 2.0.5) (Thermo Electron, San Jose, CA, USA) was used to collect and process data for all GC-MS (both polar and non-polar column) experiments and then the NIST 2014 Mass Spectral Library (version 2.2) (NIST, Gaithersburg, MD, USA) was used as reference to confirm the presence of certain compounds.

2.5.2 MassLynx™

Waters MassLynx™ software (version 4.1) (Waters Corp., Milford, MA, USA) was used to collect and process data for all the UHPSFC-MS experiments.

Chapter 3 Determination and quantification of elemental sulfur in mineral transformer insulating oil using chromatography and mass spectrometry

The focus of this Chapter is the application of chromatography and mass spectrometry to the analysis of mineral transformer insulating oil, specifically the detection of elemental sulfur. The literature review showed that some analytical techniques have been applied to determine S_8 in light hydrocarbons oils (e.g., fuels), with comparatively less reported work related to heavy oils (e.g., mineral oil). The detection of sulfur in hydrocarbon matrixes is usually conducted with the use of a sulfur chemiluminescence detector (SCD) coupled to a GC instrument, often using sulfur specific columns. Since, such instrumentation was not available in the Chemistry facilities in Southampton, a different analytical approach was required in order to progress the objectives of the current work. Bearing in mind the requirements of the project (i.e., the analytical method needed to be able to detect and quantify S_8 content in mineral oil down to low ppm levels), and the analytical instruments available to us: gas chromatography - Mass spectrometry (GC-MS) and Supercritical Fluid Chromatography - MS (UHPSFC-MS), we took the decision to develop a method based of derivatisation of S_8 . It was anticipated that derivatisation would simplify the analysis by avoiding the sulfur allotropes. It is expected that the development of these techniques will assist the identification of high value assets such as transformers that might be at risk of corrosion. National Grid plc provided mineral oil samples for analysis, some of which are believed to cause corrosion of the transformers and all with varying compositions and chemistries.

In this context, two methods for detection and quantification of S_8 in transformer mineral oil will be described in this chapter.

- The first uses GC-MS, in combination with the derivatisation method, for detection of S_8 content down to less than one ppm. The method has been applied to mineral oil samples taken from laboratory experiments and for samples of in-service mineral oil.
- A faster and more sensitive detection and quantification of TPPS can be achieved by employing UHPSFC-MS with Single Ion Recording (SIR), where parent transformer mineral oil samples with S_8 content as low as 5 ppb of can be monitored.

3.1 Derivatisation method for elemental sulfur detection

The key aims of a derivatisation method are to change the polarity of a compound, increase its volatility and thermal stability to facilitate detection in a complex medium (such as mineral oil).¹⁰⁹ Thermal stability of the derivatised compound is crucial due to high temperatures (e.g., 220 °C)

used during chromatographic analysis. The outcome of the derivatisation should realise a reduction in peak tailing and improved peak shape, detectability and selectivity.¹¹⁰ Additional advantages include the change of the retention time which can lead to improved resolution; the generation of more ions with a higher atomic mass and a more distinct mass spectrum which results in less interference from other compounds in the matrix.^{111,112} When detecting S₈, the slightly elevated temperatures (found in a standard GC injector) form an allotropic equilibrium (... S₆ ↔ S₇ ↔ S₈ ...) that leads to the complication that elemental sulfur does not elute from gas-chromatographic columns as a single well-resolved peak (as can be seen in Figure 26 – retention time (t_R): ~11 – 15 min).

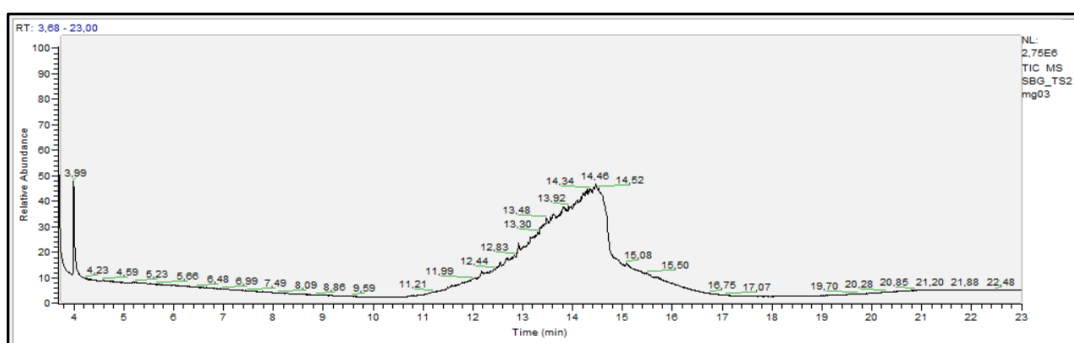


Figure 26 – GC-MS Total ion chromatogram (TIC) of 1 mg/mL of elemental sulfur in toluene. The large poorly resolved peak is due to elemental sulfur.

In addition to the issues relating to sulfur allotropes, S₈ elutes in a region in the chromatogram where other mineral oil compounds elute. In figure 27, we can see that the multitude of peaks (t_R ~10 – 17 min) obtained from the GC-MS analysis of mineral oil overlap with the elution of the S₈ (t_R ~11 – 15 min). This overlap further complicates quantification of S₈. The MS data allowed the identification of the peaks (t_R ~10 – 17 min) present in the mineral oil sample as hydrocarbon compounds with chains lengths ranging from 10 to 34 carbons (and their structural isomers), indicated by MS fragmentation patterns containing clusters of peaks 14 mass units apart (which represent the loss of (CH₂)_nCH₃).

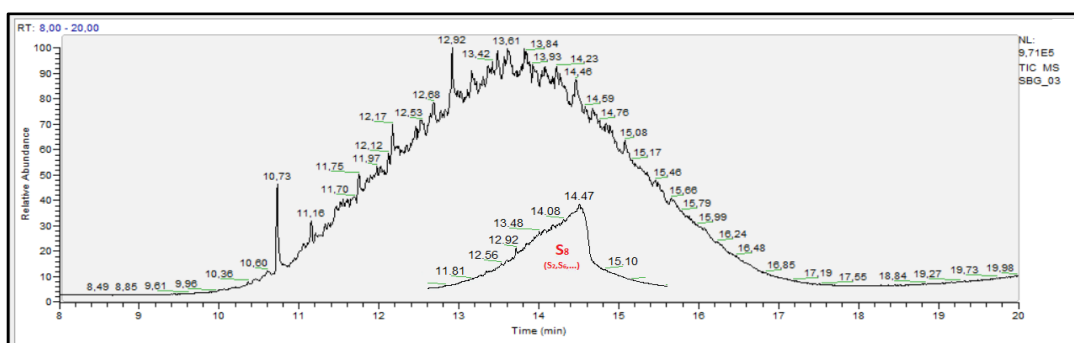


Figure 27 –TIC GC-MS Chromatograms of new mineral insulating oil A and elemental sulfur, showing how the mineral oil peaks can obscure elemental sulfur.

To overcome the problems related to overlap of the sulfur and mineral oil, and poor resolution of elemental sulfur using our instrumentation, a derivatisation method based on the rapid reaction of TPP with elemental sulfur to form TPPS was used (Figure 28).

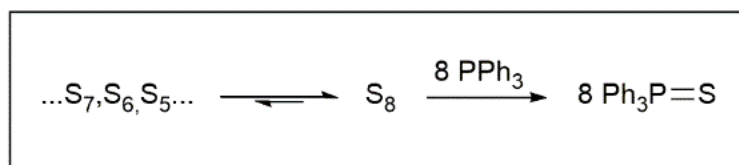


Figure 28 - Derivatisation reaction of elemental sulfur with TPP.¹¹³

There are several advantages arising from the derivatisation reaction:¹¹⁴

- Elemental sulfur is converted into a form suitable for detection with a flame ionisation detector;
- As a result of derivatisation, a 9.2-fold increase in the mass of the sulfur-containing species occurs, so a sample containing 1 ppm of elemental sulfur will contain 9 ppm of the phosphine derivative;
- All the cyclic sulfur species react to form a single product, namely TPPS;
- The derivative (TPPS) has a high boiling point and elutes in a region of the chromatogram where no mineral oil components should elute (Figure 29).

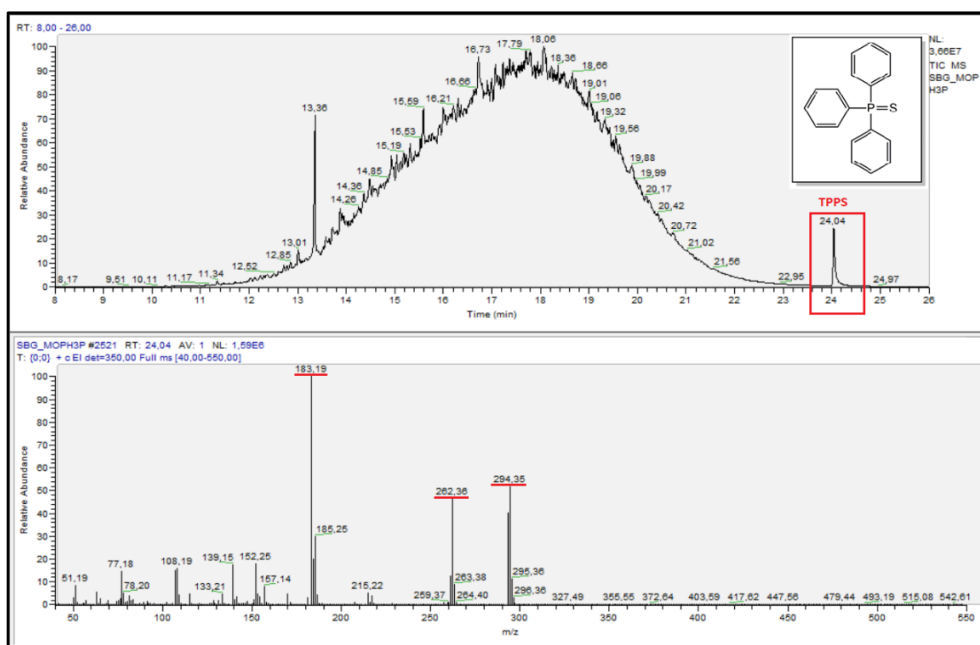


Figure 29 - GC-MS chromatogram of new mineral insulating oil **A** + 1.5 mg/mL of TPPS. The ion fragments correspond to $m/z = 183.19$ [$C_{12}H_8P$]⁺, $m/z = 262.36$ [$(C_6H_5)_3P$]⁺, and $m/z = 294.35$ [$(C_6H_5)_3PS$]⁺. The peak with $t_R \sim 13.36$ min corresponds to 2,6-di-tert-butyl-p-cresol (BHT) and multitude of peaks with $t_R \sim 10 - 17$ min correspond to the hydrocarbon matrix (10 to 34 carbons).

3.1.1 Derivatisation efficiency

Triphenylphosphine sulphide (TPPS) formation is based on the selective reaction of triphenylphosphine with elemental sulfur; Borchardt and Easty¹¹⁵ reported that the reaction was virtually instantaneous at room temperature in toluene and that the solutions were stable for at least 24 h. To ensure this was still valid for our case the conversion of elemental sulfur to TPPS was evaluated. These studies consisted in a kinetic analysis of the derivatisation reaction by ³¹P NMR, the decrease in absorbance of the elemental sulfur by UV-Vis and comparison of the theoretical and experimental concentration of TPPS by UHPSFC-MS.

3.1.1.1 Reaction rate of the derivatisation reaction by UV-vis spectroscopy

The reaction of tertiary phosphine with elemental sulfur is known to give a quantitative yield of the corresponding sulphide. Bartlett¹¹³ proposed a mechanism involving a rate limiting attack of the phosphorous on the sulfur, opening the sulfur crown-shaped ring to a linear octasulfide. The resultant dipolar ion suffers a series of rapid nucleophilic displacements to yield eight moles of the phosphine sulfide per mole of elemental sulfur (Figure 30).

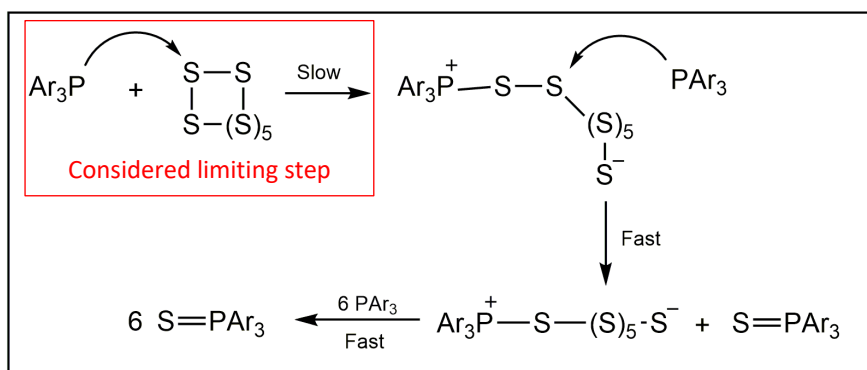


Figure 30 – Proposed mechanism of the reaction of tertiary phosphines with elemental sulfur.¹¹³

Bartlett's¹¹³ investigation also revealed that the reaction follows a second-order rate behaviour which was highly sensitive to solvent polarity. Having this in consideration a kinetic study was conducted, the rate of the derivatisation reaction was followed by UV-vis spectroscopy. The disappearance of elemental sulfur was monitored, and the results were consistent with second-order behaviour in both of the experiments. The absorbance readings were converted into concentration data and were used to obtain the reaction rate (k_2) values. The reaction rate, in the two conducted experiments, was determined at room temperature (not recorded) in toluene. The values of k_2 obtained from the two experiments conducted were $3.59 (\pm 0.30) \times 10^{-3} \text{ L} \times \text{mol}^{-1} \times \text{s}^{-1}$ and $4.14 (\pm 0.30) \times 10^{-3} \text{ L} \times \text{mol}^{-1} \times \text{s}^{-1}$. When comparing these values with that reported by Lloyd¹¹⁶ of $0.42 \times 10^{-3} \text{ L} \times \text{mol}^{-1} \times \text{s}^{-1}$ (in toluene at 25 °C, followed by UV-vis spectroscopy – disappearance of S_8) and with that reported by Bartlett¹¹³ for the same reaction

in benzene (at 25 °C, followed by titration of unreacted TPP) of $1.27 \times 10^{-3} L \times mol^{-1} \times s^{-1}$ (no absolute error was presented for both of these values), a difference between the values can be seen. The discrepancy between the obtained k_2 values and the ones reported in the literature, can be attributed to different factors. One factor is that the solvent used in the different experiments was not the same. My experiments and Lloyd's¹¹⁶ were conducted in toluene meanwhile Bartlett's¹¹³ was conducted in benzene. The influence of the solvent (usually denominated as solvent effects) on chemical reactions is something that has been studied over the years. Solvents can have an effect on rate constants, since its value can be correlated/affected with the physical characteristics of the solvent (e.g., dielectric constant, solubility parameter, viscosity, etc.).¹¹⁷ This can possibly explain the difference in rates between Bartlett¹¹³ and Lloyd¹¹⁶. The second one, is related to the temperature at which the experiments were conducted. Since, the temperature of my experiments was not controlled and Bartlett's¹¹³ and Lloyd's¹¹⁶ were conducted at 25 °C, the discrepancy between my values and theirs might be mainly associated with this fact. According to the collision model of chemical kinetics, which is a useful tool for understanding the behavior of reacting chemical species.¹¹⁸ It explains why chemical reactions often occur more rapidly at higher temperatures. If we look at the Arrhenius Equation (equation 1), which summarizes the collision model of chemical kinetics, we can observe that the rate of reaction is dependent on the temperature. Since, the temperature of my experiments was not controlled it is possible that the temperature of the room was higher than 25 °C. Which, would explain why the rate values obtained in my experiments were higher. Other factors that might influence the differences in the values obtained, could be due the fact that Lloyd's¹¹⁶ used a less sophisticated UV-Vis Spectrophotometer and that Bartlett's¹¹³ used a titration method using prepared standard solutions.

$$k = Ae^{\frac{-E_a}{RT}}$$

Equation 1 – The Arrhenius equation.

Where:

k = The rate constant.

A = The pre-exponential factor.

E_a = The activation energy for the reaction (in the same units as RT).

R = The universal gas constant.

T = The absolute temperature (in degrees Kelvin or Rankine).

Kinetic procedure (adapted from Lloyd¹¹⁶) – Stock solutions of elemental sulfur ($9.43 \times 10^{-6} mol \equiv 7.54 \times 10^{-5} mol$ of sulfur) and of triphenylphosphine ($7.54 \times 10^{-5} mol$) were prepared in 10 mL toluene. Samples of each stock solution (0.1 mL) were pipetted into the quartz

cuvette containing toluene (1.8 mL), mixed and placed in the Nicolet UV-Vis Spectrophotometer. Absorbance readings at 300 nm were taken every 15 min for 6 hours and second-order plots were derived from the data from which values of k_2 were calculated.

Calculations – For an easier interpretation and treatment of the results a second-order rate equation for two reactants at the same initial concentration, which react in a molar ratio of one to one, is used (Equation 2). For this to be valid when applied to the derivatisation reaction, the ring-opening step was considered the limiting step. The chemical equation of the reaction was then treated as: $S + TPP \rightarrow TPPS$.

$$\text{rate} = -\frac{dc}{dt} = k_2c^2$$

Equation 2 – Second-order rate equation.

Which integrates to:

$$\frac{1}{c} = k_2t + \frac{1}{c_0}$$

Equation 3 - Integrated second-order rate equation.

Where:

c = Concentration of reactants at time (t);

c_0 = Initial concentration of reactants;

k_2 = Second-order rate constant.

Therefore, a plot of $\frac{1}{c}$ vs. t yields a straight line with a slope equal to k_2 . Since the absorbance (A) of the reaction solution is proportional to c , a plot of $\frac{1}{A}$ vs t will also be a straight line, the slope of which (k_A) is proportional to k_2 .

If $A = bc$ and $A_0 = bc_0$, where A is absorbance and b is a proportionality constant equal to molar absorptivity times path length (Beer's Law) and A_0 is the absorbance at concentration c_0 , then:

$$k_2 = k_A \frac{A_0}{c_0}$$

Equation 4 – Second-order rate constant equation (UV-Vis).

Assuming this k_2 was calculated, and an example of calculation is shown below.

$$A_0 = 1.18343 ; c_0 = 3.77 \times 10^{-4} \text{ mol} \times \text{L}^{-1} ; k_A = 1.32 \times 10^{-6} \text{ s}^{-1} \text{ (see Figure 31)}$$

$$k_2 = k_A \frac{A_0}{c_0} = 1.32 \times 10^{-6} \frac{1.18343}{3.77 \times 10^{-4}} = 4.14 \times 10^{-3} \text{ L} \times \text{mol}^{-1} \times \text{s}^{-1}$$

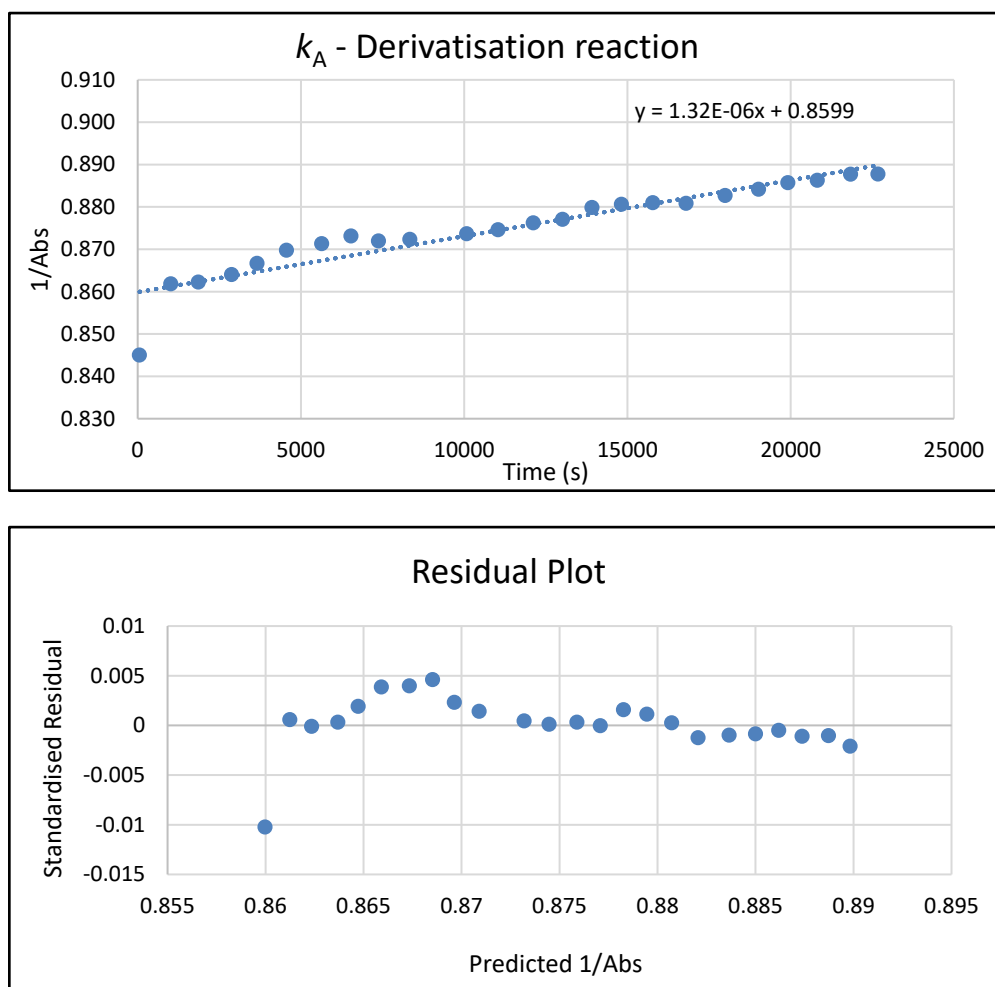


Figure 31 – Reciprocal of A vs. time of the derivatisation reaction and the associated residual plot.

In the top of Figure 31 we can see the plot of $\frac{1}{A}$ vs time of one of the kinetic studies, through the least squares regression line we can obtain the slope (k_A). In the beginning of the line, we can observe that between the two first points (60 – 1020 s) the absorbance decreased faster than during the rest of the reaction. This can be explained by the fact that the other allotropic forms of elemental sulfur (e.g., S_6) react with TPP faster than the S_8 . If we do not consider the first point, the R^2 of the regression line is ≈ 0.973 . Having this value in mind we can assume that the regression line is a straight line. As absorbance is proportional to concentration, the plot of $\frac{1}{c}$ vs. t will also yield a straight line so we can conclude that the reaction follows a second-rate order rate. This conclusion is in line with the one obtained by Bartlett.¹¹³ In the bottom of the Figure 31, the residual plot (with predicted values on the x-axis and the residual on the y-axis) is presented. By looking at the chart we can see that the plotted values seem to be pretty symmetrically distributed and tend to cluster towards the middle of the plot. If we do not take in consideration the first data point, we

can conclude that the data points are always close to the 0 of the y-axis and in general do not seem to follow a clear pattern.

3.1.1.2 Kinetic analysis of the derivatisation reaction using ^{31}P NMR

The direct measurement of chemical reaction rates has been an important tool for many years. The use of NMR techniques provides the unique capability of studying the kinetics of reactions not only *in vitro* but also *in vivo*. The ^{31}P NMR has been a crucial technique to understand and measure *in vivo* kinetics, allowing the quantification of key metabolites^{119,120} (e.g., ATP, P_i , etc.). Due to the characteristics of the derivatisation reaction, ^{31}P NMR is an excellent technique to monitor the TPP \rightarrow TPPS transformation. A control experiment was performed to assure that the resonances of TPP and TPPS were well resolved, a chemical shift of 42.06 ppm was obtained for TPPS and -5.26 ppm for TPP.

The total conversion of elemental sulfur to TPPS is essential for the validation of the analytical method. A guarantee has to be made that all of the elemental sulfur present in the transformer mineral oil sample is being quantified. For this a series of kinetic analysis were conducted to understand what conditions were optimum for total conversion and how the different conditions affect the rate of the reaction (i.e., the TPPS formation). The first ^{31}P NMR kinetic study had the purpose to determine the conversion of elemental sulfur into TPPS at RT in a solution of 50% mineral oil and 50% toluene. To achieve this a stoichiometric reaction of elemental sulfur with TPP was conducted and followed by ^{31}P NMR.

Calibration/Quantification – Standard samples containing 0.015, 0.023, 0.031, 0.038, 0.046 and 0.053 mmol of TPP and 0.027 mmol of TPPS were analysed by ^{31}P NMR. The results obtained for the calibration curve of TPP and for the TPPS standard are plotted (with number of moles (mmol) on the x-axis and the integrated peak area on the y-axis) in Figure 32.

From the visual inspection of the calibration curve of TPP (Figure 32) and the associated R^2 value of 0.9922, we can conclude that the data points have a good fit with the curve. A good correlation can also be seen between the obtained integrated peak area (1142456) for the TPPS standard (0.027 mmol) and the plotted calibration curve for TPP. By calculation, using the equation obtained in the calibration curve of TPP, the difference between the calculated value and the prepared standard TPPS sample (0.027 mmol) was of 0.0004 mmol. In face of this results, It was assumed that the detector response was equivalent/similar for TPP and TPPS. It was also assumed that the signal response obtained for TPP at the start of the experiment ($t = 0$ s) was 100% and related to the concentration loaded into the NMR tube. With this assumption, and later comproved by the experimental results, the signal obtained at the beginning for TPP (100%) and TPPS (0%) would tend

to TPP (0%) and TPPS (100%) over the time. All the kinetic analysis were performed using the integral area values obtained from the integration of the TPP and TPPS peaks.

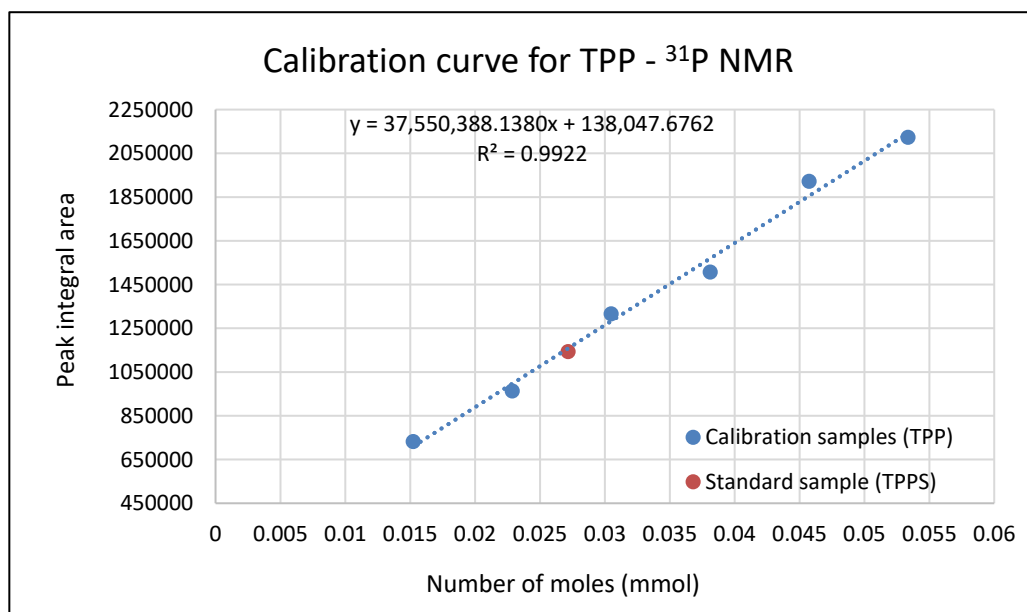
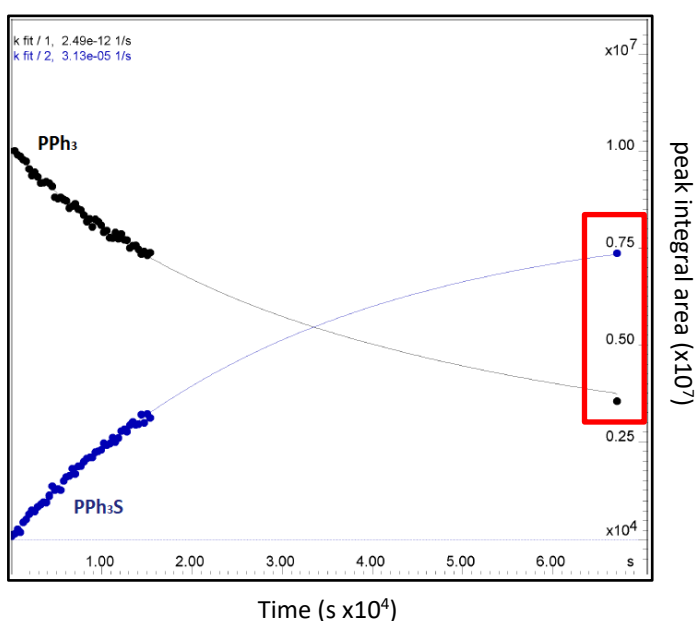


Figure 32 - Calibration results obtained from the analysis of TPP standards (0.015, 0.023, 0.031, 0.038, 0.046 and 0.053 mmol) and a TPPS standard (0.027 mmol) using the ^{31}P NMR.

Procedure – Stock solutions of elemental sulfur ($2.22 \times 10^{-5} \text{ mol} \equiv 1.78 \times 10^{-4} \text{ mol}$ of sulfur) and of triphenylphosphine ($1.78 \times 10^{-4} \text{ mol}$) were prepared in 5 mL (50% mineral oil/ 50% toluene). Samples of each stock solution (0.5 mL) were pipetted into the NMR tube ($V_f = 1\text{mL}$), mixed and placed in the Bruker AVIIIHD-500 FT-NMR Spectrometer. The sample was analysed every 5 min during 4 h 30 min and once after ≈ 18 h 30 min (red box in Figure 33), the first-order plot was derived from the data from which the value of k was calculated (Figure 33).



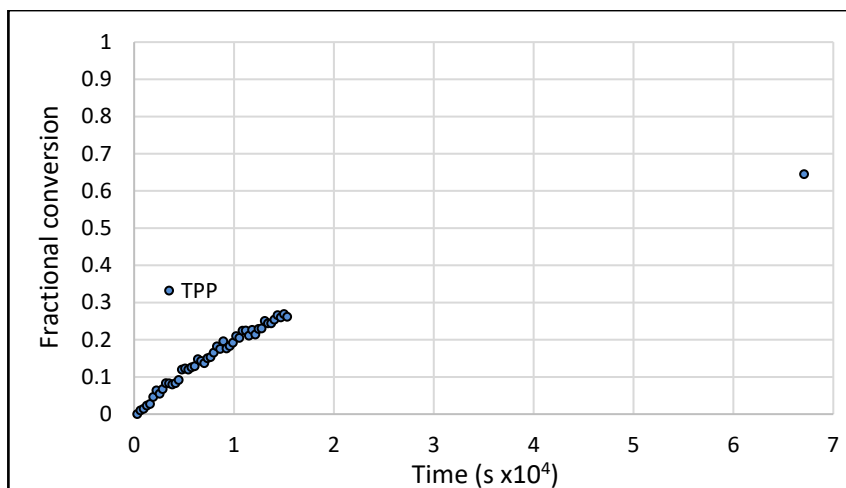


Figure 33 - ^{31}P NMR kinetic study of the derivatisation reaction at RT in 50% mineral oil and 50% toluene and the associated fractional conversion vs. time plot. ($\text{Fractional conversion} = \frac{(n_{\text{TPP}})_{\text{reacted}}}{(n_{\text{TPP}})_{\text{fed}}}$).

From Figure 33, we conclude that the reaction can be followed by ^{31}P NMR as the results fit quite nicely in the kinetic curve. The obtained shape of the curve (for TPP) is consistent with a first-order reaction, the curve obtained for the natural logarithm of TPP concentration versus time (not shown) yielded a straight line with a slope of $-k$, which is also the expected shape/result. We can also conclude that the reaction does not reach completion, the conversion of elemental sulfur to TPPS after 18 h 30 min (red box) is approximately 64%. The reaction seems to be slower than the one reported in the literature.¹¹⁵ However, some questions arise from these results:

- 1) Does the reaction reach completion using these conditions? If yes, how long does it take?
- 2) Does the presence of mineral oil affect the reaction rate?

To answer the first point, the sample was analysed by ^{31}P NMR nine days after and the NMR spectra (Figure 34).

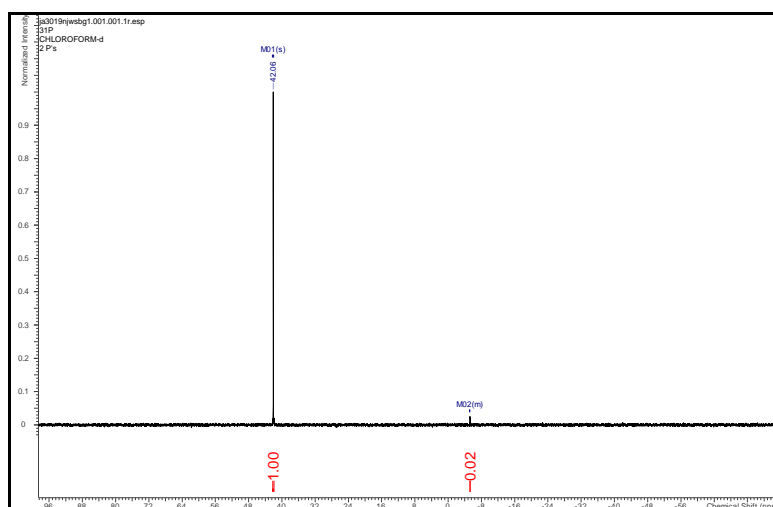
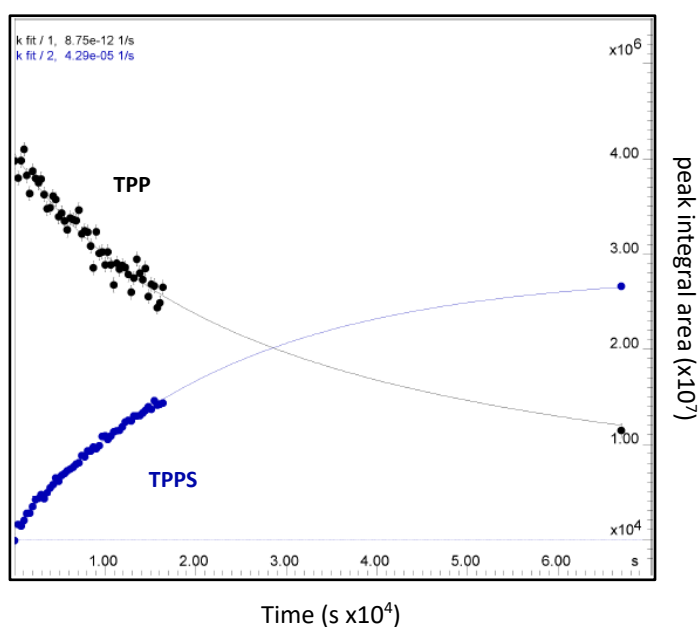


Figure 34 - ^{31}P NMR from kinetic study at RT in 50% mineral oil and 50% toluene after nine days.

After nine days the conversion of elemental sulfur in TPPS is $\geq 98\%$, this is demonstrated in Figure 33. Using the appropriate reaction rate formula and measured reaction rate (see above), it is possible to calculate/estimate the time that is needed to reach a specific concentration (e.g., can be used to calculate the time needed for the reaction to reach total conversion, i.e., $[TPP] \approx 0$). Having in mind the result obtained, we can conclude that the derivatisation reaction is reliable and proceeds to completion in the presence of mineral oil. However, the reaction time of many days is not suitable for routine analysis so further optimisation on the reaction conditions were performed (see 3.1.2). The second ^{31}P NMR kinetic study was conducted to understand the effect of the mineral oil in the reaction rate. This was accomplished by conducting a stoichiometric reaction of elemental sulfur with TPP at RT in toluene. The calibration of the first ^{31}P NMR kinetic study was used.

Procedure – Stock solutions of elemental sulfur ($8.96 \times 10^{-6} \text{ mol} \equiv 7.17 \times 10^{-5} \text{ mol}$ of sulfur) and of triphenylphosphine ($7.17 \times 10^{-5} \text{ mol}$) were prepared in 2.5 mL of toluene. Samples of each stock solution (0.5 mL) were pipetted into the NMR tube ($V_f = 1\text{mL}$), mixed and placed in the Bruker AVIIIHD-500 FT-NMR Spectrometer. The sample was analysed every 5 min during 4:30 h and once after $\approx 18:30$ h (green box in Figure 35), the first-order plot was derived from the data from which the value of k was calculated and the associated fractional conversion vs. time plot are shown in Figure 35.



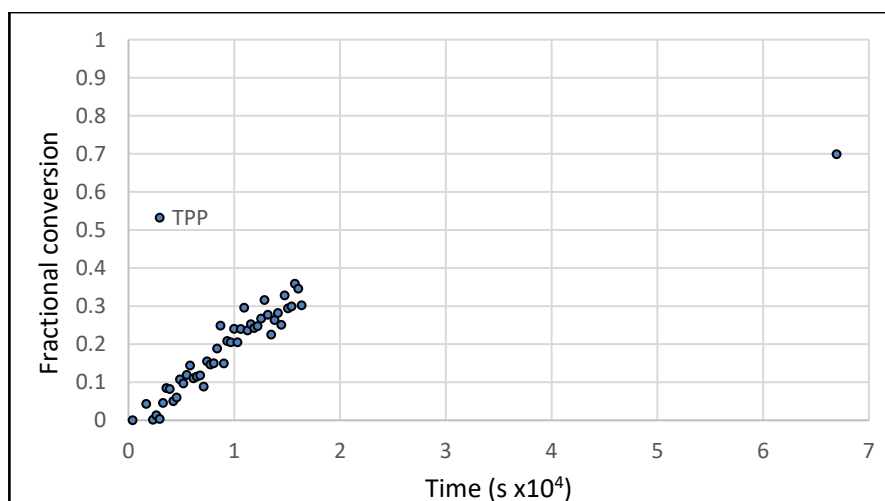


Figure 35 - ³¹P NMR kinetic study of the derivatisation reaction at RT in toluene and the associated fractional conversion vs. time plot. ($Fractional\ conversion = \frac{(n_{TPP})_{reacted}}{(n_{TPP})_{fed}}$).

After analysing the kinetic study presented in Figure 35, we can clearly see a similar pattern to the one obtained for the first kinetic study, mainly because in both cases the derivatisation reaction does not reach completion. The green box represents the last set of collected data and when derived to concentration a value of conversion around 71% was obtained. This conversion is $\approx 7\%$ higher than the one obtained for the first kinetic study. Thus, we can conclude that the presence of mineral oil has some impact on the reaction rate but is not the main responsible for the extended reaction time. Considering the results obtained, we can conclude that the derivatisation reaction does not reach full conversion as fast as reported by Borchardt and Easty.¹¹⁵ Even though the experiments were conducted in a stoichiometric ratio and with no stirring, it is practically clear that to reach full conversion in a suitable time for routine analysis the conditions of the reaction need to be optimised. The optimisation studies can be found in the next sub-chapter. Considering the approach used in the UV-Vis experiments, the second-order reaction rate was calculated using the data of the second ³¹P NMR kinetic study and following the equation here presented:

$$k_2 = k_{PA} \frac{P_{A_0}}{c_0}$$

Equation 5 – Second-order rate constant (NMR).

Where:

P_{A_0} = Peak area at time zero;

c_0 = Initial concentration of reactants;

k_{PA} = Slope of the plot $\frac{1}{P_A}$ vs time.

Assuming this the k_2 was calculated, and an example of calculation is shown below.

$P_{A_0} = 10003205$; $c_0 = 1.42 \times 10^{-2} \text{ mol} \times \text{L}^{-1}$; $k_{P_A} = 2.43 \times 10^{-12} \text{ s}^{-1}$ (see Figure 36)

$$k_2 = k_{P_A} \frac{P_{A_0}}{c_0} = 2.43 \times 10^{-12} \frac{10003205}{1.42 \times 10^{-2}} = 1.71 \times 10^{-3} \text{ L} \times \text{mol}^{-1} \times \text{s}^{-1}$$

The value of $1.71 \times 10^{-3} (\pm 0.30) \text{ L} \times \text{mol}^{-1} \times \text{s}^{-1}$ is slightly lower (factor of circa 2x) in relation with the ones obtained above in the UV-Vis experiment, and is closer to the literature rate constants reported by Lloyd¹¹⁶ and Bartlett.¹¹³ In fact, if we consider the absolute error of ± 0.30 , our experimental rate constant value is in close agreement with the one presented by Bartlett¹¹³ of $1.27 \times 10^{-3} \text{ L} \times \text{mol}^{-1} \times \text{s}^{-1}$. In Figure 36 (see below) we can observe that the slope of the plot $\frac{1}{P_A}$ vs time has a R^2 a value of 0.9885. Therefore, we can extrapolate that the derivatisation reaction follows a second-order kinetics.

The outcomes from both experiments (UV-Vis and ³¹P NMR) were quite similar, the results show that the derivatisation reaction follows a second-order kinetics and full conversion is not achieved during the time frame of the study. To validate these results a couple of ³¹P NMR kinetic experiments were performed to confirm the overall reaction order of the derivatisation reaction and the orders with respect to each component (i.e., elemental sulfur and TPP).

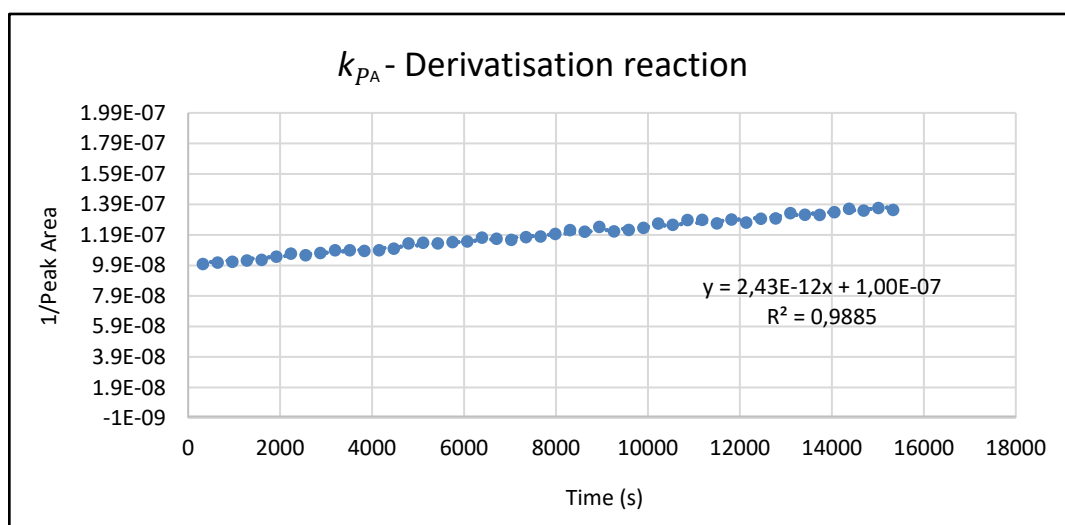


Figure 36 - Reciprocal of P_A vs. time of the derivatisation reaction.

To understand the order of reaction of the elemental sulfur and TPP the following two experiments were performed.

- 1) The second ^{31}P NMR kinetic study was repeated but this time with double the initial concentration of elemental sulfur. The kinetic procedure stayed the same and the kinetic curves obtained are presented in Figure 37.

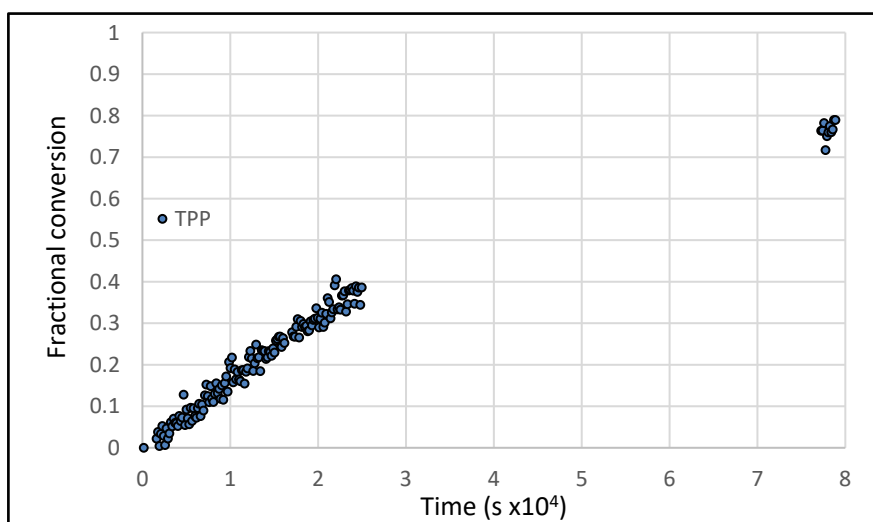
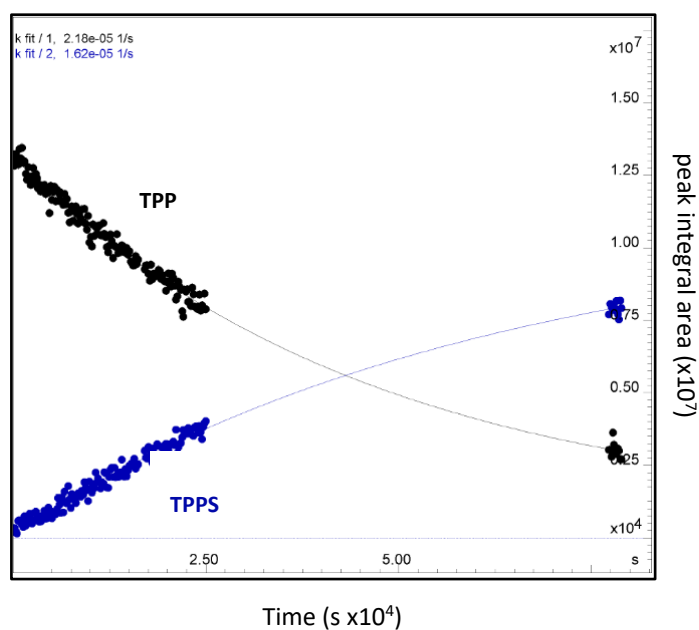


Figure 37 - ^{31}P NMR kinetic study of the derivatisation reaction between S_8 and TPP at RT in toluene with double the concentration of $[\text{S}_8]$ relative to TPP to study the order of the reaction and the associated fractional conversion vs. time plot. ($\text{Fractional conversion} = \frac{(n_{\text{TPP}})_{\text{reacted}}}{(n_{\text{TPP}})_{\text{fed}}}$).

- 2) The same kinetic study was conducted, but this time with the double of the TPP concentration. The results of this experiment are shown below (Figure 38).

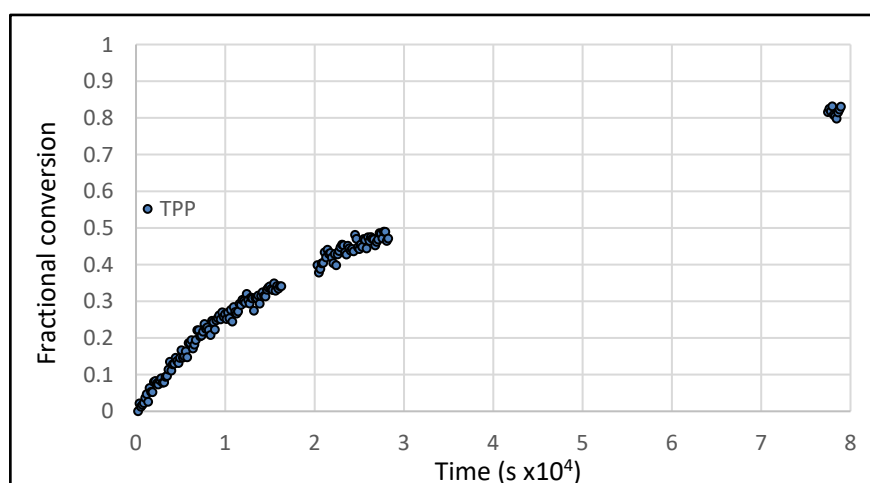
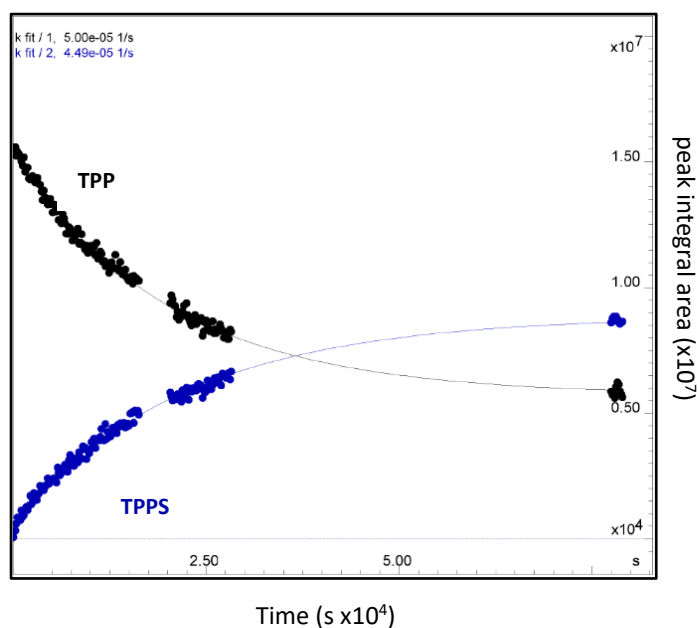


Figure 38 - ^{31}P NMR kinetic study of the derivatisation reaction between S_8 and TPP at RT in toluene with double $[\text{TPP}]$ to study the order of the reaction and the associated fractional conversion vs. time plot. ($\text{Fractional conversion} = \frac{(n_{\text{TPP}})_{\text{reacted}}}{(n_{\text{TPP}})_{\text{fed}}}$).

When comparing the three kinetic curves obtained for the ^{31}P NMR kinetic study of the derivatisation reaction, at RT in toluene, not many differences can be found (Figures 35, 37 and 38). The k value obtained for the formation of TPPS (blue line) is almost identical for Figures 35 and 38 with a value of $4.29 \times 10^{-5} \text{s}^{-1}$ and $4.49 \times 10^{-5} \text{s}^{-1}$, respectively, and slightly different for Figure 37 with a value of $1.62 \times 10^{-5} \text{s}^{-1}$. The small difference can be explained by a slight dispersion of the data points, especially on the last point. Despite this, we can say that the values are similar, and the rate of the reaction is not affected by the presence of higher concentration of elemental sulfur or TPP. With this, we conclude that the reaction is first order with respect to both elemental sulfur

and TPP, and the overall order is two. This is consistent with the results obtained previously and with the one reported by Bartlett.¹¹³

3.1.2 Optimisation of the derivatisation reaction

The derivatisation technique is widely used in analytical chemistry¹²¹ and mass spectrometry,¹²² especially to chemically modify the structure of the compounds so they can be analysed more easily by the desired technique. A good derivatisation reaction should produce the desired chemical modification of the compound of interest quantitatively, and be reproducible, efficient, and non-hazardous.¹¹⁴ Taking this into consideration, the efficiency of “our” derivatisation reaction was optimised. The optimisation was conducted having two main goals in mind:

- The full conversion should be achieved in a time frame suitable for analytical experiments;
- The reaction conditions should be as close as possible to the conditions that the mineral oil is subjected when in service.

The normal working temperature of a power transformer is 60 °C, this was the temperature that we settled for our experiments. The other parameters were optimised, and the final conditions and respective experiments are shown below. A set of three derivatisation reactions were conducted, on different days, using the optimised conditions. The efficiency of the reaction was monitored by the UHPSFC-MS (SIR method). The results of one of the UHPSFC-MS experiments is presented in Figure 39.

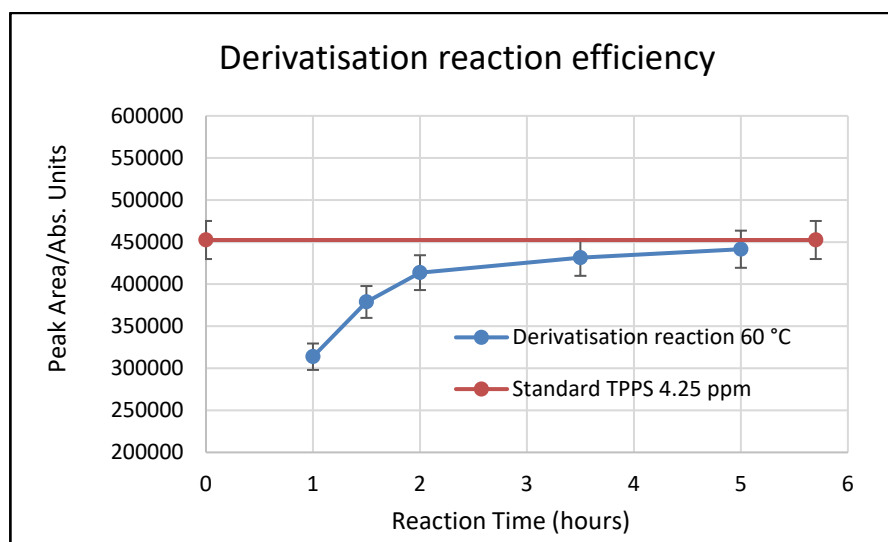


Figure 39 – First derivatisation efficiency study using the optimised conditions.

The experimental procedure consisted in a reaction of 4.5 mg of elemental sulfur (1.75×10^{-5} mol $\equiv 1.40 \times 10^{-4}$ mol of sulfur; 1 equiv.) with 250 mg of TPP (9.53×10^{-4} mol, ≈ 7 equiv.) in 10 mL (50% mineral oil / 50% toluene – optimum solvent mixture – see 3.3.1). The reaction was set to 60 °C and triplicate samples were taken after 1, 1h 30min, 2, 3h 30min and 5 hours. The autosampler vials

were prepared by dilution of 1:1000 of the samples in a solution of 50% mineral oil and 50% of toluene ($V_f = 1\text{ mL}$). The theoretical concentration of TPPS in the auto sampler if total conversion occurred is 4.13 ppm, for an easier interpretation of the results a TPPS standard of 4.25 ppm was also analysed.

In the Figure 39, the blue line displays the reaction efficiency. The well-defined curve is the expected pattern of the reaction efficiency, when we compare the results obtained with the standard concentration analysed (red line) we can conclude that the derivatisation reaction must reach completion between 3 and 5 h. For a clear understanding of the reaction time, a similar experiment was conducted. In this study the reaction efficiency was followed by ^{31}P NMR and the experimental procedure resided in a reaction of 3.38 mg of elemental sulfur ($1.32 \times 10^{-5} \text{ mol} \equiv 1.05 \times 10^{-4} \text{ mol}$ of sulfur; 1 equiv.) with 30.4 mg of TPP ($1.16 \times 10^{-4} \text{ mol}$, 1.1 equiv.) in 10 mL (50% mineral oil / 50% toluene). The reaction efficiency was analysed after 1, 2, 3 and 5 h and the results can be found below in Figure 40.

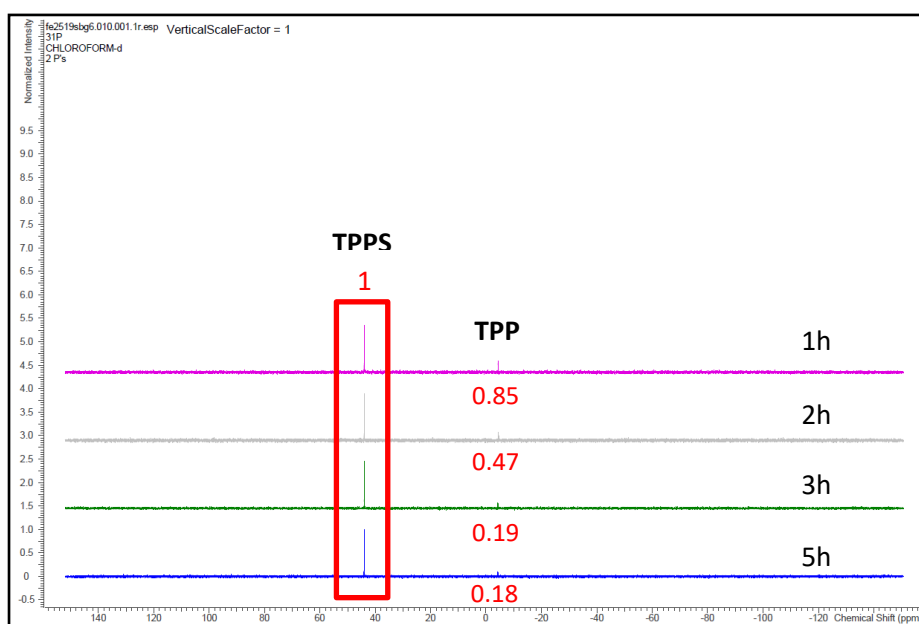


Figure 40 – Derivatisation reaction (1 equiv. S_8 : 1.1 equiv. TPP) followed by ^{31}P NMR.

From the ^{31}P NMR results obtained, the left peak (42.34 ppm) is associated with the presence of the TPPS and the right peak (-5.23 ppm) with TPP. The decrease of the TPP concentration is demonstrated by the reduction of the peak at -5.26 ppm . Although the results are similar to the ones in Figure 39, this time we can have a better understanding of when the reaction reaches completion. The TPP peak value between the 3 and 5 h is practically the same, so we can infer and conclude that the reaction reaches completion after 3 h. It was expected that the final integration values would be around of 1 (TPPS) to 0.1 (TPP), as the reaction was 1:1.1 equiv., this small discrepancy may be related to signal noise or to small differences in the relaxation time.

3.1.3 Summary

The derivatisation reaction rate was studied by UV-Vis and by ^{31}P NMR, the values obtained compare reasonably with the ones published in the literature. Following the reactions using UV-vis, the rates of reaction calculated were $3.59 \times 10^{-3} (\pm 0.30) \text{ L} \times \text{mol}^{-1} \times \text{s}^{-1}$ and $4.14 (\pm 0.30) \times 10^{-3} \text{ L} \times \text{mol}^{-1} \times \text{s}^{-1}$ in toluene at ambient temperature (actual value not controlled), for the ^{31}P NMR experiment it was $1.71 (\pm 0.30) \times 10^{-3} \text{ L} \times \text{mol}^{-1} \times \text{s}^{-1}$ at 25 °C in toluene. The obtained value in the ^{31}P NMR experiment compares more closely with that reported by Lloyd¹¹⁶ of $0.42 \times 10^{-3} \text{ L} \times \text{mol}^{-1} \times \text{s}^{-1}$ (in the same solvent – toluene) and with that reported by Bartlett¹¹³ for the same reaction in benzene of $1.27 \times 10^{-3} \text{ L} \times \text{mol}^{-1} \times \text{s}^{-1}$ than the ones obtained in the UV-vis experiments. In fact, if we consider the absolute error associated, the value of $1.71 (\pm 0.30) \times 10^{-3} \text{ L} \times \text{mol}^{-1} \times \text{s}^{-1}$ obtained in the ^{31}P NMR experiment can be considered similar to the one presented by Bartlett¹⁰⁹ of $1.27 \times 10^{-3} \text{ L} \times \text{mol}^{-1} \times \text{s}^{-1}$. The difference in measured rate constants can be explained (as discussed above) by the fact that the ^{31}P NMR experiment was conducted in a controlled environment with a temperature of 25 °C. Unfortunately, temperature control was not applied during the UV-vis kinetic experiments, and the temperature in the room, where the experiment was carried, can become quite warm. It is highly probable, that the differences in measured rate constants can be attributed to the lack of temperature control. Bartlett¹¹³ reported also that the derivatisation reaction follows second-order kinetics, being first order with respect to both elemental sulfur and TPP.

The efficiency of the derivatisation reaction was also studied, in the literature Borchardt and Easty¹¹⁵ reported that the reaction was virtually instantaneous at room temperature in toluene. Throughout the experiments, it became clear that the reaction did not reach completion as fast as reported. In the NMR studies this was confirmed when the conversion obtained after 18 h and 30 min was only around 66% for the reaction in 50% mineral oil/ 50% toluene and 75% in toluene. Optimisation of the reaction conditions were conducted and full conversion after 3 h at 60 °C was demonstrated by ^{31}P NMR and UHPSFC-MS experiments.

3.1.4 Derivatisation selectivity

The selectivity of the TPP for elemental sulfur and their reaction to form TPPS is a key requirement of this analytical method. Side reactions of the TPP with the other sulfur compounds present in the mineral oil would present us with false positives and overestimates of the S_8 concentrations. The TPP reactivity with other sulfur compounds was studied using the same conditions used in the derivatisation method. It is clearly not practical to test all sulfur compounds identified to occur in

mineral oil, so three representative sulfur compounds containing different sulfur functional groups and with different reactivities were studied.

These compounds are:

- DBDS (dibenzyl disulphide) - Figure 41.
- Benzothiophene - Figure 42.
- 4,6-Dimethyldibenzothiophene - Figure 43.

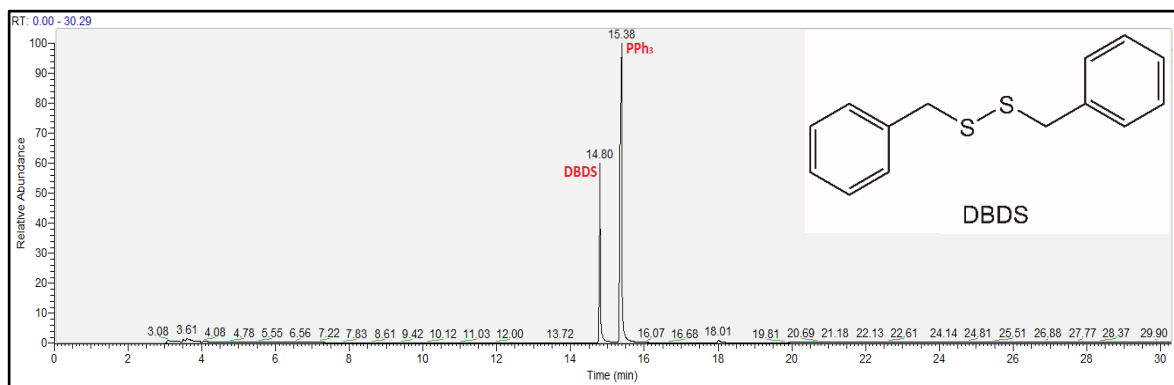


Figure 41 – GC-MS of the reaction of TPP with DBDS.

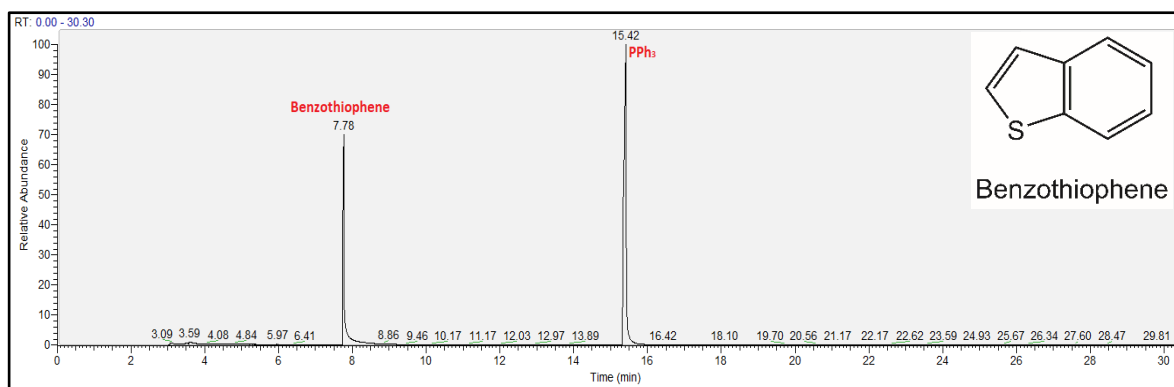


Figure 42 - GC-MS of the reaction of TPP with benzothiophene.

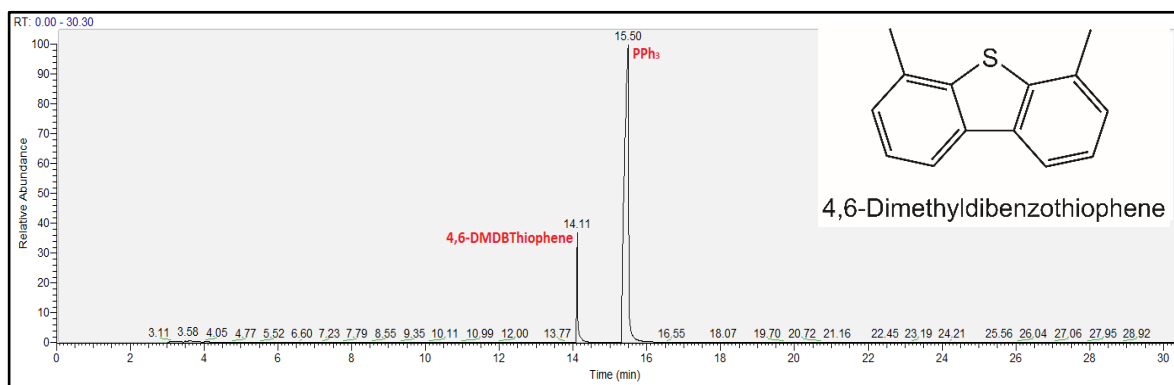


Figure 43 - GC-MS of the reaction of TPP with 4,6-Dimethyldibenzothiophene.

All three samples were analysed using a GC-MS with a non-polar column. The reactions were conducted under identical conditions, i.e., using the same reaction conditions (3 h at 60 °C) and quantities (1 equiv. of TPP to 1.1 equiv. of the sulfur containing compound). From the GC-MS results, we can conclude that the reaction of TPP with these three sulfur compounds is negligible under the chosen conditions. This leads to the conclusion that the studied sulfur compounds (e.g., DBDS) have a lower reactivity than elemental sulfur with TPP (under identical conditions). The lower reactivity can be explained by different factors, e.g., electronic, steric and stereoelectronic effects. Extrapolating this we can infer that the side reactions of TPP with the other major sulfur compounds, belonging to the same compound classes, present in mineral oil are likely to be negligible too. These results provide confidence that TPPs formed during our studies will be due to the presence of elemental sulfur and not from side reactions with typical organosulfur compounds present in mineral oil.

3.1.5 Interference from the dilution solvent

The dilution solvent, as the name suggests, is used in the GC-MS and UHPSFC-MS vial samples to dilute the solution to a concentration suitable for analysis (concentrated samples result in overloaded peaks), and to increase the solubility of TPPs, which is poorly soluble in the mineral oil. In addition, the rate of reaction of TPP with S₈ in pure mineral oil may be reduced. Due to the different optimal working conditions between the two different analytical instruments, the solvent is added to the autosampler vial in different concentrations – in our case, it is 90% of solvent concentration for the GC-MS analysis and 50% for the UHPSFC-MS analysis (see 3.3.1 for the sample mixture optimisation), immediately before the analyses are conducted. So, it is important to understand if the dilution solvent affects (possibly by the presence of trace sulfur impurities) the TPPs formed during the sample analysis. This was studied by performing the following experiment:

- 4 autosampler vials (2 samples of toluene and 2 samples of DCM) of 1 mL were prepared;
- 10 mg of TPP was added to each vial and an UHPSFC-MS (Total Ion Chromatogram (TIC) and SIR) analyses were conducted immediately.

The results for the UHPSFC-MS TIC analyses are shown below in the Figure 44.

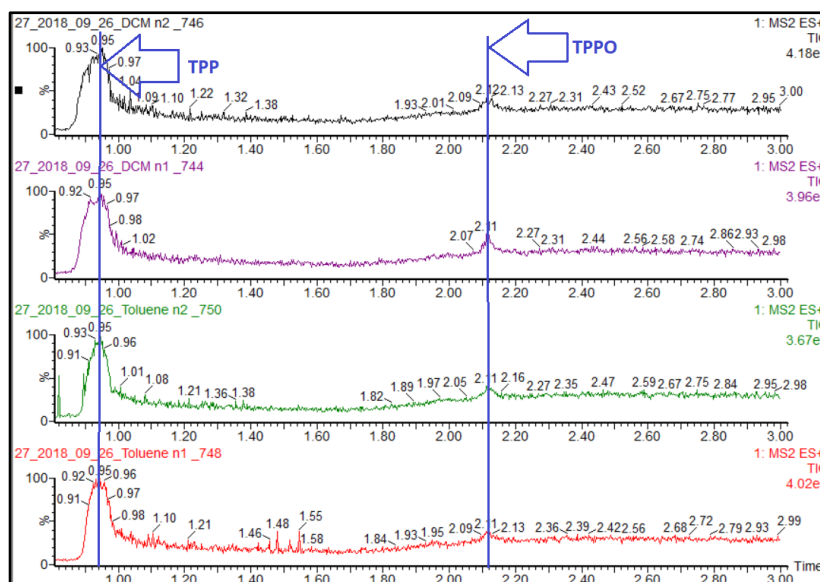


Figure 44 - TIC of DCM (#1,2) and toluene (#3,4) after reaction with TPP by UHPSFC-MS.

Inspection of the TIC chromatograms in Figure 43 reveals two peaks, shown with the blue lines, common to all of the samples. The first peak at $t_R \sim 0.50 - 1.00$ min has a very similar abundance and corresponds with the retention time of TPP. The second line indicates the peak for the triphenylphosphine oxide (TPPO) at $t_R \sim 2.55 - 2.60$ min, which is a side product due to the reaction of TPP with the atmospheric oxygen. Gratifyingly, no peak corresponding to TPPS is observed.

The UHPSFC-MS SIR (m/z : 295) results are shown in Figure 45.

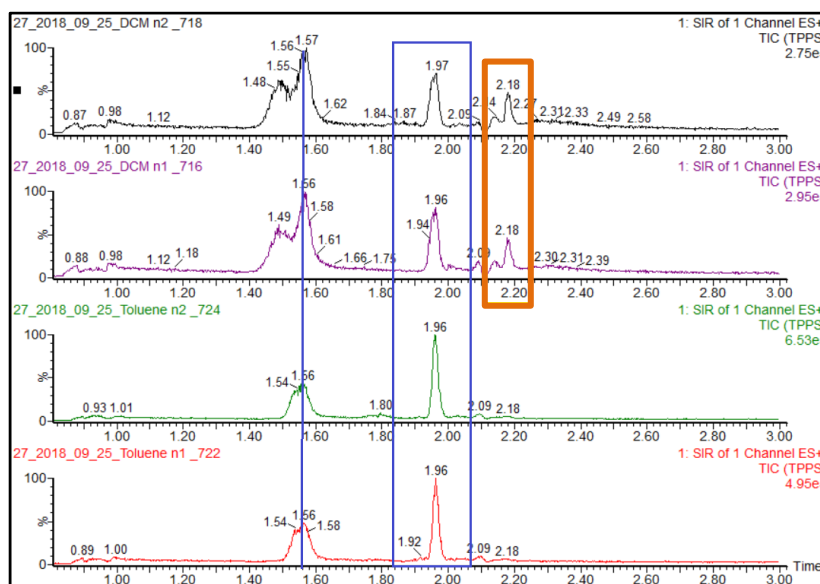


Figure 45 - SIR (m/z : 295) of DCM (#1,2) and toluene (#3,4) after reaction with TPP by UHPSFC-MS.

The UHPSFC-MS SIR chromatogram shown above, in Figure 45, shows the presence of several different peaks that allude to the presence of different ions with m/z of 295 (expected m/z for the ion of interest $[TPPS+H]^+$). For an easier interpretation, three distinct peaks/areas were identified

and marked in the chromatogram. Two of those areas (blue line and blue box) are commonly present in the toluene and DCM samples, and the orange box is only present in the DCM samples. After careful analysis of the mass spectrum, the peak with retention time of $t_R \sim 1.56$ min (blue line) was attributed to the elution of TPPS (observed ion $[\text{TPPSH}]^+$, the peak at $t_R \sim 1.96$ min (blue box) was tentatively assigned to TPPO_2^{123} (observed ion $[\text{PPh}_3\text{O}_2\text{H}]^+$) and the orange box (peak at $t_R \sim 2.18$ min) corresponds to an unidentified compound. Toluene was then recognised as the best option for dilution solvent. Due to the fact that its use presented a lower concentration of TPPS in the end (i.e., smaller peak area of the blue line peak) and the presence of less side reactions (only two peaks were present). The concentration of TPPS found in the toluene samples was less of 50 ppb, which equals to less of 5 ppb of S_8 . The presence of trace concentrations of S_8 in toluene is not desirable for their purpose as dilution solvent, but since the amount present equals to less than 5 ppb, we considered that such amount is neglectable when considering the purpose of the analysis/research project. For details regarding the determination of the limits of detection and quantification of TPPS/ S_8 for this method, please see sub-chapter 3.3.2.

3.1.6 Attempts to increase the rate of the derivatisation reaction: alternative P(III) compounds.

The conditions of the derivatisation reaction of elemental sulfur using TPP were optimised and complete conversion was accomplished. The conditions used consisted in a reaction of TPP (excess) with elemental sulfur at 60 °C for 3 h. With the aim to obtain a faster reaction rate, thus decreasing the reaction time, three different tertiary phosphines were considered (Figure 46).

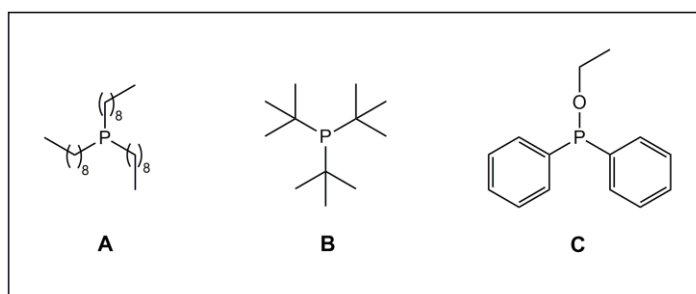


Figure 46 – Tertiary phosphines studied - trioctylphosphine (A), tri-*tert*-butylphosphine (B) and the ethyl diphenylphosphinite (C).

The trialkylphosphines **A** and **B** were available in the laboratory and compound **C** was synthesised (see organic experimental part). Compound **C** was found to be readily oxidised when in contact with air, with full conversion to the oxide occurring so rapidly that was not possible to carry out the derivatisation experiment. For the other two compounds, **A** and **B**, their suitability to be used in the derivatisation reaction was studied.

The experimental procedure consisted in a stoichiometric reaction of compound **A** (0.0312 mmol) or **B** (0.1188 mmol) with elemental sulfur at 60 °C in a solution of 50% mineral oil and 50% toluene (i.e., optimum conditions used for the derivatisation reaction). The reaction was followed during 3 h by ^{31}P NMR, and the results can be seen in Figure 46 (above) for compound **A** and Figure 47 (below) for compound **B**.

Figure 47 shows the ^{31}P NMR obtained for the derivatisation reaction using trioctylphosphine (A). Marked by the green box is the respective sulfide and by the red box the respective oxide. The reaction was followed over 3 h, and analyses of the results indicate that the formation of the oxide is a significant side reaction compared to the formation of sulfide. The final integration presented a value of 1 for the oxide, of 0.05 for the sulfide and 0.64 for the starting phosphine. By analysing the change in relative peak areas (from integration of the ^{31}P NMR spectra) of the different compounds over the course of the experiment, it is possible to see a clear increase in the amounts of the oxide but only a small increase in the sulfide over the time. It is likely that some of the oxide was already present at the beginning of the experiment, although starting material spectrum was not recorded to confirm this hypothesis.

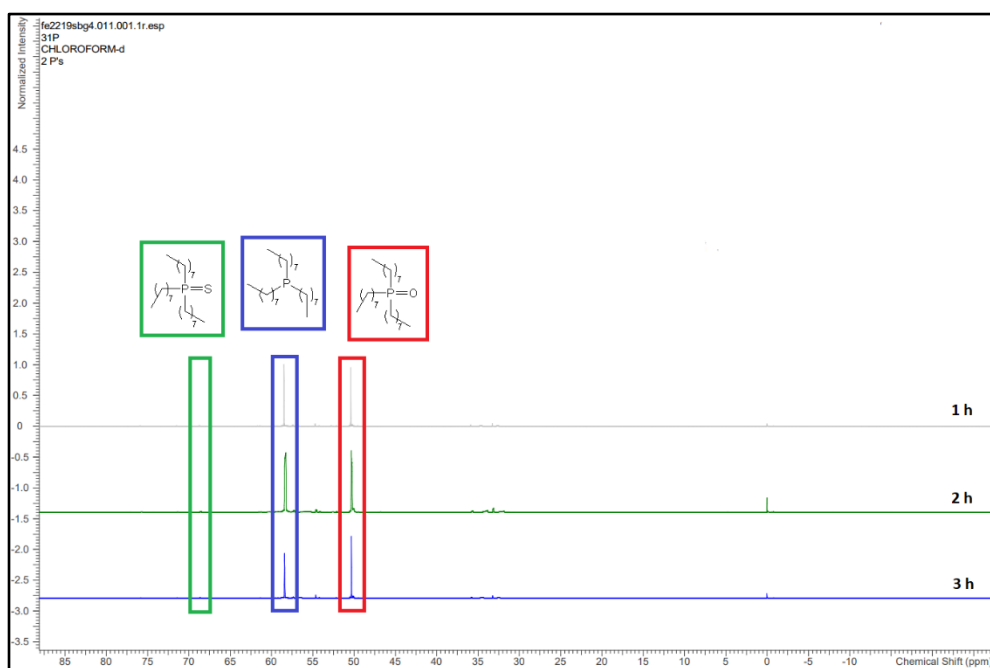


Figure 47 – ^{31}P NMR of the derivatisation reaction using the trioctylphosphine (A).

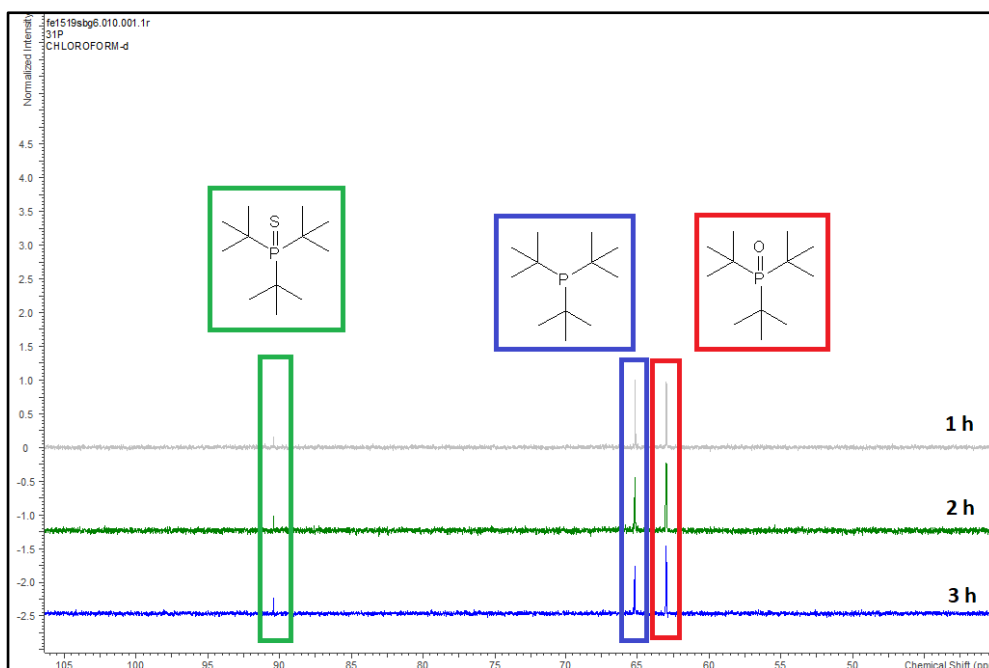


Figure 48 - ^{31}P NMR of the derivatisation reaction using tri-*tert*-butylphosphine (B).

A similar conclusion can be made after analysing the results shown in Figure 48. The starting material tri-*tert*-butylphosphine (B) is highlighted by the blue box, the respective oxide by the red box and the sulfide by the green box. In the end of the experiment, the peak of the oxide was set to 1, obtaining a value of 0.59 and 0.22 for the integration of the starting material and sulfide, respectively. The formation of the sulfide is not complete after the 3 h and by integration of the signals we can conclude that the formation of the oxide is favourable. In summary, none of the 3 alternative phosphorus(III) compounds studied is a suitable replacement for the TPP in the derivatisation reaction. In all the cases the formation of the oxide is a significant side reaction, which predominates compared to the formation of the respective sulfide. Therefore, all subsequent studies were conducted using TPP.

3.2 Development of the GC-MS method.

Different chromatography-MS approaches were investigated for quantification of TPPS in mineral oil. The use of GC coupled to an MS with electron ionisation (EI) provided an efficient method for detection of TPPS. For reliable analysis of the transformer oil samples by GC-MS, regular maintenance to prevent ion source contamination and subsequent rapid loss of sensitivity was performed. Two different columns, with different polarities were studied. The results and conclusion of this experiments are shown below.

3.2.1 Using a non-polar column

The analysis of the oil samples was initially undertaken using a non-polar column GC-MS using various parameters to investigate the best conditions for TPPS elution. In the beginning of each analysis three blanks of toluene were performed and one blank of toluene between samples to prevent carryover issues. The main parameters optimised were the split ratio, the injector temperature and the ramp rate of the temperature of the oven in order to have a better resolution and sensitivity for the TPPS. The best results were obtained when the injector temperature was set at 220 °C and the temperature program used was 60 °C for 3 min which then increased at 10 °C/min to 320 °C and then held for 10 min. For the complete configuration please check the analytical experimental part. After all the parameters were optimised, the limit of detection (LOD) of the SIR method was studied. Standard solutions of new mineral oil with different concentrations of TPPS, with a range from 2 to 20 ppm were prepared and analysed. The results for the samples with concentrations of 20, 4 and 2 ppm are shown in Figure 49. From these results, the Limit of Detection (LOD) of the method was found to be 4 ppm of TPPS, which corresponds to less than 0.5 ppm of elemental sulfur.

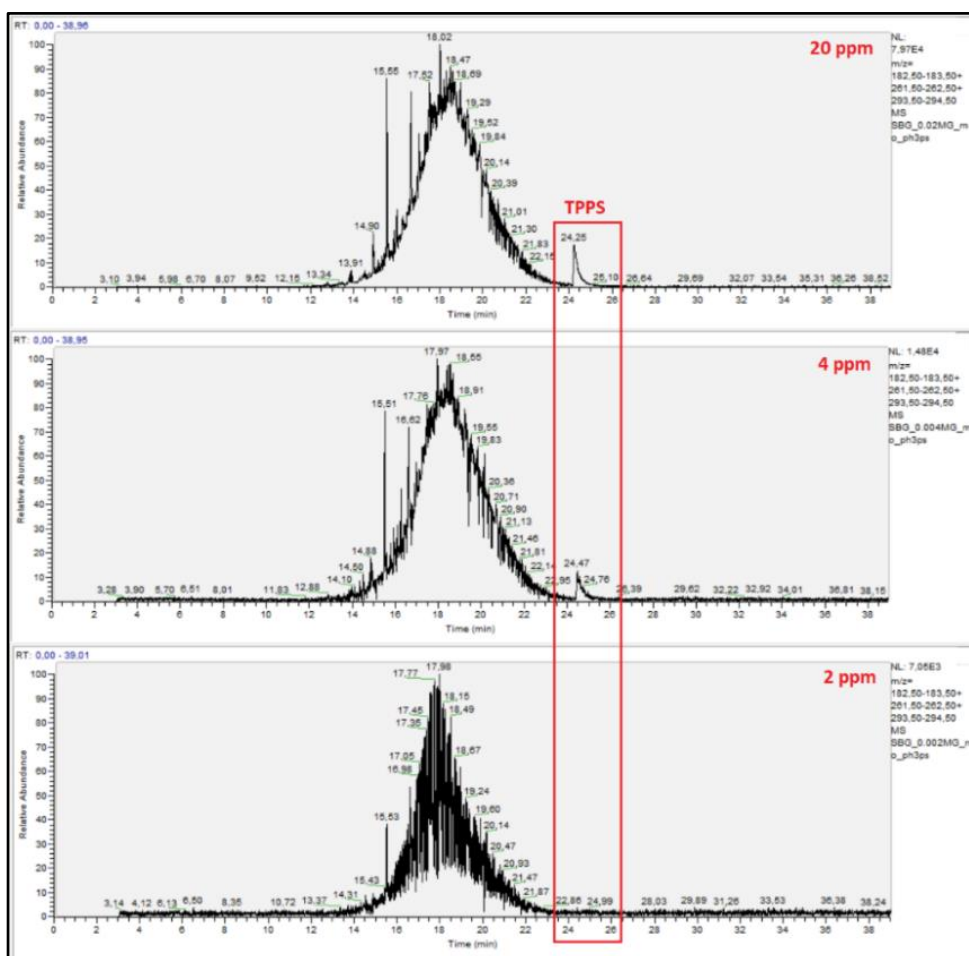


Figure 49 - Standard concentrations of TPPS (20, 4 and 2 ppm) in new mineral insulating oil analysed by GC-MS with a non-polar column.

From the data obtained a calibration curve was plotted and a value of 0.9915 was obtained for the coefficient of determination (R^2). This value shows that our calibration curve is a good representation of the detector response. By analysis of the curve, was evident that the accuracy of the calibration curve was slightly affected by the small dispersion of the data points at the low end of concentration.

This method was employed to study mineral transformer oil samples provided by National Grid plc. One of the samples, mineral oil **A**, was analysed and the result can be found in the Figure 50.

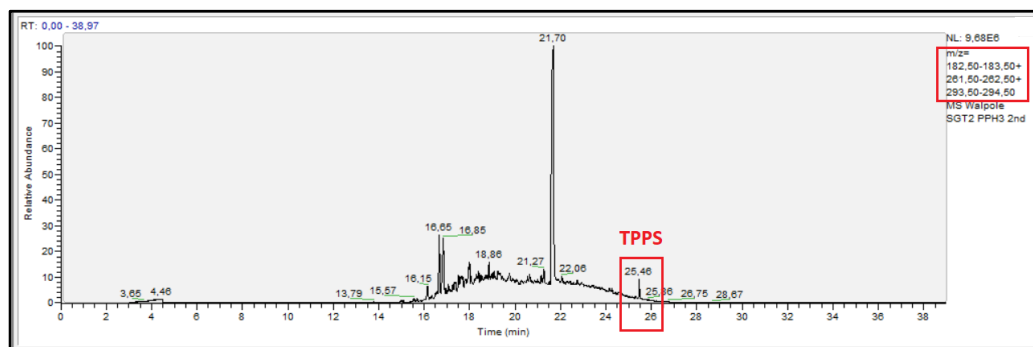


Figure 50 - SIR of the analysis of the mineral oil **A** using a non-polar column GC-MS.

The result of the analysis of the mineral oil **A** indicated the presence of elemental sulfur in the oil sample. The formation of TPPS is demonstrated in Figure 50 by the presence of the peak at t_R 25.46 min. The peak elutes with other components of the mineral oil, so quantification of the TPPS and consequently the concentration of elemental sulfur present in the sample cannot be calculated accurately.

3.2.2 Using a polar column

To investigate if a better resolution and sensitivity for the TPPS could be achieved by GC-MS, a standard solution of 20 ppm of TPPS in mineral oil was analysed using a polar column. The optimised conditions were as follows: the injector temperature was set at 220 °C and 1 μ L of sample was injected in splitless mode. The temperature program used was 40 °C for 10 min which then increased at 10 °C/min to 240 °C and then held for 20 min. For the comprehensive method conditions see 2.3.3., in the analytical experimental section. The results of the TIC and SIR analyses are shown below in Figure 51.

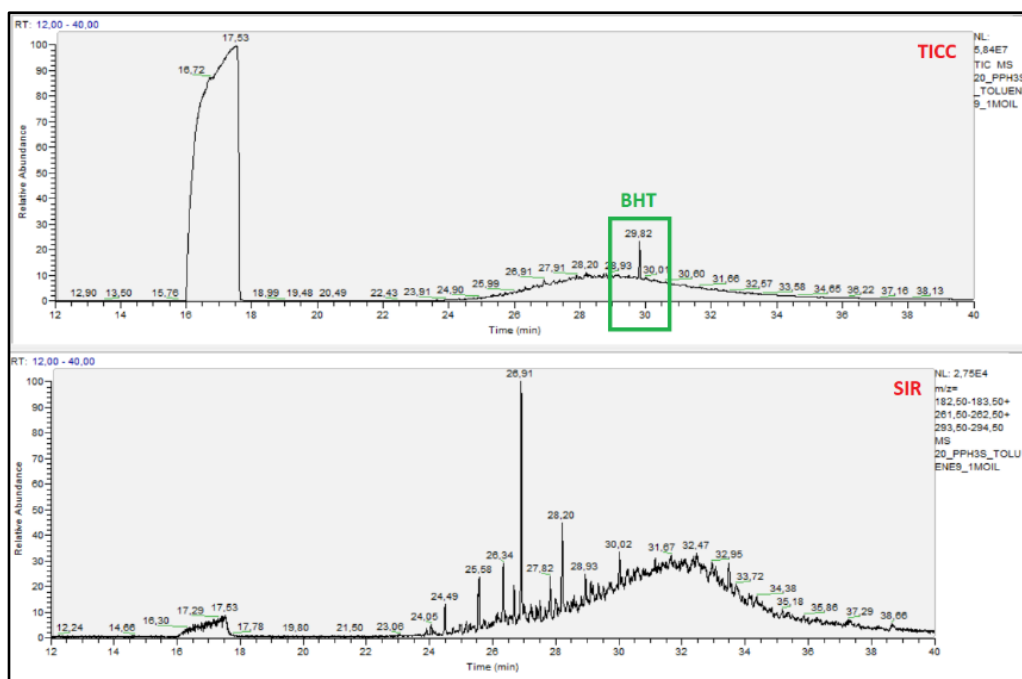


Figure 51 - TIC and SIR analyses of a 20 ppm standard solution of TPPS in new mineral insulating oil using a polar-column GC-MS.

This experiment allowed us to establish two important findings. The first one was that the polar column is not suitable for the separation of TPPS, since no peak corresponding to the elution of the TPPS can be found when analysing the TIC and SIR results. The second one, was that this method was able to point out the presence of 2,6-di-*tert*-butyl-*p*-cresol (BHT), which is an anti-oxidant added by the manufacturer of the mineral insulating oil. This is crucial as BHT is an additive used to extend the life time of the transformer, allowing this technique to be used to identify samples that could be at risk of oxidation.

3.2.3 Summary

A GC-MS method was developed for detection of elemental sulfur in diverse samples of mineral insulating oils with varying compositions and chemistries. This method uses standard GC-MS equipment that can be found in most analytical laboratories. Our technique allows the detection of trace levels of elemental sulfur levels in mineral oil down to 0.5 ppm. Due to the properties of some mineral oils, quantification might not be possible, because of the overlap of the elution of some compounds present in the mineral oil with TPPS, leading us to pursue a more sensitive method detailed in the following sections.

3.3 Development of the UHPSFC-MS method.

Triphenylphosphine (TPP) reacts quantitatively with elemental sulfur to give TPPS,¹¹¹ which displays favourable ionisation properties under positive ion ESI conditions. An excellent method to detect TPPS is to use GC-MS with electron ionisation (EI) or an element selective detector (P or S), but when the nature of the matrix is taken in consideration some limitations arise. The analytical instrument needs to be able to detect low ppb levels of the derivatised compound over the course of all the analyses, and maintaining the performance and selectivity is demanding when analysing a complex matrix such as mineral oil. A similar difficulty was faced previously by Langley and colleagues when trying to quantify the fuel marker ACCUTRACE S10 using a GC-MS instrument.¹²⁴ The issue was overcome by employing a UHPSFC-MS method to quantify the fuel marker at tank dilutions, so a similar approach was considered for the analysis of TPPS. Therefore, atmospheric pressure ionisation techniques were explored in combination with SFC to provide reliable and short analysis times. The effectiveness of the ionisation of TPPS was explored using ESI for a 1 ppm standard solution, using an ESI UHPSFC-MS Single Ion Monitoring (SIM) method (m/z 295). TPPS was found to undergo efficient ionisation, with reduced interference arising due to ionisation of the matrix. Under the selected conditions TPPS has a retention time of 1.5 min, and the protonated molecule ($[TPPS + H]^+$) is observed with a signal to noise (S/N) of 161 (Figure 52).

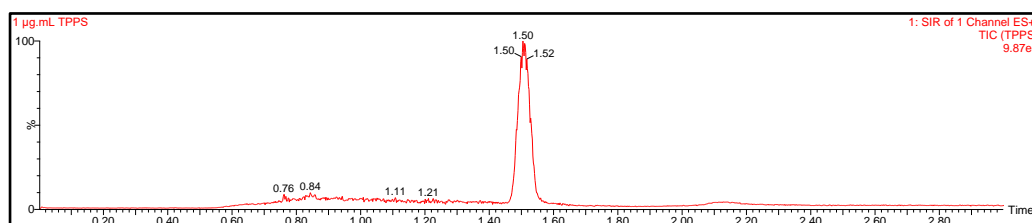


Figure 52 – ESI UHPSFC-MS SIM of TPPS at 1 ppm (S/N 161).

Positive ESI MS conditions for TPPS and the chromatographic method were optimised providing an analysis time of 3 min per sample. For quantification, an external standard calibration was employed where the ion at m/z 295 ($[TPPS + H]^+$) was used. Sample preparation was adapted to mitigate against the low solubility of TPPS in neat mineral oil and different solvents were studied based on their capacity to dissolve both TPPS and mineral oil. A 50 : 50 mineral oil/toluene mixture (v/v) provided acceptable solubility while maintaining good chromatographic efficiency and resolution (see below for the sample mixture optimisation study).

3.3.1 Sample Mixture Optimisation

Sample preparation was investigated with respect to TPPS solubility; when analysing neat mineral oil samples, poor reproducibility for TPPS concentration was obtained due to low solubility of the

analyte. Different solvents were studied (i.e., acetonitrile, dichloromethane and toluene) and based on their capability to dissolve both TPPS and mineral oil, and their chromatographic characteristics, lead to the selection of toluene as a dilution solvent. The optimum sample composition was studied by analysing samples of different concentrations of TPPS (0 to 20 ppm) in different mixtures of mineral oil : toluene (v/v). Several studies were conducted to understand which sample mixture would present the most reliable results, when analysed by our UHPSFC-MS SIR method. A representative result from this experiment is shown below. Solutions of TPPS, with concentration of 5 ppm, were prepared in different oil/toluene mixtures and analysed using the UHPSFC-MS SIR method ($m/z = 295$ ([TPPS +H]⁺).

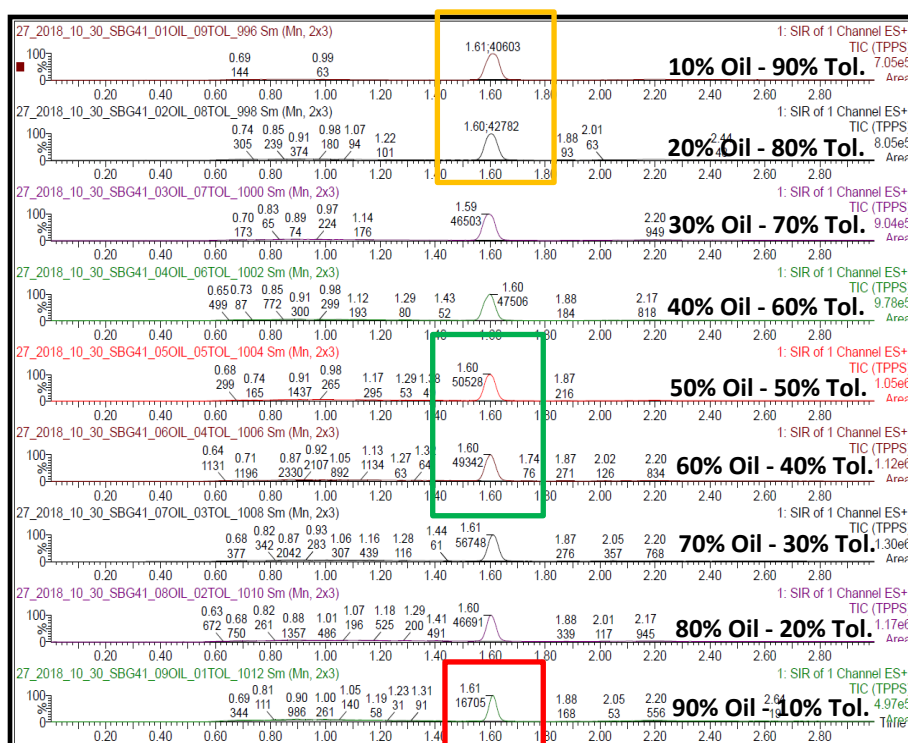


Figure 53 - UHPSFC-MS (SIR) of samples with 5 ppm of TPPS in different mixtures of mineral oil/toluene.

The data (not presented in full) showed that the detector response presented a similar behaviour throughout. It was detailed that the concentration of TPPS in the mixtures did not negatively affect the detector response, however the composition of the oil:toluene mixture was found to be important. In Figure 53, three different areas are highlighted. The green box displays the solvent mixtures that presented less interference in the analyses, and in the other hand, the orange and red boxes show the mixtures which presented a higher effect on the detector response, and per consequence in the outcome of the analyses. The orange box represents the samples with ratios of mineral oil: toluene of 10:90 and 20:80, with peak areas of 40603 and 42782, respectively. The red box identifies the sample with content of 90:10, with a peak area of 16705. In both cases, the peak area obtained is significantly lower than the ones obtained for all the other sample mixtures (e.g., peak area of 50528 for the sample mixture 50:50). In the latter case, the response of the instrument

drops 60 - 70%. This can be explained by the poor solubility of TPPS in mineral oil, from this experiment we can infer that concentrations of toluene equal or lower than 10% are not sufficient to solubilise all the TPPS in the mineral oil : toluene samples. After everything was considered, the dilutions of 50:50 and 60:40 mineral oil/toluene (v/v) were found to present the most reliable conditions to ensure solubility of TPPS and interpretation of data. Since preparation of samples plays a major role, and considering that the dilution of 50:50 it's simpler and easier to prepare, consequently less prone to measurement errors, this dilution was established as the optimum sample mixture.

3.3.2 Method validation

The first step, in the validation of the UHPSFC-MS SIR method, was to find the upper limit of quantification (ULOQ) and the lower limit of quantification (LLOQ). These limits represent the highest and lowest, points that can be used for accurate quantification of an analyte (e.g., TPPS) in a calibration/standard curve. To study the ULOQ and LLOQ of TPPS in our samples, an experiment was conducted. This study consisted in the preparation and (quadruplicate) analyses of TPPS samples that were prepared with known concentrations, ranging from 0 to 20 ppm. Standard curves were found to be linear over the range measured 0 – 5 ppm, with correlation coefficients (R^2) of 0.992 or better. A representative calibration curve is shown in Figure 54, from the obtained value for R^2 (0.9982) and from the visual inspection of the standard calibration curve, we can conclude that the data points fit/overlap with curve really well. This indicates a near-perfect positive correlation. A LLOQ of 0.05 ppm (S/N of 33) and an ULOQ of 5 ppm was set and used for all analyses, the chromatograms which served as basis for this decision are shown in Figure 55.

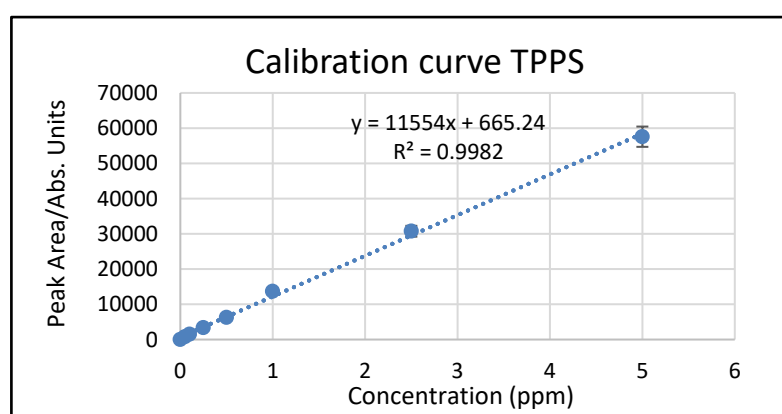


Figure 54 - Calibration curve obtained from TPPS standards (5 ppm, 2.5 ppm, 1 ppm, .05 ppm, 0.25 ppm, 0.1 ppm and 0.05 ppm) analysed using the UHPSFC-MS SIR method.

Carryover was then assessed by calculating the concentration of TPPS present in the blanks performed in between standard analysis, and was only found present when analysing samples with

concentrations close to the ULOQ and presented a value of $\leq 0.5\%$. TPPS was found to be stable for at least 24 h at ambient temperature or in the autosampler at 4 °C. Intraday reproducibility was determined by the analysis of three standard samples with different concentrations over the range of 0 - 5 ppm on three separate occasions, the method was found to be reproducible with a maximum relative standard deviation (RSD) of 2.03%. Interday reproducibility was determined by comparing TPPS concentrations calculated from several calibration curves performed on different days. This type of comparison is not possible as the response of the instrument for the same concentration was not constant. Interference of the matrix on the concentration of TPPS is minimised as most components in mineral oil are not ionized by ESI, and a SIR method is employed. Furthermore, the retention time of TPPS is separated from the vast bulk of the oil components.

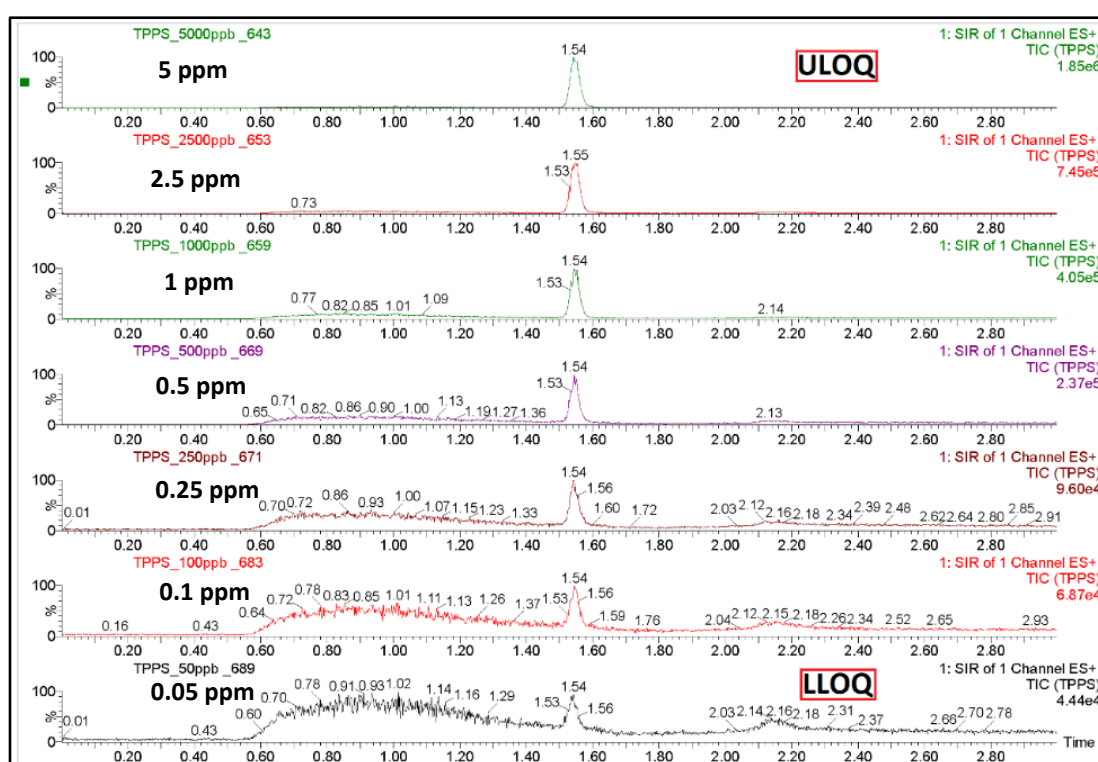


Figure 55 – ULOQ and LLOQ of the TPPS in mineral oil using the UHPSFC-MS SIR method.

3.3.3 Is elemental sulfur present in the new mineral insulating oil A?

The presence of elemental sulfur in new mineral insulating oil is of critical concern. Two studies were performed to quantify the elemental sulfur concentration in the new mineral insulating oil A, which was used in many of the power transformers from National Grid UK, and the results are shown in Figure 56.

By analyses of the chromatograms, we can conclude that TPPS was formed when TPP was added to the new mineral oil from the presence of the peak at $t_R \sim 1.56$ min (Figure 56). All the three samples present similar area peaks (6379, 6498 and 5732), which correlates to a similar value obtained for

the integration of the TPPS peak. Using the calibration curve (Figure 54) we can calculate the concentration of the elemental sulfur present in the sample. Taking in consideration the fold increase, the $[S_8]$ present in toluene (~5 ppb) and the dilution of the sample, a value of ≈ 95 ppb is obtained for the elemental sulfur concentration in the new mineral insulating oil A. Considering that the lowest value of $[S_8]$ that has been reported that might be sufficient to induce silver corrosion within the power transformer, was of 1 ppm, a value of 0.095 ppm should not present a risk.²⁰ We can safely assume that the new mineral insulating oil A, is not responsible from the silver corrosion issues in the power transformers. So, silver corrosion must be linked to the reappearance of S_8 during the usage of the oil (e.g., in the oil reclamation due to possible overheating of oil during storage in buffer tanks and/or by incomplete combustion during reactivation of clay columns).

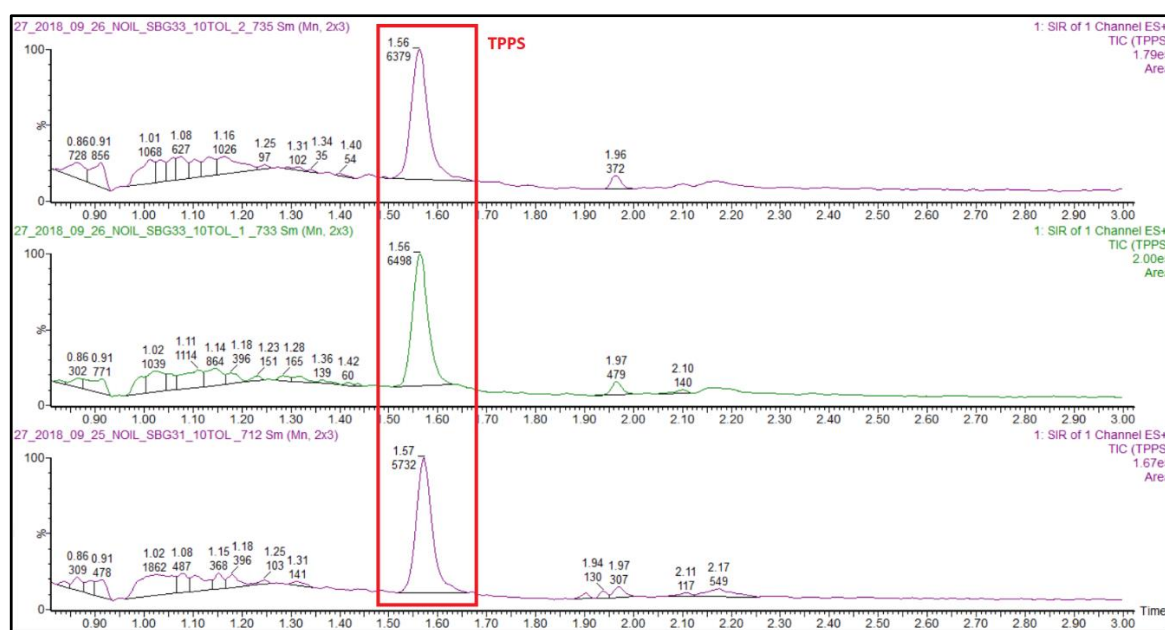


Figure 56 – Integrated chromatograms for the TPPS found in new mineral insulating oil A by UHPSFC-MS using the SIR method.

3.3.4 Analysis of ex-service mineral oil samples

Following optimisation and validation of the UHPSFC-MS method, it was then applied to the analysis of “real” mineral oil samples from power transformers, some of which were believed to be corrosive. These “real” samples are different samples from ex-service mineral oil samples, kindly supplied by National Grid UK. The example shown in Figure 57, is the SIR chromatogram obtained from a real mineral sample oil that was doped with elemental sulfur prior to the derivatisation process. The chromatogram shows a peak at a retention time of 1.62 min corresponding to TPPS ($[TPPS + H]^+$) and two additional clear peaks at 2.05 and 2.21 min (identification of the molecules was not possible). The peaks do not elute in the same region as the TPPS peak, so accurate quantification of TPPS is not compromised. An additional useful finding from analysis of the ex-service transformer

oils is that the different chemistries inherent to each sample, due to different working conditions, did not appear to have any negative effect on the analysis performed.

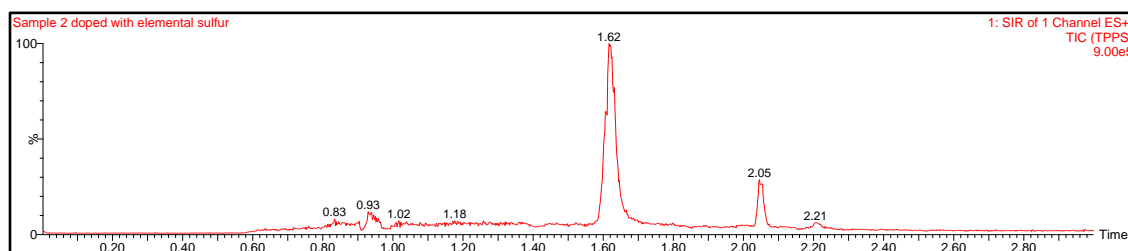


Figure 57 – UHP-SFC-MS SIR chromatogram from a real mineral oil sample doped with S₈.

From the real oil samples tested only one, designed as ex-service mineral insulating oil B, presented a concentration of S₈ around 17 ppm, that was considered high enough to present a corrosive risk for the transformer. The SIR chromatogram of one of the triplicate analyses is shown below in Figure 58.

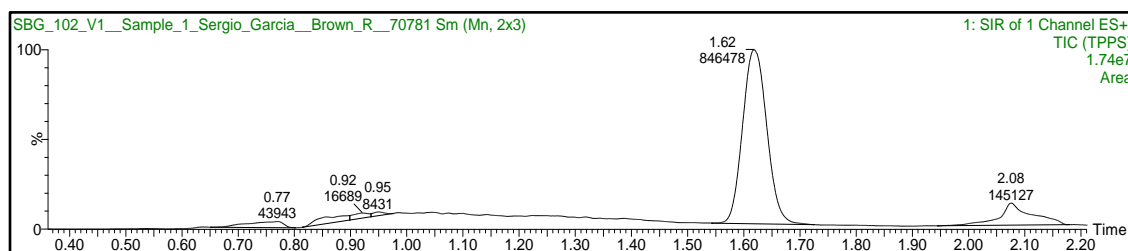


Figure 58 - UHP-SFC-MS SIR chromatogram from the ex-service mineral oil sample B.

The peak at 1.62 min with area of 846478 corresponds to TPPS. Using the appropriate calibration curve, with an equation of $y = 116.5x + 15114$ where x is the concentration of TPPS in ppb and considering all the relevant dilutions the concentration of S₈ was calculated. A medium value of ≈ 16 ppm of S₈ was obtained, from the other analyses, values of ≈ 17 and ≈ 18 ppm were attained. The concentration of the real oil sample B was then set to be ≈ 17 ppm, a value that in according to the literature should present a corrosive risk for the power transformer.²⁰ To gain qualitative evidence that the oil B was indeed corrosive, the sample was evaluated by subjecting it to the silver standard corrosion test (DIN 51353).¹⁸ This standard specifies a qualitative method to detect sulfur species in insulating mineral oils that are corrosive towards silver, classifying an oil sample as corrosive or non-corrosive. The samples are classified as corrosive if they cause a visible discoloration of the silver strip due to formation of silver sulfide. The principle of the test consists in emerging a silver strip in the sample oil of interest for 18 hours at 100 °C, followed by inspection of the silver strip for discoloration. The limit of detection of the test for elemental sulfur is 2 mg of elemental sulfur in 1 Kg of oil (2 ppm). The detailed procedure is provided in the experimental section. For ex-service oil B, a black coloration of the silver strip is clearly evident due to the presence of silver sulfide on the silver strip surface (Figure 59). This result undoubtedly indicates

that the oil sample B is corrosive towards silver, presenting a considerable risk for the power transformer. Due to the corrosive nature of oil B together with confirmation of the presence of S_8 by the analytical method, we decided to utilise ex-service oil sample B in all our reclamation processes (see chapter 4).



Figure 59 - Corrosion test result of the ex-service mineral oil sample B subjected to the standard corrosion test (DIN 51353). The presence of the black colouration (silver sulfide) indicates that the oil is corrosive.

3.3.5 Reproducibility of the UHPSFC-MS method when applied to ex-service mineral oil samples

To test the reproducibility of the UHPSFC-MS method to quantify the presence of S_8 in ex-service mineral oil samples, two different samples supplied by National Grid were analysed three times and on different days. A new calibration curve was plotted each day, to prevent errors associated with small differences in the detector response.

These samples, designated ex-service mineral oil samples C and D, represent samples of the same ex-service oil (R) taken before (sample C) and after (sample D) a reclamation process that was conducted in the field to restore the properties of the mineral insulating oil. Our investigation aimed to understand not only the reproducibility of the method when applied to ex-service samples but also gather useful information about the effectiveness of the reclamation process to reduce/increase the S_8 concentration in the oil. The analyses were divided in three experiments, two of them were performed on the same day and the last one was performed on the successive day. Although, each experiment was conducted in triplicate only one representative analysis will be presented here. The results for the sample C are shown in Figure 60 and for sample D in Figure 61 (see below). The concentration of S_8 (in ppm) obtained for each experiment was calculated using the according calibration curve and the summary can be found in table 7. The values presented are the medium obtained from the triplicate analysis.

Results for Sample C:

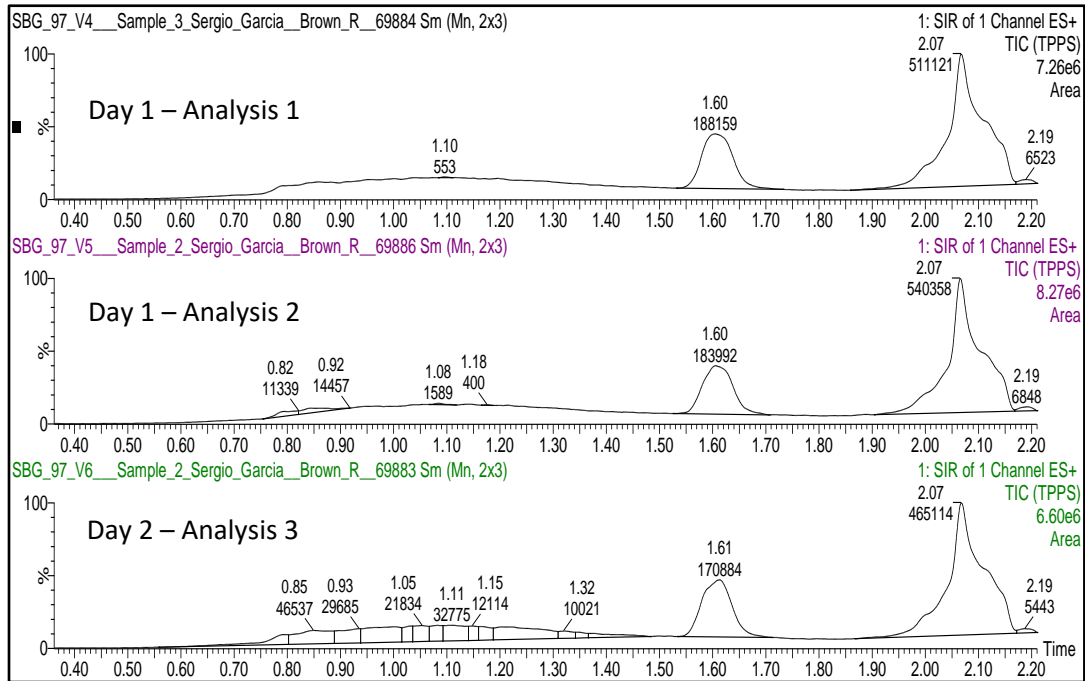


Figure 60 – Reproducibility of analyses: Three different analyses of ex-service oil sample C showing similar TPPS peak areas ($t_R \sim 1.60$ min), indicating reproducibility of the method when applied to ex-service oil samples.

Results for Sample D:

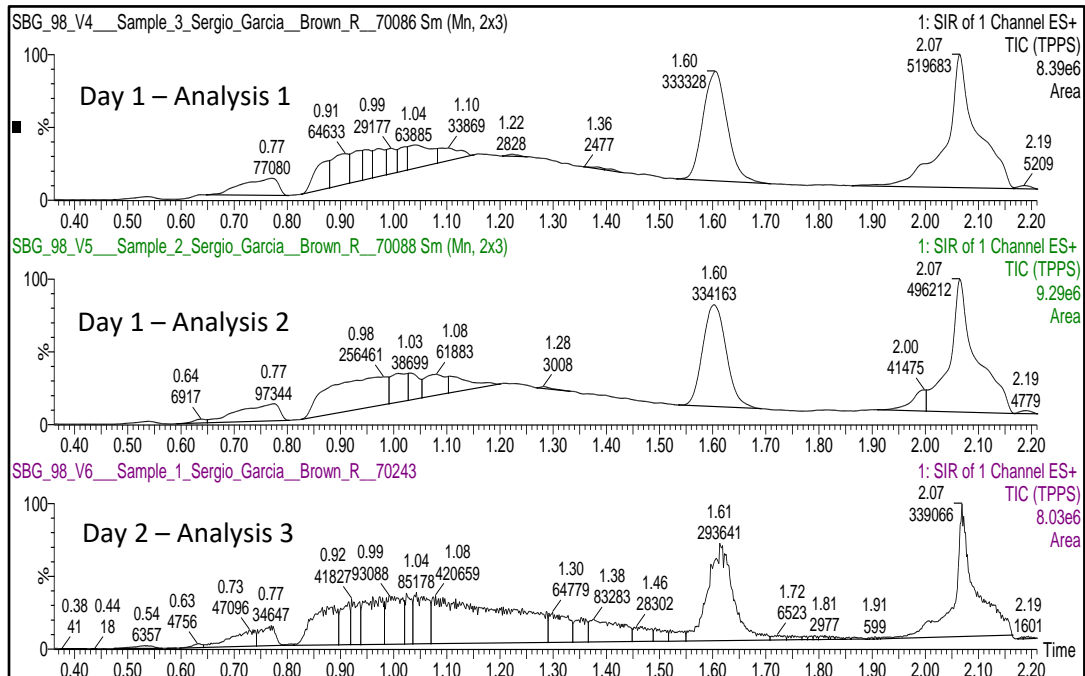


Figure 61 – Reproducibility of analyses: Three different analyses of ex-service oil sample D showing similar TPPS peak areas ($t_R \sim 1.60$ min), indicating reproducibility of the method when applied to ex-service oil samples.

Table 7 – Intraday and Interday reproducibility of the UHPSFC-MS method when analysing ex-service mineral oil samples.

*Values of concentration are in ppm of S ₈		Sample C	Sample D
Day 1	Analysis 1	0.539	0.739
	Analysis 2	0.542	0.737
Day 2	Analysis 3	0.524	0.694

This experiment demonstrated, summary of results shown in Table 7, that a really good intraday and interday reproducibility is achieved when the UHPSFC MS method is applied to the analysis of ex-service mineral oil samples. The maximum deviation in the results obtained was of 6 %, this corresponds to the analyses of sample D, when a value of 0.739 ppm of S₈ was obtained for the first result of day 1 and 0.694 ppm for the 2nd day result. This proves that the verification of results can be conducted in the same or in a different day, without compromising the validity/legitimacy of the outcome, which is always an amazing feature to have. An interesting observation from the analyses is that the concentration of S₈ in the ex-service mineral oil sample (R) suffered a slight increase from before the reclamation (sample C) to after the reclamation (sample D). This increase was from ≈ 0.535 ppm (before reclamation process) to ≈ 0.723 ppm (after reclamation process). Although in this case the increase did not present a risk to the transformer, it does show that elemental sulfur levels can be increased following reclamation. As the origin of the increase in S₈ following reclamation is not clear, a regular quantification of S₈ should be conducted to ensure that the oil does not become corrosive to silver.

3.3.6 Identification of elemental sulfur in mineral insulating oil - Standard corrosive test (DIN 51353) vs. Analytical approach

The intent of this work was to evaluate and compare the capability of two methods to identify oil samples that might present a risk for the power transformer. For this, Transformer mineral oil samples were spiked with different concentrations of S₈ (1, 2, 5 and 10 ppm). These samples were then analysed by the standard corrosive silver test (DIN 51353) and by the analytical method (UHPSFC-MS) for S₈ content. The experiments were then evaluated, for the standard corrosive silver test the evaluation was conducted following the visual rating process and for the analytical method, the concentration of the S₈ was expressed in ppm.

3.3.6.1 Corrosion test results

The spiked oil samples were tested for corrosion using the standard DIN 51353. The unused silver strip used as reference is shown in Figure 62. The corrosion results for the mineral transformer oil samples spiked with 1, 2, 5 and 10 ppm are shown in Figure 63, 64, 65 and 66, respectively. Lastly, for an easier visualisation and comprehension of the corrosion tests all the results are compiled and shown in Figure 67. From the results, we can clearly observe that the test gives a positive result for all the samples. These results will be further discussed below in 3.3.6.3.



Figure 62 – Silver strip (showing both sides) used as reference for the standard DIN 51353 corrosion tests.



Figure 63 - Corrosion test result of the oil sample spiked with 1 ppm of S_8 subjected to the standard corrosion test (DIN 51353). The silver strip (showing both sides) presents black colouration (silver sulfide), which indicates that the oil is corrosive.



Figure 64 - Corrosion test result of the oil sample spiked with 2 ppm of S_8 subjected to the standard corrosion test (DIN 51353). The silver strip (showing both sides) presents black colouration (silver sulfide), which indicates that the oil is corrosive.

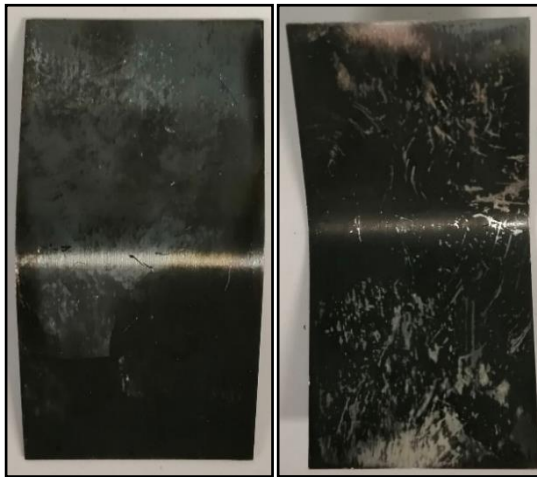


Figure 65 - Corrosion test result of the oil sample spiked with 5 ppm of S_8 subjected to the standard corrosion test (DIN 51353). The silver strip (showing both sides) presents black colouration (silver sulfide), which indicates that the oil is corrosive.

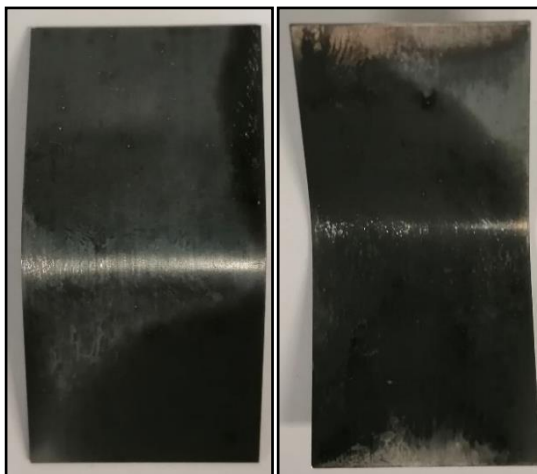


Figure 66 - Corrosion test result of the oil sample spiked with 10 ppm of S_8 subjected to the standard corrosion test (DIN 51353). The silver strip (showing both sides) presents black colouration (silver sulfide), which indicates that the oil is corrosive.

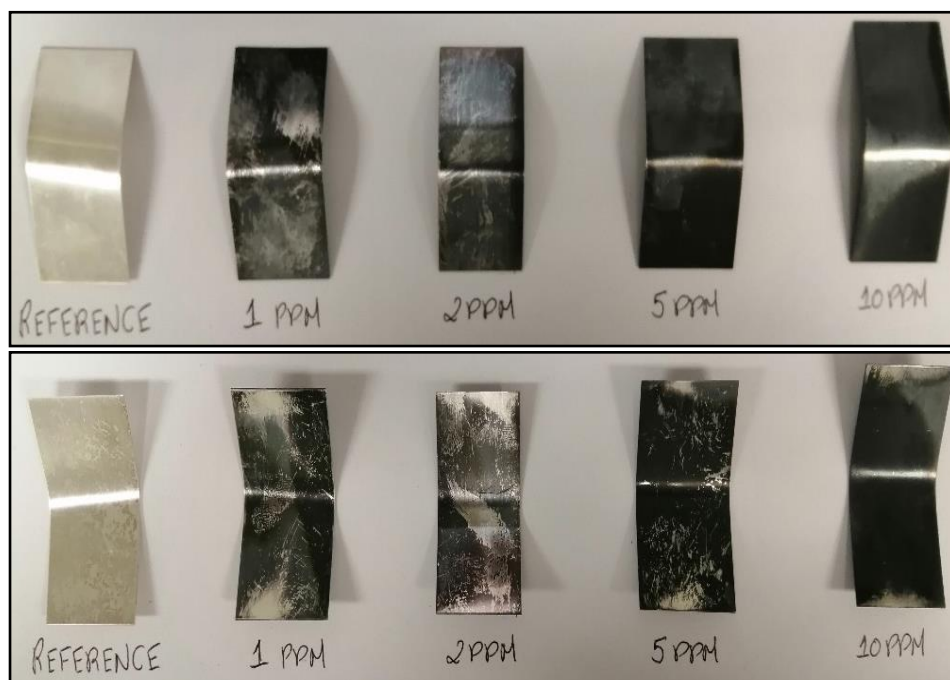


Figure 67 - Compiled results from the oil samples spiked with 1, 2, 5 and 10 ppm of S_8 subjected to the standard corrosion test (DIN 51353).

3.3.6.2 Analytical method results

The four spiked samples were subjected to the derivatisation reaction and then analysed for TPPS content. The results of these analyses are shown in the figures 68-71 below; the inspection of the chromatogram shows a peak at a retention time of 1.58 min, corresponding to TPPS. The concentration of TPPS is directly proportional to the concentration of S_8 , and from the images is clear that the analytical method is capable of detecting the presence of S_8 in all the spiked samples. Further discussion can be found in the next sub-topic (3.3.6.3).

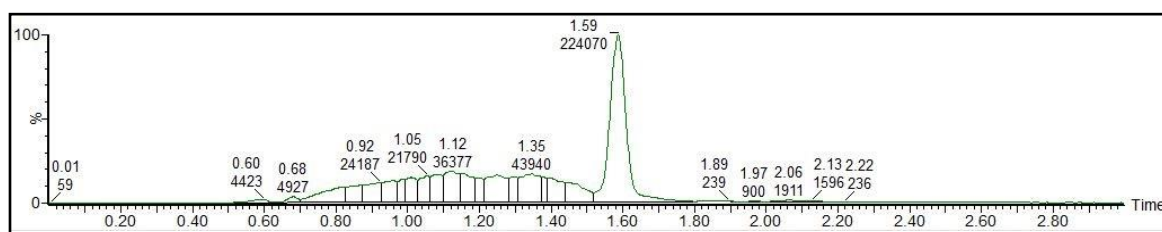


Figure 68 - Chromatogram of the oil sample spiked with 1 ppm of S_8 .

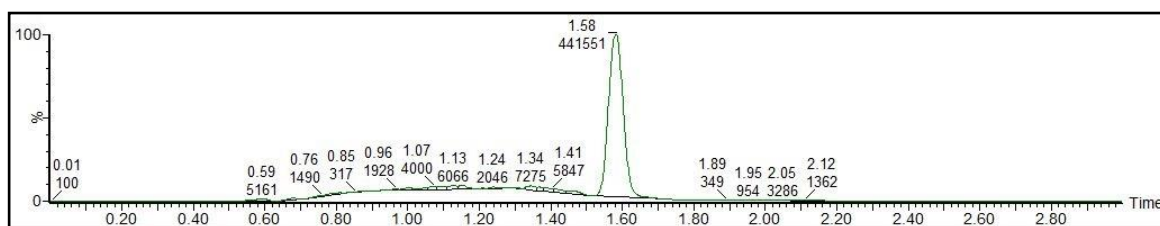


Figure 69 - Chromatogram of the oil sample spiked with 2 ppm of S_8 .

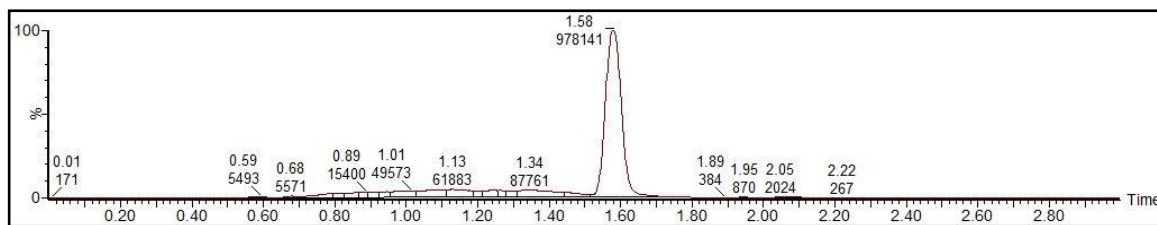


Figure 70 - Chromatogram of the oil sample spiked with 5 ppm of S₈.

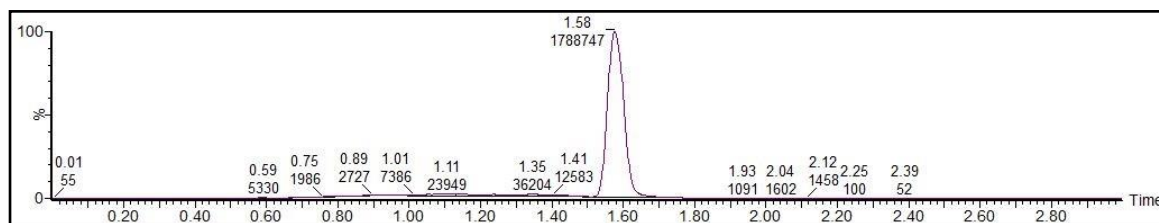


Figure 71 - Chromatogram of the oil sample spiked with 10 ppm of S₈.

3.3.6.3 Discussion

In this study the detection of S₈ in transformer mineral oil was investigated using the DIN 51353 and an analytical (UHPSFC-MS) method. From the results obtained, we can conclude that both techniques are capable to detect S₈ at low ppm levels, demonstrating that both methods have the sensitivity to identify oil samples that might present a risk of corrosion for the transformer. Although the DIN 51353 was able to positively identify all the spiked samples, this may not be the case when applied to ex-service oil samples with different compositions (e.g., concentration of antioxidant). In addition to this, due to the qualitative aspect of the method is not possible to deduce the concentration of S₈ present in the sample just by the discoloration obtained. This is better understood from our corrosion tests results, where the silver strip subjected to oils containing 1 and 2 ppm of S₈ appear almost identical, and the same is seen for the 5 and 10 ppm samples. On the other hand, the concentration of elemental sulfur is obtained directly by using our analytical (UHPSFC-MS) method. This method is capable of accurately quantifying low ppm of S₈ in mineral transformer oil, and due to the ionization technique employed, the chemical composition of the oil samples does not affect the reliability of the method.

3.3.6.4 Conclusions

The UHPSFC-MS SIR method proved to be a robust and reliable tool to specifically quantify S₈ in samples of mineral insulating oil. Although the suitability of this method has not been rigorously evaluated to be used/considered as a standard, the experiment showed that it could provide reliable results, including in ex-service oil samples. These results could be used to not only validate the ones obtained from the standard corrosion test DIN 51353, but also to provide a reliable result for real oil samples where the inherent chemical composition could affect the outcome of the

standard test. This method was found to be capable in identifying insulating oils that could become a risk for the transformer.

3.4 Summary of the chapter

In this chapter it was demonstrated that the developed GC-MS and UHPSFC-MS methods can be used to detect and quantify the presence of S_8 in transformer insulating mineral oil (new and ex-service). The established GC-MS method is able to monitor elemental sulfur concentrations as low as ~0.5 ppm, while the UHPSFC-MS method can detect and quantify trace levels of elemental sulfur in mineral insulating oils as low as 0.5 ppb. Both methods were found to be reliable, reproducible, and robust, making them as ideal analytical tests that can be used routinely or to confirm the presence of elemental sulfur in samples where corrosion has occurred. The developed methods provide an alternative to the use of a GC with a chemiluminescent detector, with the main advantage of providing the same detection/quantification (ppb levels) capabilities without the requirement of an element selective detector. This derivitisation method is advantageous for application in laboratories that do not have specialised equipment for sulfur analysis. This study also verified that the UHPSFC-MS method can be used in conjunction with the standard corrosion test DIN 51353, to provide a valid and quantitative result in cases where the qualitative side of the DIN 51353 might not be sufficient to deliver a reliable result. This analytical method was used to analyse the final concentration of elemental sulfur in the samples subjected to our laboratory reclamation process (see next chapter) for selective removal of elemental sulfur from new and ex-service mineral oil samples, and to evaluate how effective it is.

Chapter 4 Reclamation process - Selective removal of elemental sulfur from mineral transformer insulating oil

The mitigation of future corrosion has received a lot of focus during the last years, primarily on the research and development of processes for remediation of transformers categorised as being “corrosive”. The “corrosiveness” of the transformer mineral oil is generally diagnosed using a relevant corrosion test (e.g., DIN 51 353). Since the oil quality is reliant on the outcome of the test, oils that present a positive result are no longer suited to be used as insulating oils and need to be replaced/regenerated. The replacement of the mineral insulating oil of a power transformer is not only costly but also harmful for the environment, so regeneration processes are usually applied. A common method for regeneration/reclamation of aged and/or corrosive oils is the use of bauxite clays. The reclamation consists mainly of filtering the oil through the clay, and was considered largely successful, although a sporadic, but increasing number of failures and corrosion linked with the reclamation process itself have been observed. The corrosion observed is due to elemental sulfur and affects silver metallic surfaces such as the tap changers present in transformers. A better understanding of the chemistry that occurs during the oil reclamation is expected to identify possible modifications of the process, which will ultimately lead to an increase of the life-expectancy of the transformer. This chapter describes initial studies of sulfur removal using two different reclamation processes, one technique is based on the reclamation process that is currently employed by National Grid and the other is a novel method based on using various phosphine-bound polymers.

4.1 Reclamation process using montmorillonite clay

A laboratory investigation was performed to study the effectiveness of a reclamation process based on the use of a clay. The method employed was based on the one generally used by National Grid for the regeneration of used mineral insulating oil, but instead of using a bauxite clay, we use a montmorillonite clay. The main differences between the two clays is associated with the crystal system and structure that they possess. The bauxite clay consists of one aluminium octahedral sheet and one silica tetrahedral sheet per repeating unit while the montmorillonite clay consists of two silica tetrahedral sheet and aluminum octahedral sheet per repeating unit. In Figure 72, the molecular structure of montmorillonite is shown. The selectivity of the clay for removal of elemental sulfur is the main desirable characteristic, as removal of other sulfur compounds (e.g., thiophenes) might have a detrimental effect on the dielectric properties of the oil.

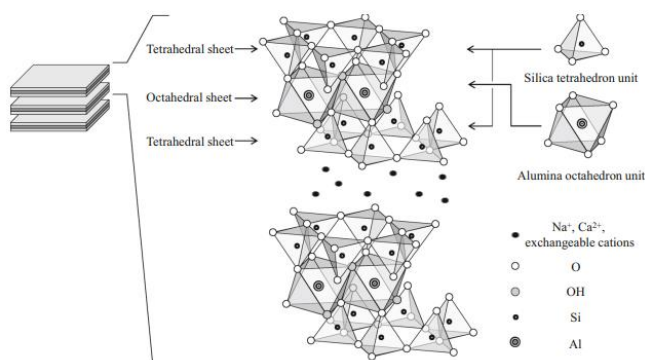


Figure 72 – Representation of the molecular structure of montmorillonite clay.¹²⁵ Reprinted from reference [125] with permission of Springer.

In order to simplify the analysis, *n*-hexadecane was used in place of the more complex mineral oil matrix. The selectivity of the clay was studied by adding a known amount of DBDS and benzothiophene to the *n*-hexadecane (which is used as model for the mineral oil), followed by filtration at room temperature (RT) through the montmorillonite clay. The initial mixture and the mixture after the filtration were analysed using GC (Figure 73).

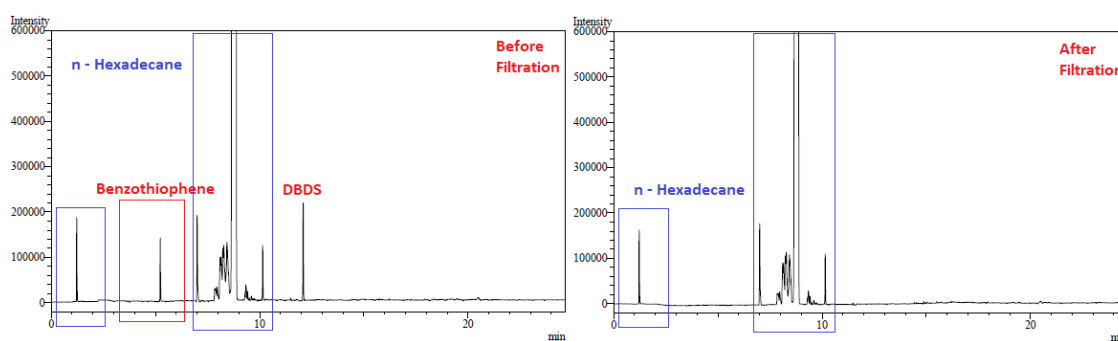


Figure 73 – GCs of a solution of DBDS and benzothiophene in *n*-hexadecane before filtration (left) and after filtration (right) using the montmorillonite clay.

The absence of the peaks for the DBDS and benzothiophene can be clearly seen from the chromatogram of the sample after filtration. We can conclude that montmorillonite clay is effective in removal of these two organosulfur compounds from *n*-hexadecane. Therefore, use of montmorillonite clay for removal of elemental sulfur of mineral insulating oil may not be appropriate, as the process will also remove some of ubiquitous anti-oxidant compounds such as benzothiophenes that are found in mineral oils, which may compromise the electrical properties and thermal/chemical stability of the mineral oil. Bauxite clay is expected to exhibit similar behaviour, since both clays present comparable structural composition (i.e., both present a relative high aluminium content). According to the literature, bauxite clay has already been studied/used as an inexpensive adsorbent for removal of different contaminants (e.g., removal of DBDS from mineral oil).¹⁵ The reactivity of the clay can be further enhanced (usually referred to as activation of the clay), which is generally accomplished by chemical/physical treatment of the clay (i.e., heating or acid treatment).¹⁶

4.1.1 Conclusion

This study demonstrated that if the montmorillonite clay would be used in the reclamation process of a transformer mineral oil sample, its use can/would lead to the unwanted removal of different organosulfur compounds (e.g., benzothiophenes) that are beneficial for the stability of the oil. So, the use of a method that is selective for the removal of S_8 is essential to maintain the optimal thermal/electrical properties of the transformer mineral oil. Therefore, a novel laboratory reclamation method that can be used for the selective removal of S_8 from mineral oil was developed. This method consisted in the use of trisubstituted-phosphine polymers scavengers to selectively remove S_8 from the mineral insulating oil.

4.2 Selection of trisubstituted-phosphine polymer scavengers used in the selective removal of S_8 from mineral oil

Having realised a quantitative method for analysis of S_8 in mineral oil using a derivatisation reaction with TPP, it was logical to consider TPP, or a derivative, as a potential desulfurisation agent for the reclamation process. This potential was not only associated with its selectivity for S_8 but also as it is convenient to use, relatively low in cost, and widely available due to its use in the synthetic chemistry. In organic chemistry, TPP is utilised as a reagent in several types of reactions (e.g., Wittig, Mitsunobu), where its respective oxide is usually generated as a by-product. In some cases, in order to avoid difficult separations, insoluble polymer-bound TPP derivatives are used to “trap” the oxide and simplify separations. Several different types of TPP-containing polymers are commercially available, and we initially identified use of polystyrene-bound TPP (100-200 mesh, extent of loading: ~ 1.6 mmol/g, crosslinked with 2% divinylbenzene (DVB), CAS N^o 39319-11-4). A search of different commercially available trisubstituted polymer-bound compounds was also conducted, but only benzyldiphenylphosphine, polystyrene-bound (100-200 mesh, ~ 2.5 mmol/g loading, crosslinked with 2% DVB) was found and purchased. Simplified structures of these polymers (denominated **A** and **C**) are depicted in Figure 74.

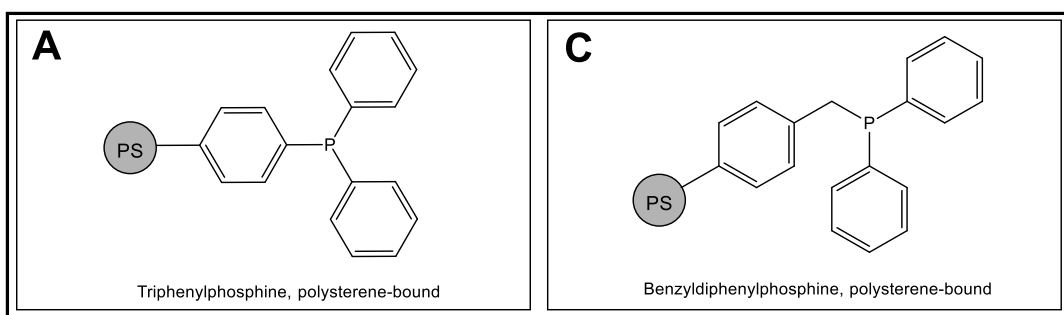


Figure 74 – Triphenylphosphine and benzyldiphenylphosphine polystyrene-bound (polymer A and C).

Bartlett and Meguerian,¹¹³ published a paper on the uncatylsed reaction between S_8 and different tertiary phosphines. Therefore, it was reasonable to consider other phosphorous (III) compounds for a quantitative production of the corresponding sulfide during our reclamation process. Three alternative tertiary phosphines were studied as suitable alternatives. The compounds studied were the trioctylphosphine, tri-*tert*-butylphosphine and the ethyl diphenylphosphinite. The results of the reactions of these phosphines with S_8 are fully described in Chapter 3, and in all cases, formation of the oxide was a significant side reaction, which predominated compared to the formation of the respective sulfide. Therefore, none of these more reactive P(III) compounds were considered to be suitable to be used in our reclamation process, and it was then evident that for the purpose of our study less reactive, or more “oxygen-stable”, phosphines were required.

A review of the literature revealed suitable polymer-bound triphenylphosphine derivatives that could be relatively easily synthesised and used in our reclamation process. A suitable example was found in a paper published by Charette *et al.*,¹²⁶ where they describe the synthesis of a triphenylphosphine derivative coupled to a non-crosslinked polystyrene support. The major difference for our application was that a Merrifield resin crosslinked with 1% DVB was used to obtain a polymer structure that would be insoluble, since insolubility of the polymer-bound reagent is a fundamental requirement for our desired process. The generalised structure and synthesis of this trisubstituted polystyrene-bound (polymer **D**) is shown below in Figure 75. The full experimental synthetic procedure can be found in the sub-chapter 6.3.4.

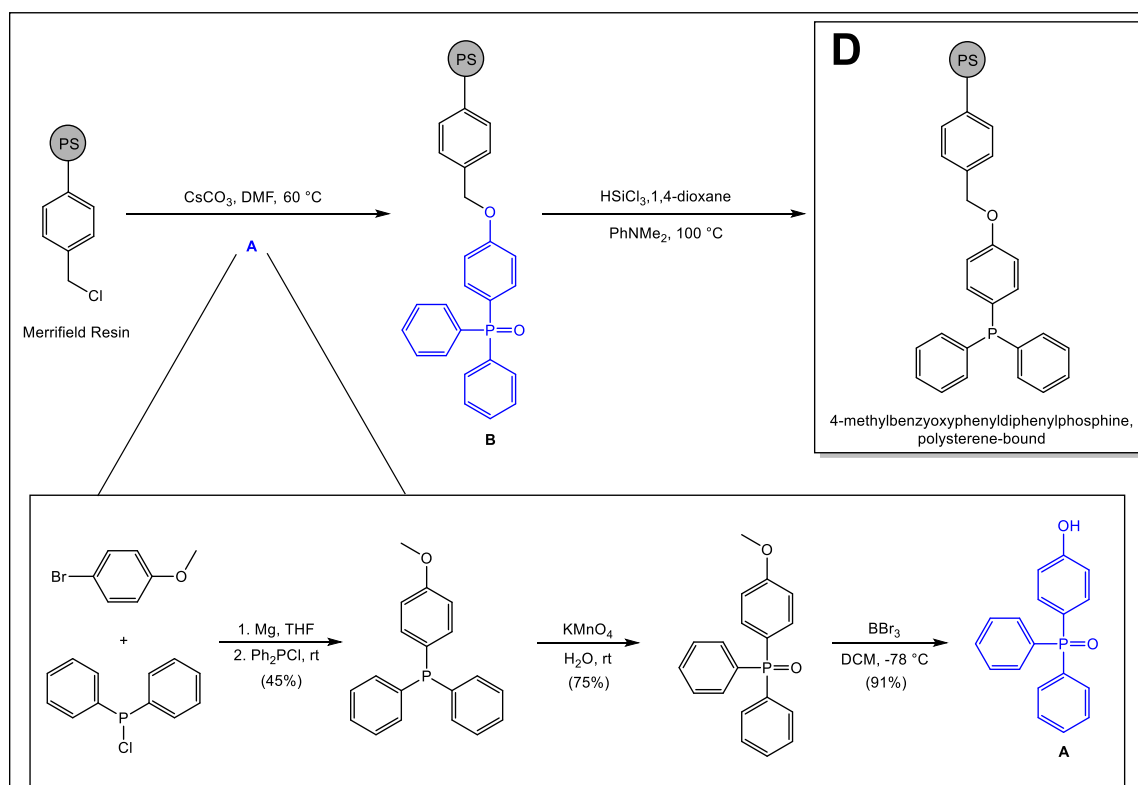


Figure 75 – Synthesis of polystyrene-bound 4-methylbenzyoxyphenyldiphenylphosphine (Polymer **D**).

Polymer D was synthesised in two steps from Merrifield resin (crosslinked with 1% DVB) by immobilisation of 4-hydroxyphenylphosphine oxide (**A**) (Figure 75).¹²⁶ The required 4-phosphine oxide **A** was synthesised in three steps from 4-bromoanisole,¹²⁷ starting with Grignard reagent formation and reaction with the phosphorus (III) electrophile. Permanganate oxidation led to the formation of the correspondent monomethoxy phosphine oxide, which was subsequently *O*-demethylated to afford the desired phosphine oxide **A**. No significant modification was required to transfer the coupling methodology from the soluble polymer to the crosslinked Merrifield resin. The reaction of the caesium salt, obtained from deprotonation of **A** using CsCO₃, with Merrifield resin gave polystyrene-bound phosphine oxide **B** (gel phase ³¹P NMR, δ = 27.89 ppm). Subsequent reduction of phosphorus (V) compound **B** with trichlorosilane gave the desired phosphine polymer **D**, which was confirmed by gel phase ³¹P NMR (δ = -7.16 ppm).

With three different polystyrene-bound phosphorous (III) polymers already in hand, we also wanted to understand if the actual material of the solid support had an impact on the reactivity/ability to remove S₈ from the mineral oil. We therefore synthesised a fourth type of polymer that was expected to possess better “swelling” in the mineral oil, i.e., easier access of the oil to the reactive P(III) centres within the polymer, which was expected to lead to higher reactivity and consequently to shorter removal times. The polymer in question is a poly(lauryl methacrylate) crosslinked with DVB and loaded with TPP (Figure 76 – polymer **B**).

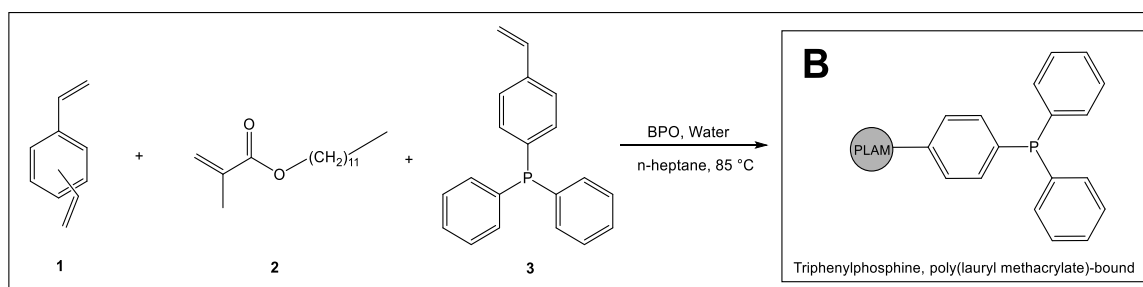


Figure 76 – Synthesis of poly(lauryl methacrylate)-bound triphenylphosphine (polymer **B**).

No literature was found that specifically described the synthesis of a poly(lauryl methacrylate) P(III)-containing polymer. Therefore, a general literature method for FRP polymerisation was first investigated, which consisted in the reaction of a mixture of monomers (DVB, lauryl methacrylate (LMA) and 4-(diphenylphosphino)styrene (SDP)) with benzoyl peroxide (BPO) (0.5% - 1% wt. in respect to the total monomer) and *N,N*-dimethylaniline (PhNMe₂) (1/1 molar ratio to BPO) in different solvents (acetic acid, methanol, or acetonitrile) at RT for 48 h. The monomer mixture was always degassed prior to the reaction by bubbling argon for 15 min. No obvious polymeric material was obtained under these homogeneous conditions, despite various adaptations to the procedure (Table 8, entries 2-6). Ultimately, a successful polymer synthesis was found only when prior

oxidation of the phosphine SDP monomer **3** to the phosphine oxide was performed (Table 8, entry 7), which was confirmed by gel phase ^{31}P NMR ($\delta = 28.86$ ppm). An explanation for this is that the P(III) SDP monomer was oxidised by the BPO, inhibiting the polymerisation reaction as the initiator was being consumed. Although the polymer synthesis was possible using the phosphine oxide monomer, the obtained material was a fine powder and not considered suitable physical form to be used in the reclamation process (i.e., material obtained should be able not only to withstand the pressure of the oil flow passing through it but also be of a particle size that would allow oil to freely pass and also not block the oil filters). In addition, further reduction of the phosphine oxide to the phosphine was still needed, even though it was expected to be more challenging for the ester-based polymer the reduction of the P=O was found to be successful with trichlorosilane (gel phase ^{31}P NMR, $\delta = -6.56$ ppm ; sub-chapter 6.3.3.2). Efforts to increase the bead size by changing the concentrations of DVB and/or decreasing the amount of BPO were tried, each produced similar small polymer beads (Table 8, entries 7-12). Finally, following a general procedure described by Garcia-Diego and Cuellar, using a biphasic water/*n*-heptane system at 65 °C, we were able to obtain the phosphorus-containing polymers with desirable physical properties.¹²⁸ The first successful attempt at biphasic polymerisation used the oxidised form of the 4-(diphenylphosphino)styrene (SDP) (gel phase ^{31}P NMR, $\delta = 28.48$ ppm Table 8, entry 14), but further experiments demonstrated that prior oxidation of the SDP was not necessary, making it possible to perform the synthesis of the desired polymer in a single step (Table 8, entry 15), which was confirmed by gel phase ^{31}P NMR ($\delta = 29.36$ (P=O) (~10%), -5.78 (P) (~90%) ppm). A possible explanation is that due to the different solubility characteristics of SDP and BPO, they are dissolved in different phases preventing oxidation of the phosphine by BPO. During the synthesis it was also found that increasing SDP wt. % in the initial monomeric mixture from ~9% to ~15% (Table 8, entry 16) led to polymers with more gel-type characteristics, rather than a solid type. For this reason, the wt. % of SDP was not further increased from ~9% (sub-chapter 6.3.3).

Table 8 – Conditions tried for the synthesis of polymer **B**.

Entry ^a	Monomers (mmol)				BPO ^c	PhNMe ₂ ^d	Solvent	Temp.	Successful Synthesis
	DVB	LMA	SDP	SDPO ^b					
1	16.924	16.875	-	-	1	1	Acetic Acid	RT	✓
2	17.426	17.531	1.638	-	1	1	Acetic Acid	RT	✗
3	11.543	17.498	1.569	-	1	1	Acetic Acid	RT	✗
4	17.581	17.464	1.542	-	0.5	1	Acetic Acid	RT	✗

5	17.511	17.589	1.598	-	1	1	Acetonitrile	RT	✗
6	17.612	17.575	1.498	-	1	1	Methanol	RT	✗
7	17.564	17.608	-	1.627	1	1	Methanol	RT	✓ ^e
9	11.897	17.635	-	1.579	1	1	Methanol	RT	✓ ^e
10	17.528	17.691	-	1.534	0.5	1	Methanol	RT	✓ ^e
11	11.487	17.614	-	1.543	0.5	1	Methanol	RT	✓ ^e
12	11.637	17.682	-	1.652	0.5	1	Methanol	50 °C	✓ ^e
13	11.125	23.439	-	-	0.5	-	Water/n-Heptane	85 °C	✓
14	6.249	24.869	-	2.624	0.5	-	Water/n-Heptane	85 °C	✓
15	5.612	22.243	2.627	-	0.5	-	Water/n-Heptane	85 °C	✓
16	5.579	23.198	4.251	-	0.5	-	Water/n-Heptane	85 °C	✓ ^e

^a All the experiments were conducted for 48 h. ^b 4-(diphenylphosphino)styrene oxide, obtained from oxidation of SDP (sub-chapter 6.3.3.1). ^c Wt. % with respect to the total monomer. ^d Molar ratio with respect to BPO. ^e Obtained material not suitable for the reclamation process, i.e., material obtained was powder/small beads or had gel-type properties.

The laboratory reclamation process to selectively remove S₈ from mineral oil, and consequently reduce silver corrosion from power transformers, was studied using the four different trisubstituted-phosphine polymers (**A**, **B**, **C** and **D**) (see Figures 74, 75 and 76) and the outcome of these experiments are described later in this chapter.

4.2.1.1 Future work - Synthesis of an end-functionalised trisubstituted-phosphine polymer to be used in the selective removal of S₈ from mineral oil

Initial studies were conducted towards the synthesis of a trisubstituted-phosphine polymer where the chemical composition of the end-substituent was controlled. The manipulation of such characteristics had one main purpose in mind; to allow the polymer to be attached to different surfaces (e.g., glass, silica). The direct loading of the polymer onto a desired surface, ideally possessing a high surface area, was expected overcome some issues (e.g., overloading, erosion/compression and low flow rates) that can arise from when using resin-like polymers in the form of small beads. Such feature would open the possibility of the reclamation process to be

conducted in different ways. For example, instead of a single reclamation process similar to the one usually employed, a continuous reclamation process would be then feasible within the transformer.¹²⁹ The synthesis of end-functionalised trisubstituted-phosphine polymer was attempted by adaptation of a procedure by Mansky *et al.*¹³⁰ The synthesis used a functionalised TEMPO initiator (NMP agent) to control the end-function of copolymers of styrene and methylmethacrylate. Using the same principle, i.e., using the same functionalised TEMPO initiator, the synthesis of a copolymer of styrene, lauryl methacrylate and SDP was attempted. For an easier comparison, both approaches are shown below in Figure 77.

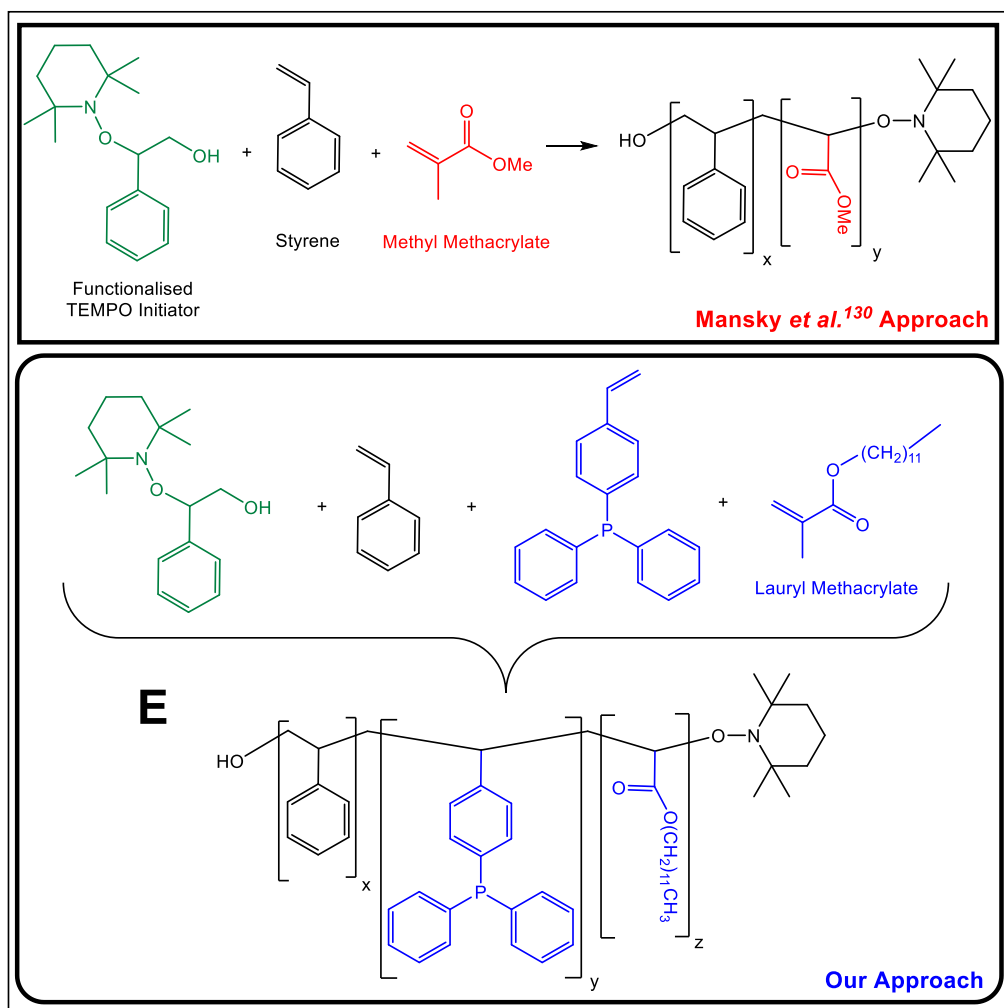


Figure 77 –Literature,¹³⁰ and our adapted approach to end-functionalised polymers.

Prior to attempting end-functionalised polymer synthesis, the functionalised TEMPO initiator had to be prepared. This NMP agent was synthesised in two steps from TEMPO (Figure 78).^{133,134} The first step involved the reaction of TEMPO with BPO in an excess of styrene followed by hydrolysis with potassium hydroxide to give the desired hydroxyl derivative **7**. Once the functionalised TEMPO initiator **8** was obtained, the synthesis of the end-functionalised polymer **E** was attempted.

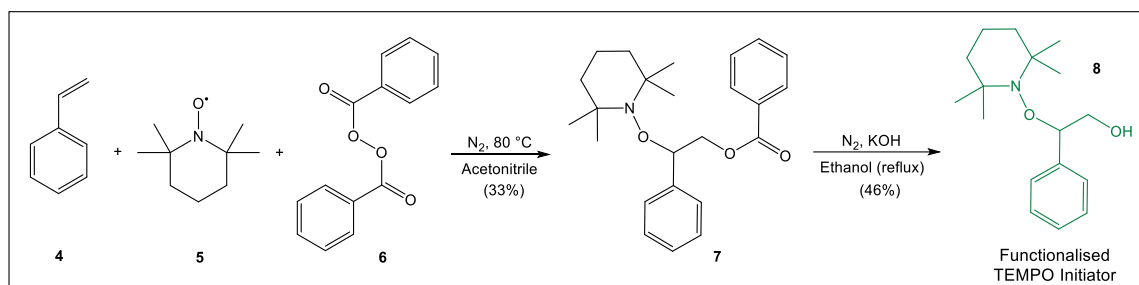


Figure 78 – Synthesis of the functionalised TEMPO initiator (NMP agent).

The general experimental procedure reported by Mansky *et al.* was followed,¹³⁰ the only difference being the mixture of monomers used. In our case, we used a monomer mixture that consisted of styrene, lauryl methacrylate, and SDP (Figure 77). The monomer mixture was then reacted with the functionalised TEMPO initiator (in xylene) at 130 °C for 72 hours. The obtained molecular product (a white powder) was then analysed by ³¹P NMR, showing the presence of a P=O peak. Indicating that phosphine containing groups had undergone oxidation during the attempted polymerisation reaction. This observation would also account for inhibition of the polymerisation reaction, and isolation of the obtained molecular compound. Unfortunately, as this work was carried out at the end of the period of research, it was not attempted a second time. A potential solution, as previously demonstrated, would be prior oxidation of the phosphine containing group to the phosphine oxide. Experimental details may be found in sub-chapter 6.3.5.

The use of a RAFT polymerisation agent was considered instead of the functionalised TEMPO initiator shown in Fig 78. The use of RAFT agents provides the ability to control polymerisation of most monomers, including the monomers of interest such as methacrylates and styrenes. RAFT polymerisation would also provide other advantages, such as; a narrow molecular weight distribution, suitable for synthesis of block copolymers and end functional polymers. These characteristics were essential as the ultimate purpose was to synthesise an end functionalised polymer (-OH) which could be then attached to different surfaces (e.g., glass, silica). Unfortunately, an appropriate RAFT agent, which would provide/lead to the synthesis of the desired end-functionalised polymer was not commercially available.

4.2.1.2 Summary

Four different trisubstituted phosphine-loaded polymers that were studied in this work for their ability to selectively remove S₈ from mineral insulating oil (Figure 79). The triphenylphosphine and benzyldiphenylphosphine polystyrene polymers were obtained from commercial suppliers while another two were synthesised for the purpose of this work. By adaptation of published synthetic procedures, two different polymers (**B** and **D**) were synthesised. These procedures were optimised for the synthesis of polymers **B** and **D**, giving convenient access to such polymers in a reproducible

way. The results, conclusions, and experimental procedures of the selective removal of S_8 from transformer mineral oil using polymers **A**, **B**, **C** and **D** are presented later on in this chapter.

An attempt to the synthesis of an end-functionalised polymer-bound triphenylphosphine was attempted unsuccessfully. It is believed that the triarylphosphine functionality present may be incompatible with the polymerisation conditions, with oxidation to triarylphosphine oxide being observed. The synthesis of end-functionalised polymers could open the possibility of new ways to conduct the reclamation process for mineral oil in power transformers, by providing the possibility to immobilise the scavenging polymers onto different materials. These processes could bring, to the industry, systems that are more environmentally friendly and inexpensive (e.g., continuous on-line system), with the possibility of regenerating the polymers after use.

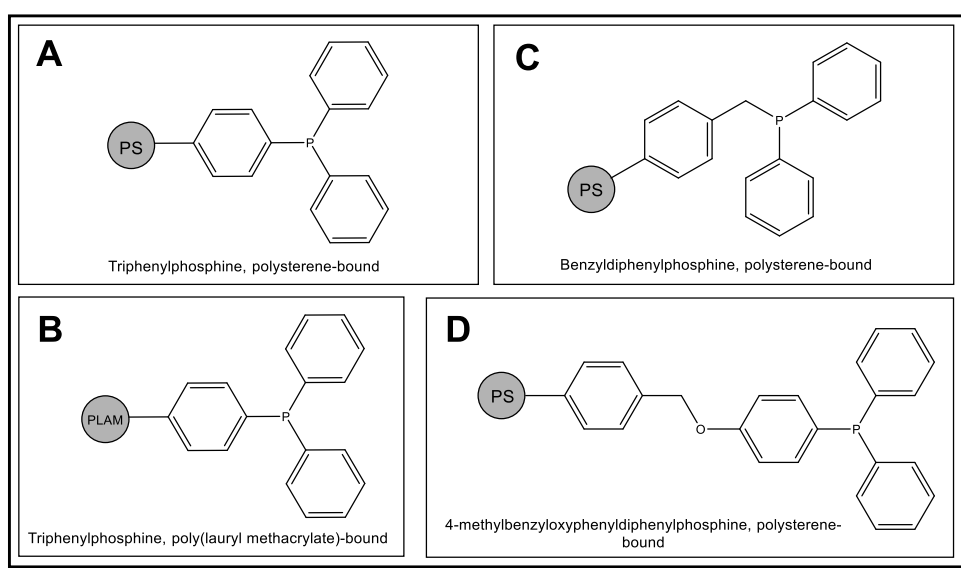


Figure 79 – Four different trisubstituted phosphine-loaded polymers used in the laboratory reclamation studies.

4.3 Design and commission laboratory reclamation rig to be used on the selective removal of S_8 from transformer mineral oil

As discussed above, the life expectancy and reliability of a transformer is strongly influenced by the state of the oil insulation. As an alternative to replacing, and disposing of, the large volume of “corrosive” insulating oil, reclamation provides an economical and more environmentally friendly alternative that restores the properties of the oil close to the values of new oil. However, standard reclamation processes are not effective in removal of elemental sulfur, and corrosion of silver surfaces, such as tap changers present in transformers, has been identified following reclamation. This sub-chapter focuses not only on the selective removal of elemental sulfur from mineral oil but

also on the development of a lab scale reclamation process that may be scaled so that it could be replicated in the field.

4.3.1 Initial studies on the selective removal of S₈ from transformer mineral oil

This reclamation process that uses a novel method for the selective removal of elemental sulfur from mineral insulating oil is based on a selective chemical reaction of triphenylphosphine (TPP) with elemental sulfur. In the first instance, the polymer studied was a commercially available triphenylphosphine polymer-bound triarylphosphine derivative, with a cross-linked polystyrene backbone (Figure 80).

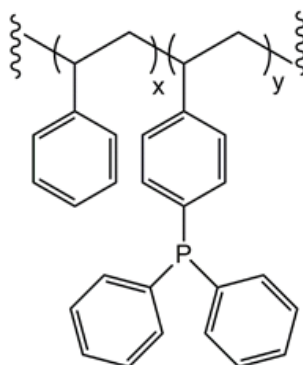


Figure 80 - Triphenylphosphine polymer-bound (100-200 mesh, extent of labelling: ~1.6 mmol/g loading, crosslinked with 2% Divinylbenzene (DVB), CAS N^o 39319-11-4).

The reclamation process is based on the fact that the triphenylphosphine present on the polymer will react selectively with the elemental sulfur to give triphenylphosphine sulfide. Once the reaction occurs the phosphine sulfide is formed and in this way the elemental sulfur is converted in a suitable form to be removed, through its incorporation into the insoluble polymer. At the end of the reclamation process, the polymer will have retained the reactive elemental sulfur and the oil that has passed through will contain reduced levels of elemental sulfur depending on the conditions. This chemical transformation is shown below in the Figure 81.

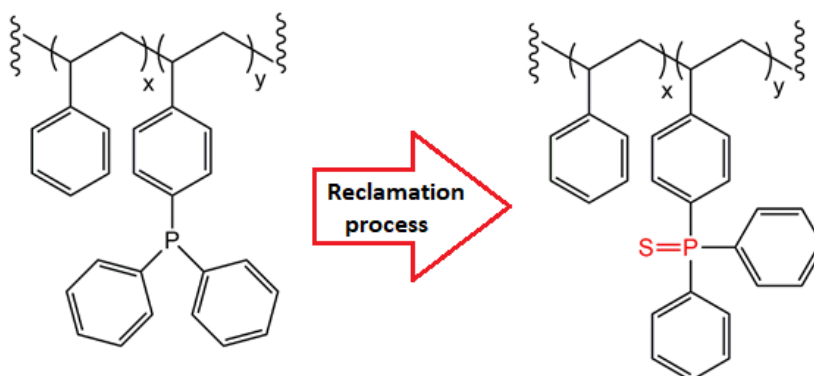


Figure 81 – Chemical transformation that occurs to the triphenylphosphine polymer-bound during the reclamation process.

Reclamation conditions were optimised in terms of reaction time, the temperature and the stoichiometry of the amount of elemental sulfur and the active triphenylphosphine bound to the polystyrene polymer. These initial studies consisted basically of adding known amounts of mineral oil, triphenylphosphine polymer-bound and S₈ to a round bottom flask at a constant temperature with continuous stirring. After appropriate sets of time the samples would be then analysed for elemental sulfur content using the analytical method previously described (previous chapter). During these initial studies and by adjusting only the conditions described before the efficiency of the removal never reached values higher than 60%, this was probably due to the fact that:

- a) The polystyrene resin beads are/were not well swollen in the mineral oil, which can result in:
 - Poor reaction site accessibility by the mineral oil/S₈, leading to diminished reaction rates for the removal of S₈ (i.e., reaction between active site of polymer and S₈ present in the mineral oil is slower/non-existent).
 - The resin beads aggregate and “stick” on the bottom of the round bottom flask, which leads to a smaller area of contact and so to a slower rate for the removal of S₈.

- b) Compounds present in the oil are “blocking” the reaction site of the polymer.

To understand if the removal efficiency of the S₈ was being hampered due to the poor swelling of the polystyrene beads in the mineral oil, the same experiment (as described above) was conducted. But at this time the polymer-bound triphenylphosphine was added at two stages, half in the beginning and the other half after 15 min. The result of this study is shown in the Figure 82.

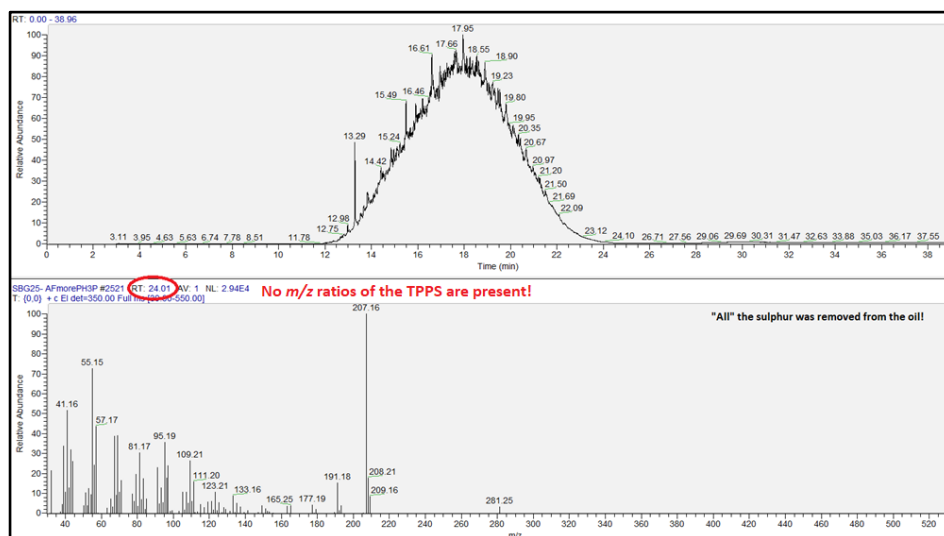


Figure 82 – GC-MS result for TPPS content of a reclamation process where the triphenylphosphine polymer-bound was added at two different stages.

Using the analytical method for elemental sulfur described in the previous chapter, inspection of the chromatogram shows that the peak from the TPPS derivative is not visible, indicating that very little sulfur is present in the oil after filtration (Figure 82). Given that the LoD for the analysis was determined to be 0.5 ppm of S_8 (the experimental data can be found in section 3.2 of this thesis), we can conclude that the polymer-bound phosphine was $\geq 99.5\%$ effective in removing the elemental sulfur from the mineral insulating oil.

4.3.2 Design and optimisation of the reclamation rig

Due to the excellent initial experimental results using polymer-bound phosphine to remove elemental sulfur, a reclamation rig was designed (Figure 83). The design was conceived having in mind that it should be able to be adapted for use in the field, uncomplicated and economically viable (Figure 84).

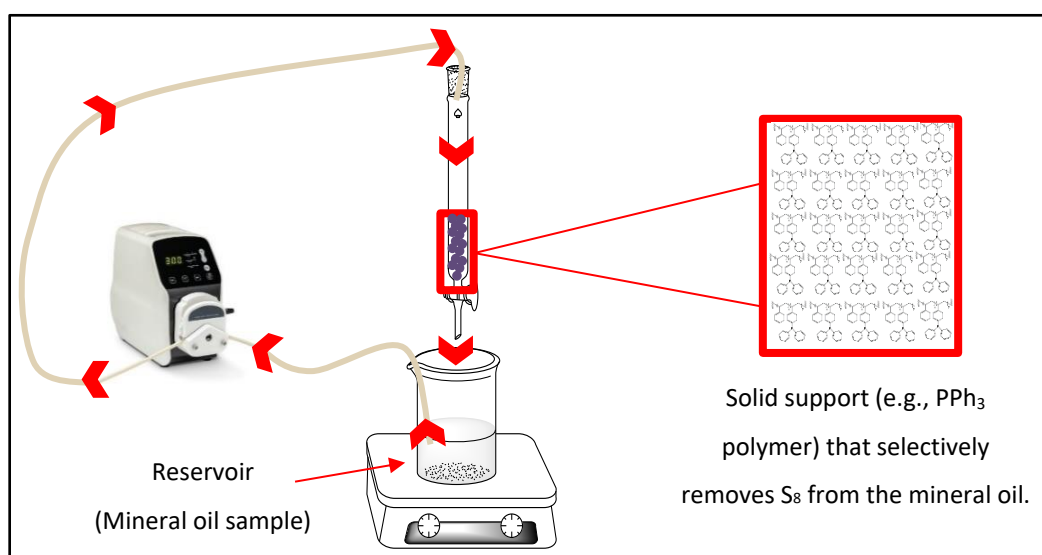


Figure 83 – Design of the lab scale reclamation rig.

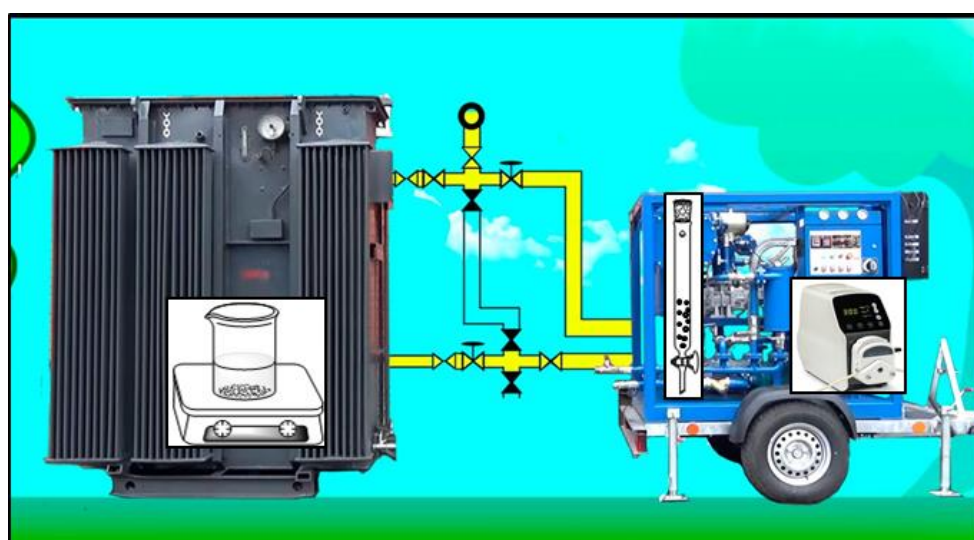


Figure 84 – How the reclamation rig can be adapted to the field.

The laboratory-scale reclamation set-up suffered some changes (i.e., column used, flow rate achieved, etc...) during the testing and validation phase, the first working set-up is shown in Figure 84. This working set up allowed for a flow rate of 1 to 10 mL/min, which translated to a number of cycles between 4 to 60, with a loading of the polymer-bound triphenylphosphine of 2 g, at a temperature of 60 ° C and under reduced pressure (value not measured). The main discovery during the initial test phase was that in order to achieve a significant flow rate (of around 1 to 10 ml/min) a pumped system (using a fish pump, as seen in the figure below) had to be utilised to recycle the test mixtures through the polymer matrix. The working reclamation set-up was used in a series of preliminary reclamation processes to selectively remove elemental sulfur from mineral oil (see below).



Figure 85 – First working lab scale reclamation rig.

4.3.2.1 Preliminary reclamation processes to selectively remove S₈ from transformer mineral oil

The first working reclamation rig (Figure 85) was used for the study of the selective removal of elemental sulfur from mineral oil using the polymer-bound triphenylphosphine (Figure 80). This study consisted in a series of five experiments, presented in chronological order , and the conditions used were optimised along the way.

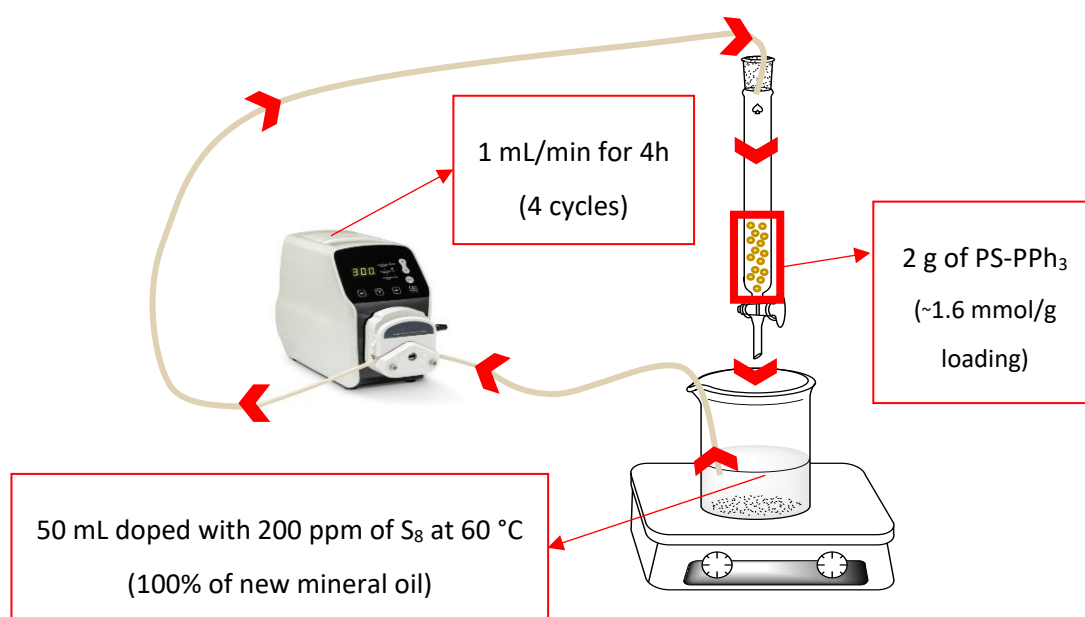
The general concept of this preliminary reclamation process experiment consisted in using the triphenylphosphine polymer-bound to selectively to remove elemental sulfur from different samples of mineral oil (or mixtures of oil/organic solvent).

The general procedure involved loading of two grams of polymer-bound triphenylphosphine (re-used in all five experiments) to an empty column, where a piece of cotton was used as frit (a control test was performed to ensure that the cotton would not remove S_8). The doped mineral oil was warmed in a RBF using an aluminium heat transfer block placed on a heating plate (60 °C), with stirring, and then continuously pumped through the system and samples were taken every hour until the end of the experiment. The oil samples were then subjected to derivatisation by reaction with TPP at 60 °C for 3 h (for experimental details see page 36), and immediately analysed for TPPS content using our SFC-MS SIR method (each analysis, including sample preparation, took around 20 minutes). This method showed a LLOQ of 0.05 ppm (S/N of 33), for experimental data see sub-chapter 3.3.2 and 3.3.3.

To ensure that an accurate estimation of the final S_8 concentration was obtained in situations where evaporation (of solvent) was a significant factor, for example when mixtures containing toluene or THF were used, the final volume was corrected to take this into consideration. The results taking evaporation into consideration are designated as “[S_8] corrected” in the result tables presented below. In this case, the value obtained would be recalculated using the initial volume (V_0), the final volume (V_{fin}), and the volume taken for the analyses (V_{anal}). The equation used for this calculation is $[S_8]_{corrected} = \frac{[S_8]_{in\ the\ sample} \times (V_0 - V_{anal})}{V_{fin}}$. During the experiment, the sample volume would be measured by weight and converted to volume using the solvent, or the density of the mineral oil in the cases where oil/solvent mixtures were studied.

Experimental results:

- Experiment 1:



The sample was pumped continuously to the top of the column containing polymer at 1 mL/min, where it passed through under pressure, back into the reservoir of oil. Approximately four volumes of 60 mL passed through the polymer during the 4 h of the experiment. Every hour a sample (5 mL) of the oil was taken to be analysed for S_8 content using the UHPSFC-MS SIR method. Since the amount of S_8 present in the sample is directly proportional to the TPPS peak area, its value was calculated using the appropriate calibration curve and also considering the dilution factor (a dilution of 1:400 was used in this case). A summary of the obtained results is presented below in Table 9.

Table 9 – Results of the preliminary reclamation experiment 1 to selectively remove S_8 from mineral oil.

Time (h)	Peak area ^a (TPPS)	Calculated [TPPS]	[TPPS] in the sample ^b	[S_8] in the sample	[S_8] corrected ^c	Removal efficiency ^d
0	n/a	n/a	n/a	200.0 ^e ppm	200.0 ^e ppm	n/a
1	1358092	4.43 ppm	1774 ppm	192.8 ppm	n/a	~4%
4	1103115	4.06 ppm	1625 ppm	176.6 ppm	n/a	~12%

^a Area from integration of the peak at approximately 1.57 min corresponding to TPPS in the UHPSFC chromatogram. ^b The value obtained for the concentration of TPPS after dilutions are taken in consideration

^c The corrected value takes into consideration the decrease in the total sample volume due to evaporation of solvent. ^d Removal efficiency is the proportion of S_8 removed during the process expressed as a percentage.

^e Original (t = 0) concentration of S_8 added to the sample in study.

By analysis of the data shown in table 9 we can see that the removal efficiency of the experiment (after 4 h) was only 12%. This can be explained by the fact that the swelling of the polymer in the oil is poor, and the sulfur could not efficiently access the phosphine sites within the polymer, limiting the rate of the reaction. Furthermore, the low flow rate only allowed for four volumes of the oil to cycle through the polymer resin. To investigate how properties of the oil, such as polarity and viscosity, influence polymer swelling the flow rate, the oil sample was mixed with THF (1:1). THF is an organic solvent that is known to swell the polymer beads efficiently (see experiment 2 below) and will also decrease the viscosity.

- Experiment 2:

The experiment was conducted in a similar way as the previous one, in this experiment a sample (50 mL, 50% of new mineral oil / 50% THF) was doped with 2.5 mg of elemental sulfur and was pumped continuously for 5 h, under reduced pressure. The flow rate achieved was around 3 mL/min, which allowed for 18 cycles. Every hour a sample (5 mL) was taken for quantification of elemental sulfur by UHPSFC-MS, due to solvent evaporation the final volume was 10 mL (instead of the expected 25 mL). The concentration of TPPS was then translated to concentration of S_8 in the

sample, the obtained value was achieved also considering the dilution (1:100 in this case). The summary of the obtained results is presented below in Table 10 and Figure 85.

Experimental conditions changed from experiment 1: Increase of flow rate (1 → 3 mL/min), decreased concentration of $[S_8]$ (200 → 50 ppm), extended reclamation time (4 → 5 h) and “oil sample” diluted with THF (50% of new mineral oil/ 50% THF (v/v)).

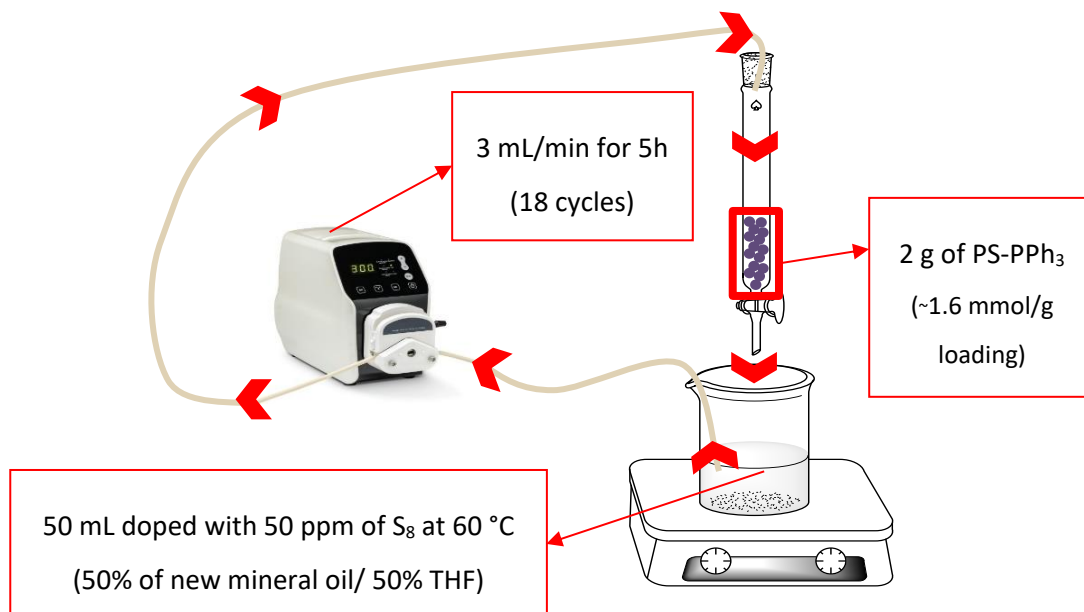


Table 10 – Results of the reclamation experiment 2 to selectively remove S₈ from mineral oil.

Time (h)	Peak area ^a (TPPS)	Calculated [TPPS]	[TPPS] in the sample ^b	[S ₈] in the sample	[S ₈] corrected ^c	Removal efficiency ^d
0	n/a	n/a	n/a	50.0 ^e ppm	50.0 ^e ppm	n/a
1	61439	3.53 ppm	353 ppm	38.5 ppm	-----	-----
2	47981	2.76 ppm	276 ppm	30.1 ppm	-----	-----
3	44497	2.56 ppm	256 ppm	27.9 ppm	-----	-----
4	34604	1.99 ppm	199 ppm	21.7 ppm	-----	-----
5	29890	1.72 ppm	172 ppm	18.7 ppm	7.50 ppm	~85%

^a Area from integration of the peak at approximately 1.53 min corresponding to TPPS in the UHPSFC chromatogram. ^b The value obtained for the concentration of TPPS after dilutions are taken in consideration

^c The corrected value takes into consideration the decrease in the total sample volume due to evaporation of solvent. ^d Removal efficiency is the proportion of S₈ removed during the process expressed as a percentage.

^e Original (t = 0) concentration of S₈ added to the sample in study.

During the experiment was clear that the addition of THF to the oil sample helped to swell the polymer (i.e., increased volume of the beads and also lowered the viscosity), allowing to an increase

of the flow rate from 1 to 3 mL/min due to the faster passage of the oil/THF solution through the beads. Using the data shown in Table 10, the final concentration of S_8 was calculated and a value of 7.48 ppm was obtained. This corresponds to a reclamation efficiency of close to 85 %, which represents a significant increase from the first/last experiment. This improvement can be easily seen in the Figure 86, where the decrease of the TPPS in the sample is evident just by looking to the corresponding peak (1.53 min – marked by the black box) during the 5 h of the experiment.

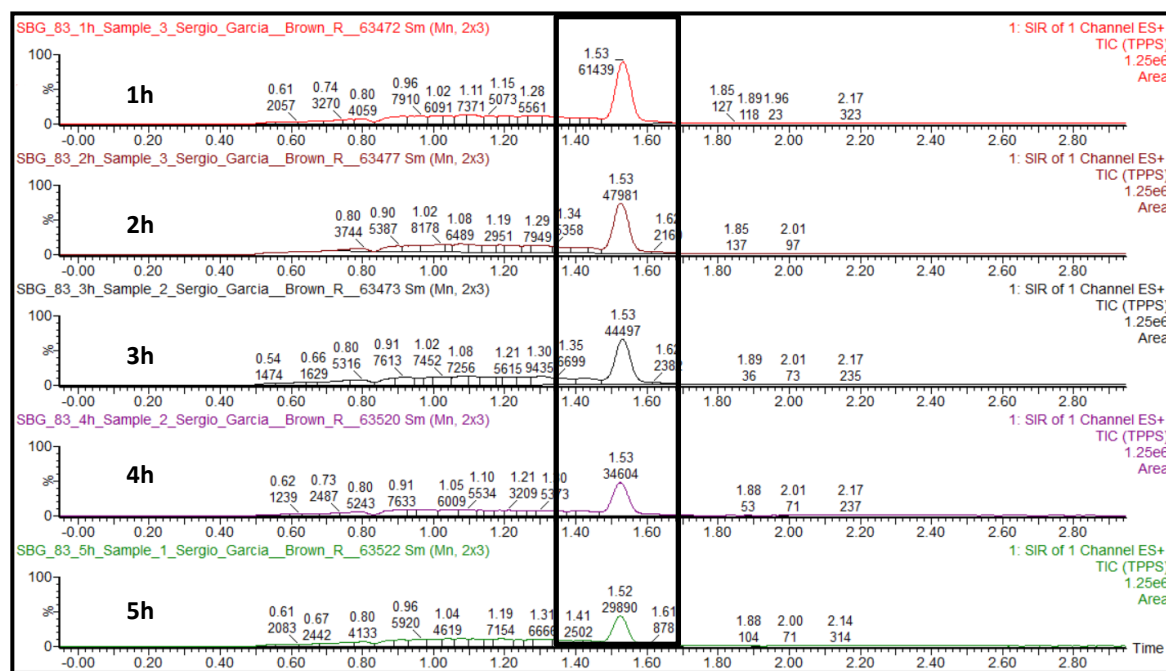


Figure 86 - SFC-MS chromatogram showing the change in concentration of S_8 in the second experiment.

Although, the use of an organic solvent (THF) is not adequate to be used in the field, this experiment proved not only that the increase of flow rate and swelling of the polymer promotes a higher removal efficiency of S_8 from mineral oil but also that the use of triphenylphosphine is adequate for the selective removal of the S_8 . It is likely that pre-swelling of the beads with THF and the utilisation of a closed system would further promote the increase of the flow rate and minimise the solvent loss by evaporation. However, these conditions are not compatible with application in the field (i.e., use of organic solvents is not possible and power transformers are “open to air”). The use of a mixed solvent system clearly demonstrated the importance of swelling of beads on efficient removal of elemental sulfur, and further experiments using THF were not conducted. Although the polymer beads used were not optimum for use in sulfur removal from oil, the scavenging efficiency was further explored using other solvent media. Subsequent experiments (3 and 4) were conducted in toluene, its higher boiling point (compared to THF), should mitigate/reduce the solvent loss due to evaporation during the study. These experiments were carried out with the main goal of establishing if the polymer being studied (when used in “optimal” conditions, i.e., good swelling and flow rate) would provide efficient removal of S_8 .

- Experiments 3 and 4:

In both experiments the sample in study was prepared by addition of 2.5 mg of elemental sulfur to 50 mL of toluene. Similarly, to the other experiments, the sample under study was then pumped continuously for 5 h, at a flow rate of 7 mL/min, which allowed for 42 cycles. Samples were taken every hour and the results for both experiments, 3 and 4, are presented below in Table 11 and 12, respectively. Despite major efforts, significant evaporation was observed in both experiments, leading to a final volume of 6 mL in the experiment 3 and 6.5 mL in the experiment 4.

Conditions changed from experiment 2: Increased flow rate (3 → 7 mL/min) and sample medium is Toluene.

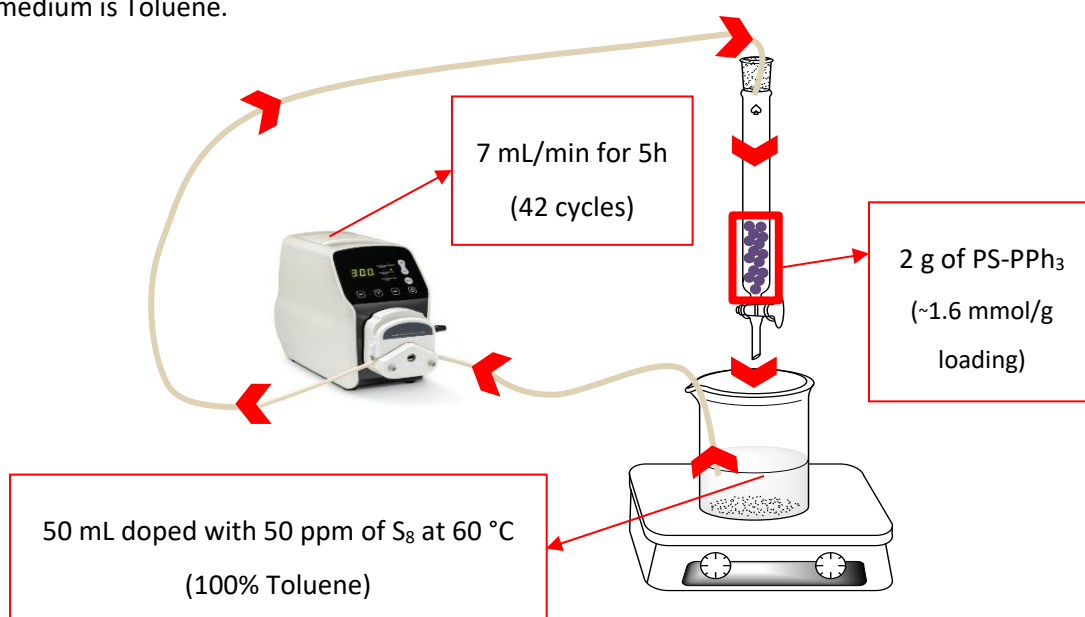


Table 11 – Results of the preliminary reclamation experiment 3 to selectively remove S₈ from mineral oil.

Time (h)	Peak area ^a (TPPS)	Calculated [TPPS]	[TPPS] in the sample ^b	[S ₈] in the sample	[S ₈] corrected ^c	Removal efficiency ^d
0	n/a	n/a	n/a	50.0 ^e ppm	50.0 ^e ppm	n/a
1	29918	1.72 ppm	172 ppm	18.7 ppm	-----	-----
5	9023	0.52 ppm	52 ppm	5.6 ppm	1.4 ppm	~97%

Table 12 – Results of the preliminary reclamation experiment 4 to selectively remove S₈ from mineral oil.

Time (h)	Peak area ^a (TPPS)	Calculated [TPPS]	[TPPS] in the sample ^b	[S ₈] in the sample	[S ₈] corrected ^c	Removal efficiency ^d
0	n/a	n/a	n/a	50.0 ^e ppm	50.0 ^e ppm	n/a
1	62679	3.59 ppm	359 ppm	39.2 ppm	-----	-----
5	24924	1.43 ppm	143 ppm	15.6 ppm	4.1 ppm	~92%

^a Area from integration of the peak at approximately 1.47 min corresponding to TPPS in the UHPSFC chromatogram. ^b The value obtained for the concentration of TPPS after dilutions are taken in consideration. ^c The corrected value takes into consideration the decrease in the total sample volume due to evaporation of solvent. ^d Removal efficiency is the proportion of S_8 removed during the process expressed as a percentage. ^e Original ($t = 0$) concentration of S_8 added to the sample in study.

From these experiments we were able to conclude and prove that the increase of the flow rate, and a better swelling of the polymer, lead to high removal efficiency of S_8 . Unfortunately, even with the use of a higher boiling point solvent toluene, significant evaporation was observed in both experiments. The results obtained were similar in both cases, with values of removal efficiency of around 97% for experiment 3 and around 92% for experiment 4. Since an increase of flow rate seemed to increase the efficiency of removal of S_8 , a similar experiment to 1 was conducted next. Where the use of a new peristaltic pump allowed the increase of flow rate of 1 mL/min to 5 mL/min when using samples of mineral oil, for the results see below.

Experiment 5:

In this experiment 3 mg of elemental sulfur were added to 50 mL of new mineral oil. A peristaltic pump was used to pump the sample continuously 7 h in the first day and 8 h in the next day. During the study a flow rate of around 5 mL was achieved, samples were collected every hour between 1 and 7 h, and then at 9:30 h and 15 h. The results are shown above in Table 13. Note: Samples from 1 to 6 h were analysed but the data obtained had been compromised by instrument issues during the collection. Fortunately, the samples corresponding to 7, 9:30 and 15 h were analysed in a different day and “good” data was obtained.

Conditions changed from experiment 3/4: Decreased flow rate (7 → 5 mL/min), $[S_8]$ (50 → 60 ppm) and increased reclamation time (5 → 15 h).

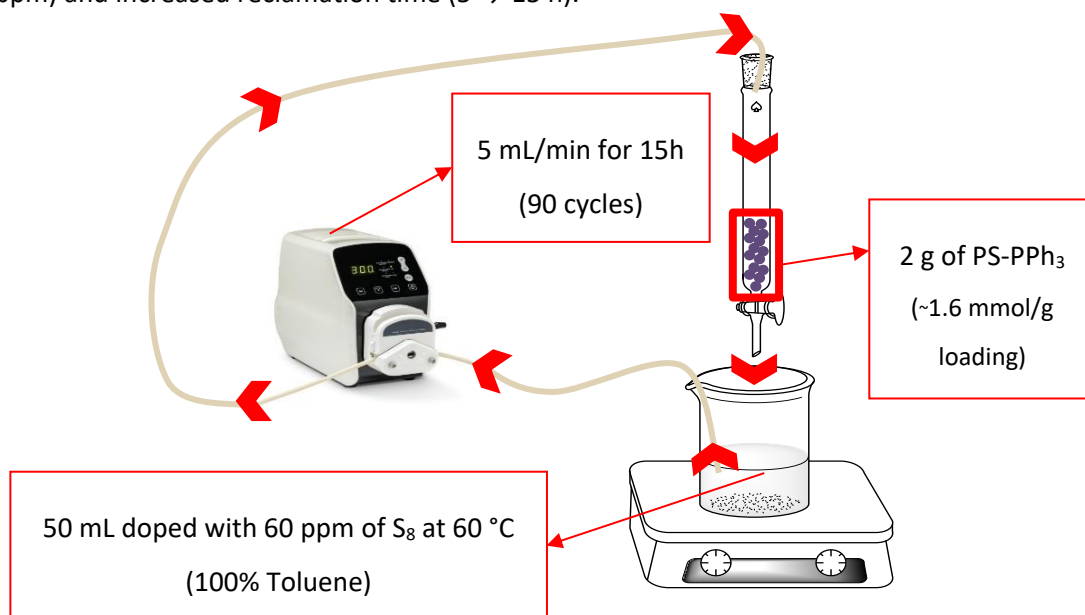


Table 13 – Results of the preliminary reclamation experiment 5 to selectively remove S₈ from mineral oil.

Time (h)	Peak area ^a (TPPS)	Calculated [TPPS]	[TPPS] in the sample ^b	[S ₈] in the sample	[S ₈] corrected ^c	Removal efficiency ^d
0	n/a	n/a	n/a	60.0 ^e ppm	60.0 ^e ppm	n/a
7	177528	3.69 ppm	185 ppm	20.1 ppm	n/a	~66%
9.5	144709	3.01 ppm	151 ppm	16.4 ppm	n/a	~73%
15	112551	2.34 ppm	117 ppm	12.7 ppm	n/a	~79%

^a Area from integration of the peak at approximately 1.47 min corresponding to TPPS in the UHPSFC chromatogram. ^b The value obtained for the concentration of TPPS after dilutions are taken in consideration

^c The corrected value takes into consideration the decrease in the total sample volume due to evaporation of solvent. ^d Removal efficiency is the proportion of S₈ removed during the process expressed as a percentage.

^e Original (t = 0) concentration of S₈ added to the sample in study.

The main purpose of this study was to understand if a higher flow rate and reclamation time could compensate the poor swelling of the polymer by the mineral oil. By analysis of the results obtained, we can conclude that even if the swelling of the polymer was poor, the decrease in concentration of S₈ in the mineral oil sample is noticeable. From this, we can then infer that if the oil is pumped long enough the elemental sulfur will be completely removed. In the field, reclamation processes usually take place during days or even weeks.

4.3.2.1.1 Summary of the results

The results obtained in these five experiments were compiled and are shown in Table 14, a brief discussion and conclusion is found in the next subchapter.

Table 14 – Summary of the obtained results of the preliminary reclamation experiments to selectively remove S₈ from mineral oil.

Experiment	Sample in study	Flow rate (mL/min)	Reclamation Time (h)	Initial [S ₈] in the sample	Final [S ₈] in the sample	Removal efficiency
1	New Mineral Oil	1	4	200 ppm	176.6 ppm	~12%
2	1:1 New Mineral Oil/THF	3	5	50 ppm	7.5 ppm	~85%
3	Toluene	7	5	50 ppm	1.4 ppm	~97%
4	Toluene	7	5	50 ppm	4.1 ppm	~92%

5	New Mineral Oil	5	15	60 ppm	12.7 ppm	~79%
---	-----------------	---	----	--------	----------	------

4.3.2.1.2 Conclusion of the preliminary reclamation processes to selectively remove S₈ from transformer mineral oil

The capability of a laboratory reclamation rig to remove elemental sulfur from mineral oil (and mixtures with mineral oil) was demonstrated during the last study, and most importantly not only demonstrated a really high efficiency of S₈ removal can be achieved (< 90%) but also allowed the reclamation conditions to remain stable during all the experiment and that the conditions could be replicated. The polymer-bound triphenylphosphine (Figure 77) was found to efficiently remove elemental sulfur from different samples. When applied to the removal of elemental sulfur from toluene the removal efficiency reached values as high as ~97%. In the experiments where mineral oil was used, the complete removal of elemental sulfur was not achieved in the time frame of the experiment due to the decreased flow rate/poor swelling of the polymer in the presence of the oil. Although these experiments were not entirely successful, they demonstrated that extending the reclamation time would invariably lead to higher removal efficiencies. Therefore, in order to achieve faster reclamation times - two main parameters were optimised, which lead to:

- An increasing of the flow rate (i.e., increased number of cycles of the oil through the polymer).
- Improved swelling of the polymer in the mineral oil.

The optimisation/final conditions of these parameters are detailed in the following sub-chapters.

4.3.2.2 Optimisation of the flow rate

From the preliminary results for removal of elemental sulfur using the triarylphosphine polymer it was evident that a higher flow rate was necessary to achieve not only more efficient removal of sulfur but also to provide conditions that could be more easily reproduced in the field. To achieve this a number of different parameters were varied, but significant increase of the flow rate was only achieved when the column was changed so that the solution could be pumped directly through the polymer. Different columns were tried, the best results were obtained when an empty column (Biotage® Sfär - empty 10 g column with frits) was employed (Figure 87).



Figure 87 - Column that was utilised in the optimised lab. reclamation rig.

4.3.2.3 Swelling of the polystyrene polymer in the mineral oil

It was evident that the polystyrene backbone of our solid support was not the most appropriate to be used in mineral oil. The poor swelling of the polystyrene in the mineral oil leads to a decrease in the surface area, and consequently negatively affecting the number of active sites available for the removal of S_8 . This phenomenon is illustrated in Figure 88. In oil, we can see that the surface area of the polymer is at least half of the one that is shown in the figure where the solid support is in toluene caused by the toluene entering into the polymer beads and solvating the chains. This does not occur efficiently in the highly nonpolar mineral oil, limiting access of the sulfur to the internal sites. With this in mind, we can presume that the use of a different backbone for our solid support, one that would present good swelling properties in oil would increase the efficiency of the polymer support to remove S_8 . This increase could then lead to faster reclamation processes. A different backbone for the solid support that is more compatible with the mineral oil would be advantageous. Our plan was to investigate a superhydrophobic poly(lauryl methacrylate) back-bone polymer that should present good swelling properties in mineral oil. The synthesis of this polymer, designated as polymer B, is described in full in Chapter 6.

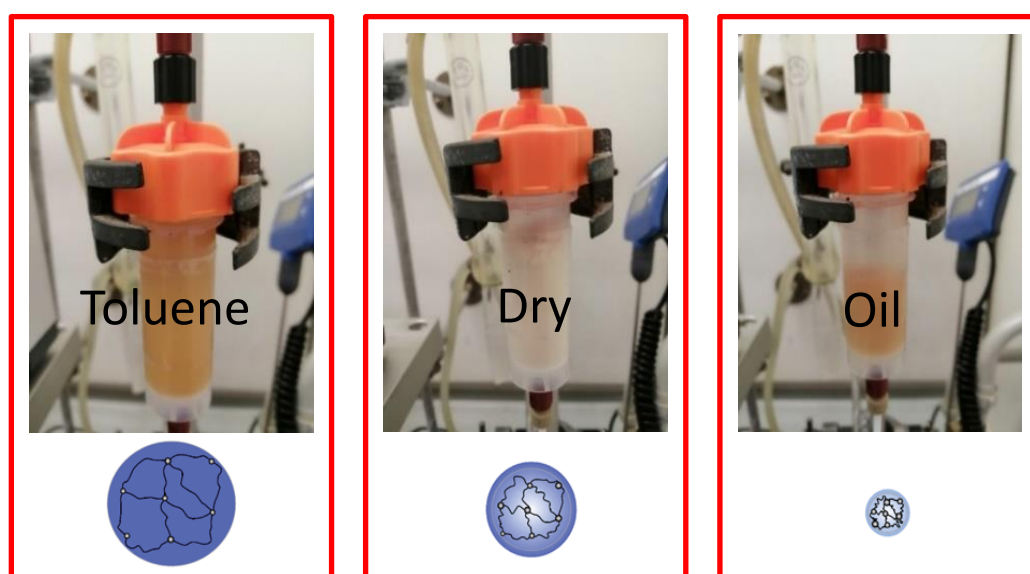


Figure 88 - Solvent effect on the swelling of the polystyrene-triphenylphosphine polymer.

4.3.3 Optimised reclamation process to selectively remove S₈ from transformer mineral oil

The general procedure involved the loading of seven grams of the trisubstituted phosphine-loaded polymer under evaluation into an empty column (Biotage® Sfär - empty 10 g column with frits). The mineral oil (250 mL) under study (in a RBF) was warmed using a aluminium heat transfer block placed on a heating plate at 60 °C, with stirring, and then continuously pumped (50 mL/min) through the system. Analyses for S₈ content would be performed every 6-8 hours. The experiment would be deemed complete once the concentration of S₈ present in the oil sample would be ≤ 100



Figure 89 - Optimised laboratory reclamation rig set-up used for the selective removal of elemental sulfur from mineral oil.

ppb. To note that the volume of the mineral oil would be measured by weighing after every analysis, to ensure an accurate calculation. The pump used in our work was a Masterflex L/S digital miniflex pump (item number: WZ-07525-40) and the tubing was Masterflex L/S® precision pump tubing (part number: 06424-16). The optimised laboratory set-up used for elemental sulfur removal is shown below in Figure 89.

In this work four different trisubstituted phosphine-loaded polymers were studied in terms of their ability to selective remove S₈ from the mineral insulating oil B. The polymers are identified as polymers A, B, C and D (Figure 90). Polymers A (same as used in the preliminary experiments) and C were purchased from Sigma-Aldrich and used as received, polymers B and D were synthesised as

part of this work. The synthetic experimental section will be discussed later on, in the organic experimental part (Chapter 6).

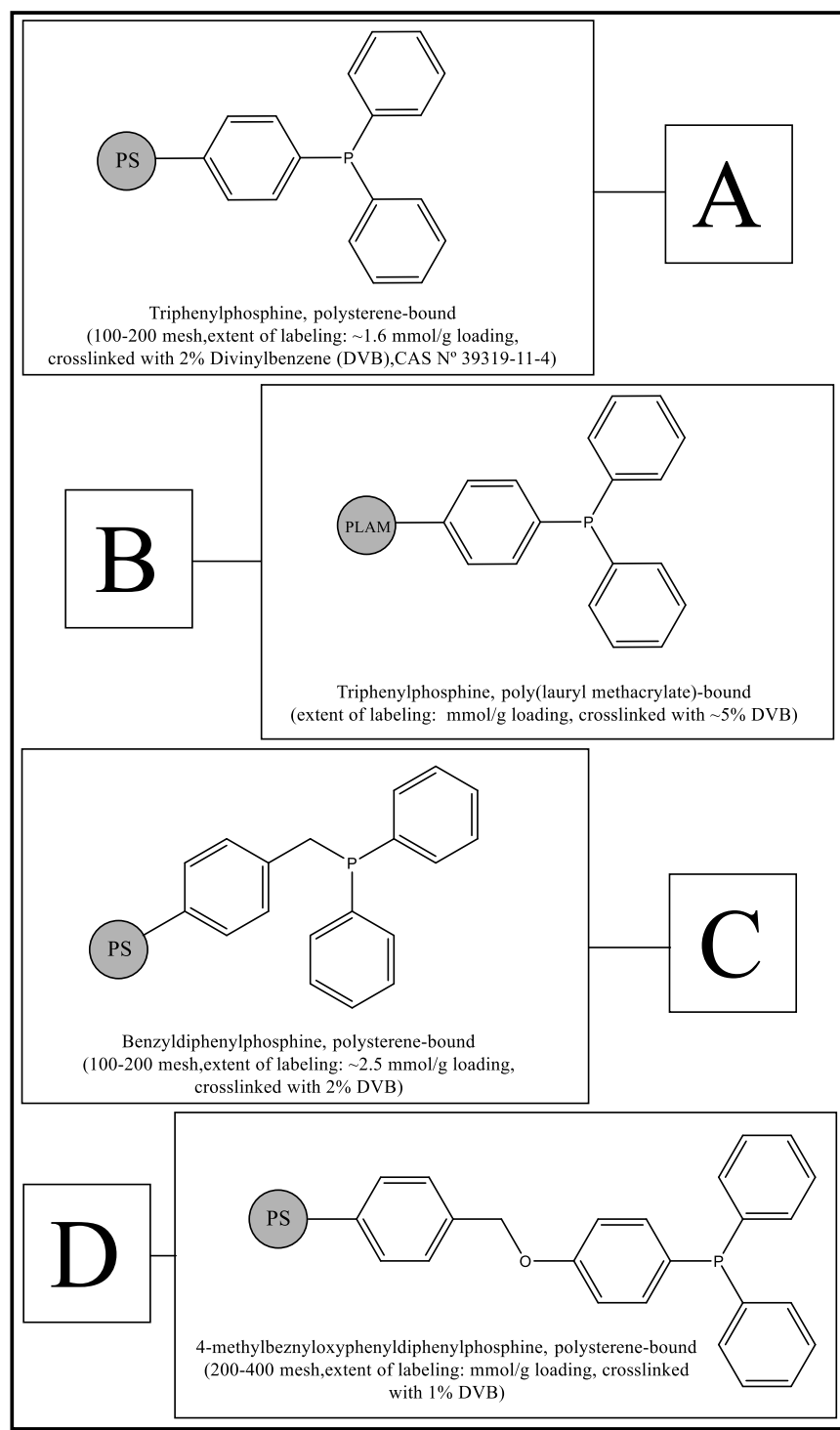


Figure 90 – The different trisubstituted phosphine-loaded polymers that were studied in their ability to selectively remove S_8 from mineral oil.

4.3.3.1 Effectiveness of the laboratory reclamation strategy with respect to reducing silver corrosion

The success of the reclamation process was evaluated using a simple visual testing strategy for corrosion. After having been subjected to our reclamation process for removal of S_8 , the mineral oil sample under study would be tested using the standard silver corrosion test (DIN 51 353). If the test presented a negative result the experiment would be considered successful, if a positive result was presented the oil sample would be once more subjected to our reclamation process until a negative result was obtained. The corrosion tests would be supported by elemental sulfur analysis using the method described in chapter 2. An overview of the strategy is shown in the Fig. 91.

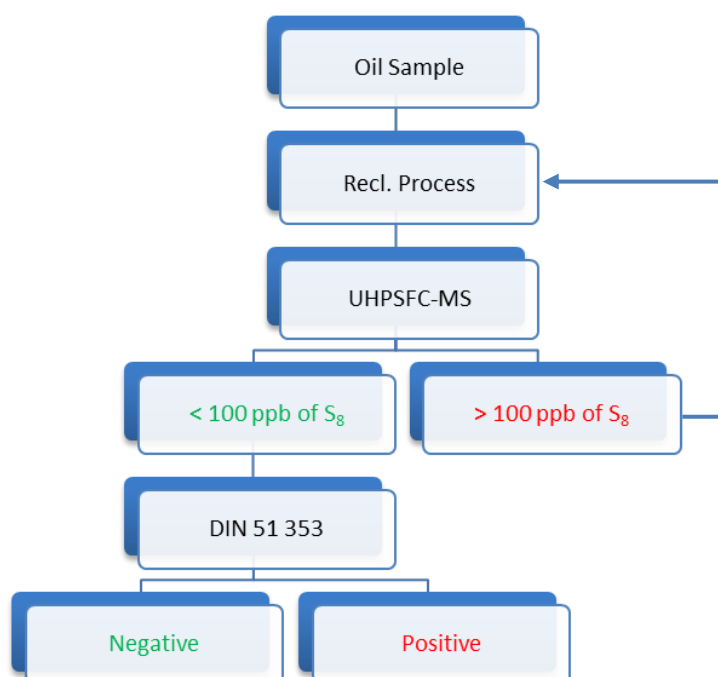


Figure 91 - Strategy to study the effectiveness of our reclamation process in reducing silver corrosion.

4.3.3.2 Reclamation of a new transformer mineral oil sample spiked with S_8 using polymer A

The new and optimised reclamation rig was first tried with a 250 mL sample of new transformer oil spiked with 100 ppm of S_8 . In this experiment the sample was continuously pumped at 50 mL/min through a column loaded with 7.00 g of the PS-PPh₃ polymer A. Aliquots were removed periodically and subjected to the derivatisation method and analysed using UHPSFC-MS (dilutions employed varied depending on the concentration of S_8 remaining in the oil sample), once the [S_8] present in the sample would be ≤ 100 ppb the experiment would stop. The set-up and the results of this experiment are shown below.

Conditions changed from experiment 5 (page 100): Flow rate (5 → 50 mL/min), [S₈] (60 → 100 ppm) and 100% oil sample.

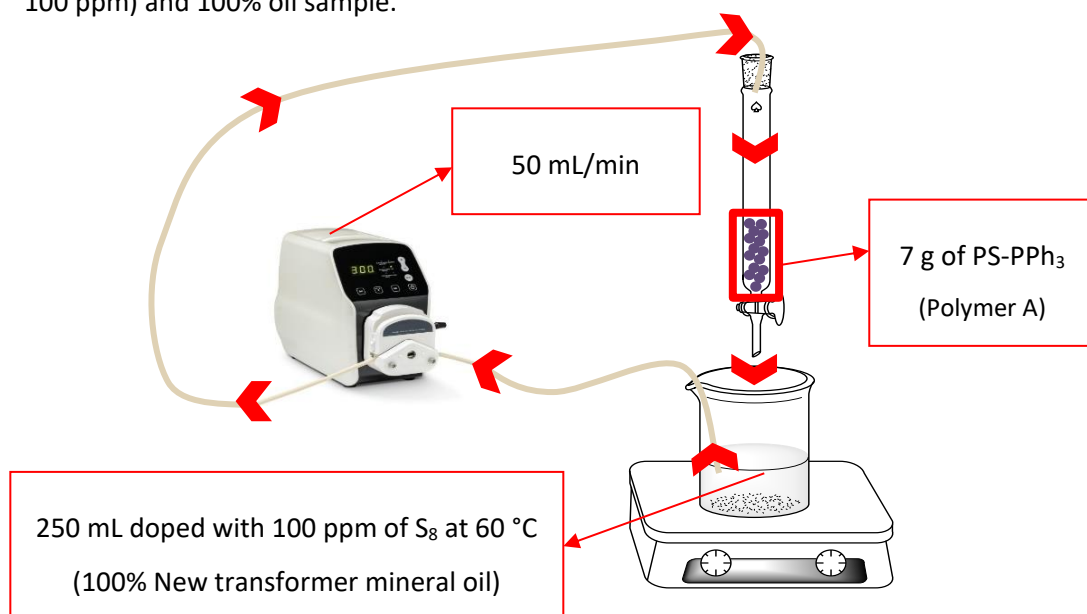


Table 15 – Results of the reclamation of new transformer mineral oil sample spiked with S₈ using polymer A to selectively remove S₈.

Time (h)	Peak area ^a (TPPS)	Calculated [TPPS]	[TPPS] in the sample ^b	[S ₈] in the sample	Removal efficiency ^c
0	n/a	n/a	n/a	100.00 ^d ppm	n/a
6.5	763161	2.54 ppm	508 ppm	55.27 ppm	~45%
24	54752	1.28 ppm	64 ppm	6.96 ppm	~93%
32	11290	0.26 ppm	13 ppm	1.43 ppm	~99%
42	638	0.015 ppm	0.7 ppm	0.08 ppm	~100%

^a Area from integration of the peak at approximately 1.50 min corresponding to TPPS in the UHPSFC chromatogram. ^b The value obtained for the concentration of TPPS after dilutions are taken in consideration

^c Removal efficiency is the proportion of S₈ removed during the process expressed as a percentage. ^d Original (t = 0) concentration of S₈ added to the sample in study.

Looking at the results obtained we can observe that the concentration of S₈ in the sample decreases to levels of less than 100 ppb. Meaning that the reclamation efficiency of this experiment is close to 100%. It is also evident that the decrease of the S₈ concentration in the mineral oil sample seems to follow an exponential decay. Which indicates that most of the S₈ removal is achieved in the first hours of the reclamation process. This result proved our initial beliefs/conclusions that higher flow rates in conjunction with higher reclamation times would inevitably lead to the removal of all the S₈ present in the mineral oil sample.

With a successful demonstration using sulfur-spiked new oil, we decided to perform the reclamation process on an ex-service oil sample from Nation Grid with four different trisubstituted phosphine-loaded polymers (Figure 88). The chosen oil sample for this study was the one that presented a concentration of ~17 ppm of S_8 (denominated previously as Oil sample B – see 3.3.4 for the analytical data). Which is a value that presents a corrosive risk for the transformer, as demonstrated in the performed silver corrosion test – the results are shown in Figure 58/Page 71. See below for the results and conclusions of these experiments.

4.3.3.3 Reclamation process of an ex-service transformer mineral oil sample (B) using the polymer A

Conditions changed from experiment 4.3.3.2 (above): Oil sample under study is the ex-service oil - Sample B with $[S_8]$ (100 → 17 ppm).

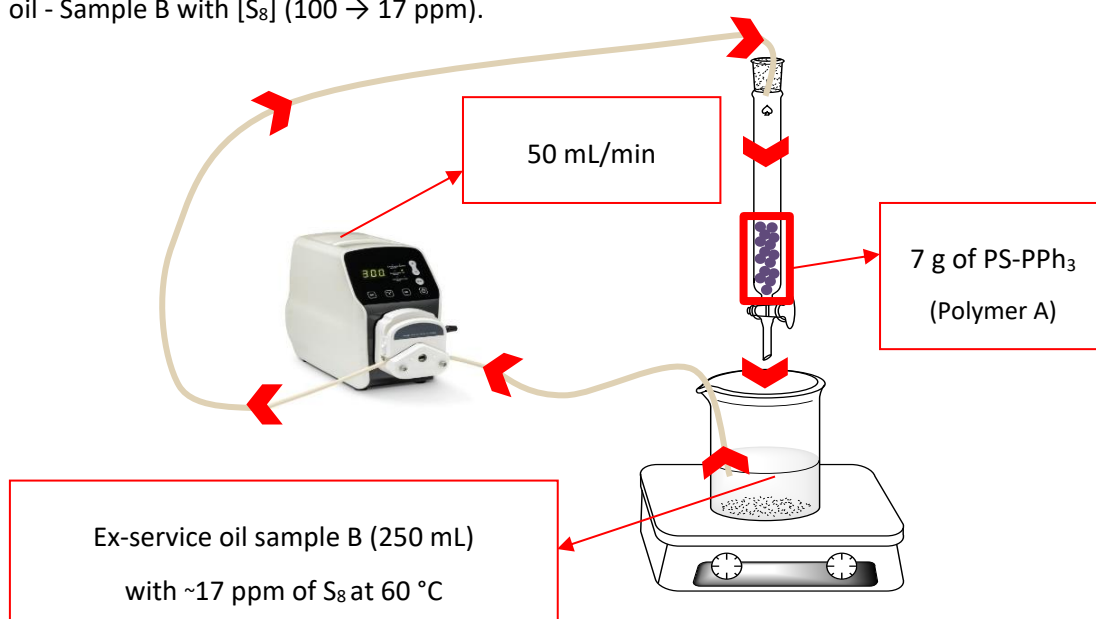


Table 16 – Results of the reclamation of ex-service oil sample B using polymer A to selectively remove S_8 .

Time (h)	Peak area ^a (TPPS)	Calculated [TPPS]	[TPPS] in the sample ^b	$[S_8]$ in the sample	Removal efficiency ^c
0	n/a	n/a	n/a	17.0 ^d ppm	n/a
14	127501	2.24 ppm	112 ppm	12.14 ppm	~29%
22	67826	1.36 ppm	68 ppm	7.38 ppm	~57%
50	799	0.016 ppm	0.8 ppm	0.09 ppm	~100%

^a Area from integration of the peak at approximately 1.50 min corresponding to TPPS in the UHPSFC chromatogram. ^b The value obtained for the concentration of TPPS after dilutions are taken in consideration

^c Removal efficiency is the proportion of S_8 removed during the process expressed as a percentage. ^d Original (t = 0) concentration of S_8 in the sample in study.

The variation of the concentration of S_8 during the experiment is demonstrated in Table 15. It is clear, from the results obtained that the total removal of S_8 from an ex-service corrosive mineral oil sample is possible. As we have discussed before, the lower the concentration of S_8 present in the oil the longer it seems that takes to remove it.

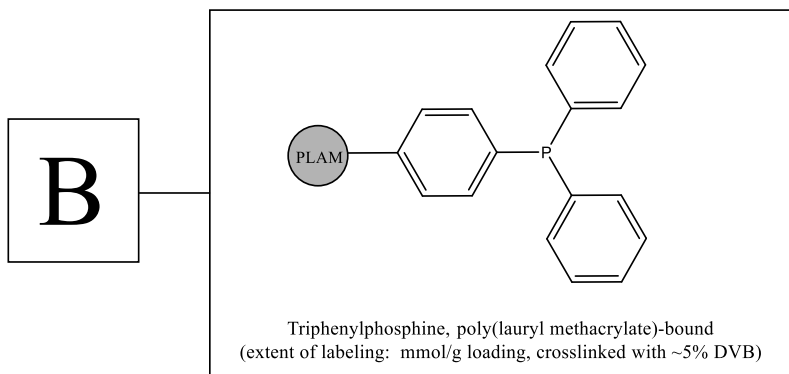
To confirm that the reclamation process was indeed successful, the reclaimed sample was subjected to the silver corrosion test (DIN 51 353), and the result of this test is shown below in Figure 92. For a better understanding and comparison purposes of the results, a reference silver strip, and the result of the corrosion test before the reclamation process are also shown.



Figure 92 - Result of the silver corrosion test obtained from the oil sample B after being subjected to our reclamation process with polymer A. * Yellow colouration is due to the thermal stress.

From the Figure 92, we can clearly see that the silver strip gave a negative result for the silver corrosion test after the reclamation experiment. We can then conclude that not only we were able to transform a corrosive sample into a non-corrosive one, but we were also able to demonstrate that the near total removal of the S_8 from ex-service oils can be achieved. To prove that this outcome could be reproduced, the experiment was reconducted and a similar result was obtained. The polymer being reused without being regenerated, did not have a clear effect on the reclamation process time. This means that the polymer probably only needs to be regenerated once the concentration of free phosphine is depleted. Having now established the proof of principle, we decided to perform our reclamation process also with the other trisubstituted phosphines (Polymer B, C and D). The experiments were conducted in the same way as described before, and the results of these experiment are demonstrated below.

4.3.3.4 Reclamation process of an ex-service transformer mineral oil sample (B) using polymer B



Conditions changed from experiment 4.3.3.3 (above): Polymer in study is changed to polymer B.

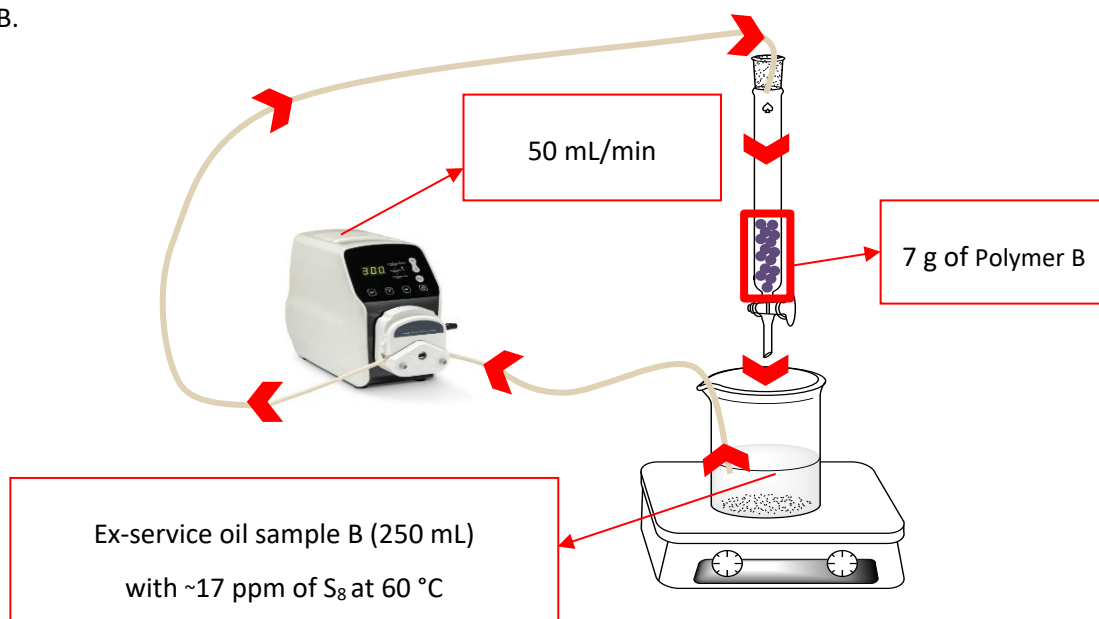


Table 17 – Results of the reclamation of ex-service oil sample B using polymer B to selectively remove S₈.

Time (h)	Peak area ^a (TPPS)	Calculated [TPPS]	[TPPS] in the sample ^b	[S ₈] in the sample	Removal efficiency ^c
0	n/a	n/a	n/a	17.00 ^d ppm	n/a
20	153505	2.95 ppm	59 ppm	6.41 ppm	~62%
32	40562	0.78 ppm	7.8 ppm	0.85 ppm	~95%
42	4647	0.09 ppm	0.9 ppm	0.098 ppm	~100%

^a Area from integration of the peak at approximately 1.58 min corresponding to TPPS in the UHPSFC chromatogram. ^b The value obtained for the concentration of TPPS after dilutions are taken in consideration

^c Removal efficiency is the proportion of S₈ removed during the process expressed as a percentage. ^d Original (t = 0) concentration of S₈ in the sample in study.

The results obtained are in accordance with the ones previously obtained for the reclamation process with polymer A. The results in Table 17, demonstrate that polymer B can also successfully remove S_8 from the mineral oil sample B. This also confirms the previous results/conclusions, that most of the S_8 removal is achieved in the first hours of the reclamation process, which is an excellent feature when we consider its viability to be applied in an industrial set up. Where the primary goal is the transformation of a corrosive oil sample into a non-corrosive one, and not the total removal of S_8 . This means that less time would be needed for a successful reclamation process, which would not only translate in economic advantages, but also in a more reliable and effective transmission grid. To confirm this line of thought, a silver corrosion test was not only conducted at the end of the reclamation process (i.e., when $[S_8] < 100$ ppb) but also during the reclamation time once the concentration of S_8 was believed to drop to levels of no risk for the transformer. In this case, a corrosive silver test was also conducted at the 32 h mark, when the $[S_8]$ was < 1 ppm. The results of the two silver corrosion tests conducted in this experiment are shown below, Figure 93.

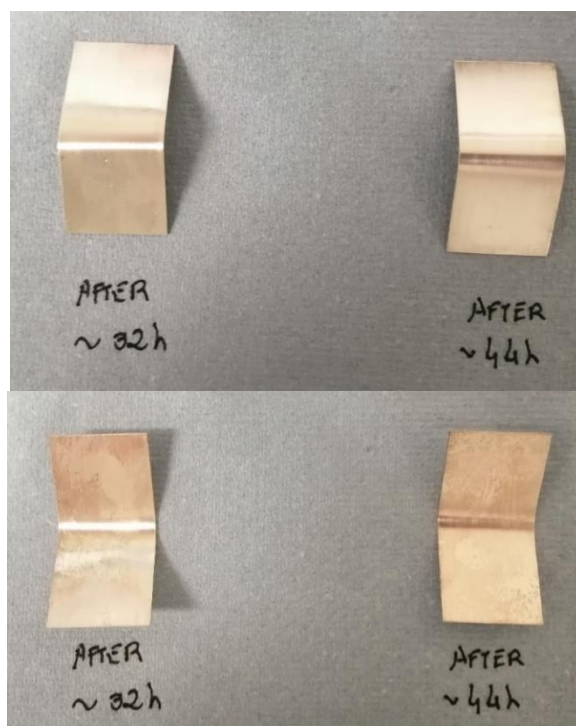


Figure 93 – Results of the corrosion tests of the oil sample B after 32 and 44 h of reclamation with Polymer B.

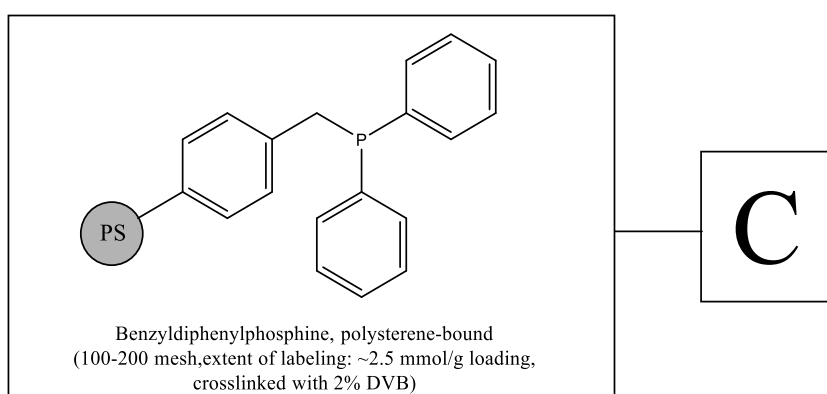
From the results obtained from the corrosion tests, Figure 93, is clear that no corrosion occurred during the test. This double negative result is very interesting, this shows that to transform a corrosive sample into a non-corrosive one a total removal of S_8 is not necessary. Another interesting outcome of this experiment was the lack of yellow colouration at the end of the silver corrosion test. This outcome was confirmed by conducting another corrosion test and similar results were obtained. This was not studied in detail but an “explanation” for this was found when looking at the

polymer B before and after the reclamation process. The polymer changed from presenting a clear colour to a yellowish/brown colouration. It is possible that the compounds responsible for the yellow colouration of the strip are being “trapped” in the polymer gel. This can be easily seen by analysing the Figure 94.



Figure 94 – Change in colour of the polymer B due to reclamation process of the oil sample B.

4.3.3.5 Reclamation process of an ex-service transformer mineral oil sample (B) using the polymer C



Conditions changed from experiment 4.3.3.4 (above): Polymer under study is now polymer C.

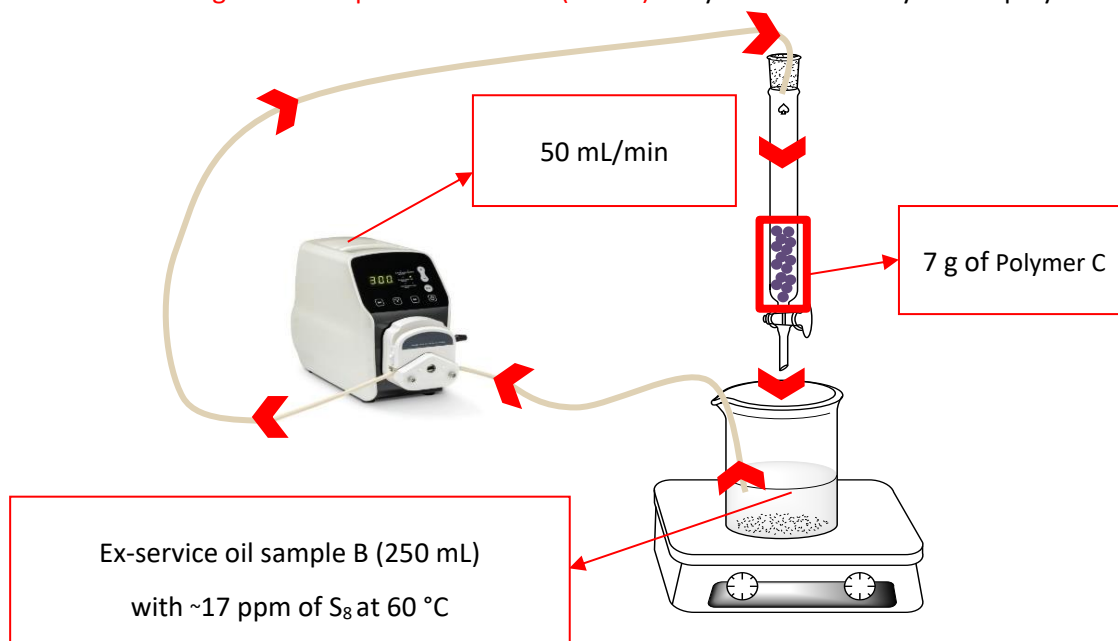


Table 18 – Results of the reclamation of ex-service oil sample B using polymer C to selectively remove S₈.

Time (h)	Peak area ^a (TPPS)	Calculated [TPPS]	[TPPS] in the sample ^b	[S ₈] in the sample	Removal efficiency ^c
0	n/a	n/a	n/a	17.00 ^d ppm	n/a
35	66033	1.21 ppm	61 ppm	6.63 ppm	~61%
49	37366	0.69 ppm	13.8 ppm	1.5 ppm	~93%
63	5921	0.11 ppm	1.1 ppm	0.12 ppm	~100%

^a Area from integration of the peak at approximately 1.52 min corresponding to TPPS in the UHPSFC chromatogram. ^b The value obtained for the concentration of TPPS after dilutions are taken in consideration

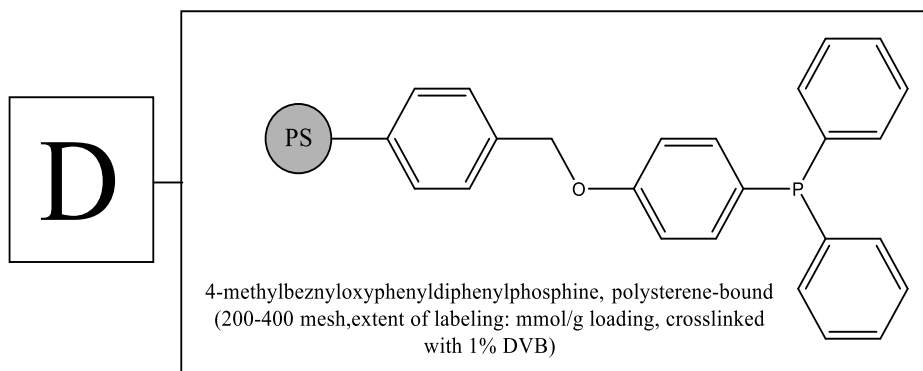
^c Removal efficiency is the proportion of S₈ removed during the process expressed as a percentage. ^d Original (t = 0) concentration of S₈ in the sample in study.

The removal of the S₈ was also successful with polymer C, this can be seen from the obtained results shown in Table 18. In this case the reclamation process took more time than in the previous two cases. This will be discussed in further detail later on, once the results of the four studied polymers are presented. The corrosive standard test that resulted from this experiment is shown in Figure 95, and as we can observe it provided a negative outcome.



Figure 95 - Result of the silver corrosion test obtained from the oil sample B after being subjected to our reclamation process with polymer C.

4.3.3.6 R Reclamation process of an ex-service transformer mineral oil sample (B) using the polymer D



Conditions changed from experiment 4.3.3.5 (above): Polymer under study is polymer D.

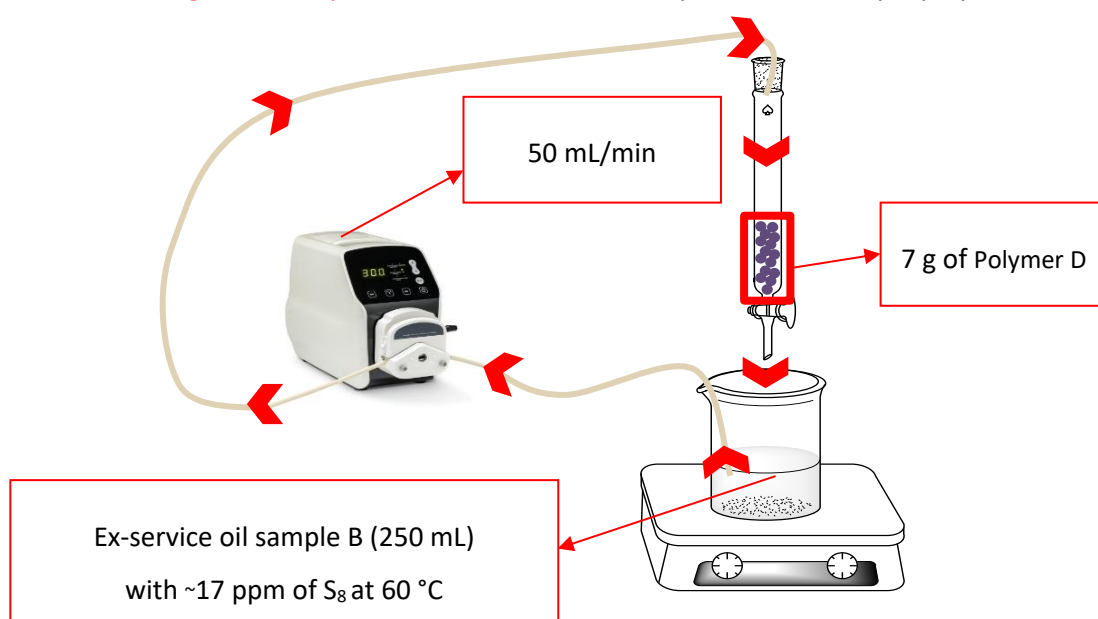


Table 19 – Results of the reclamation of ex-service oil sample B using polymer D to selectively remove S₈.

Time (h)	Peak area ^a (TPPS)	Calculated [TPPS]	[TPPS] in the sample ^b	[S ₈] in the sample	Removal efficiency ^c
0	n/a	n/a	n/a	17.00 ^d ppm	n/a
32	52719	0.94 ppm	47 ppm	5.11 ppm	~70%
40	34181	0.61 ppm	12.2 ppm	1.33 ppm	~92%
56	5148	0.09 ppm	0.9 ppm	0.1 ppm	~100%

^a Area from integration of the peak at approximately 1.53 min corresponding to TPPS in the UHPSFC chromatogram. ^b The value obtained for the concentration of TPPS after dilutions are taken in consideration

^c Removal efficiency is the proportion of S₈ removed during the process expressed as a percentage. ^d Original (t = 0) concentration of S₈ in the sample in study.

The outcome from this experiment, that is presented in Table 19, clearly demonstrates that polymer D is able to remove S_8 from the mineral oil sample. The reclamation time of 56 h goes in line with the obtained with the other polystyrene polymers. In Figure 96 the result of the standard corrosive test that was conducted after the reclamation process with polymer D is presented. Once again, a negative result was obtained, demonstrating once more the capability of our reclamation process to remove selectively all the elemental sulfur present in the ex-service oil sample B.

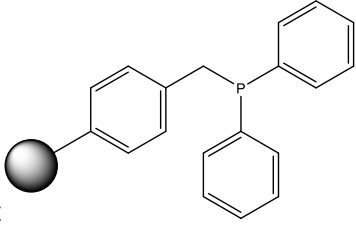
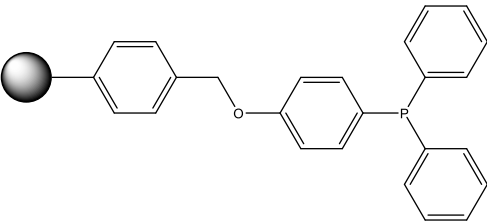


Figure 96 - Result of the silver corrosion test obtained from the oil sample B after being subjected to our reclamation process with polymer D.

4.3.3.7 Summary of the obtained results

Table 20 - Results obtained from the reclamation processes experiments of the ex-service oil sample B.

Solid Support	UHPSFC-MS	Standard corrosion test DIN 51 353	Reclamation Time (h)
<p>A</p>	<100 ppb of S_8	Negative	50
<p>B</p>	<100 ppb of S_8	Negative	42

 <p>C</p>	<100 ppb of S ₈	Negative	63
 <p>D</p>	<100 ppb of S ₈	Negative	56

The results obtained from the reclamation process of the corrosive ex-service oil sample B with the four different trisubstituted phosphine-loaded polymers is summarised in the Table above. We can conclude that the polymer B presented the best result among all of the studied polymers, with a reclamation time of around 42 h. The influence of the backbone and the P-active site is discussed in further detail below.

4.3.3.8 Reactivity of the different polymers

Two different back-bones were utilised for our P-containing polymers. Three of the polymers, A, C and D, have a polystyrene back-bone (Polymer A (P-active loading = ~ 1.6 mmol/g), C (P-active loading = ~ 2.5 mmol/g) and D (theoretical P-active loading = ~ 3 mmol/g)) and the fourth polymer B (theoretical P-active loading = ~ 0.4 mmol/g) had a poly(lauryl-methacrylate) back-bone. Polymers A and C were acquired from commercial suppliers and polymers B and D were synthesised. In addition to the different back-bones our polymers also presented different phosphine structures and loadings, which would lead to different reactivities towards the S₈. In this way we could not only compare the effect of having different P-active sites but also how the back-bone would affect the reactivity. It is important to note the difference in the reclamation time observed using polymers A (50 h), C (63 h) and D (56 h), despite all three polymers possessing the same polystyrene back-bone. The reclamation experiments indicate that A is the most active polystyrene-based polymer in terms of rate of removal of sulfur from mineral oil. This result is hard to rationalise on the basis of P loading, which is lower for polymer A, compared to C or D. It is also hard to rationalise based on the structures of the phosphines, where more electron-rich (polymer D) or less hindered phosphines (polymer C) would be expected to have greater inherent reactivity. The discrepancy may be attributed to the physical properties of the polymers where polymer A possibly presented more accessible P-active sites that originated from the polymer synthesis method. For example, the phosphine sites may be on the exterior of the beads, which poorly swell in mineral oil, rendering internal sites much less accessible for reaction. Having this in mind, and considering that polymer

B presented a faster reclamation time than its polystyrene homologous (polymer A), we can lastly conclude that the major property affecting the reactivity, and per consequent the reclamation efficiency, is the composition of the back-bone of the polymer. This result can be associated with the fact that the polymer B presented a better swelling when in contact to the oil sample B than the other polymers. A better swelling leads to an increasingly accessible P-active sites, which leads to a more efficient removal of the S_8 , that per consequence leads to a faster reclamation process.

4.3.3.9 Analysis of trisubstituted phosphine-loaded polymers after being used in the reclamation experiments

To understand if the elemental sulfur was selectively removed by the P-active site of the polymer, the polymers utilised in the reclamation process experiments were analysed by ^{31}P NMR (Gel Phase). Since, the concentration of S_8 that we were trying to remove from the oil sample in study was always in the low ppm range, we did not expect to be able to observe any peaks related to the P=S bond in the ^{31}P NMR results (due to the lower limit of detection of the instrument). This was found to be true for most of the polymers, but not for polymer A. The increased amount of polymer bound $\text{R}_3\text{P}=\text{S}$ can be explained due to the fact that polymer A was utilised in most of the experiments, not only for the removal of S_8 from the corrosive ex-service oil sample B, but also used in all the preliminary studies. The ^{31}P NMR (Gel Phase) results obtained for Polymer A are shown in Figure 97.

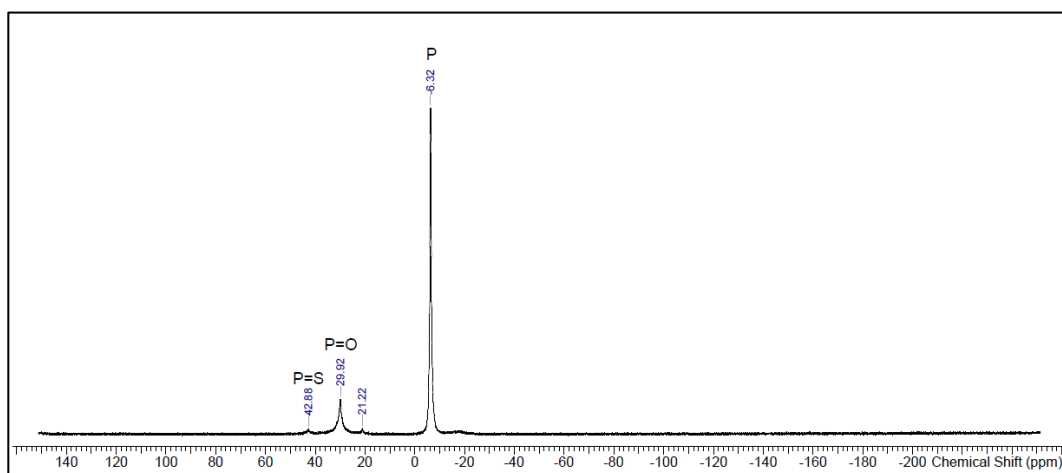


Figure 97 – ^{31}P NMR (Gel Phase) of the Polymer A after being used in all the reclamation experiments to remove S_8 from mineral oil.

By analysis of Figure 97, we can see that several peaks are present in the ^{31}P NMR spectrum. The obtained data were compared to published literature,¹²¹ and the peak at -6.32 ppm was attributed to R_3P , the peak at 29.92 ppm to P=O and the peak at 42.68 to the P=S bond. The presence of the P=S peak demonstrates that polymer A removed and transformed the S_8 that was present in the mineral oil sample. We can also conclude that the polymer A is capable of maintaining good S_8

removal capability even after dozens of experiments, which is confirmed by the peak size relative to the free P. Despite the presence of the P=O peak, which shows that a small part of the polymer A was oxidised, most likely by air (O₂), when considering that the polymer was in contact to air for hundreds of hours during the different reclamation process, we can conclude that such phenomena should not compromise the optimal function of the polymer.

4.3.3.10 Chemical recycling of the trisubstituted phosphine-loaded polymer A

The possibility of reusing the trisubstituted phosphine-loaded polymers, would bring not only an environmental advantage to their use but would also significantly decrease their cost overtime. Having this in mind, polymer A was subjected to a chemical recycling process. This approach consisted in the chemical reduction of the phosphorus (V) sites with trichlorosilane to produce the desired phosphorous (III) moiety. The results of this experiment can be seen below in Figure 98.

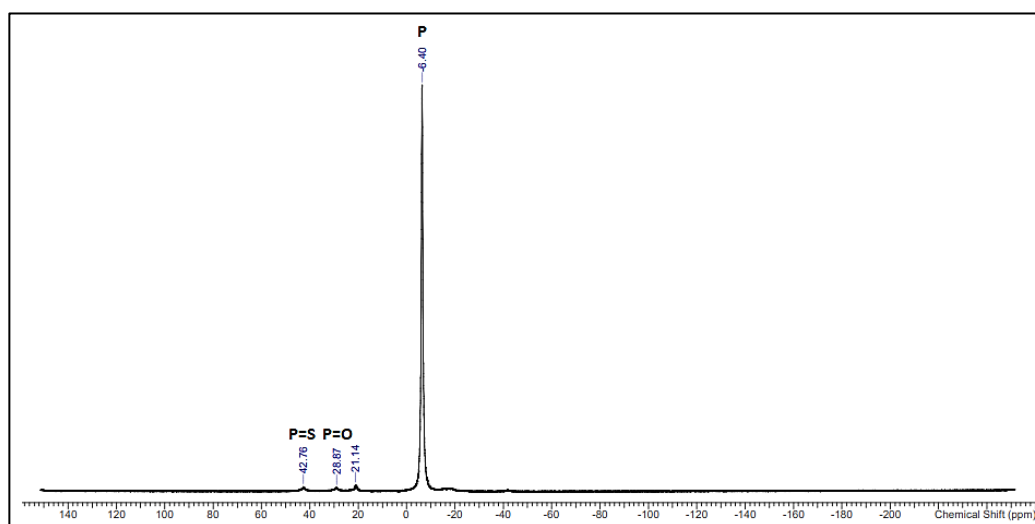


Figure 98 - ³¹P NMR (Gel Phase) of the Polymer A after being chemically recycled.

By analysis of the obtained gel-phase ³¹P NMR and by comparison with the one obtained in Figure 98, we can clearly see that the peak of P=O ($\delta = 28.87$ ppm) decreased to a baseline level. Showing that the reduction of the P=O bond is feasible, regarding the P=S peak ($\delta = 42.76$ ppm) the change on the intensity of the peak is not clearly seen. This was probably due to the fact that the peak intensity of the P=S bond, was already at a base line level before the chemical recycling process was conducted. With this result we can conclude that the chemical recycling process to restore the properties of trisubstituted phosphine-loaded polymers is possible, demonstrating that reuse of these type of polymer scavengers for elemental sulfur is conceivable.

4.3.3.11 Scale up of our reclamation process to be used in the field

The equipment and time frame used for the laboratory reclamation rig should be compatible to scale up for field work. All the equipment is already commonly used and the frame time of 40-50 hours per reclamation, is well suited to be divided into a working schedule of 8 hours a day during a week.

In terms of the economic viability, as an example, if we consider 500 L of mineral insulating oil with a concentration of ~17 ppm of S_8 . To remove all the S_8 present, a quantity of at least 188 g (1:1 eq.) of Polymer A (See table above; loading of triphenylphosphine = 1.4 mmol/g) would be necessary. The polymer A can be purchased as a laboratory reagent from a variety of different providers. No quotes for larger bulk quantities were requested and the best on-line “catalogue price” was £430.00 for 100 g of Polymer A (loading = 1.4 - 2.0 mmol/g of triphenylphosphine). However, once used, polymer A can be chemically recycled and reused. This recycling needs to be conducted in a laboratory and would have a cost of ~£150 in chemical reagents to reduce the 188 g of polymer A.

These values were estimated under the assumption that all the P-active sites on the polymer would be active for the removal of the S_8 and that the decreasing number of available active sites would not affect the removal rate of S_8 . This assumption was made to simplify the calculations, but in reality, only a fraction of the P-active sites will be used, since some of them will be less accessible and some may undergo air oxidation. For large-scale practical application, it is likely that a higher loading of the phosphine would be required. On the other hand, the cost of materials would also be expected to be reduced considerably when purchased in bulk quantities.

4.4 Summary of the chapter

During this work an effective laboratory reclamation strategy that reduces the silver corrosion in mineral oil samples from power transformers has been developed. This is applicable to corrosion present in power transformers that operate in the field by the national grid. This strategy demonstrated the possibility of transforming a corrosive sample of insulating mineral oil into a non-corrosive one. This opens the possibility of reusing samples that presented a corrosive risk to the power transformer, without the environmental and economic concerns regarding the disposal of used mineral insulating oil. The use of trisubstituted phosphine-loaded polymers enabled not only the selective removal of S_8 from mineral oil but also the possibility of the polymer regeneration. This proved to be a fast, reliable and robust system that can be applied to extend the life-time of oil insulated power transformers.

4.5 Current and further work

Despite the scale-up capability of the developed reclamation process, initial studies were conducted to find a more practical solution than the single reclamation process. For this solution, a longer-term decontamination option was considered. The option consisted of a continuous online operation, where the decontaminant system would be directly attached to the in-service transformer to be reclaimed. This system would not only extend the lifetime of the transformer, but also reduce to overall cost of the reclamation process.

The decontaminant system would essentially operate in the same principle as the single reclamation process, i.e., the oil would pass through a cartridge filled with an appropriate decontaminant (e.g., Polymers A, B, C and D) that would selectively remove the S_8 from the oil. This cartridge could be then regenerated/swapped whenever necessary. This would overcome some issues (e.g., overloading, erosion/compression) that could arise from using decontaminants in the form of small beads, different solid supports could be used.

Initial studies were conducted on the synthesis of a polymer (for synthesis details please see below - sub-chapter 6.3.5) that could be attached to different solid supports (e.g., glass, silica), without affecting its capabilities to selectively remove S_8 from mineral oil. This would open the possibility of several different combination of cartridges/polymers. To conclude, possible future work could comprise the synthesis of different solid supports that could be used with different cartridges. This would give valuable information on which combination of cartridge/decontaminant would present better properties and characteristics to be used in a continuous online reclamation process to selectively remove S_8 from mineral oil.

Chapter 5 Conclusions

The main aim of the research described in thesis was to identify strategies to quantify and remove elemental sulfur from insulating transformer mineral oil. This work was mainly motivated by the necessity to prevent and reduce silver corrosion issues in power transformers, which consequently would not only improve their working condition but also in a vital way extend their life-time. The chosen experimental approach led ultimately to the development of a reliable and robust system that can be used by the respective industry to tackle the silver corrosion issue. The main outcomes and developed techniques are briefly described below

Two analytical methods focused on the evaluation of S_8 content in transformer mineral oil were developed. This work established and optimises a GC-MS method to monitor S_8 concentrations as low as ~0.5 ppm. A rapid UHPSFC-MS method was also developed to detect and quantify trace levels of S_8 in mineral insulating oils. In comparison with existing methods for S_8 detection, this technique was found to be much faster (3 min), more sensitive and interference free. Concentrations as low as 0.5 ppb of elemental sulfur can be detected and concentrations of 5.5 ppb can be quantified. These methods can be used as a routine test or to confirm the presence of S_8 in samples where corrosion has occurred. The UHPSFC-MS method was also used to analyse the final concentration of S_8 in the samples subjected to our reclamation process for selective removal of S_8 .

During this work an effective laboratory reclamation strategy to remove elemental sulfur from mineral insulating oil was also developed. The method operates under practical conditions, which could potentially be extended for use in the field by the respective industry. Removal of sulfur is relevant to reducing silver corrosion in power transformers, and this strategy demonstrated the possibility of transforming a corrosive oil sample into a non-corrosive one. This opens the possibility of reusing samples that presented a corrosive risk to the power transformer, without the environmental and economic concerns regarding the disposal of used mineral insulating oil. The use of trisubstituted phosphine-loaded polymers enabled not only the selective removal of S_8 from mineral oil but also the possibility of the polymer regeneration. In this work, all four polymers studied were able to selectively remove S_8 from the ex-service oil sample B. From the experimental results, we can conclude that Polymer B was the best performing over the timescale of the reclamation experiments. The better performance of polymer B, can be mainly explained due to the fact that it possessed a poly(lauryl-methacrylate) back-bone that presented good swelling properties when used in the mineral oil, which consequently led to a more efficient removal of S_8 from mineral oil, when compared to the polystyrene back-bone based polymers A, C and D. Taking everything in consideration, these experiments demonstrated that the method/system used/studied, is reliable, robust. Therefore, the methodology reported shows promise for

application in the field for reclamation of mineral oil containing elemental sulfur, and could be used as part of a mitigation strategy to extend the life-time of oil insulated power transformers.

Chapter 6 Organic experimental part

6.1 Chemicals

Chemicals were purchased from Sigma-Aldrich, Alfa Aesar, Fluorochem. Reaction solvents were used as received. Anhydrous DMF was purchased from Sigma-Aldrich. All glassware used was oven dried prior to use. Quantities of materials are quoted to either three significant figures or two decimal places where appropriate.

6.2 Instrumentation

6.2.1 Nuclear Magnetic Resonance (NMR)

^1H NMR, $^{13}\text{C}\{^1\text{H}\}$ NMR and $^{31}\text{P}\{^1\text{H}\}$ NMR spectra were recorded on a Bruker DPX-400 spectrometer at 400 MHz, 100 MHz, and 162 MHz, respectively. The experiments were performed in deuterated chloroform (CDCl_3) (purchased from Cambridge Isotope Laboratories, Inc.) at 298 K. Chemical shifts for proton and carbon signals are reported on the δ scale in ppm and were referenced to residual solvent: 7.27 ppm for ^1H NMR spectra and 77.00 ppm for $^{13}\text{C}\{^1\text{H}\}$ NMR spectra. For the $^{31}\text{P}\{^1\text{H}\}$ NMR experiments, the chemical shifts were referenced to phosphoric acid (H_3PO_4 , external reference). All spectra were reprocessed using ACD/Spectrus Processor 2017.1.

6.2.2 Fourier-transform - Infrared Spectroscopy (FT-IR)

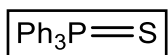
The FT-IR spectra were collected on a Nicolet iS5 FT-IR Spectrometer using OMNIC software package. The analyses were performed at room temperature, the spectra were collected as a result of 16 running scans in the range between 500–4000 cm^{-1} . The Infrared spectra are reported in wavenumbers (cm^{-1}).

6.2.3 Melting point

The reported melting points (m.p.) were obtained using a Gallenkamp Electrothermal apparatus and are not corrected.

6.3 Preparation and characterisation of the compounds synthesised

6.3.1 Synthesis of triphenylphosphine sulphide



C₁₈H₁₅PS

Mol Wt: 294.35 g.mol⁻¹

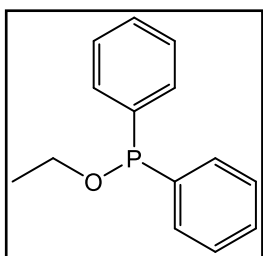
Following the procedure of Lloyd *et al.*,¹¹⁶ triphenylphosphine sulphide was prepared by the reaction of elemental sulphur (0.16 g, 5.09 mmol, 1.05 equiv.) with triphenylphosphine (1.25 g, 4.77 mmol, 1 equiv.) under reflux in toluene (20 mL). The reaction mixture was heated for 45 min. After cooling to at RT, the solvent was removed by rotary evaporation. The resulting white solid was recrystallised from the minimum volume of acetone to give Ph₃PS as a white crystalline solid (0.99 g, 3.35 mmol, 70.2%). Physical and spectroscopic data are consistent with those previously reported.¹¹⁶

¹H NMR (400 MHz, CDCl₃): δ_H (ppm) = 7.78 - 7.72 (6H, m), 7.56 – 7.52 (3H, m), 7.49 – 7.44 (6H, m).

LRMS (EI) *m/z* = 183.2 (100%) [C₁₂H₈P]⁺, 262.4 (20%) [(C₆H₅)₃P]⁺, 294.4 (80%) [M]⁺.

mp: 168.2 -168.5 °C [Lit.¹¹⁶ 162 - 164 °C].

6.3.2 Synthesis of ethoxydiphenylphosphane



$C_{13}H_{13}OP$

Mol Wt: 216.22 g.mol⁻¹

Following the procedure by Spreider and Breit,¹³² the ethoxydiphenylphosphane was prepared. A solution of ethanol (EtOH, 0.28 mL, 0.23 g, 4.88 mmol, 1.8 equiv.) and pyridine (0.24 mL, 0.24 g, 2.98 mmol, 1.1 equiv.) in Et₂O (10 mL) was added dropwise to a stirred solution of Ph₂PCl (0.5 mL, 0.59 g, 2.71 mmol, 1 equiv.) at RT under nitrogen atmosphere. The resulting mixture was stirred 1 h before it was filtered. The solvent was removed under reduced pressure and the dried under high vacuum.

Note: The compound prepared is oxidised readily in the presence of air, only a ³¹P NMR was conducted before total oxidation occurred. The compound was not resynthesised, because one of the requirements for the experiments was to be stable in the presence of air.

³¹P{¹H} NMR (162 MHz, CDCl₃): δ_P = 111.39 ppm.

6.3.3 Synthesis of the poly(lauryl-methacrylate) resin-bound phosphine (B)

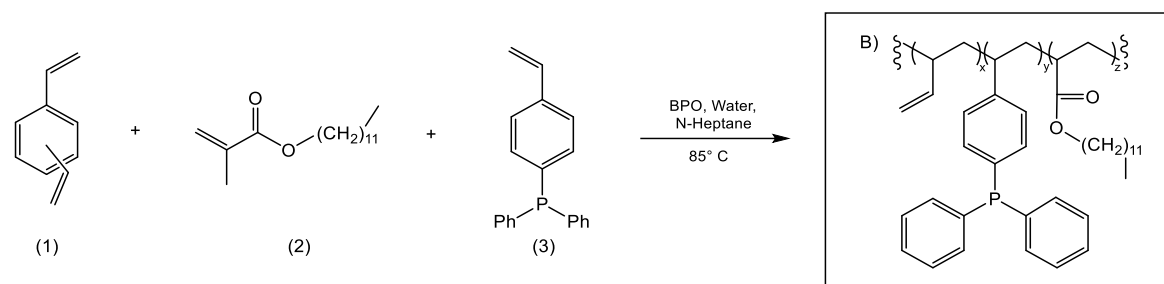


Figure 99 - Synthesis of the phosphine-bound poly(lauryl-methacrylate) resin (B).

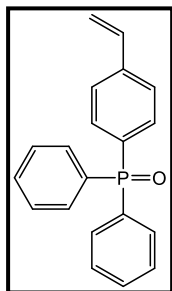
The synthesis of polymer **B** was accomplished by using a modified procedure based on the original report by Garcia-Diego and Cuellar.¹²⁸ To deionised water (25 mL) in a 100 mL round bottom flask heated at 85 °C using a dry syn, a mixture of divinylbenzene (DVB) (7.5 mL, 5.612 mmol), lauryl methacrylate (LMA) (6.0 mL, 22.24 mmol), 4-(diphenylphosphino)styrene (SDP) (0.8 g, 2.63 mmol) and benzoyl peroxide (BPO) (5.0 mL of a 0.5 wt. % sol in *n*-heptane). The mixture was under magnetic stirring for 48 h. The resulting solid was washed thoroughly with hot water (65 °C), then with methanol and then vacuum filtered. The solid was dried under vacuum in an oven at 50 °C for 24 h.

Physical and spectroscopic data are consistent with those previously reported.¹²⁸

FT-IR (neat): ν_{\max} 2921 (w), 2852 (s), 1723 (s), 1456 (m), 1198 (w, br), 1088 (m) cm^{-1} .

Gel Phase $^{31}\text{P}\{^1\text{H}\}$ NMR (162 MHz, CDCl_3): δ_{P} = 29.36 (P=O) (~10%), -5.78 (P) (~90%) ppm.

6.3.3.1 Synthesis of 4-(diphenylphosphino)styrene oxide (SDPO)



$C_{20}H_{17}OP$

Mol Wt: 304.33 g.mol⁻¹

Following the procedure of Kusumaatmaja *et al.*,¹³⁵ 4-(diphenylphosphino)styrene oxide (SDPO) was prepared by the reaction of 4-(diphenylphosphino)styrene (SDP) (1.02 g, 3.56 mmol) with a saturated aqueous solution of oxone (4.28 g, 13.9 mmol) in 1,2-dichloroethane (20 mL). The reaction mixture was left stirring for 2h at RT. The reaction mixture was then transferred to a separating funnel where the organic layer was separated, the solvent was then removed by rotary evaporation. The resulting brown oil was then washed with cyclohexane (2x10 mL) and then filtered to give SDPO as a white powder (0.78 g, 2.56 mmol, 71.9%).

Physical and spectroscopic data are consistent with those previously reported.¹³⁵

¹H NMR (400 MHz, CDCl₃): δ_H (ppm) = 7.74 - 7.39 (14H, m, ArH), 6.75 (1H, dd, J = 17.6 and 10.9 Hz, CH), 5.86 (1H, d, J = 17.6 Hz, CH₂), 5.38 (1H, d, J = 11.0 Hz, CH₂).

³¹P{¹H} NMR (162 MHz, CDCl₃): δ_P = 29.01 (P=O) ppm.

LRMS (EI) m/z = 183.2 (100%) [C₁₂H₈P]⁺, 277.1 (70%) [(C₆H₅)₃OP], 304.1 (30%) [M]⁺.

6.3.3.2 Reduction of the of the poly(lauryl-methacrylate) resin-bound phosphine (B)

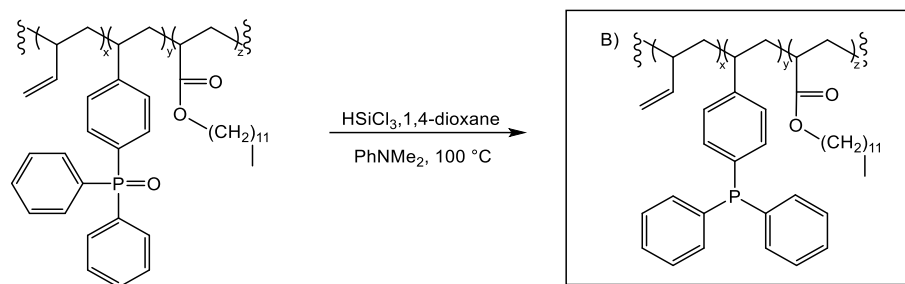


Figure 100 - Reduction of the of the poly(lauryl-methacrylate) resin-bound phosphine (B).

By adaptation of a procedure by Charette *et al.*,¹²⁶ the polymer B was prepared by the addition of *N,N*-dimethylaniline (4.0 mL, 3.82 g, 31.0 mmol) to a solution of the polymer oxide (3.10 g, 3.04 mmol) in 1,4 – dioxane (50 mL). The reaction mixture was put in an ice bath and then trichlorosilane (1.0 mL, 1.35 g, 9.97 mmol) was added and subsequently heated at 100 °C (reflux) for 17 h under magnetic stirring. The solution was then poured on methanol (300 mL) under magnetic stirring thus precipitating the polymer. The polymer suspension was then filtered using a glass filter, rinsed with THF and methanol to be subsequently placed in a vacuum oven at 70 °C for 6 h.

The physical and spectral data recorded were consistent with reported literature values.¹²⁶

FT-IR (neat): ν_{\max} 2921 (w), 2852 (s), 1723 (s), 1456 (m), 1198 (w, b), 1088 (m) cm^{-1}

Gel Phase ³¹P{¹H} NMR (162 MHz, CDCl₃): δ_{P} = 31.28 (P=O) (~3%), - 6.03 (P) (~97%) ppm.

6.3.4 Synthesis of the polystyrene resin-bound phosphine (D)

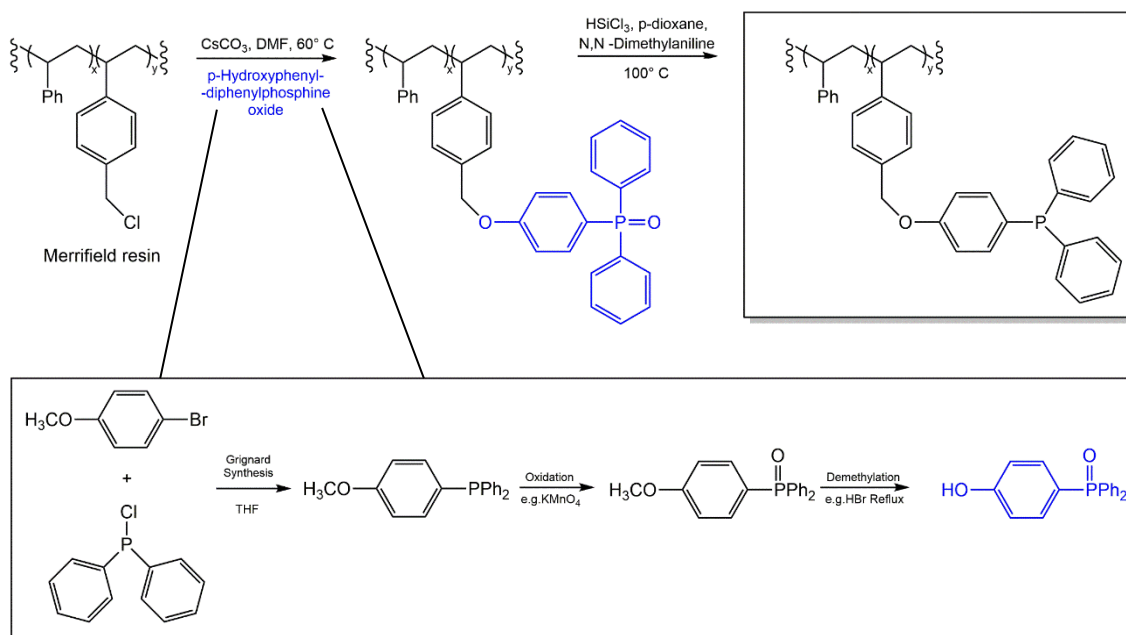
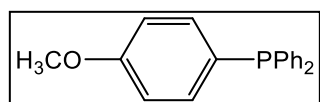


Figure 101 - Synthesis of the phosphine-bound polystyrene resin (D).

6.3.4.1 (4-Methoxyphenyl)diphenylphosphine (1)



$C_{19}H_{17}OP$

Mol Wt: 292.10 g.mol⁻¹

By adaptation of a procedure by Whitaker *et al.*,¹²⁷ the Grignard reagent of 4-bromoanisole was prepared by reaction of 4-bromoanisole (2.0 mL, 15.9 mmol, 1.5 equiv.) with magnesium turnings (0.50 g, 20.1 mmol, 1.9 equiv.) of under N₂. The magnesium was added to a three-neck-round bottom flask and covered with THF (2.0 mL), then a solution of 4-bromoanisole in THF (2.0 mL) was slowly added to the magnesium. The flask content was then stirred 1 h at RT. Subsequently, PPh₂Cl (2.0 mL, 2.46 g, 11.2 mmol, 1 equiv.) was added dropwise to the stirred mixture. The reaction was stirred overnight and then poured into an ice-cooled solution of 10% HCl (60 mL). The mixture was extracted with Et₂O (3x20 mL), and the combined organic solution was dried (MgSO₄). The solvent was removed to afford a white solid. Recrystallisation from methanol gave the title phosphine as a white crystalline solid (1.44 g, 4.91 mmol, 45.3%).

The physical and spectral data recorded were consistent with reported literature values.¹²⁷

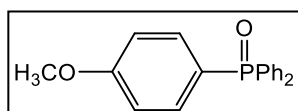
FT-IR (neat): ν_{\max} 1596 (w), 1176 (w), 1100 (m) cm⁻¹.

¹H NMR (400 MHz, CDCl₃): δ_H (ppm) = 7.36 – 7.28 (12H, m), 6.92 – 6.88 (2H, m), 3.84 (3H, s).

¹³C{¹H} NMR (CDCl₃, 100 MHz): δ_C (ppm) = 160.45 (1C), 137.80 (d, 2C, J_{PC} = 10.7 Hz), 135.74 (d, 4C, J_{PC} = 11.3 Hz), 135.52 (1C), 133.45 (d, 2C, J_{PC} = 11.1 Hz), 128.51 (d, 4C, J_{PC} = 10.1 Hz), 127.43 (d, 2C, J_{PC} = 10.6 Hz), 114.28 (d, 2C, J_{PC} = 12.6 Hz), 55.20 (-OCH₃).

LRMS (EI) m/z = 183.2 (100%) [C₁₂H₈P]⁺, 215.1 (60%) [C₁₃H₁₂OP]⁺, 292.2 (25%) [M]⁺.

6.3.4.2 (4-Methoxyphenyl)diphenylphosphine oxide (2)



$C_{19}H_{17}O_2P$

Mol Wt: 308.10 g.mol⁻¹

By adaptation of a procedure by Whitaker *et al.*,¹²⁷ the oxidation of (1) (1.44 g, 4.91 mmol, 1 equiv.) to its oxide (2) was accomplished using aqueous $KMnO_4$ (0.81 g, 5.15 mmol, 1.06 equiv.) in 70 mL of water. The reaction was stirred at RT overnight. Extraction was carried out with use of chloroform (3x25 mL). The combined organic layers were washed with water (3x15 mL) and then dried over magnesium sulphate. The solvent removal gave origin to the oxide (2) as a clear, colourless oil. Purification by recrystallization from cyclohexane gave the pure oxide (2) as white, crystalline needles (1.12 g, 3.63 mmol, 74.9%).

The physical and spectral data recorded were consistent with reported literature values.¹²⁷

FT-IR (neat): ν_{max} 1597 (w), 1116 (w), 1070 (m) cm^{-1} .

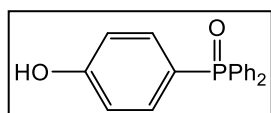
¹H NMR (400 MHz, $CDCl_3$): δ_H (ppm) = 7.70 – 7.64 (4H, m), 7.63 – 7.52 (4H, m), 7.48 – 7.43 (4H, m), 7.00 – 6.95 (2H, m), 3.85 (3H, s).

¹³C{¹H} NMR ($CDCl_3$, 100 MHz): δ_C (ppm) = 162.48 (1C), 133.95 (2C, J_{PC} = 11.1 Hz), 133.54 (d, 4C, J_{PC} = 11.1 Hz), 132.04 (d, 2C, J_{PC} = 9.5 Hz), 131.76 (C), 128.42 (d, 4C, J_{PC} = 12.1 Hz), 124.19 (1C), 123.10 (1C), 114.08 (d, 2C, J_{PC} = 13.3 Hz), 55.33 (-OCH₃).

LRMS (EI) m/z = 215.1 (100%) [$C_{12}H_{12}OP$]⁺, 231.1 (75%) [$C_{12}H_{12}O_2P$]⁺, 308.1 (40%) [M]⁺.

mp: 120.2-120.7 °C [Lit.¹²⁷ 117 - 119 °C].

6.3.4.3 (4-hydroxyphenyl)diphenylphosphine oxide (**3**)



$C_{18}H_{15}O_2P$

Mol Wt: 294.08 g.mol⁻¹

By adaptation of a procedure by Whitaker *et al.*,¹²⁷ in a round bottom flask under N₂ atmosphere compound **2** (1.12 g, 3.63 mmol) was dissolved in DCM (70 mL). The solution was cooled down to -78 °C and a 0.57 M solution of BBr₃ in DCM (24.2 mL, 0.06 mol) was added dropwise over a period of 120 min. The resulting mixture was stirred at RT. After 72 h the reaction mixture was slowly poured into cold water (600 mL). DCM was removed under reduced pressure and the aqueous phase was extracted with ethyl acetate (3 x 25 mL). The combined organic layers were dried over MgSO₄, filtered and the solvent was removed by rotary evaporation. The obtained oil was dissolved in the minimum amount of EtOAc to afford crystallization. The desired product **3** was obtained as a white solid with a 90.6% yield (0.95 g, 3.24 mmol).

The physical and spectral data recorded were consistent with reported literature values.¹²⁷

FT-IR (neat): ν_{\max} 3053 (s, br), 1483 (w), 1116 (w) cm⁻¹.

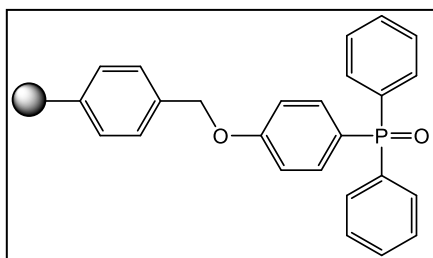
¹H NMR (400 MHz, CDCl₃): δ_H (ppm) = 10.23 (1H, s (br)), 7.71 – 7.64 (4H, m), 7.59 – 7.53 (2H, m), 7.49 – 7.45 (4H, m), 7.43 – 7.36 (2H, m), 7.00 – 9.96 (2H, m).

¹³C{¹H} NMR (CDCl₃, 100 MHz): δ_C (ppm) = 161.65 (s, 1C), 133.98 (d, 2C, J_{PC} = 10.9 Hz), 133.86 (d, 2C, J_{PC} = 10.2 Hz), 132.13 (1C), 132.02 (1C), 131.99 (d, 4C, J_{PC} = 9.5 Hz), 128.57 (d, 4C, J_{PC} = 11.2 Hz), 121.56 (1C), 116.23 (d, 2C, J_{PC} = 12.9 Hz).

LRMS (ESI+) found m/z = 295.1 [M+H]⁺.

mp: 244.9-245.4 °C [Lit.¹²⁷ 237 - 239 °C].

6.3.4.4 4-methylbenzyloxyphenyldiphenylphosphine oxide, polymer-bound (4)



200-400 mesh;

To be calculated mmol of P(III)/g loading;

Cross-linked with 1% DVB.

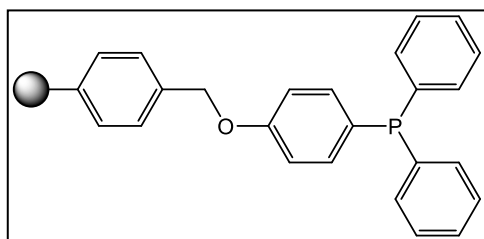
By adaptation of a procedure by Charette *et al.*,¹²⁶ the polymer (4) was prepared by adding (4-hydroxyphenyl)diphenylphosphine oxide (3) (0.95 g, 3.24 mmol) to a solution of Merrifield's resin (0.93 g, 3.24-4.24 mmol Cl⁻/g) in 30 mL of DMF. Caesium carbonate (1.77 g, 5.01 mmol) was then added to the reaction and heated to 60 °C for 16 h under magnetic stirring. The solution was then poured on methanol (150 mL) under magnetic stirring thus precipitating the polymer. The polymer suspension was then filtered under pressure, rinsed with methanol, and subsequently placed in a vacuum oven at 70 °C for 20 h.

The physical and spectral data recorded were consistent with reported literature values.¹²⁶

FT-IR (neat): ν_{\max} 1593 (w), 1175 (s), 1115 (m) and 997 (m) cm^{-1} .

Gel Phase $^{31}\text{P}\{^1\text{H}\}$ NMR (162 MHz, CDCl_3): $\delta_{\text{P}} = 27.89$ ppm.

6.3.4.5 4-methylbenzyloxyphenyldiphenylphosphine oxide, polymer-bound (5)



200-400 mesh;

To be calculated mmol of P(III)/g loading;

Cross-linked with 1% DVB.

By adaptation of a procedure by Charette *et al.*,¹²⁶ the polymer (5) was prepared by the addition of *N,N* – dimethylaniline (2.0 mL, 1.91 g, 15.78 mmol) to a solution of the polymer oxide (4) (1.39 g, 1.33 mmol) in 1,4 – dioxane (25 mL). The reaction mixture was put in an ice bath and then trichlorosilane (1.0 mL, 1.35 g, 9.97 mmol) was added and subsequently heated at 100 °C (reflux) for 17 h under magnetic stirring. The solution was then poured on methanol (300 mL) under magnetic stirring thus precipitating the polymer. The polymer suspension was then filtered using a glass filter, rinsed with THF and methanol to be subsequently placed in a vacuum oven at 70 °C for 6 h.

The physical and spectral data recorded were consistent with reported literature values.¹²⁶

FT-IR (neat): ν_{\max} 1591 (w), 1175 (s), 1088 (m) cm^{-1} .

Gel Phase $^{31}\text{P}\{^1\text{H}\}$ NMR (162 MHz, CDCl_3): $\delta_{\text{P}} = -7.16$ ppm.

6.3.5 Attempt to the synthesis of the poly(lauryl-methacrylate) resin-bound phosphine (E) using a TEMPO based initiator

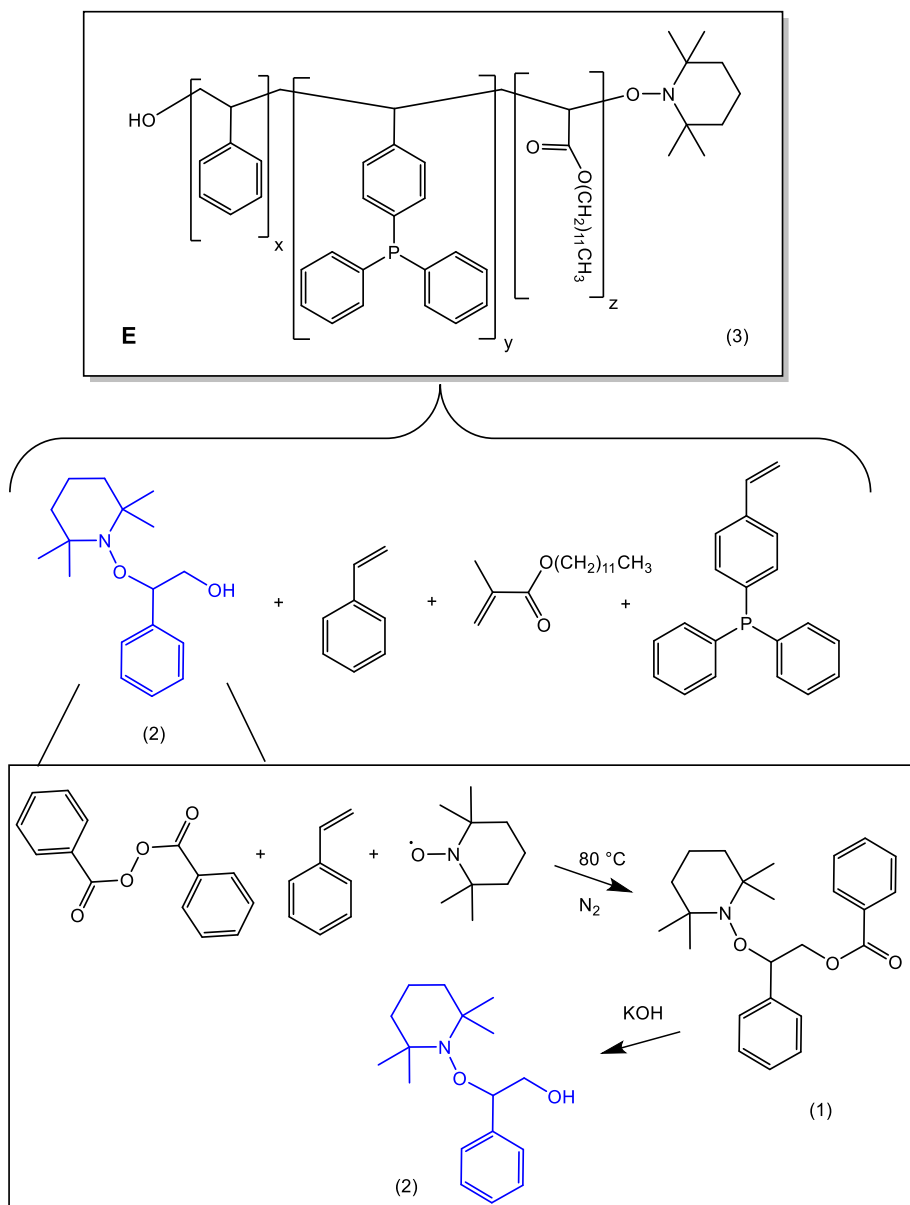
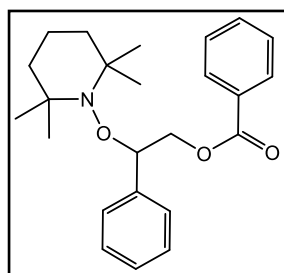


Figure 102 - Synthesis of the poly(lauryl-methacrylate) resin-bound phosphine (E).

6.3.5.1 1-Benzyloxy-2-phenyl-2-(2',2',6',6'-tetramethylpiperidinyl-1-oxy)ethane (1)



$C_{24}H_{31}NO_3$

Mol Wt: 381.52 g.mol⁻¹

By adaptation of a procedure by C. J. Hawker,¹³³ compound (**1**) was prepared. To a solution of benzoyl peroxide (1.56 g, 6.43 mmol), styrene (2.0 mL, 1.82 g, 17.46 mmol) and acetonitrile (10 mL) was added 2,2,6,6-Tetramethyl-1-piperidinyloxy (TEMPO) (0.50 g, 3.21 mmol) and the solution was heated at 80 °C under nitrogen for 20 hours. After cooling, the solution was evaporated to dryness and purified by column chromatography (1st separation with 1:1 hexane/dichloromethane and 2nd separation with Dichloromethane + 5% of Methanol). The desired modified TEMPO initiator was obtained as a yellow/brown oil (0.31 g, 0.81 mmol, 33 %).

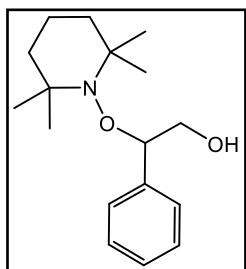
The spectral data recorded were consistent with reported literature values.¹³³

FT-IR (neat): ν_{max} 3110 (s), 1731 (s), 1552 (s), 1205 (m) cm⁻¹.

¹H NMR (400 MHz, CDCl₃): δ_H (ppm) = 7.93 – 7.95 (2H, m), 7.24 – 7.30 (8H, m), 5.11 - 5.06 (1H, m), 4.85 (1H, dd, J = 5.0 and 11.1 Hz), 4.55 (1H, dd, J = 6.2 and 11.0 Hz) 1.47 – 1.52 (6H, m), 0.85 – 1.13 (12 H, m).

LRMS (EI) found m/z = 77.0 (100%) [C₆H₅]⁺, 140.1 (65%) [C₉H₁₈N]⁺, 381.2 (10%) [M]⁺.

6.3.5.2 1-Hydroxy-2-phenyl-2-(2',2',6',6'-tetramethyl-1-piperidinyloxy)ethane (2)



$C_{17}H_{27}NO_2$

Mol Wt: 277.41 g.mol⁻¹

By adaptation of a procedure by C. J. Hawker,¹³⁴ compound **(2)** was synthesised by adding aqueous sodium hydroxide (5.0 mL of a 2M solution) to a solution of the benzyl ester **(5.3.5.1)** (0.308 g, 0.807 mmol) in 10 mL of ethanol. The resulting solution was heated at reflux and under nitrogen for 2 hours. After cooling the solution was evaporated to dryness, washed with water (50 mL) and dichloromethane (50 mL). The aqueous layer was extracted with DCM (2 x 25 mL). The combined organic layers were dried, evaporated to dryness and the crude product purified by column chromatography (1:4 hexane/dichloromethane + 5% methanol). The desired product was obtained as a yellow/brown oil (0.114 g, 0.411 mmol, 46%).

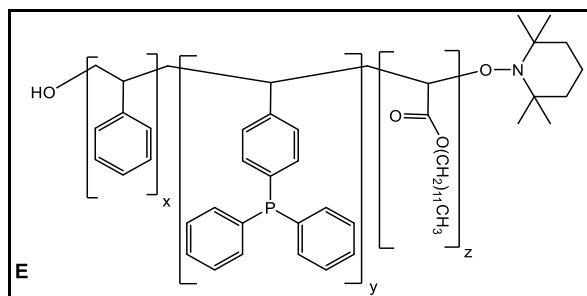
The spectral data recorded were consistent with reported literature values.¹³⁴

FT-IR (neat): ν_{\max} 3053 (s, br), 1532 (s), 1105 (m) cm⁻¹.

¹H NMR (400 MHz, CDCl₃): δ_H (ppm) = 7.32 – 7.44 (5H, m), 5.88 (1H, br s), 5.27 (1 H, dd, J = 2.1 and 3.4 Hz), 4.21 (1H, dd, J = 2.1 and 5.8 Hz), 3.71 (1H, d, J = 2.4 Hz) 1.42 – 1.55 (6 H, m), 1.01 – 1.37 (12 H, m).

LRMS (ESI+) found m/z = 278.4 [M+H]⁺.

6.3.5.3 Poly(lauryl-methacrylate) resin-bound phosphine (**E**)



The synthesis of polymer (**E**) was attempted using an adaptation of a procedure by P. Mansky *et al.*¹³⁰ A solution of the modified TEMPO initiator (**2**) (0.114 g, 0.411 mmol), styrene (4.0 mL, 3.636 g, 34.911 mmol), lauryl methacrylate (8.0 ml, 6.944 g, 27.295 mmol) and 4-(Diphenylphosphino)styrene (0.503 g, 1.745 mmol) was prepared in 25 mL of xylene. The solution was then heated at 130 °C, with stirring, under nitrogen for 72 hours. The reaction mixture was then dissolved in dichloromethane (25 mL) and precipitated into hexane (250 mL), followed by reprecipitation in methanol (250 mL). A white powder was obtained (0.241 g).

The product obtained was studied by ³¹P NMR, which confirmed that the product obtained was not the desired one. The results showed a P=O peak, which indicated that the phosphine containing molecule was probably oxidated by the TEMPO molecule. Preventing this way, the occurrence of the polymerization reaction. The reaction was not attempted a second time, but prior oxidation of the phosphine containing molecule might solve this issue. The P=O contained in the final polymer, could be then reduced (e.g., HSiCl₃ – 6.3.4.5 for general conditions) leading this way to the desired product.

Appendix A

A.1 Copyright permissions to reuse - IEEE

The IEEE does not require individuals working on a thesis to obtain a formal reuse license; however, you may print out this statement to be used as a permission grant: Requirements to be followed when using any portion (e.g., figure, graph, table, or textual material) of an IEEE copyrighted paper in a thesis:

- 1) In the case of textual material (e.g., using short quotes or referring to the work within these papers) users must give full credit to the original source (author, paper, publication) followed by the IEEE copyright line © 2011 IEEE.
- 2) In the case of illustrations or tabular material, we require that the copyright line © [Year of original publication] IEEE appear prominently with each reprinted figure and/or table.
- 3) If a substantial portion of the original paper is to be used, and if you are not the senior author, also obtain the senior author's approval.

Requirements to be followed when using an entire IEEE copyrighted paper in a thesis:

- 1) The following IEEE copyright/ credit notice should be placed prominently in the references: © [year of original publication] IEEE. Reprinted, with permission, from [author names, paper title, IEEE publication title, and month/year of publication]
- 2) Only the accepted version of an IEEE copyrighted paper can be used when posting the paper or your thesis on-line.
- 3) In placing the thesis on the author's university website, please display the following message in a prominent place on the website: In reference to IEEE copyrighted material which is used with permission in this thesis, the IEEE does not endorse any of University of Southampton's products or services. Internal or personal use of this material is permitted. If interested in reprinting/republishing IEEE copyrighted material for advertising or promotional purposes or for creating new collective works for resale or redistribution, please go to:

http://www.ieee.org/publications_standards/publications/rights/rights_link.html to learn how to obtain a License from RightsLink. If applicable, University Microfilms and/or ProQuest Library, or the Archives of Canada may supply single copies of the dissertation.

Appendix B

B.1 Copyright permission for reuse – Analyst

Quantitative UHPSFC-MS analysis of elemental sulfur in mineral oil *via* derivatisation with triphenylphosphine: application to corrosive sulfur-related power transformer failure

S. B. Garcia, J. Herniman, P. Birkin, J. Pilgrim, P. Lewin, G. Wilson, G. J. Langley and R. C. D. Brown, *Analyst*, 2020, **145**, 4782

DOI: 10.1039/D0AN00602E

This article is licensed under a Creative Commons Attribution 3.0 Unported Licence – Link to the license: <http://creativecommons.org/licenses/by/3.0/>. Material from this article can be used in other publications provided that the correct acknowledgement is given with the reproduced material.

Reproduced material should be attributed as follows:

- For reproduction of material from NJC: [Original citation] - Published by The Royal Society of Chemistry (RSC) on behalf of the Centre National de la Recherche Scientifique (CNRS) and the RSC.
- For reproduction of material from PCCP: [Original citation] - Published by the PCCP Owner Societies.
- For reproduction of material from PPS: [Original citation] - Published by The Royal Society of Chemistry (RSC) on behalf of the European Society for Photobiology, the European Photochemistry Association, and RSC.
- For reproduction of material from all other RSC journals: [Original citation] - Published by The Royal Society of Chemistry.

List of References

- 1) Faraday, M. and Neufeld, C. Experimental Researches in Electricity. Volume I, Library of Alexandria, 2016.
- 2) The association for renewable energy and clean technology (REA). Energy Storage, Available: <https://www.r-e-a.net/wp-content/uploads/2019/10/Energy-Storage-FINAL6.pdf> (accessed, May 2022).
- 3) National Grid UK. Network route maps, Available: <https://www.nationalgrid.com/uk/electricity-transmission/network-and-infrastructure/network-route-maps> (accessed, February 2021).
- 4) UK Parliament. The future of Britain's electricity networks - Energy and Climate Change, Available: <https://publications.parliament.uk/pa/cm200910/cmselect/cmenergy/194/19404.htm#n3> (accessed, February 2021).
- 5) Digest of United Kingdom Energy Statistics (DUKES), 2020.
- 6) Energy networks association. Electricity transmission and distribution operators, Available: <https://www.energynetworks.org/operating-the-networks/whos-my-network-operator> (accessed, May 2022).
- 7) National Council on Electricity Policy. Brown, M. H., Sedano, R. P. Electricity Transmission – A Primer (2014), Available: <https://www.energy.gov/sites/prod/files/oeprod/DocumentsandMedia/primer.pdf> (accessed, February 2021).
- 8) Paynter, R. T. and Boydell, B. J. T. Introduction to electricity. Volume I, Pearson, 2010.
- 9) Heathcote, M. J. The J & P Transformer Book: A Practical Technology of the Power Transformer, Newnes, 2007.
- 10) Donev, J. *et al.* Energy Education – Transformer (2020), University of Calgary. Available: https://energyeducation.ca/encyclopedia/Transformer#cite_note-3 (accessed, February 2021).
- 11) Mahanta, D. K. and Laskar, S. Electrical insulating liquid: A review. *J. Adv. Dielectr.*, 07, 04, 1730001, 2017.
- 12) Rouse, T. O. Mineral insulating oil in transformers. *IEEE Electr. Insul. Mag.*, 14, 3, 6 - 16, 1998.
- 13) IEC TC 10. Fluids for electrotechnical applications - Unused mineral insulating oils for transformers and switchgear (BS EN 60296), BSI Std., 2012.

- 14) Scatiggio, F. *et al.* Corrosive sulfur in insulating oils: its detection and correlated power apparatus failures. *IEEE Trans. Power Deliver.*, 23, 508 - 509, 2008.
- 15) Copper Sulphide in Transformer Insulation. *CIGRE Technical Brochure n°378*, WG A2.32, 1, 1 - 23, 2009.
- 16) Copper Sulphide Long Term Mitigation and Risk Assessment. *CIGRE Technical Brochure n° 625*, WG A2.40, 1, 1 - 98, 2015.
- 17) IEC 60422. *Supervision and Maintenance Guide for Mineral Insulating Oils in Electrical Equipment*, 4, 11, 2013.
- 18) Standard DIN 51353. Testing of insulating oils - Detection of Corrosive Sulfur – Silver strip test, 1, 1 - 3, 1985.
- 19) ASTM D1275-15. *Standard Test Method for Corrosive Sulfur in Electrical Insulating Liquids*, 4, 1 - 3, 2015.
- 20) Khiar, M. S. A. *et al.* On-Line Quantification of Corrosive Sulfur Content in Large Autotransformers, *IEEE Trans. Dielectr. Electric. Insul.*, 27, 6, 1787-1794, 2020.
- 21) Wan, T. *et al.* Suppressive mechanism of the passivator irgamet 39 on the corrosion of copper conductors in transformers, *IEEE Trans. Dielectr. Electr. Insul.*, 19, 454–459, 2012.
- 22) Akshatha, A. *et al.* Laboratory validation of method of solvent extraction for removal of sulphur compounds from mineral oil, *IEEE Trans. Dielectr. Electr. Insul.*, 22, 2572–2580, 2015.
- 23) Qian, Y. H. *et al.* Synthesis and adsorption performance of ag/gamma-al₂o₃ with high adsorption capacities for dibenzyl disulfide, *Ind. Eng. Chem. Res.*, 59, 6164–6171, 2020.
- 24) Kato, F. *et al.* Suppressive effect and its duration of triazole-based passivators on copper sulfide deposition on kraft paper in transformer, *IEEE Trans. Dielectr. Electr. Insul.*, 20, 1915–1921, 2013.
- 25) Wan, T. *et al.* Removal of corrosive sulfur from insulating oil with adsorption method, *IEEE Trans. Dielectr. Electr. Insul.*, 22, 3321–3326, 2015.
- 26) Zhao, Y. *et al.* Inhibition effectiveness and depletion characteristic of irgamet 39 in transformer oil, *IEEE Trans. Dielectr. Electr. Insul.*, 23, 3382–3388, 2016.
- 27) Facciotti, M. *et al.* XPS study on direct detection of passivator irgamet 39 on copper surfaces aged in insulating mineral oil, In: Proceedings of International Conference IEEE Conference on Electrical Insulation and Dielectric Phenomena, 1097–1100, Shenzhen, China, 2013.

- 28) Facciotti, M. *et al.* Passivators, corrosive sulfur and surface chemistry. New tools in the investigation of an effective protection. In *MyTransfo 2014: Oil and Transformer*, 1, 27–35, 2014.
- 29) Amimoto, T. *et al.* Duration and Mechanism of Suppressive Effect of Triazole-based Passivators on Copper-sulfide Deposition on insulating paper. *IEEE Trans. Dielectr. Electr. Insul.*, 16, 257, 2009.
- 30) Matejkova, M. *et al.* Removal of Corrosive Sulfur from Insulating Oils by Natural Sorbent and Liquid-Liquid Extraction, *IEEE Trans. Dielectr. Electr. Insul.*, 24, 2383-2389, 2017.
- 31) Ding, D. *et al.* Removal of dibenzyl disulfide (DBDS) by polyethylene glycol sodium and its effects on mineral insulating oil, *IEEE Access.*, 7, 121530–121539, 2019.
- 32) Dahlund, M. *et al.* Understanding the Presence of Corrosive Sulfur in Previously Non-Corrosive Oils Following Regeneration, *77th Doble Client Conference*, Boston, MA, USA, IM – 5, 2010.
- 33) S. Samarasinghe, H. *et al.* Investigating passivator effectiveness for preventing silver sulfide corrosion in power transformer on-load tap changer, *IEEE Trans. Dielectr. Electr. Insul.*, 27, 1761 - 1768, 2020.
- 34) S. Samarasinghe, H. *et al.* Investigations of silver sulfide formation on transformer OLTC tap selectors and its influence on oil properties, *IEEE Trans. Dielectr. Electr. Insul.*, 2, 1926 - 1934, 2019.
- 35) Selley, R. C. and Sonnenberg, S. A. *Elements of Petroleum Geology*, Academic Press, 3rd Edition, 1-528, 2014.
- 36) Javadli, R. and de Klerk, A. Desulfurisation of heavy oil. *Appl. Petrochem. Res.* 1, 3 – 19, 2012.
- 37) Srivastava, V. C. An evaluation of desulfurisation technologies for sulfur removal from liquid fuels, *Rsc. Adv.*, 2, 759-783, 2012.
- 38) Kabe, T. *et al.* Hydrodesulfurization of Sulfur-Containing Polyaromatic Compounds in Light Oil. *Ind. Eng. Chem. Res.*, 31, 1577-1580, 1992.
- 39) Topsøe, H. *et al.* *A review of: "Hydrotreating Catalysis Science and Technology"*, 1st ed., Springer, 1465 – 1468, 1996.
- 40) Jeong, K. E. *et al.* Selective oxidation of refractory sulfur compounds for the production of low sulfur transportation fuel, *Korean J. Chem. Eng.*, 30, 509-517, 2013.
- 41) Sharipov, A. K. and Nigmatullin, V. R. Oxidative desulfurization of diesel fuel (a review), *Petrol. Chem.*, 45, 371-377, 2005.
- 42) Gupta, N. *et al.* Biotechnology of desulfurization of diesel: prospects and challenges. *Appl. Microbiol. Biot.*, 66, 356-366, 2005.
- 43) Tumiatti, V. *et al.* IEC 62697-2012: State of the Art Methods for Quantification of DBDS and Other Corrosive Sulfur Compounds in Unused and Used Insulating Liquids. *IEEE Trans. Dielectr. Electr. Insul.*, 19, 1633-1641, 2012.
- 44) Lewand, L., The role of corrosive sulfur in transformers and transformer oil (2002). Doble Engineering Company, USA. https://www.doble.com/wp-content/uploads/2002_3B.pdf (accessed, February 2021).

- 45) Andersson, J. T. and Holwitt, U. An Advantageous Reagent for the Removal of Elemental Sulfur from Environmental-Samples, *Fresen. J. Anal. Chem.*, 350, 474-480, 1992.
- 46) Borchardt, L. G. and Easty, D. B. Gas chromatographic determination of elemental and polysulfide sulfur in kraft pulping liquors, *J. Chromatogr. A*, 299, 471 - 476, 1984.
- 47) Struble, D. L. Quantitative Determination of Elemental Sulfur by GLC with an Electron Capture or a Flame Photometric Detector, *J. Chromatogr. Sci.*, 10, 57 - 59, 1972.
- 48) Junk, G. A. *et.al.* Use of macroreticular resins in the analysis of water for trace organic contaminants, *J. Chromatogr. A*, 99, 745 – 762, 1974.
- 49) Guinon, J. L. *et.al.* Determination of elemental sulfur, mercaptan and disulfide in petroleum naphtha by differential-pulse polarography, *Fresenius J. Anal. Chem.*, 337, 372 – 376, 1990.
- 50) Clark, P. D. and Lesage, K. L. Quantitative Determination of Elemental Sulfur in Hydrocarbons, Soils, and Other Materials, *J. Chromatogr. Sci.*, 27, 259 – 261, 1989.
- 51) Sid Kalal, H. S *et.al.* Determination of trace elemental sulfur and hydrogen sulfide in petroleum and its distillates by preliminary extraction with voltammetric detection, *Analyst*, 125, 903 – 908, 2000.
- 52) Olofsson, B. R. Determination of elemental sulfur in jet fuel by differential pulse polarography, *Anal. Chim. Acta*, 177, 167 - 173, 1985.
- 53) Taylor, B. F. *et.al.* Assay of sulfur as triphenylphosphine sulfide by high performance liquid chromatography: application to studies of sulfur bioproduction and sulfur in marine sediments, *J. Microbiol. Methods*, 9, 221 – 231, 1989.
- 54) Woods, G. D. and Fryer, F. I. Direct elemental analysis of biodiesel by inductively coupled plasma-mass spectrometry, *Anal. Bioanal. Chem.*, 289, 753 - 761, 2007.
- 55) Geiger, W. M. *et.al.* Application of ICP-MS as a multi-element detector for sulfur and metal hydride impurities in hydrocarbon matrices, *J. Chromatogr. Sci.*, 45, 677 - 682, 2007.
- 56) Djokic, M. R. *et.al.* Quantitative on-line analysis of sulfur compounds in complex hydrocarbon matrices, *J. Chromatogr. A*, 1509, 102 – 113, 2017.
- 57) Yan, X. Review: Sulfur and nitrogen chemiluminescence detection in gas chromatographic analysis, *J. Chromatogr. A*, 976, 3 – 10, 2002.
- 58) Meyer, B. Elemental Sulfur, *Chem. Rev.*, 76, 367 – 388, 1976.

- 59) Heilmann, J. and Heumann, K. G. Development of a Species-Unspecific Isotope Dilution GC-ICPMS Method for Possible Routine Quantification of Sulfur Species in Petroleum Products, *Anal. Chem.*, 80, 1952 – 1961, 2008.
- 60) Bartlett, P. D. and Meguerian, G. Reactions of Elemental Sulfur. I. The Uncatalyzed Reaction of Sulfur with Triarylphosphines, *J. Am. Chem. Soc.*, 78, 3710 – 3715, 1956.
- 61) Pauls, R. E. Determination of elemental sulfur in gasoline by gas chromatography with on-column injection and flame ionization detection following derivatization with triphenylphosphine, *J. Chromatogr. Sci.*, 48, 283 – 288, 2010.
- 62) ASTM D7800/D7800M-14, Standard Test Method for Determination of elemental sulfur in Natural Gas, 5, 1 - 13, 2014.
- 63) Strain, H. *et.al.* M. Tswett: Adsorption analysis and chromatographic methods: Application to the chemistry of chlorophylls, *J. Chem. Educ.*, 4, 238 - 242, 1967.
- 64) Ettre, L. S. Nomenclature for Chromatography (IUPAC Recommendations 1993). *Pure & Appl. Chem.*, 65, 819-872, 1993.
- 65) James, A. T. and Martin, A. J. P. Gas-liquid partition chromatography: the separation and micro-estimation of volatile fatty acids from formic acid to dodecanoic acid, *Biochem.*, 50, 679-690, 1952.
- 66) McNair, H. M. and Miller, J. M. Basic gas chromatography, 2nd ed., *John Wiley & Sons, Inc.*, 2009.
- 67) Image: Gas Chromatography-vector.svg. In Wikipedia. Retrieved February, 2021, from https://commons.wikimedia.org/wiki/File:Gas_chromatograph-vector.svg
- 68) Berger, T. A. Separation of polar solutes by packed column supercritical fluid chromatography. *J. Chromatogr. A*, 785, 3-33, 1997.
- 69) Ruixiang, H *et al.* Analysis of sulfur - containing compounds in crude oils by comprehensive two - dimensional gas chromatography with sulfur chemiluminescence detection, *J. Sep. Sci.*, 27.9: 691-698, 2004.
- 70) Grob, R. L. and Barry, E. F. Modern practice of gas chromatography, 4th ed., *Wiley-Interscience*, 2004.
- 71) Cong, H. *et al.* Study on Sulfide Distribution in the Operating Oil of Power Transformers and Its Effect on the Oil Quality, *Appl. Sci.*, 8, 1577-1589, 2018.
- 72) Yaku, K. and Morishita, F. Separation of drugs by packed-column supercritical fluid chromatography, *J. Biochem. Bioph. Meth.*, 43, 59-76, 2000.
- 73) Gere, D. R. Supercritical Fluid Chromatography, *Science*, 222, 253-259, 1983.
- 74) Garzotti, M. *et.al.* Coupling of a supercritical fluid chromatography system to a hybrid (Q-TOF 2) mass spectrometer: on-line accurate mass measurements, *Rapid Commun. Mass. Sp.*, 15, 1187-1190, 2001.
- 75) Fischer, H. *et.al.* Reaction monitoring of aliphatic amines in supercritical carbon dioxide by proton nuclear magnetic resonance spectroscopy and implications for supercritical fluid chromatography, *Anal. Chem.*, 75, 622-626, 2003.

- 76) Daintree, L. S. *et.al.* Separation processes for organic molecules using SCF technologies, *Adv. Drug Deliver. Rev.*, 60, 351-372, 2008.
- 77) Bower, N. W. Principles of Instrumental Analysis. 4th edition (Skoog, D. A.; Leary, J. J.), *J. Chem. Educ.*, 69, A224, 1992.
- 78) Chapman, S. Carrier Mobility Spectra of Spray Electrified Liquids, *Phys. Rev. Series II*, 52, 184-190, 1937.
- 79) Fenn, J. B. *et.al.* Electrospray Ionization for Mass-Spectrometry of Large Biomolecules, *Science*, 246, 64-71, 1989.
- 80) Fenn, J. B. Electrospray wings for molecular elephants (Nobel lecture). *Angew. Chem. Int. Ed.*, 42, 3871-3894, 2003.
- 81) Kott, L. An overview of supercritical fluid chromatography mass spectrometry (UHPSFC-MS) in the pharmaceutical industry (2013), *Am. Pharm. Rev.*, Online: <https://www.americanpharmaceuticalreview.com/Featured-Articles/131177-An-Overview-of-Supercritical-Fluid-Chromatography-Mass-Spectrometry-SFC-MS-in-the-Pharmaceutical-Industry/> (accessed, February 2021).
- 82) Image: Schematic of an ESI interface. In University of Bristol Website. Retrieved February, 2021, from: <http://www.bristol.ac.uk/chemistry/facilities/nerc-lsmsf/techniques/hplcms/>
- 83) Image: Schematic of an ion source. In University of Bristol Website. Retrieved February, 2021, from: <https://www.bristol.ac.uk/chemistry/facilities/nerc-lsmsf/techniques/gcms/>
- 84) Hoffman, E. d. and Stroobant, V. *Mass Spectrometry: Principles and Applications*, 3rd ed., John Wiley & Sons Ltd, 2007.
- 85) Paul, W. Electromagnetic Traps for Charged and Neutral Particles, *Angew. Chem. Int. Ed.*, 29, 739-748, 1990.
- 86) Image: Quadrupole mass analyser. In University of Alabama at Birmingham Website. Retrieved February, 2021, p.8, from: https://www.uab.edu/proteomics/pdf_files/2018/GBSC%20724%2001-24-18.pdf on February 2021.
- 87) Dawson, P. H. Quadrupole mass spectrometry and its applications, 1st ed., Elsevier scientific publishing company, 1976.
- 88) William, B. J. The Origin of the Polymer Concept, *J. Chem. Educ.*, 85, 5, 624, 2008.
- 89) The Nobel Prize in Chemistry 1953. In NobelPrize.org. Accessed, February 2021, <https://www.nobelprize.org/prizes/chemistry/1953/summary/>
- 90) The Nobel Prize in Chemistry 1963. In NobelPrize.org. Accessed, February 2021, <https://www.nobelprize.org/prizes/chemistry/1963/summary/>
- 91) Nesvadba, P. Radical Polymerization in Industry. In *Encyclopedia of Radicals in Chemistry, Biology and Materials* (eds C. Chatgililoglu and A. Studer), 2012.
- 92) Lamers, B. A. G. *et.al.* Consequences of Molecular Architecture on the Supramolecular Assembly of Discrete Block Co-oligomers, *Macromolecules*, 53, 10289-10298, 2020.
- 93) Solomon, D. H. Polymerization Process and Polymers Produced Thereby, *US Pat. 4581429-A*, 1986.

- 94) Wang, J. and Matyjaszewski, K. Controlled/"living" radical polymerization. atom transfer radical polymerization in the presence of transition-metal complexes, *J. Am. Chem. Soc.*, 117, 5614-5615, 1995.
- 95) Le, T. P. *et.al.* Polymerization with living characteristics, *Int. Pat. WO9801478-A1*, 1998.
- 96) Moad, G and Solomon, D. H. Comprehensive Polymer Science, Pergamon, Chapter 8, 101-104, 1996.
- 97) Gutiérrez-Villarreal, M. H. and Guzmán-Moreno, J. G. Surface graft polymerization of N-vinylcaprolactam onto polylactic acid film by UV irradiation, *J. Polym. Res.*, 20, 149 - 155 , 2013
- 98) Paul L. Flory, Principles of Polymer Chemistry, Cornell University Press, Ithaca, New York, 1953.
- 99) Lee, N. S. and Wooley, K. L. Block Copolymer Synthesis Using a Commercially Available Nitroxide-Mediated Radical Polymerization (NMP) Initiator, *Material Matters*, 5.1, 9, 2010
- 100) Grubbs. R. B. Nitroxide-Mediated Radical Polymerization: Limitations and Versatility, *Poly. Rev.*, 51:2, 104-137, 2011.
- 101) Hawker, C. J. Molecular Weight Control by a "Living" Free-Radical Polymerization Process, *J. Am. Chem. Soc.*, 116, 11185-11186, 1994.
- 102) Kreutzer, J. and Yagci, Y. Metal Free Reversible-Deactivation Radical Polymerizations: Advances, Challenges, and Opportunities, *Polymers* 10, 35, 2018.
- 103) Ley, S. V. Multi-step organic synthesis using solid-supported reagents and scavengers: a new paradigm in chemical library generation, *J. Chem. Soc., Perkin Trans. 1*, 24, 3815–4195, 2002.
- 104) Kecili, R. *et. al.* Removal of acrolein from active pharmaceutical ingredients using aldehyde scavengers, *Org. Process Res. Dev.*, 16, 6, 1225–1229, 2012.
- 105) Merrifield, R. B. Solid Phase Peptide Synthesis. I. The Synthesis of a Tetrapeptide, *J. Am. Chem. Soc.*, 85, 2149-2154, 1963.
- 106) Brown, R. C. D. Recent developments in solid-phase organic synthesis, *J. Chem. Soc., Perkin Trans. 1*, 19, 3293 – 3320, 1998.
- 107) Vaino, A. R. and Janda, K. D., Solid-Phase Organic Synthesis: A Critical Understanding of the Resin, *J. Comb. Chem.*, 2, 579-596, 2000.
- 108) Cankařová, N. *et.al.* Traceless Solid-Phase Organic Synthesis, *Chem. Rev.*, 119, 12089-12207, 2019.
- 109) Braithwaite, A. and Smith, F. J., Chromatographic Methods, 5th ed., Kluwer Academic Publishers, 1999.
- 110) Telepchak, M. J. *et.al.* Forensic Science and Medicine: Forensic and Clinical Applications of Solid Phase Extraction, 1st ed., Humana Press Inc., 2004.
- 111) Halket, J. M. Handbook of Derivatives for Chromatography, 2nd ed., John Wiley & Sons, Ltd., 1993.
- 112) Levine, B. Principles of Forensic Toxicology. 2nd ed., American Association of Clinical Chemistry, 2006.
- 113) Bartlett, P. D. and Meguerian, G. Reactions of Elemental Sulfur. I. The Uncatalyzed Reaction of Sulfur with Triarylphosphines, *J. Am. Chem. Soc.*, 78, 3710 – 3715, 1956.

- 114) Pauls, R. E. Determination of elemental sulfur in gasoline by gas chromatography with on-column injection and flame ionization detection following derivatization with triphenylphosphine, *J. Chromatogr. Sci.*, **48**, 283 – 288, 2010.
- 115) Borchardt, L. G. and Easty, D. B. Gas chromatographic determination of elemental and polysulfide sulfur in kraft pulping liquors, *J. Chromatogr. A*, **299**, 471 - 476, 1984.
- 116) Lloyd, J. R. *et.al.* Kinetics and mechanism of the reaction of trico-ordinate phosphorus compounds with octasulfur, *J. Chem. Soc., Perkin Trans. 2*, **11**, 1813-1817, 1985.
- 117) Abraham, M. H. Solvent effects on reaction rates, *Pure & Appl. Chem.*, **57**, 8, 1055 - 1064, 1985.
- 118) Steinfeld, J. I. *et.al.* Chemical Kinetics and Dynamics, 2nd ed., Pearson, 14-17, 1998.
- 119) Xavier, K. B. *et.al.* Kinetic analysis by in vivo ³¹P nuclear magnetic resonance of internal Pi during the uptake of sn-glycerol-3-phosphate by the pho regulon-dependent Ugp system and the glp regulon-dependent GlpT system, *J. Bacteriol*, **177**, 699-704, 1995.
- 120) Brown, T. *et.al.* ³¹P nuclear magnetic resonance measurements of ATPase kinetics in aerobic Escherichia coli cells. *Proceedings of the National Academy of Sciences*, **74**, 5551-5553, 1977.
- 121) Knapp, D. R. Handbook of analytical derivatization reactions, 1st ed., John Wiley & Sons, 1979.
- 122) Gross, M. L. The Encyclopedia of Mass Spectrometry: Molecular Ionization, 1st ed., Elsevier science, 2004
- 123) Itzstein, M.V. and Jenkins, I. D. The reaction of diols with triphenylphosphine and di-isopropyl azodicarboxylate. Part 2. Formation of cyclic phosphoranes from 1,5–1,12-diols, *J. Chem. Soc., Perkin Trans. 1*, 1987, 2057-2060, 1987.
- 124) Langley, G. J. *et.al.* Detection and Quantitation of ACCUTRACE S10, a New Fiscal Marker Used in Low-Duty Fuels, Using a Novel Ultrahigh-Performance Supercritical Fluid Chromatography–Mass Spectrometry Approach. *Energ. Fuel*, **32**, 10580-10585, 2018.
- 125) Park, J. *et.al.* Application of montmorillonite in bentonite as a pharmaceutical excipient in drug delivery systems. *J. Pharm. Investig.*, **46**, 363-375, 2016.
- 126) Charette, A. B. *et.al.* Synthesis of a Triphenylphosphine Reagent on Non-Cross-Linked Polystyrene Support: Application to the Staudinger/Aza-Wittig Reaction. *Org. Lett.*, **2**, 3777-3779, 2000.
- 127) Whitaker, C. M. *et.al.* Synthesis and solid-state structure of substituted arylphosphine oxides. *J. Org. Chem.*, **60**, 3499-3508, 1995.
- 128) Garcia-Diego, C. and Cuellar, J. Synthesis of Macroporous Poly(styrene-co-divinylbenzene) Microparticles Using n-Heptane as the Porogen: Quantitative Effects of the DVB Concentration and the Monomeric Fraction on Their Structural Characteristics, *Ind. Eng. Chem. Res.*, **22**, 8237, 2005.
- 129) Jain, M. On-Line transformer oil purification. 17th IERE general meeting and Canada forum, 18th May, 2017. Accessed, November 2021, <https://www.iere.jp/events/forum/2017-canada/Presen/S4-1.pdf>
- 130) Mansky, P. *et.al.* Controlling Polymer-Surface Interactions with Random Copolymer Brushes, *Science*, **275**, 1458-1460, 1997.
- 131) Albright, T. A. *et. al.*, Nuclear magnetic resonance studies. IV. Carbon and phosphorus nuclear magnetic resonance of phosphine oxides and related compounds. *J. Org. Chem.*, **40**, 23, 3437–3441, 1975.

- 132) Spreider, P. A. and Breit, B. Palladium-Catalyzed Stereoselective Cyclization of in Situ Formed Allenyl Hemiacetals: Synthesis of Rosuvastatin and Pitavastatin. *Org. Lett.*, 20, 3286-3290, 2018.
- 133) Hawker, C. J. Molecular Weight Control by a "Living" Free-Radical Polymerization Process, *J. Am. Chem. Soc.*, 116, 11185-11186, 1994.
- 134) Hawker, C. J. Architectural Control in "Living" Free Radical Polymerizations: Preparation of Star and Graft Polymers, *Angew. Chem. Int. Ed.*, 34, 1456 – 1459, 1995.
- 135) Kusumaatmaja, A., *et. al.*, Synthesis and photoproperties of Eu(III)-bearing star polymers as luminescent materials. *J. Polym. Sci. Part A: Polym. Chem.*, 51: 2527-2535, 2013.

